THE UNIVERSITY *of* EDINBURGH

Acquisition of renogenic competence in the early mouse embryo and embryonic stem cells

Veronika V. Ganeva

Doctor of Philosophy

Centre for Integrative Physiology
School of Biomedical Sciences
The University of Edinburgh

2011

To Stefan

for his love, care and support

Contents

Abstract

The acquisition of renogenic competence (the ability to give rise to kidney) during embryonic development is not yet fully understood. Clarifying the temporal and molecular aspects of this process is equally essential for understanding excretory system development and for devising methods for successful differentiation of embryonic stem cells (ESCs) to renal cells for disease modeling, toxicology screening and potential cell replacement therapies.

In embryo development, the metanephric (permanent) kidney arises as a result of inductive interactions between two embryonic structures that arise in the intermediate mesoderm - the ureteric bud (UB, a diverticulum of the Wolffian duct) and the metanephric mesenchyme (MM). The UB develops into the collecting duct system and the MM undergoes an epithelial-to-mesenchymal transition to form the secretory units of the kidney - the nephrons.

In this thesis, I used a tissue disaggregation-reaggregation method that allows the reconstruction of mouse organotypic kidney rudiments to place different embryonic cells in the environment of a developing kidney and assess their potential to integrate into kidney epithelia and differentiate to renal cells. First, the suitability of this method was evaluated and a quantitative assay for evaluating the numbers of test cells integrating in various renal compartments was developed. Second, the reaggregation method was used to characterise the renogenic potential of undifferentiated mouse ESCs, ESC-derived cells after Notch inhibition, and cells derived from the presumptive nephrogenic regions of embryos at various stages of development.

ESCs are isolated from the inner cell mass of an embryo and have the potential to differentiate to any tissue of the body when injected into mouse blastocysts. Strategies have successfully been devised for ESC differentiation to many lineages, but very few studies reported any success with the differentiation of ESCs to a renal lineage.

Undifferentiated ESCs showed a very good ability to form chimeric structures with developing kidney tubules (both nephrons and extending UBs). Nevertheless, the

resulting structures were morphologically different from renal epithelia in most cases and integrated ESC-derived cells were not positive for several combinations of kidney markers. These results suggested that the influence of the niche was not sufficient for a successful ESC differentiation to renal cells. Treatment of ESC with an inhibitor of the Notch pathway to increase the proportion of mesodermal cells did not improve this outcome. On the basis of these results, it was speculated that the earliest lineage to which embryonic stem cells must be differentiated in order to become competent to make renal cells should first be identified. I addressed this by determining the developmental stage at which cells able to contribute to the formation of metanephric epithelia first appear in mouse embryo development. When mixed in embryonic kidney reaggregates labelled cells isolated from the nephrogenic regions of E9.5 embryos integrated into various renal compartments. These cells were seen in UBs, nephrons, glomeruli and the condensing mesenchyme. Marker expression studies showed that the exogenous E9.5 cells expressed an array of kidney markers - Pax2 in renal epithelia and the condensing mesenchyme, Wt1 in glomeruli and Six2 in the condensing mesenchyme. Furthermore, exogenous E9.5 cells also co-expressed Pax2/Wt1 in the condensing mesenchyme, Megalin/E-cadherin in the proximal tubule and Pax2/E-cadherin in renal epithelia. This provides evidence that challenges the existing model and suggests that some cells from the intermediate mesoderm at a stage where the metanephric blastema is yet formed are competent to contribute to kidney structures. Furthermore, experiments with E8.5 embryos showed that such a renocompetence could be acquired even before the specification of intermediate mesoderm.

These findings contribute to our knowledge about kidney cell specification and provide valuable information to guide future attempts to develop an efficient method for deriving renal cells from ESCs. Furthermore, the reported ability of ESC-derived non-kidney cells to form chimeric structures with renal tubules provides a proof-of-principle that it might be possible to use exogenous types of cells for physiological support to injured kidney tubules, thus offering a possible novel approach for cell replacement therapies.

Declaration

This thesis has been composed entirely by myself and represents my own unaided work, except where otherwise acknowledged. This work has not been submitted for any other degree or professional qualification.

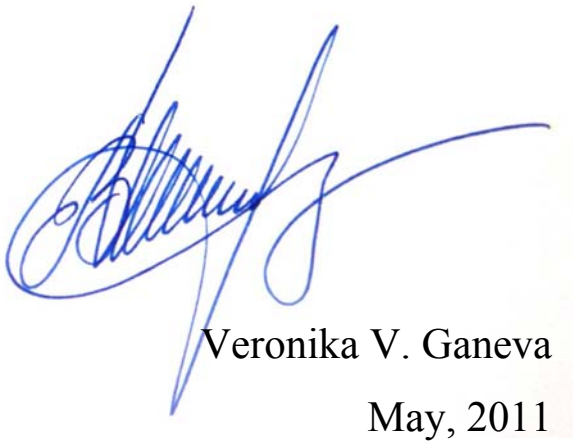

Veronika V. Ganeva

May, 2011

Acknowledgments

I would first like to express my gratitude to my PhD supervisor, Prof. Jamie Davies, for guiding me and encouraging me throughout my PhD work. His expertise and love of science have been an inspiration for me during the past several years. I am also very thankful for Jamie's support and appreciation of my work in public engagement and science communication.

I would like to thank all members of the Jamie Davies lab for their support, scientific advice and good time spent together. I am especially grateful to Dr. Mathieu Unbekandt for providing me with useful advice on so many occasions and to Ms. Weijia Liu for helping me with my thesis submission. Many thanks to Dr. Nils Lindstrom and Dr. Peter Hohenstein for the inspiring and challenging discussions and my gratitude to Dr. Jane Brennan, Dr. Chris Armit, Dr. Jane Armstrong, Dr. Guangping Tai and Ms. Sue Lloyd-MacGilp for their kind support.

Many thanks to the whole EU FP6 consortium KIDSTEM for giving me the opportunity to perform this work and for the multitude of opportunities to attend scientific meetings and improve my knowledge and understanding of science.

My sincere thanks go to Dr. Thomas Pratt who kindly provided the TgTP6.3 mice used in this work. Without his support this work would not have been possible.

Many thanks to the members of BRR-CIP who have provided general animal care and allowed me to work in the facility along with them. Also thanks to Dr. Trudi Gillespie for her assistance with confocal microscopy.

I cannot miss thanking Dr. John West for his patient and useful advice and his sense of humour. Many thanks to Dr. Thomas Theil for showing me how to dissect early mouse embryos. Dr. Jane Quinn has kindly provided our group with tauGFP mouse embryonic stem cells. Oct4-GFP mouse embryonic stem cells were a generous gift from Dr. Patricia Murray, University of Liverpool. Dr. Paul de Sousa welcomed me

to his lab to perform the human embryonic stem cell experiments. I am also very thankful to all members of the de Sousa lab for welcoming me as a new colleague and as a new friend. Many thanks go to Dr. Steve Pells, Dr. Alexander Ermakov, Ms. Heidi Mjoseng, Ms. Yanina Tsenkina, Ms. Eirini Koutsouraki, Ms. Bruna Corradetti, Ms. Sara Valencia, Ms. Martina Mrsnik and Mr. Cairnan Duffy.

I really appreciate the opportunities to take part in public engagement and science communication activities provided to me by Mr. Andrew Smith (Manager of ESTOOLS). It was only thanks to these opportunities that I was awarded the Anne McLaren Award for multidisciplinary contribution to human embryonic stem cell research. Andrew has made my work with ESTOOLS extremely interesting and enjoyable.

Much love to my friends from the CIP – Dr. Petrina Georgala, Dr. Panagiotis Douvaras, Mr. Giuseppe Gallone, Mr. Fabio Simony and Dr. Oforiwa Gorleku.

Also many thanks to my Edinburgh friends – Svilen Svilenov, Mostafa Afgani, Polly Hristova, Andrea Louise Kane, Diana Tasseva for their friendship and good time spent together.

List of abbreviations

°C - degrees Centigrade

Å - angstrom (1 angstrom = 1.0×10^{-10} metres)

AC - anchor cell

AChE - acetylcholinesterase

ADAM - A disintegrin and metalloproteinase

AFP - alpha fetoprotein

AFSC – amniotic fluid stem cell

ANOVA - analysis of variance

AP - alkaline phosphatase

Aqp2 - aquaporin 2

BMP - bone morphogenetic protein

bp - base pairs

CD - collecting duct

CD1 - mouse strain

CD44 - cluster of differentiation 44

cDNA - complementary DNA

CKCM - complete kidney culture medium

CM - cap mesenchyme

CMV - cytomegalovirus

c-Myc - myelocytomatosis oncogene

CO_2 - carbon dioxide

c-Ret - Receptor tyrosine kinase c-Ret

CSL - CBF1/RBP-Jκ, Su(H), Lag1

[DNA] – DNA concentration

DX – where X is a number – day X

DAPI - 4',6-diamidino-2-phenylindole

DAPT - N-[N-(3,5-Difluorophenacetyl-L-alanyl)]-S-phenylglycine t-Butyl Ester (also referred to as gamma secretase inhibitor)

DBA - Dolichos biflorus agglutinin

DIA - differentiation inhibitory activity

DMEM - Dulbecco's Modified Eagles Medium

DMSO - dimethyl sulfoxide

DNA - deoxyribonucleic acid
dNTPs – deoxyribonucleotide triphosphate
DT - distal tubule
EB - embryoid body
EC - embryonal carcinoma
ECM - extracellular matrix
EDTA - Ethylene diamine tetraacetic acid
EGF - epidermal growth factor
EMT - epithelial-to-mesenchymal transition
Emx1/2 - empty spiracles homeobox 1/2
ESCs (or ES cells) - embryonic stem cells
EX.X - in embryonic development - X.X days post coitum
Eya1 - eyes absent homologue 1
FACS - fluorescence-activated cell sorting
FBS - fetal bovine serum
FCS - fetal calf serum
FGF - fibroblast growth factor
FITC - fluorescein isothiocyanate
Flk1 - fetal liver kinase 1
Fox - forkhead box
G418 - Geneticin
GAPDH - Glyceraldehyde 3 phosphate dehydrogenase
GATA3 - GATA-binding protein 3
GBM - glomerular basement membrane
GDNF - glial cell line-derived neurotrophic factor
GFRα1 - GDNF family receptor alpha 1
GFP - green fluorescent protein
Gp130 - glycoprotein 130
Gpc3 - glypican 3
h - hours
HATs - histone acetyltransferases
Hes - hairy and enhancer of split genes
hESC - human embryonic stem cells
HGF - hepatocyte growth factor
HIF1α - hypoxia inducible factor 1, alpha subunit

Hox - homeobox genes
Hs2st - heparan sulfate 2-O-sulfotransferase
HSC - hematopoietic stem cells
ICM - inner cell mass
IHC - immunohistochemistry
IM - intermediate mesoderm
iPSC (or iPS cells) - induced pluripotent stem cells
IRES - internal risbosome entry site
IVC - individually ventilated cell
JNK - c-Jun N-terminal kinase
KD - kidney development
kDa - kilodalton
Klf4 - Kruppel-like factor 4
KO-DMEM - KnockOut Dulbecco's modified Eagle's medium
KSP-cadherin – kidney-specific cadherin
LIF - leukaemia inhibitory factor
LIFR – LIF receptor
Lim1 - LIM homeobox protein 1
LOH - loop of Henle
LTL - Lotus tetragonolobus agglutinin
μ - micro
M – molar
MD - macula densa
MDCK - Madin-Darby Canine Kidney cells
MEFs - mouse embryonic fibroblasts
MEM - Minimal Essential Medium
mESC - mouse embryonic stem cells
MET - mesenchymal-to-epithelial transition
μF - microfarad
μg - microgram
mg – milligram
μL - microliter
mL - milliliter
μm - micrometer
μM - micromolar

mm - millimeter
MM - metanephric mesenchyme
mRNA - messenger RNA
MSC - mesenchymal stem cells
n - nano
Na^+/K^+ ATPase - sodium/potassium adenosine triphosphatase
N-CAM - neural cell adhesion molecule
NeXT - Notch extracellular truncation
NFκB - nuclear factor kappa-light-chain-enhancer of activated B cells
ng - nanogram
NICD - Notch intracellular domain
NIH - National Institute of Health
NRR - negative regulatory regions
ns - not standard
Oct4 - octamer-binding transcription factor 4
Osr1 - odd-skipped-related 1
Pax2/8 - paired-box gene 2/8
PBS - Phosphate buffered saline
PCR - polymerase chain reaction
PDGF - platelet-derived growth factor
PEST - proline, glutamate, serine and threonine-rich domain
PFA - paraformaldehyde
Pkd1/2 - polycystic kidney disease 1/2
PNA - peanut agglutinin
PS - primitive streak
PT - proximal tubule
Ptn - Pleiotrophin
RA - retinoic acid
RAM - RBPjκ-association module
Rara/Rarb - retinoic acid receptor alpha/beta
RCM1 - Roslin Cells Manchester - 1 human embryonic stem cell line
RNA - ribonucleic acid
RNase - ribonuclease
ROCK - Rho-associated, coiled coil-containing potein kinase 1
ROCKi - ROCK inhibitor

RT - room temperature
RV - renal vesicle
Sall1 - sal-like 1
SC - spinal cord
SEM - standard error of the mean
siRNA - small interfering RNA
Six2 - sine oculis homeobox 2
SME - smooth muscle actin
SOP - sensory organ precursor
Sox2 - SRY-box containing gene 2
sqPCR - semi-quantitative PCR
STAT3 - signal transducer and activator of transcription 3
STO (feeder cells) - mouse embryonic STO (S, SIM; T, 6-thioguanine resistant; O, ouabain resistant) cell line
T - Brachyury
TAE - buffer solution containing Tris base, acetic acid and EDTA
TRITC - Tetramethyl rhodamine isothiocyanate
U - unit(s)
UB - ureteric bud
VU - ventral uterine precursor cell
WD - Wolffian duct
Wnt - wingless-type MMTV integration site family
WT - wild type
WT1 - Wilms' tumour 1

List of figures and tables

(in chronological order)

Chapter 1

Chapter 2

Chapter 3

Chapter 4

Chapter 5

Chapter 6

Chapter 7

Appendix II - Supplementary Figures

Chapter 1

Introduction to early embryo development, kidney development and stem cell biology

1.1 Aims

The focus of this thesis is on understanding more about the process of how cells acquire a renal fate *in vivo* and *in vitro*. This problem has been approached from two very different angles - trying to understand how embryonic stem cells (ESC) can be differentiated into renal cells and looking at early embryo development to dissect how and when this process happens *in vitro.*

The aim of the former approach, which targets ESC differentiation, is to investigate whether these cells can differentiate into renal cells when subjected to the environment of a developing embryonic kidney rudiment, at the stage where nephrogenic processes are just starting to define the morphology of the kidney. Furthermore, it is important to see how pre-differentiation of ESCs compares to using undifferentiated cells, still in combination with exposing the test cells to the inductive signals present in the embryonic kidney. As discussed more extensively in section 1.6.2, the differentiation of pluripotent cells to kidney cells has not been well described and the processes and steps taking place have not been characterised. On the basis of previous publications, it becomes clear that much more work is necessary to understand these processes.

The aim of the second approach in this work was to find out more about the processes naturally occurring in a developing mouse embryo, which are related to the production of kidney cells. For example, it would be extremely useful to pinpoint the stage in embryonic development where cells acquire competence to produce renal cells. This will contribute to understanding the process of lineage specification in the embryo. It will also make possible the isolation and possibly propagation of these progenitor cells, which would be an extremely valuable tool for studying kidney cell specification and stem cell differentiation *in vitro*. Identification of the first developmentally occurring cells, capable of giving rise to kidney cells independently of the signals provided by the embryo, would also answer the question of which lineage do embryonic stem cells have to be differentiated to, in order to be able to produce renal cells efficiently.

1.2 Chapter introduction

As mentioned in the previous section, the main focus of this thesis (in short) is to explore the potential of embryonic stem cells to differentiate to kidney cells in certain conditions and to investigate when cells in the early embryo acquire renogenic capacity. These two aims are a part of a bigger scientific endeavour to understand how nature works and devise ways of correcting it when it stops working. Since the interlinks between stem cell biology, kidney development and therapeutic potential are quite complex, a separate section (section 1.7 of this chapter) was dedicated to demonstrating how the work of this thesis is positioned in a more global initiative. Before these concepts can be discussed and the results of this work examined several different scientific areas need to be introduced – how the kidney functions, what developmental processes lead to the formation of a functional kidney in embryogenesis, what are embryonic stem cells and their potential applications.

I will start this introduction by providing information about the function and anatomy of the kidney as a general overview of the complexity of this organ. Understanding these concepts first is a prerequisite to exploring how they come into being. Then, important processes of early embryo development will be examined, to clarify the origins of the kidney and to demonstrate the complex processes that cells undergo to acquire renocompetence. In this work renocompetence is defined as the ability of test cells to give rise to kidney cells *in vitro*, independently of the signals provided by the embryo. Examining some aspects of early embryo development in depth will be particularly relevant to Chapter 6 of this thesis, where cell mixing experiments containing early embryo cells will be described to assess the renogenic potential of these tissues. The focus of embryo development will be narrowed down to the formation of mesoderm and intermediate mesoderm, from which the kidneys are derived. Furthermore, the specification of the transient embryonic kidneys, the pronephros and mesonephros will be described prior to that of the permanent metanephros. Since the first two are formed earlier, this information will be especially important when discussing the cell mixing experiments mentioned above to study the acquisition of renogenic potential of early embryo tissues. This will be followed by an introduction of the metanephros and the morphogenetic and

regulatory processes that allow its development to a fully functional kidney after the completion of embryo development. Then, a transition will be made to stem cell biology. All information mentioned up to here will also be relevant to the ESC differentiation experiments described in Chapter 4 and 5. First, understanding how the metanephros develops and where it originates from might be key to the successful differentiation of ESCs to renal cells. When studying directed differentiation of ESCs, it might be necessary to try to reproduce embryonic development *in vitro* and try to transition these cells (in a directed manner) first to mesoderm and then intermediate mesoderm to push them to acquire renogenic ability. In addition, information will be provided about ESCs, their discovery and properties, together with concepts of differentiation and directed differentiation. A literature summary about differentiation of ESCs to renal cells will critically review the current advancements in this field. Finally, the impact and perspectives of a work integrating stem cell biology with kidney development and embryo development will be provided, accompanied by some perspectives to translational studies.

1.3 The kidney - function and anatomy

Many aspects of kidney anatomy, function, development and disease have already been described. A recent summary of these is provided in the book "The kidney: from normal development to congenital disease" (eds. Vize, Woolf and Bard, 2003). This source has been used for most of this section as it provides a modern summary of kidney anatomy. Additional sources are cited as appropriate.

The kidneys are bean-shaped organs located at the posterior abdominal wall. They have an excretory function and are a part of the urinary system, together with the ureters (connecting the kidney and the bladder), the bladder and the urethra, the latter two located at the midline caudally from the kidneys. Each kidney has a collecting duct system, leading to a ureter, which clears urine to the bladder and out of the body. The kidney is often described as having two layers referred to as the cortex (outer) and the medulla (inner). The renal medulla is composed of structures called pyramids, which are not clearly separated, but divided by septa of cortical tissue, known as the columns of Bertin. Although the medulla and cortex do not have a

physical boundary, the corticomedullary junction can be distinguished visually due to the differences in appearance of those two compartments (reviewed by Hallgrimsson et al.., 2003). Urine flows from the medulla, out of the pyramids, into the minor calyces via a porous region called the cribriform plate. The human kidney contains a highly branched and complex drainage system, in which the minor calyces converge to form major calyces, which also converge to become the renal pelvis. The calyces and the renal pelvis are contained into a recess - the renal sinus. The renal sinus also contains the blood vessels, lymphatic vessels and nerves entering the kidney through the hilum, or the exit point of the ureter. After passing through the minor and major calyces, the urine produced in nephrons flows through the renal pelvis and the ureter to reach the bladder - an elastic musculomembranous organ, which serves for the storage of urine. The bladder is composed of four coats called serous, muscular, submucous and muscous (Gray, 1918). The contraction of the muscle layers, in combination with other processes, leads to voiding of the bladder and expelling urine out of the body.

The nephron is a structure responsible for the filtration of blood and production of urine. A human kidney contains about 500,000 to 1,500,000 nephrons (Sariola and Philipson, 1999). Although nephrons are essentially hollow tubes able to transport fluid to the collecting duct system, their structure and mechanism of work are much more complex than originally thought. The mature functional nephron is made up of more than 14 different types of cells (Herzlinger et al, 1992).

The two main components of the nephron are the renal corpuscle and the renal tubule (Little et al., 2007). The renal corpuscle consists of Bowman's capsule and the glomerulus. The renal tubule is segmented into proximal tubule (with convoluted and straight parts), the thin limbs of the loops of Henle, the thick ascending limb, the distal tubule (which also consists of a convoluted and distal part) and the connecting segment, which takes fluid into the collecting duct system (reviewed by Madsen et al., 2007). The positioning of nephrons in the kidney is not random, but rather organised. Nephrons can be classified according to the length of their loops of Henle, which can be either long or short (reviewed by Hallgrimsson et al., 2003).

The part of the nephron responsible for the filtration of blood is the renal corpuscle. As mentioned before, it consists of the Bowman's capsule and a glomerulus, along with connective tissue that supports them. The glomerulus is a vascular tuft that invades the renal corpuscle from the vascular pole (reviewed by Hallgrimsson et al., 2003). The primary mechanism for filtration of blood in the renal corpuscle involves three barriers - a fenestrated endothelium, a 1200-1500Å - thick glomerular basement membrane (GBM) and the slit diaphragm of the glomerular visceral epithelial podocytes (Farquhar et al., 1961; Kestila et al., 1998). The endothelia of the invading capillaries have numerous fenestrations that are 500-1000Å in diameter and do not have diaphragms. The fenestrations contain a glycocalyx secreted by the endothelial ells and are responsible for retaining cellular components and large macromolecules (reviewed by Satchell and Braet, 2009; Miner, 2011; Hallgrimsson et al., 2003). Unlike the other two layers, the second component of the filtration barrier, the GBM, is acellular. It is a specialised matrix, which consists of primarily laminin-521 (α5β2γ1), collagen IV (α3α4α5), nidogen1, nidogen2 and agrin (reviewed by Miner, 2011). Even though the GBM shares a lot of similarities with other more typical basement membranes, it is unusually thick and has a more unusual composition. Evidence has been shown that both the endothelial cells and podocytes synthesise and secrete components of the GBM (Abrahamson, 1985; St. John and Abrahamson, 2001; Abrahamson et al., 2009)

The outermost layer of the filtration barrier consists of highly specialised epithelial cells called podocytes. These cells possess primary (trabeculae) and secondary foot processes (pedicels), which interdigitate to form a tight meshwork, which sits on top of the GBM (reviewed by Madsen et al., 2007). The podocytes are anchored to the GBM by α3β1 integrin. The spaces between foot processes are referred to as filtration slits and are joined by a slit diaphragm (reviewed by Mundel and Shankland, 2002; Ruotsalainen et al., 1999. Farquhar et al., 1961). The mesh-like mechanical filter excludes all molecules larger than albumin (69kDa, radius 3.6nm). In addition to the purely physical filtration of fluid, the negatively charged components of the filtration barrier, such as glycoproteins and heparan sulfate (components of the glycocalix of the secondary processes of podocytes, the GBM

and the internal membrane of the capillary endothelial cells), repel negatively charged proteins, which causes them to be retained in the blood (reviewed by Hallgrimsson et al., 2003). The produced filtrate, called ultrafiltrate, is expelled into Bowman's space and then enters the proximal tubule. Furthermore it is important to emphasise on the importance of the three barriers in the glomerulus for the proper functioning of the kidney. An example is the protein nephrin, which is found on the slit diaphragm of podocytes (Ruotsalainen et al., 1999). A mutation in the gene encoding for this protein has been implicated in the cause of congenital nephrotic syndrome of the Finnish type and leads to a massive leakage of albumin and larger plasma proteins in the urine (Kestila et al., 1998). This is a result of podocytes failing to form normal foot processes.

A very different type of cells sit in the spaces between the glomerular capillaries and these are the mesangial cells, which help maintain the structural integrity of glomerular capillary loops. They generate extracellular matrix, regulate capillary flow and ultrafiltration surface and produce prostaglandins and cytokines (reviewed by Schlondorff, 2009).

Up to this point in the introduction it was demonstrated that a lot of structural and functional complexity is implicated in only one of the many steps on the way of producing urine. The ultrafiltrate resulting from the direct passage of water and small molecules from blood to the tubular units undergoes a lot of further processing when it passes through the whole length of the nephron, as it still contains many valuable components. Proteins, amino acids, glucose, water and salts are resorbed in the proximal tubule (PT; Sekine et al., 2011). The beginning of the PT is morphologically defined by the zone of transition from the simple squamous epithelium of the Bowman's capsule, to the cuboidal epithelium of the tubule. (Bulger, 1979). In some species (for example the rat), the PT consists of three subsegments (S1, S2 and S3), which show different protein expression patterns and function (Walmsley, 2010). These cells are equipped with a dense brush border of microvilli to maximise the area available for resorption (Heidrich et al., 1972). The PT leads to the thin limbs of the loop of Henle (Bulger, 1979). The short cortical

nephrons tend to lack the thin ascending portion, while the juxtamedullary ones have long ascending and descending limbs. The three segments of the loop of Henle are also responsible for the transport of salts and water and have great differences in their permeability (reviewed by Hallgrimsson et al., 2003). This part of the nephron is extremely important in establishing and maintaining the osmotic gradient in the renal medulla. The following segment of the nephron, the distal tubule (DT), also contributes to this process by removing salts from the tubule lumen by remaining impermeable to water. The DT consists of a straight and convoluted part and begins with the thick ascending limb (Bulger et al., 1979). Two different configurations of the epithelium lining the thick ascending limb have been reported. Some cells have a rough surface with numerous microprojections, while others have a smooth surface. Most cells possess one or two cilia (Madsen et al., 2007). The thick ascending limb possesses a specialised structure called the macula densa. It is a specialised region where the DT can be seen immediately adjacent to the hilus of the glomerulus (Bulger et al., 1979). The cells of the macula densa interdigitate with the mesangial glomerular cells (Barajas, 1979). This connection with the juxtaglemerular apparatus, serves as an important checkpoint for the content of urine in the distal tubule and is able to regulate the secretion of renin - an essential component of the renin - angiotensin - aldosterone system, which is crucial for control of blood pressure and volume (Skeggs et al., 1954; Goormaghtigh, 1940).

1.4 Development

The previous section illustrated the complexity of the kidney, both in terms of structure and function. In order to be able to address the problems of acquisition of renocompetence in ES cells or in embryonic development, it is first necessary to look at the known developmental processes, with three aims. An introduction of mouse embryonic development is necessary to follow the processes of cell specification that lead to the formation of the kidney primordia. Since the kidneys have been shown to derive from the intermediate mesoderm, its formation from mesoderm should also be discussed. The existence of three types of kidneys present in embryonic development will be covered with relevance to analysing cell mixing experiments in Chapter 6, containing tissues from early embryos. Finally, the mechanisms, which lead to the

formation of the adult kidney will be described to understand the mechanism of kidney formation and the properties of renocompetent cells. All these are also necessary for trying to understand what pathways ESCs should take to acquire the ability to make kidney cells *in vitro.*

1.4.1 Mouse embryonic development

1.4.1.1 Early embryo development

The beginning of a new organism starts by the fusion of the male and female gametes to produce a conceptus. The fertilised egg, or zygote, starts undergoing consecutive cleavages. The cells that result from these divisions are called blastomeres. One feature that distinguishes mammalian early development from that of other organisms is a process called rotational cleavage (Gulyas, 1975). Usually blastomere cleavages are symmetrical. In mammals, the first cleavage produces 2 blastomeres and happens meridionally, while in the second division one of these divides meridionally and the other – equatorially (Piotrowska-Nitsche and Zernicka-Goetz, 2005). Another major specificity of early mammalian development is the asynchrony of cell division, which rather than producing 4-cell, 16-cell and etc stages, often produces an odd number of cells (Mulnard, 1978).

One of the most crucial distinct features in mammalian development is the phenomenon of compaction. The blastomeres of an 8-celled mouse embryo are spherical and clearly distinct from each other (Pratt et al., 1982). At this stage, the cells begin the process of compaction, which results in the cells getting very tightly packed next to one another, forming a compact ball of cells (Pratt et al., 1982). This process is stabilised by the formation of tight junctions by the cells located on the outside of the ball, which essentially isolate the inner side of the sphere. In contrast, the inner cells start expressing gap junctions, which allow for easy exchange of signals and transport of small molecules (Ducibella and Anderson, 1975). During compaction, E-cadherin becomes localised to the cell-cell adhesion surfaces of blastomeres and remains evenly distributed in the inner cell mass after progression to the blastocyst (Vestweber et al., 1987).

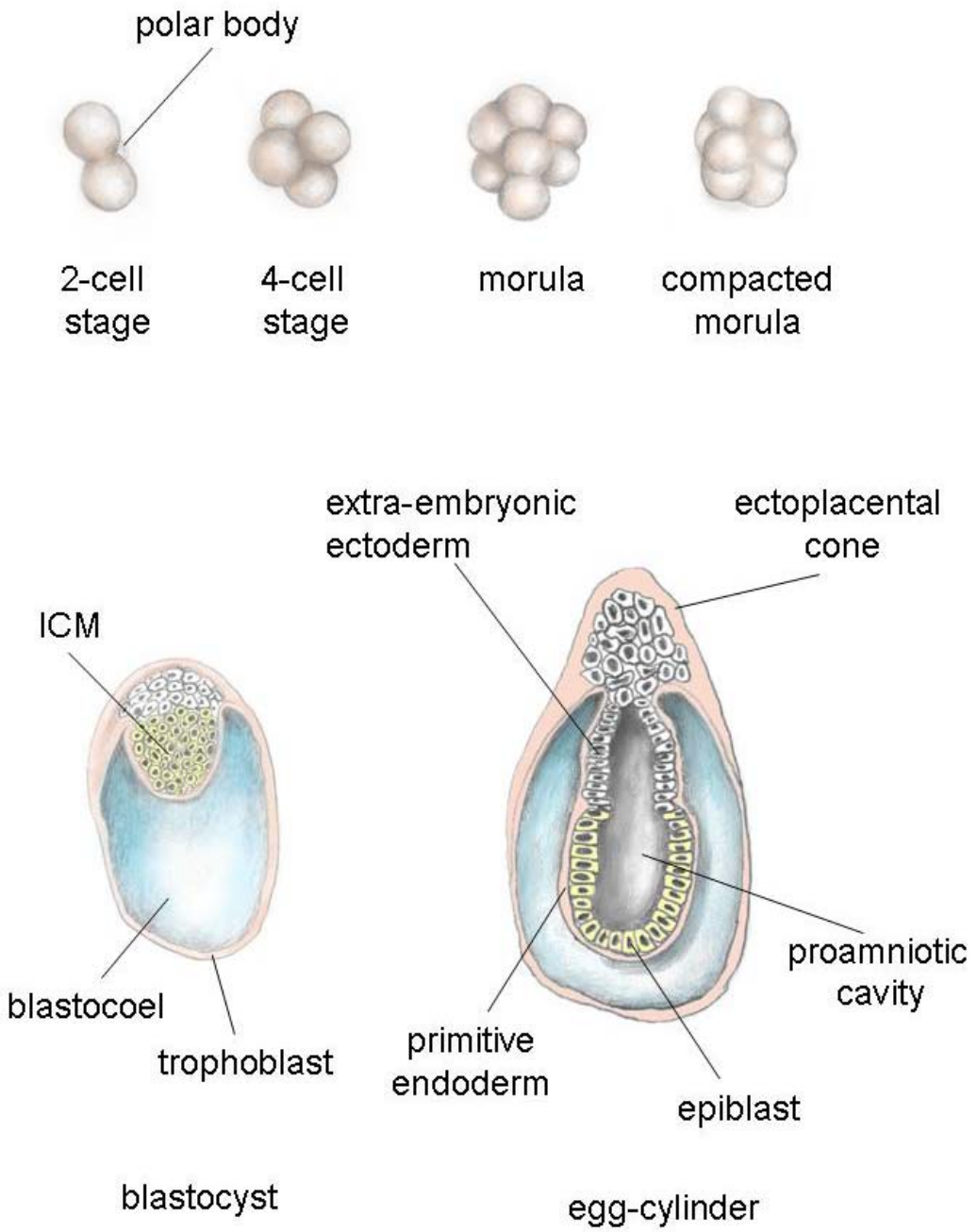

Figure 1.1 - Early development in the mouse

The cells of a compacted 8-cell embryo divide a fourth time to produce 16-cells or a morula. At that stage, the fate of the cells on the outside of the ball starts to be specified - they are going to produce the trophectoderm or the extraembryonic component (for example, the chorion and the placenta; Papaioannou, 1982). The cells on the inner side of the ball will give rise to the embryo proper, yolk sac,

allantois and amnion. From about the 32-cell stages these cells start to be called the inner cell mass and at the 64-cell stage are approximately 13 cells. This stage is considered as a landmark for the first differentiation process in embryogenesis - the differentiation of trophectoderm and inner cell mass (ICM; Rossant, 1975). Although, these become two separate cell populations, the trophectoderm is being supported by the ICM by the secretion of FGF4 (Leunda-Casi et al., 2001). Its cells start secreting fluid, which supports the formation of a blastocoel and initiate the process of cavitation of the morula (Watson et al., 1990). This leads to the formation of another developmental stage, specific of mammalian development - the blastocyst. The next important process that happens during embryonic development is the hatching of the blastocyst - it squeezes through a small hole lysed in the wall of the zona pellucida enwrapping it. At that stage, the trophectodermal cells become exposed and the embryo is ready to implant in the endometrium (uterine wall). In the mouse this process happens at around E4.5 (Theiler, 1989).

Post implantation, the three germ layers of the embryo start to be formed by extremely complex morphogenetic movements in the process of gastrulation. The primary function of gastrulation is to ensure the correct placement of precursor tissues for subsequent morphogenesis (reviewed by Tam and Behringer, 1997). After implantation into the uterus, the mouse embryo develops as a cylindrical structure and subsequently changes dramatically in size and shape during a very short period of time. Epithelisation of the ICM occurs concomitantly with the formation of the proamniotic cavity, which results in the specification of two layers - the inner epiblast and the outer visceral endoderm. At this stage, the mouse embryo is called the egg cylinder. It has a well defined embryonic and extraembryonic component and starts to specify the dorsal-ventral and proximal-distal axes. The epiblast cells, or embryonic ectoderm, are recruited to a transient embryonic structure called the primitive streak. The primitive streak also defines the antero-posterior axis as it is situated at the posterior of the developing embryo. At the primitive streak, the cells of the epiblast undergo an extremely interesting process, in which they change their identity from epithelial to mesenchymal (reviewed by Hay, 1995). This is called epithelial-to-mesenchymal transition (EMT) and at this particular instance in

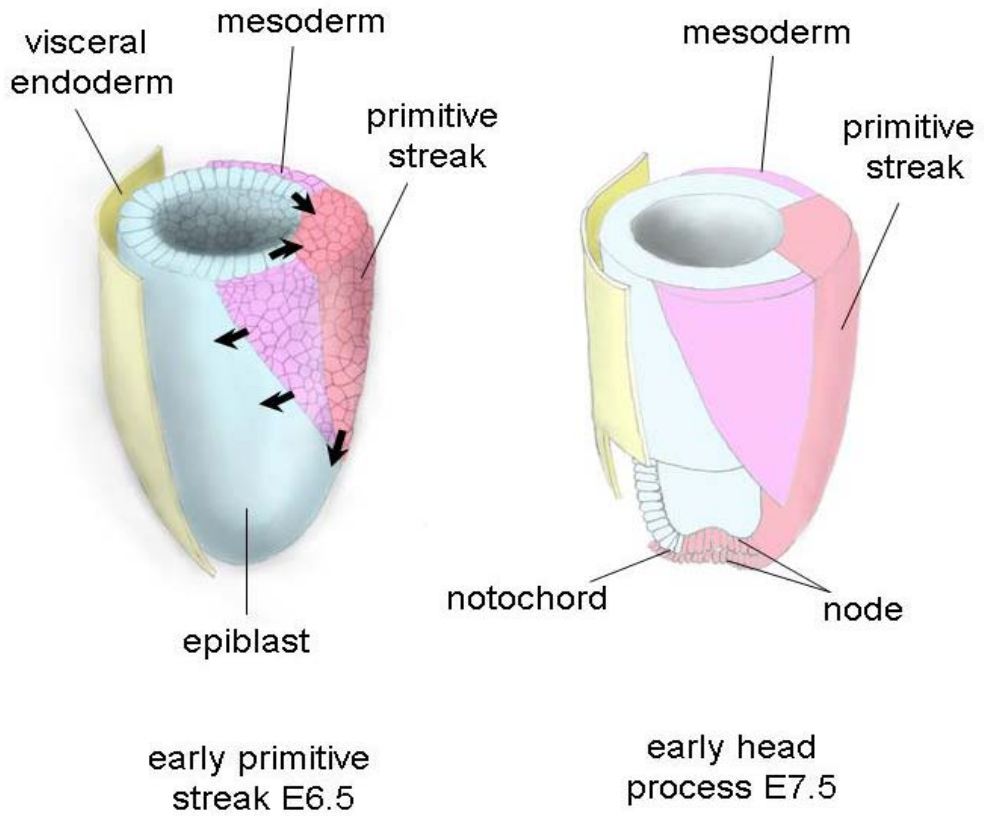

Figure 1.2 - Gastrulation in the mouse embryo
The embryo shown on the left is approximate age E6.5, while the embryo on the right - E7.5. During gastrulation, epiblast cells (shown in blue) move through the primitive streak (red) to give rise to mesoderm and definitive endoderm (not shown).

development, initiates the formation of either the definitive endoderm or mesoderm. The newly formed mesoderm appears as a new layer of cells emanating from the primitive streak, which is often referred to as the "mesodermal wings" (Tam and Behringer, 1997).

1.4.1.2 Mesoderm

Many aspects of mammalian embryonic development are tightly interlinked and work in cooperatively to allow further embryogenesis, for example, induction of neighbouring tissues, formation of signalling gradients, cell migration, spatial arrangements, cell contact and etc. Although, the importance of these could not be overestimated, I would like to focus on providing more background information

about the mesodermal lineage in particular, as mesoderm is considered to the precursor of the more specified renal lineages of cells.

Several experimental techniques have proven absolutely essential for studying cell origin, for instance, cell mapping analysis. Single epiblast cells are marked and followed in development or cells are orthotopically transplanted (Lawson et al., 1991). Such experiments have proved that there are domains in the three germ layers, which form distinct populations of cells that will form most of the major tissue types present in an adult organism (Beddington, 1982). The mechanisms of how this happens are also starting to be uncovered. Recent experiments, for example, have shown that well before primitive streak formation, epiblast cells form two counter-rotating vortices, which merge at the posterior part of the embryo (Chuai et al., 2006). The authors have also shown that FGF signalling is implicated in this process leading to primitive streak and therefore also mesoderm formation.

The mesoderm, in particular, is found between the progenitors of the ectoderm and the vegetal or extraembryonic tissues. It is formed in the process of gastrulation by ingression of the embryonic ectoderm, which migrates through the primitive streak (reviewed by Tam and Behringer, 1997). It appears that in the migratory movements, mesodermal cells use extra cellular matrix (ECM) components (like fibronectin, type IV collagen and heparan sulfate proteoglycan) as a migratory substratum during gastrulation (Smith et al., 2009). When epiblast cells undergo EMT at the primitive streak to give rise to mesodermal cells, they downregulate E-cadherin, the calcium-dependent cell-cell adhesion molecule present in epithelial cells, and start expressing the cytoskeletal protein vimentin, characteristic of primitive streak mesoderm (Burdsal et al., 1993). During the 12-24h following primitive streak formation, the streak elongates and forms a specialised structure at its anterior end, known as the node. The node is considered analogous to the organising centre of other vertebrate embryos (Zhou et al., 1993). It generates axial mesendoderm, which consists of: 1 - the mesoderm that will populate the midline of the embryo (prechordal plate and notochord); and 2 - the definitive gut endoderm. The lateral plate mesoderm and

paraxial mesoderm emerge from the intervening levels of the streak (Beddington and Robertson, 1999).

At neurula stage, the mesoderm can be divided into five regions. For example, the chordamesoderm forms the notochord, a structure present only in embryonic development, which is a source of midline signals responsible for patterning the surrounding tissues, for example, neural tube patterning and establishing left-right asymmetry (reviewed by Stemple, 2005; Kingsbury, 1920). The paraxial mesoderm, which is also known as somitic dorsal mesoderm, will form the somites, as the name suggests. The somites are distinct regions of mesodermal cells, situated symmetrically on both sides of the neural tube. They produce many of the connective tissues of the embryo, such as bone, muscle, cartilage, and dermis (Ordahl and Douarin, 1992). The lateral plate mesoderm, which as the name suggests, is the most distant from the notochord mesodermal layer, gives rise to the heart, blood vessels of the circulatory system, the lining of the body cavities and to all mesodermal components of the limbs except the muscles (Garcia-Martinez and Schoenwolf, 1993; reviewed by Noden and Francis-West, 2006). The head mesenchyme forms the connective tissues and the musculature of the face. The intermediate mesoderm, or the mesodermal layer situated between the paraxial and lateral plate mesoderm, will be discussed more extensively in the following section, as it gives rise to the urogenital system.

1.4.1.3 Intermediate mesoderm

Fate mapping experiments have been performed to identify the location of early embryo cells that are destined to form the intermediate mesoderm. Smith et al. (1994) have tracked the migration of cells after injections of a labelling reagent in different positions of the mouse primitive streak. These experiments determined that cells located at intermediate positions in the E7.5 mouse blastocyst contribute mainly to the lateral plate and intermediate mesoderm (Smith et al., 1994). Furthermore, it was reported that cells from the posterior streak also seemed to contribute to the intermediate mesoderm. The cells were observed to migrate first bilaterally from the injection site and then anteriorly.

Although little is known about the signalling molecules that specify its formation, some processes in the formation of intermediate mesoderm are starting to be understood better. The transcription factor Osr1 is one of the genes expressed earliest in the intermediate mesoderm. In mice, transcripts can be seen as early as E7.5 in the regions of presumptive nephrogenic tissue, but also in the lateral plate mesoderm (James et al., 2006). Mugford et al., (2008) have demonstrated that descendants of Osr1+ cells contribute to many intermediate mesodermal derivatives, such as the adrenal gland, gonad and metanephric kidney. Further studies have provided evidence that Osr1 expression is activated by Bmp signalling (James et al., 2005). James et al. (2005) have also proposed a mechanism for the role of Bmp signalling in trunk mesodermal pattering, where low levels of Bmp are able to inhibit repressors in the medial mesoderm, therefore activating intermediate mesodermal gene expression, but high levels of Bmp are able to repress both medial and intermediate mesoderm gene expression at the expense of lateral plate genes.

Much more information would need to be collected to understand the specification of the intermediate mesoderm. The interplay of gene expression patterns and molecule gradients becomes increasingly complex with the progress of embryo development and will probably require taking into account the global processes, which steer embryo patterning. The idea that there is global and local positional information that patterns the embryo increases in popularity (Burke, 2000; Barak, 2005). The global positional information determines timing, major developmental events and patterning, while local positional information might be responsible for the final specification of a cell type. More evidence towards this idea might prove key for a new approach to studying development.

1.4.2 Kidney development

The previous sections of this chapter present only a short overview of embryo development, mesoderm and intermediate mesoderm formation. Although a much larger body of literature would have to be summarised for a complete overview, the information presented hitherto provides the developmental sequence of events leading to the development of the kidney from intermediate mesoderm. In mammals,

nephrogenesis progresses through three stages - the pronephros, mesonephros and metanephros, which develop in a temporal and spatial sequence. The pronephros and mesonephros are temporary and degenerate, while the metanephros remains functional throughout the life of the organism. In order to understand the development of the metanephros, we would need to look at the development of the preceding two stages, first.

1.4.2.1 The nephric duct

One of the first steps towards the formation of the urogenital system starts with the formation of the nephric duct. The morphogenetic processes and changes that the intermediate mesoderm undergoes to form the nephric duct have been studied in the development of a large variety of organisms, which include teleosts, amphibians, birds and mammals (Drummond et al., 1998; O'Connor, 1938; Davies, 1950; Fraser, 1920). The nephric (pronephric) duct has received so much scientific attention, as it is a central component of the excretory system throughout development. It is a result of one of the first mesenchymal-to-epithelial transitions (MET), which occur in embryogenesis and has been mapped to the intermediate mesoderm (Bouchard et al., 2002). The duct is derived from a thickening localised in the pronephric region (Fraser, 1950). Early observations in *Amblystoma tigrinum* and *Triton taeniatus* have reported that the pronephric duct comes from "an independent outgrowth of the first nephric rudiment" (O'Connor, 1938). Furthermore, evidence has been demonstrated that the first nephric rudiment is derived in a segmental manner, where the cranial portion forms the pronephros, and the caudal portion forms the pronephric duct (O'Connor, 1938). Similar observations have been made in the cat - discrete vesicular structures along the length of the posterior part of the intermediate mesoderm were thought to fuse to form the rostral parts of the duct (Fraser, 1950). Nephric duct progenitors are thought to migrate caudally as a cord of mesenchymal cells and then transform into a tubule with a central cavity possessing a nephron-inducing ability (O'Connor, 1938; Obara-Ishihara et al., 1999). After extension, in later developmental stages, the pronephric duct is called the mesonephric or Wolffian duct. It is an essential component for later morphogenetic events, which give rise to the urogenital system (Torres et al., 1995). It induces the neighbouring intermediate

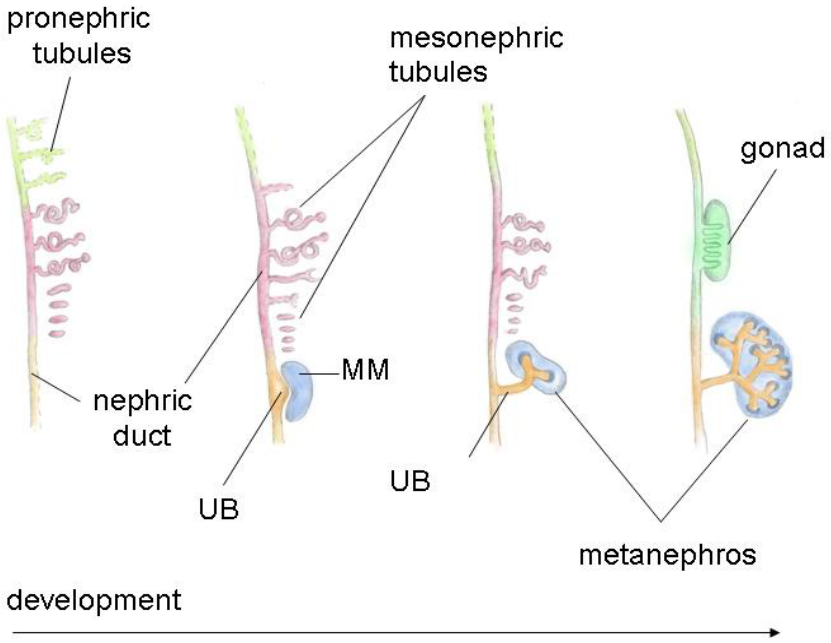

Figure 1.3 - Development of the pronephros, mesonephros and metanephros

mesoderm to give rise to the mesonephric tubules. The nephric duct functions as a drainage channel of the functional pronephros and mesonephros and is key for the development of the metanephros as it gives rise to the ureteric bud - an epithelial duct continuous with the WD, which will branch and develop into the collecting duct system of the adult kidney (Saxen, 1987).

Several genes implicated in nephric duct specification have been identified. One of them encodes for the homeobox gene *lim1*. Shawlot and Behringer (1995) have reported that a targeted disruption of the gene results in a complete loss of duct formation. Retinoic acid (RA) has been identified as another important component for duct morphogenesis - in *Xenopus,* treatment with retinoic acid leads to ectopic *lim1* expression (Taira et al., 1994), while deletion of the RA synthetic enzyme, leads to an absence of nephric duct formation (Niederreither et al., 1999). These studies have also demonstrated that the action of RA might be to mediate *lim1* expression, which in turn supports initiation of nephric duct formation. Obara-Ishihara et al. (1999) reported that BMP signalling is important for the maintenance of duct markers, although evidence for its role in initiation of the duct has not been demonstrated. Surface ectoderm and BMP4 have been shown to be essential for

nephric duct formation from the intermediate mesoderm. The importance of paraxial mesoderm for differentiation of the intermediate mesoderm has also been shown in the chick (Mauch et al., 2000). In the initial stages of development Pax2 mutants show a normal formation of the nephric duct, but subsequently it fails to extend caudally and degenerates (Torres et al., 1995).

1.4.2.2 The pronephros

The complexity and fate of the pronephros varies from species to species. Entirely developed and functional pronephroi are found in all embryonic fish and all larval amphibians and they are also essential for their survival (Howland, 1921). In fish for example, although pronephroi function transiently, they are essential for maintaining water balance. Due to their habitat, freshwater fish larvae are subject to a constant water influx, which means that huge amounts of dilute urine have to be excreted, while maintaining a very high efficiency in recovering solutes to retain osmotic balance. There is some evidence that functional pronephroi are also molecular filters efficient in recovering solutes from the filtrate and can contribute to the regulation of blood pH (reviewed by Drummond and Majumdar, 2003). There is much more variation in complexity in reptiles, where the less advanced species have more advanced pronephroi. Birds and mammals do not have well-developed pronephroi and the latter persist only during embryonic development. In mice, pronephric tubules are rudimentary and exist only for a short period of time (Sainio et al., 1997).

The pronephros develops from the intermediate mesoderm around E9.0 of mouse development (Kaufman, 2001). The pronephric ridge is first formed as a thickening of the somatic wall and as described in the previous section is closely associated with nephric duct formation. The pronephros consists of three main components - the glomus (external glomerulus), or the filtration unit of the organ; the tubules, which are responsible for resorption and excretion; and the duct, which drains the urine (Vize et al., 1995). The organ has a very simple structure, which produces filtrate similarly to metanephric glomeruli with the difference that the liquid is expelled in a coelom rather than in Bowman's space (Davies, 1950). In *Bufo viridis* tadpoles there are two cranial and two caudal pronephroi, each of which consists of an external

glomerulus and a single convoluted tubule (Møbjerg et al, 2000). The pronephric tubule opens into the coelom via three nephrostomes and consists of three proximal tubule branches, a common proximal tubule and a distal tubule (Møbjerg et al, 2000). The nephrostomes are thin epithelial ciliated tubules of the nephron, which collect the filtrate from the coelom and channel it to the proximal tubule which functions in solute resorption and waste secretion. After water is resorbed when the filtrate passes through the distal tubule, the urine is passed down the pronephric duct to the cloaca (reviewed by Vize et al., 2003).

1.4.2.3 The mesonephros

The mesonephros is the second excretory organ that appears in embryonic development. It starts to appear posteriorly to the pronephros and is also derived from the nephrogenic cord mesenchyme (Fraser, 1920). Mesonephric tubules have a more complicated structure and unlike pronephric tubules might be functional during the embryonic life of mammals (Torres et al., 1995). Even though mesonephroi degenerate in mammalian development, they form functional adult organs in amphibians and teleost fish (Zhou et al., 2010; Haugan et al., 2010). The most cranial renal vesicles of the mesonephros appear at about E9.0 in the mouse (Vetter and Gibley, 1966) and the maximal number of tubules is 18-26. It is also interesting to note that there are two types of mesonephric tubules. The 4-6 anteriormost are connected to the nephric duct and have a short distal segment that might be partially derived from it. Most mesonephric nephrons are located posteriorly and can be seen "hanging" next to the WD, but never fused to it (Sainio et al., 1997).

In mesonephros development, the nephric duct has a role in inducing nephrons in the mesonephric blastema. The cells of the mesonephric blastema condense to form renal vesicles and S-shaped bodies, which fuse with the WD and this process concludes in the maturation of a nephron with a small glomerular-like structure with primitive endothelial tufts (Lawrence, 1992; de Matino and Zamboni, 1966). Diverticulae of the mesonephric tubules of reptiles have been described, as well as forking of these in avian and mammalian embryos (Friebova-Zemanova and Goncharevska, 1982 and

the references therein). Mesonephric branching has also been described in a review by Sainio (2003).

Relatively few genes implicated in mesonephros development have been described. Not surprisingly many of them are also involved in metanephros development, as will be detailed in section 1.5. An example is the transcription factor *Pax2* (Dressler et al., 1990). Other genes important for mesonephros development include *Wt1* (Kreidberg et al., 1993), *Emx2* (Miyamoto et al., 1997), *Foxc1* (Kume et al, 2000) and *Gata3* (Labastie et al., 1995; Grote et al., 2006).

1.4.2.4 The metanephros

The metanephros is the functional kidney in adult mammals and is formed last in the triad of embryonic kidneys (Bremer, 1916 and references therein). Its function and adult structure have been described earlier in this chapter (section 1.3). The development of the metanephros starts by the reciprocal inductive interactions of two progenitor tissues - the ureteric bud (UB) and the metanephric mesenchyme (MM; Grobstein, 1953). Evidence for these inductive interations and more information about the inductive properties of various tissues has been provided by experiments, in which the MM and UB have been surgically separated and cultured separately, re-combined in culture, or cultured with heterologous tissues (Grobstein, 1953; Grobstein, 1955; Saxen, 1987). It was first determined that the UB was the natural inducer of the MM in embryonic development (Grobstein, 1953). Later, it was discovered that other heterologous tissues were also able to induce the formation of renal tubules in isolated MMs (Grobstein, 1955). Experiments showed that an impressive number and variety of embryonic tissues were able to induce tubulogenesis in E11.0 mouse metanephric mesenchymes. In addition to the UB, embryonic neural tissues (spinal cord, medulla, brain) and neural teratomas, embryonic mesenchymes (salivary, jaw, head, and bone), and submandibular embryonic epithelium were found to have inductive abilities on combination with MM (reviewed by Saxen, 1987).

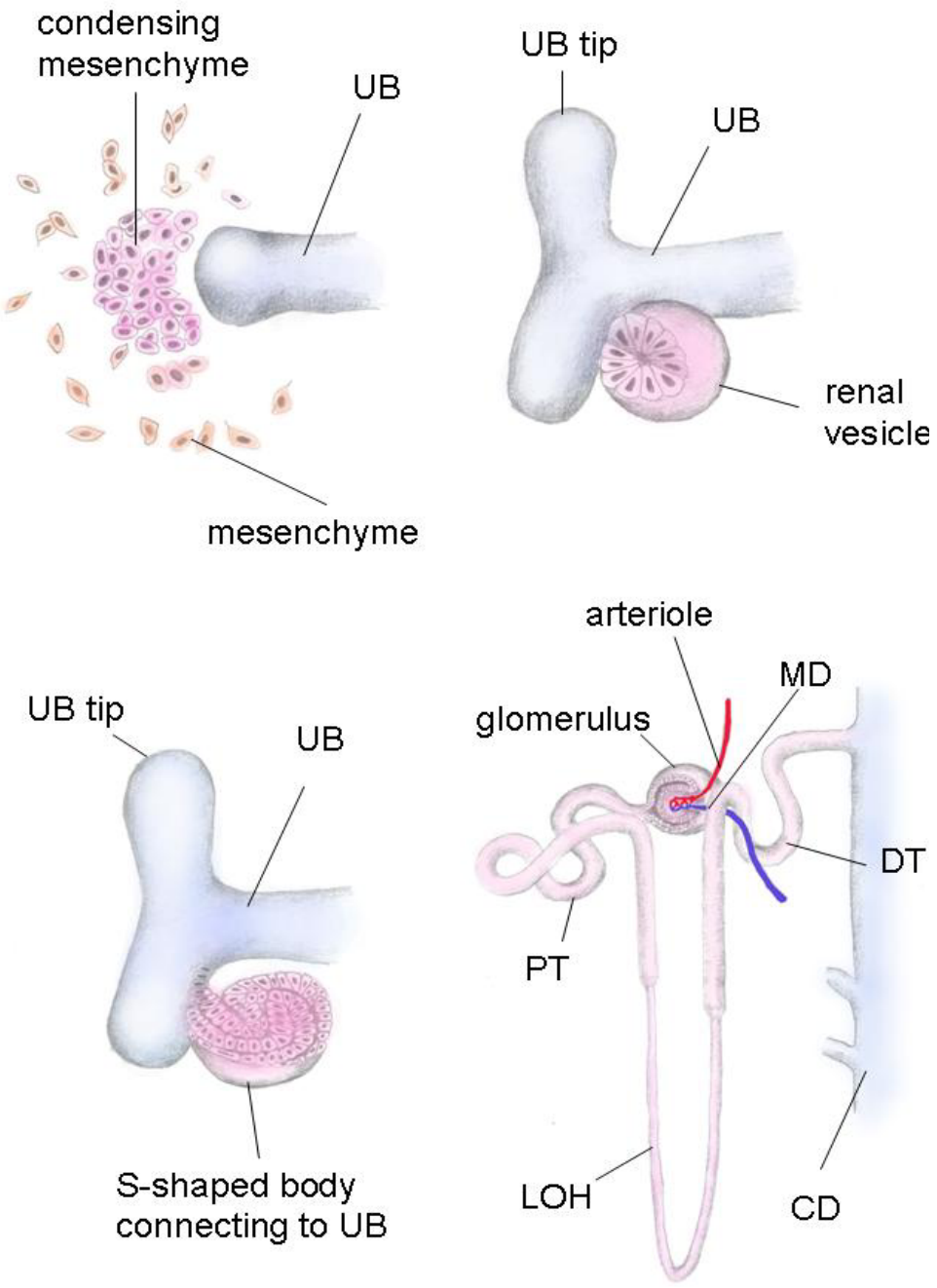

Figure 1.4 - Development of the metanephros
The schematic drawing shows invasion of the UB in the MM, induction of condensation, formation of the renal vesicle, formation of S-shaped body and fusion to the UB, and formation of a nephron with a glomerulus, PT, limbs of the loop of Henle, DT and collecting duct

In development, the MM and UB are formed in two distinct developmental processes and originate from two different descendents of the intermediate mesoderm (Fraser, 1920; Vetter and Gibley, 1966). The UB starts to form at about E10.0 in the mouse as a diverticulum of the WD. Its formation is induced by the cells of the metanephric blastema, which secrete GDNF (Sainio, 1997). Experiments have shown that the UB fails to form upon removal of the adjoining MM. In embryo development, upon evagination, the UB grows laterally towards the MM and projects into the metanephric blastema (also known as the metanephric anlage). Multiple bifurcations of he UB create a branching tree, which will become the collecting duct (CD) system of the adult kidney (reviewed by Saxen, 1987).

The MM or blastema is composed of a few thousand mesenchymal cells that will give rise to stromal cells and all renal epithelia, but the collecting duct (CD). Although this is not the favoured hypothesis, some studies have suggested that cells from the MM are also able to contribute to UB structures (Qiao et al., 1995). There has been a lot of debate about the nature of the cells of the MM and whether there is a single stem or progenitor cell able to give rise to all types of cells present in the adult kidney including neuronal and endothelial cells (Herzlinger et al., 1992). A second hypothesis proposes that the metanephric blastema might consist of a heterologous cell population that might contain progenitors of the different kidney lineages.

At E10.0 - E10.5 in the mouse, the metanephric blastema is visible as an accumulation of cells at the posterior end of the urogenital ridge, at the region of the intermediate mesoderm (Vetter and Gibley, 1966). The loose MM cells respond to the inductive signals from the UB by condensation and aggregation. The cells start to show signs of epithelisation and undergo MET to form a renal vesicle. As the ureteric bud grows and undergoes dichotomous branching, the renal vesicles remain associated with the UB at the side (Saxen, 1987; Georgas et al., 2009). The MET induces the expression of new cadherin genes and the formation of a basement membrane on the outside of the renal vesicle (Ekblom, 1980; Cho et al., 1998). Morphological shaping of the vesicles results in the formation of a structure called a

comma-shaped body (due to the formation of a cleft on one side of the vesicle), which then progresses to an S-shaped body (after the acquisition of a second cleft; Jokalainen, 1963). After the initial growth phase of cells, the first diversification can be noticed at the comma-shape stage. The proximal cells of the forming nephron elongate, their nuclei change position and cells at different positions become funnel-shaped (reviewed by Saxen, 1987). At the stage of an S-shape, the nephron is already compartmentalised with a proximal and distal part. The most distal cells establish a contact with the cells of the UB, and both of these structures undergo morphogenetic changes to form a continuous lumen between the nephron and the UB (Georgas et al., 2009). The cleft positioned away from the UB forms the glomerular epithelium, consisting of visceral epithelium (podocytes) and the parietal epithelium of Bowman's capsule (reviewed by Saxen et al., 1987). At this stage, the presumptive podocytes can already be distinguished from the rest of the cells by their reactivity to the lectins - peanut agglutinin (PNA) and soya bean agglutinin (Laitinen et al., 1987). A functional glomerulus is formed only after the invasion of endothelial cells, which form the glomerular tuft and nephron maturation continues thereafter (reviewed by Daniel and Abrahamson, 2000).

Although this process describes how a nephron is formed, it does not give an account of how more than 20,000 nephrons in the mouse kidney arise from the 12,000 cells in the metanephric mesenchyme (Karner et al., 2011). The generation of nephrons does not occur in a single burst of epithelialisation of MM cells, but rather proceeds continuously throughout embryo development. This implies that the progenitor population of cells should be replenished or that a population of cells with the ability to proliferate and differentiate to all cells of a nephron should be present in the MM. Recently these cells have been identified as Six2+ progenitors in the mesenchyme adjacent to the UB tips (cap mesenchyme; Kobayashi et al., 2008; Karner et al., 2011; Self et al., 2006). Kobayashi et al. (2008) have demonstrated that the Six2+ cap mesenchyme contains multipotent progenitor cells, which seemed to have the ability to self-renew and to give rise to all cell types within the main body of the nephron. With the progression of kidney development, Six2+ cells are no longer seen

in the inner parts of the kidney where nephrons have already formed, but only at the periphery where nephrogenesis proceeds (Kobayashi et al., 2008).

1.5 Important genes expressed during embryonic kidney development and nephron formation

Although a thorough review of all signalling molecules would need many more pages, the aim of this chapter section is to give sufficient information about some of the main genes and molecular mechanisms governing early or later developmental or morphogenetic processes for kidney development. The expression profiles and functional importance of these genes are described here with two aims; 1 – to further describe the signals driving renogenesis in embryo development; and 2 – as some of them will be referred to in future chapters, as markers of renal progenitor cells.

As it is relevant to one of the first processes defining metanephric development, I would like to go back to the mechanism by which the UB evaginates from the WD and invades the neighbouring MM. As shortly previously mentioned, this process is mediated by c-Ret-GDNF signalling (Vega et al., 1996; Sainio et al., 1997). c-Ret is a receptor tyrosine kinase localised on the membrane of WD cells. It is a receptor for glial cell line-derived neurotrophic factor or GDNF, which is secreted by the MM. GDNF is already expressed at low levels by the uninduced MM, but is highly upregulated in the cap mesechyme (Hellmich et al., 1996; Sainio et al., 1997). GDNF has been implicated in ureteric bud evagination and branching. On WD cells, GDNF binds to and activates a receptor complex, consisting of namely the Ret receptor tyrosine kinase and the GDNF family receptor α1 or GFRα1 (Sainio et al., 1997). Sainio at al. (1997) have shown that beads soaked in GDNF are able to induce the formation of supernumerary diverticula from the WD, which project towards the source of the chemical. A recent study by Kuure et al. (2005) has demonstrated that another major pathway, the Jagged1/Notch, is also implicated in the initiation of UB sprouting. They report a co-expression of molecules from both pathways starting immediately after the specification of intermediate mesoderm. Jagged1 (a ligand for Notch) colocalises with both GDNF receptors on the WD and *Gdnf* expression in the cap mesenchyme. GDNF seems to upregulate *Jagged1* through Ret/GFRα1

signalling. The Ret/GFRα1/Gdnf system might coordinate UB growth acting together with other secreted factors, for example, pleiotrophin (Ptn) and bone morphogenetic protein 4 (Bmp4). *Pleiotrophin* expression has been detected in the MM and can stimulate the branching of explanted UBs *in vitro*, together with Gdnf, indicating that these two factors are sufficient for branching (Sakurai et al., 2001). Bmp4 has also been found important for UB branching by an indirect mechanism related to MM differentiation (Raatikainen-Ahokas et al., 2000). Bmp4 is expressed by the mesenchymal cells, which surround the WD and UB stalks, and might be involved in supporting their growth. *Bmp4* heterozygous mutants form cystic kidneys (Dunn et al., 1997). It seems like there are some differences between observations in organ culture and *in vivo* studies, where in the latter situation gene regulation of UB growth and branching might be considerably more complex (reviewed by Vainio and Lin, 2002).

Another whole group of proteins important for kidney development (and more particularly for the formation of nephrons from MM) are adhesion molecules. Condensation of the MM is associated with an increase in intercellular adhesion (reviewed by Ekblom, 1989). Proteins, which were reported to be involved in the epithelialisation of the MM are the extracellular matrix components collagen I and III, fibronectin and tenascin, as well as the adhesion proteins laminin, E-cadherin (uvomorulin), N-CAM, as well as P- and N-cadherin. During MET, N-CAMs, interstitial collagens and fibronectin (common for mesenchymal cells), gradually disappear to be replaced by molecules characteristic of epithelial cells, such as laminin and E-cadherin (reviewed by Ekblom et al., 1989). Also, it should be mentioned that some of the signals driving MET have already been identified. Experiments in the rat confirmed that the UB secreted factors that drive the epithelialisation of the MM and also identified that one of these factors was the IL-6 type glycosylated cytokine LIF (leukemia inhibitory factor, Barasch et al., 1999). LIF activated STAT3 in rat MMs and induced a program of epithelial gene expression in precursors maintained or expanded by FGF2. The epithelialisation of the MM could also be induced by other IL-6 type cytokines (cardiotrophin, ciliary neurotrophic factor and oncostatin M). LIF was further found to cooperate with TGFb2 (in

addition to FGF2) to enhance and accelerate renal tubule formation in rat metanephric explants through a Wnt-dependent mechanism (Plisov et al, 2001).

I would like to give a little more attention to another gene that has proven absolutely essential for early kidney development and will be frequently referred to in later chapters of this work - *Pax2*. *Pax2* is frequently described together with another gene, *Pax8*, as it is another closely related member of the Pax-family sequence-specific transcriptional regulators (reviewed by Chi and Epstein, 2002). The reason for this is that Pax2 and Pax8 are thought to have redundant functions at E9.5 of mouse embryonic development (reviewed by Dressler, 2011). *Pax2* is expressed primarily in embryogenesis and - more specifically - during excretory system and central nervous system development. In the nervous system, it localises to the hindbrain, spinal cord, the otic vesicle and the optic cup (Dressler et al., 1990). In kidney development, *Pax2* expression has been reported both in the ductal and mesenchymal components (Torres et al., 1995). Dressler et al. (1990) have reported that in mesoderm-derived tissues in the mouse, *Pax2* starts to be expressed in the pronephric tubules and the nephric duct at about E9.0 whereas no expression is detected in the renogenic intermediate mesoderm prior to pronephros formation. In contrast, another study suggests that *Pax2* expression starts earlier, being already detectable in the intermediate mesoderm at E8.5, before the nephric duct has been formed (Torres et al., 1995). Nevertheless, both studies agree that gene transcripts have been seen in the mesonephros, as well as the metanephros. *Pax2* expression is characteristic of the UB, renal vesicles after they have started to condense from mesodermal cells and acquire epithelial properties, and the subsequent epithelial components of the nephron (Dressler et al., 1990; Narlis et al., 2007). On the other hand, the similar *Pax8* starts to be expressed at the renal vesicle stage and continues to be maintained, together with *Pax2,* until the end of nephron differentiation (Narlis et al., 2007). It is interesting to note that *Pax2* expression declines with the maturation of renal tubules. At embryonic day 17, *Pax2* expression is discontinued in the glomerular crevices, but still seen in the perimeter of the growing kidney, and can no longer be detected in adult kidneys (Dressler et al., 1990).

The expression of *Pax2* is essential for formation of pronephric, mesonephric and metanephric tubules. It has been reported that *Pax2* is not only expressed, but also required for multiple steps in metanephros development (Torres et al., 1995; Bouchard et al., 2002). *Pax2* homozygous mutants fail to form metanephroi (Torres et al, 1995). Although the nephric duct forms normally at E9.0-E10.0, it fails to extend caudally and no initiation of UB formation takes place. The MM of these animals does not undergo mesenchymal-to-epithelial transformation, which results in renal agenesis. It has also been demonstrated that Pax2 is necessary for the expression of Gdnf (Brophy et al., 2001).

In kidney development, Pax2 and Pax8 participate in interconnected and extremely complex genetic networks, which still remain to be clarified. Mouse embryos lacking both *Pax2* and *Pax8* are not able to form pronephroi or later kidney structures due to an arrest of the MET that normally happens in the intermediate mesoderm to produce the nephric duct (Bouchard et al., 2002). Failure to initiate *Lim1* and *c-Ret* expression occurs, accompanied by apoptotic loss of the nephrogenic intermediate mesoderm, one day after failed pronephric induction. At the same time, forced expression of *Pax2* by retroviral vectors leads to the production of ectopic nephric structures in the intermediate mesoderm and genital ridge of chick embryos (Bouchard et al., 2002). Recent studies have indentified signals both upstream and downstream of Pax2. The c-Jun N-terminal kinase (JNK) was found to activate Pax2 by phosphorylation. There is some evidence that Pax2 causes changes in methylation to establish renal epithelial fate (reviewed by Dressler, 2011)

Data showing that double *Pax2/8* mutants have a much more severe phenotypic effect than single mutants, suggests that there is a functional redundancy between those two genes (Bouchard et al., 2002). Heterozygous *Pax2/8* mutants show a significantly reduced nephron number in correlation with a decrease in expression of the key developmental regulator *Lim1*, as well as an increase in the apoptotic index of nephron progenitor cells. Downregulation of *Pax2/8* in mature nephrons results in differentiation defects of the distal convoluted tubules and UBs display branching defects associated with a downregulation of *Wnt11* gene expression (Narlis et al.,

2007). Narlis et al., 2007 have suggested a model, in which *Fgf8* and *Pax* genes act in consort to activate *Lim1* in renal vesicles, thereby allowing the differentiation of nephrons to proceed. Pax2 might also act by activating signalling via *Wnt4* in the cells of the MM (Torban et al., 2006). These findings suggest that in kidney development *Pax* genes are important regulators for differentiation and branching morphogenesis.

Another gene important for kidney development is the tumour-suppressor Wt1 (Wilms' tumour). It encodes a zinc-finger transcription factor, which has at least 24 different isoforms resulting from combinations of alternative splicing, alternative start codons and RNA editing (Hohenstein and Hastie, 2006). *Wt1* is expressed at low levels in the metanephric blastema at E10.5, but its expression increases in aggregates, comma-shaped bodies, and persists at high levels in podocyte precursors and epithelia of the Bowman's capsule (Self et al., 2006; Pritchard-Jones et al., 1990). Wilms' tumour is an embryonic kidney neoplasia, which is characterised by undifferentiated mesenchymal cells and disorganisation of the renal epithelia and surrounding stromal cells (reviewed by Davies et al., 1999). Wilms' tumours have provided a lot of insight into kidney development as the genes responsible for it are thought to control early kidney development. Studies have suggested that *Wt1* is absolutely required for renogenesis (Kreidberg et al., 1993). Homozygous mutants had a complete absence of a UB and although a metanephric blastema was present it underwent apoptosis leading to a renal agenesis. Since MM apoptosis could not be rescued *in vitro*, the authors concluded that Wt1 is important for MM survival and early differentiation.

The function of Wt1 is extremely complex and information in the literature is contradictory. The *Wt1* promoter has been described as a target of Pax2 (Dehbi et al., 1996; McConnell et al., 1997), while on the other hand Wt1 appears to be a regulator of *Pax2* (Hartwig et al., 2010) and repressor of *Pax2* and *Wt1* (Rupprecht et al., 1994; Ryan et al., 1995). A recent large-scale study identified 1663 genes bound by Wt1, which is only an example of the complexity and significance of this gene (Hartwig et al., 2010).

At the start of metanephric kidney development, the metanephric blastema acts as an accumulation of kidney progenitor cells that will proliferate and differentiate to form all structures essential for the formation of a functional kidney. In this respect, the MM could be regarded as a site where multipotent renal progenitors or stem cells are contained. Many groups are currently working on isolating putative stem cells from embryonic kidney rudiments (Herzlinger et al., 1992; Maeshima et al., 2003; Oliver et al., 2002; Lusis et al., 2010). Evidence is accumulating that the transcription factor Six2 might be central for multipotent kidney cells (Self et al., 2006; Kobayashi et al., 2008; Lusis et al., 2010). *Six2* is a homeobox gene, which is expressed throughout the development of the excretory system, including in the nephrogenic cords and metanephroi. At around E10.0 of mouse embryonic development, expression can be detected in the metanephric blastema before UB invasion (Oliver et al., 1995). At E10.5, *Six2* expression localises to the mesenchyme surrounding the UB tips and at E11.5 it is found in the cap mesenchyme - the induced MM surrounding UB tips. It has been described that *Six2* is expressed at different levels in different compartments - high levels were observed on the dorsal side of the UB and lower levels were found on the ventral side, near the ureteric stalk, where renal vesicles are formed. *Six2* expression is shut down in epithelialised nephrons, but remains expressed in the nephrogenic zone (at the periphery of the kidney) while the kidney develops (Self et al., 2006). Self et al. (2006) have also demonstrated that in *Six2*-null mice, ectopic renal vesicles form on the cortical side of the ureteric bud, rather than on the medullary as expected in a normally developing metanephros. The authors have shown that there is a depleted progenitor pool, which is progressively lost leading to a termination of nephrogenesis after induction of only a few nephrons. It has been proposed that *Six2* might at least in part act by blocking the action of *Wnt9b* thus permitting self-renewal of uncommitted nephron progenitors (Kobayashi et al., 2008). It has also been suggested that *Six2* might act by activating *Gdnf* expression and that it is able to auto-activate its own promoter (Brodbeck et al., 2004).

Wnts are a large family of secreted proteins that regulate key steps in kidney development and in embryogenesis, in general. When separated from the UB, MMs

usually die in cultures. In series of experiments, it has been determined that heterologous tissues, such as spinal cord, were able to rescue isolated MMs from cell death and induce nephron formation. Wnt1, for example, has been identified as the factor, which has the effect of spinal cord to induce nephron formation in isolated MMs (Herzlinger et al., 1994). Interestingly, it is not normally expressed in kidney development indicating that it must have a redundant function with another Wnt protein (also Kispert et al., 1998). Wnt4, for example, is expressed in the condensates of the induced MM. In double *Wnt4* mutants, the ability of the MM to condense upon induction is retained, but MET fails and no tubules are formed (Stark et al., 1994). In experiments with Wnt4-producing cells and spinal cord, it has been found that these signals are sufficient to initiate *ex vivo* tubule formation, which pinpoints Wnt4 as an important tubule-inducing factor (Kispert et al., 1998). These studies of the role of Wnts in nephron induction have also provided insight about the ability of spinal cord to induce nephrons in explanted MMs. Other Wnts are also important for kidney development. Two examples are Wnt9b and Wnt11. Wnt9b is required for differentiation of the condensed mesenchyme via FGF8 and Fgflr1. Wnt11 seems to promote GDNF expression and therefore survival and branching of the UB (reviewed by Hendry et al., 2011).

Although many more genes are involved in and important for different aspect of early or late kidney development, it would not be possible to cover all of them in the current work. The information in the text about genes important for kidney development and some additions are been given in Table 1.1.

1. 6 Embryonic stem cells

1.6.1 The biology of embryonic stem cells

One of the two major foci of this thesis is embryonic stem cell differentiation to renal cells with two aims – to obtain a model system for studying renal lineage specification, and to obtain ESC-derived kidney cells for testing the usefulness of cell replacement therapies in treating kidney disease or testing the efficacy of drugs. To be able to discuss these concepts in subsequent chapters successfully, several aspects of embryonic stem cells have to be introduced. First, a general overview of

Table 1.1 - A summary of some mutant genes, which show a kidney phenotype
The expression profile is not given in detail. UB-ureteric bud; MM-metanephric mesenchyme; S- s-shaped body
Modified from Vainio and Lin, 2002 and Carroll and McMahon, 2003

Gene name (Genotype)	Tissue expressed in	Phenotype	References
Transcription factors			
Emx1	UB, MM	Kidneys, UB, genital tract completely missing	Miyamoto et al., 1997
Eya1	MM	Absence of UB growth and failure of MM induction	Xu et al., 1999
Foxc1	MM	Two kidneys and double Ubs	Kume et al., 2000
Foxd1	S	Mutant kidneys are small, few nephrons fused longitudinally	Hatini et al., 1996
Pax2	UB, MM	Deficient UB outgrowth, MM not induced	Brophy et al., 2001
Rara, Rarb	UB, S, MM	Hypoplasia, agenesis	Mendelsohn et al., 1999
Sall1	MM	Failure of UB outgrowth	Nishinakamura et al., 2001
Wt1	MM	MM undergoes unrescuable apoptosis	Kreidberg et al., 1993
Six2	MM	Premature and ectopic differentiation of MM cells, depletion of the progenitor pool	Self et al., 2006
Pod1	MM	abnormalities in epithelial branching and morphogenesis, podocyte defects	Quaggin et al., 1999
Growth factors			
Bmp4 (het)	MM	Hypoplasia, dysplasia, hydroureters, ectopic uterovesical junction, double collecting duct	Miyazaki et al., 2000
Bmp7	UB, MM	Severe hypoplasia, few nephrons and collecting ducts	Dudley et al., 1995; Dudley and Robertson, 1997
Fgf7	S	Small kidneys, less UB branches and nephros	Qiao et al., 1999
Gdnf	MM	No kidney as UB evagination fails	Moore et al., 1996; Sanchez et al., 1996; Pichel et al., 1996
Wnt4	MM	Failure of kidney tubule formation	Stark et al., 1994
Growth factors/receptors			
Gfra1	UB, MM	Agenesis of the kidney as in *Ret* and *Gdnf*	Enomoto et al., 1998
Notch2	MM**	Glomerular defects	McCright et al., 2001
Ret	UB	Failure of UB outgrowth	Schuchardt et al., 1994
Nephrin	podocytes	Foot process effacement, proteinuria, early postnatal death	Putaala et al., 2001

PdgfB	mesangial cells	absence of glomerular tufts and mesangial cells	Leveen et al., 1994
Integrin α8	MM	reduced UB growth and branching, defective epithelialisation of MM cells	Muller et al., 1997
Integrin α3β1	UB, glom	decreased branching, proximal tubular epithelia contain excess lysosomes or become microcystic, podocytes do not form mature foot processes	Kreidberg et al., 1996
Proteoglycans and their biosynthetic enzymes			
Hs2st	UB, MM	Renal agenesis due to lack of UB branching and mesenchymal condensation	Bullock et al., 1998
Gpc3	UB, MM	Selective degeneration of medullary collecting duct	Cano-Gauci et al., 1999
Others			
Laminin α5	UB, MM	absence of normal GBM, disarrayed glomerular epithelial cells, absence of vascularised glomeruli	Miner and Li, 2000
Pkd1	UB, MM	enlarged cystic kidneys	Lu et al., 1997
Pkd2	UB, MM	cyst formation	Wu et al., 2000

the history, biology and use of embryonic stem cells is provided together with the key players in regulating pluripotency. Then, ES cell differentiation is discussed with a focus on literature reports for the derivation of renal cells from ES cells. Other types of stem cells are mentioned briefly to illustrate their limited differentiation potential in comparison to ESC or other pluripotent cells.

1.6.1.1 Characteristics of embryonic stem cells

Embryonic stem cells are pluripotent cells derived from the inner cell mass of a blastocyst-stage embryo (Evans and Kaufman, 1981; Martin, 1981). These cells have attracted the interest of the scientific community with their abilities to self-renew indefinitely and to differentiate into all derivatives of the three germ layers - the endoderm, mesoderm and ectoderm (Evans and Kaufman, 1981). The true pluripotent stem cell has to fulfil a number of requirements to be considered pluripotent (reviewed by Smith, 2001). These have been summarised in Figure 1.5. The characteristics of ESCs are very different from these of adult stem cells or other stem cells found in extraembryonic tissues. This will be discussed in a later section.

1.6.1.2 The discovery of embryonic stem cells

The first publications, reporting successful attempts to isolate and maintain in culture murine ESCs have been published in two independent studies by Martin Evans and Matthew Kaufman (Department of Genetics, University of Cambridge) and Gail Martin (Department of Anatomy, University of California, San Francisco) in 1981 (Evans and Kaufman, 1981; Martin, 1981). Also, Martin was the first person to use the term "embryonic stem cell". Evans and Kaufman used the term "EK" cells to distinguish the blastocyst-isolated pluripotential cells from EC cells or embryonal carcinoma cells. The potential of ESCs to form embryoid bodies (EBs), to differentiate into a multitude of cells and to form teratomas when injected in mice, has been reported together with their discovery (Evans and Kaufman, 1981).

It is important to note that pluripotency and the ability to form chimeric animals is not a property exclusive to ESCs. Cells derived from teratocarcinomas of germ cell or embryonic cell origin also have shown such properties. These cells, known as embryonal carcinoma (EC) cells or teratocarcinoma stem cells, have demonstrated an ability to differentiate to the three germ layers (McBurney, 1976) and to form chimeric animals (Brinster, 1974; Papaioannou et al., 1975, 1978).

Scientists spent a lot of years trying to isolate the human equivalent of mouse ES cells. Finally, the breakthrough happened when researchers led by James Thomson (University of Wisconsin-Madison) were able to prove a technique for the isolation and maintenance of human ESCs in culture (Thomson et al., 1998). This was an important event in stem cell biology, as it introduced the possibility of using hESC for differentiation and subsequent application in the treatment of disease by cell replacement therapies or other more indirect medical applications. Such a use of hESCs harboured many challenges, both scientific and ethical. The ethical debate about hESC is based on the fact that they are derived from the blastocyst stage of an embryo, which involves its destruction. To solve this, scientists have been looking for other sources of pluripotent cells. This led to the cornerstone discovery of 4 key factors, which were able to induce pluripotency in somatic cells (Takahashi and Yamanaka, 2006). This has rekindled many efforts for future developments in the

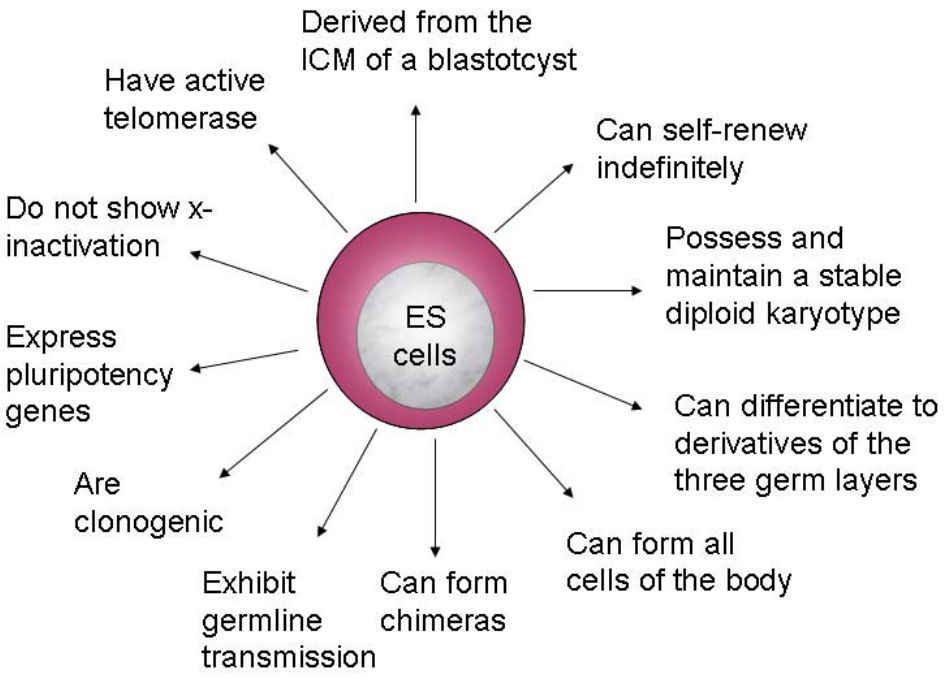

Figure 1.5 - The characteristics of a true embryonic stem cell
After Smith, 2001

field of regenerative medicine.

Takahashi and Yamanaka (2006) showed that the genes Oct4, Klf4, c-Myc and Sox2 can induce pluripotency when introduced into a terminally differentiated cell. The resulting cells are thus called induced pluripotent stem cells or iPS cells. Although direct therapeutic results by means of cell transplantation of iPSC-derived cells are not yet possible for safety concerns, iPS cells have proved of a great significance for the creation of models of human disease and provided us with an invaluable tool to study the molecular mechanisms of some pathologies and to test for potential therapeutic targets, *in vitro* and on human tissue. This means that once methods for the differentiation of ESCs have been established, they could also be transferred to the differentiation of iPS cells to renal cells.

1.6.1.3 How is pluripotency maintained?

The two properties of ES cells, which make them extremely interesting, are their abilities to differentiate to all germ layers and to self-renew indefinitely. At the dawn of embryonic stem cell research, there was no scientific evidence of what governed

pluripotency and managed to maintain these cells undifferentiated in *in vitro* culture. ES cells were first cultured on STO feeders and in conditioned medium obtained from teratocarcinoma cell lines (Martin, 1981). The unknown factor, which could be obtained from STO mouse fibroblasts or from buffalo rat liver cells, was shown to maintain embryonal carcinoma cells and embryonic stem cells in an undifferentiated state (Smith and Hooper, 1987; Koopman and Cotton; 1984). Thus, it was referred to as DIA, or differentiation inhibitory activity (Williams et al., 1988). Williams et al. (1988) noticed a structural similarity between partially purified DIA and myeloid leukaemia inhibitory factor (LIF). They managed to prove that supplementing cultures of mouse ESCs with LIF was able to maintain them in pluripotent state, as shown by chimera formation. Nowadays, it is possible to culture mESCs without feeders in LIF-containing medium (Smith et al., 1988; Williams et al., 1988). Furthermore, the pathways governing pluripotency start to be understood much better than before, which has led to the development of a chemically defined medium based on inhibitors, which is not only able to maintain the undifferentiated state of mESCs, but proves to be better than conventional methods (Silva et al., 2008). In mouse ES cell culture, LIF and serum (BMP) block differentiation by activation of STAT3 and inhibition of differentiation proteins. However, these pharmacological inhibitors (CHIR99021, PD184352 and SU5402) were sufficient for maintenance of pluripotency in mESCs (Ying et al., 2008). They act upstream of LIF/Stat3 by blocking phospho-Erk-mediated signalling from the FGF receptor and inhibition of GSK3 to enhance ES cell proliferation and survival (Ying et al., 2008). These studies have also led to the theory that ESCs do not require external signals to remain pluripotent and will do so as long as differentiation signals are absent, which was named the “ground state of pluripotency”.

Further aspects of the major regulatory pathways implicated in the maintenance of pluripotency have also been described. It has been reported that Stat3 activation by gp130 (glycoprotein 130, which interacts with the LIF receptor) is essential for maintenance of pluripotency (Niwa et al., 1998). It is also dependent on the intrinsic activity of the octamer-binding transcription factor Pou5f1 (Oct3/4). Chambers et al. (2003) have also further indentified that Stat3/Oct4 can be bypassed by the

overexpression of the transcription factor Nanog to sustain pluripotency. At the same time, Oct4 and Sox2 (which belongs to the SRY-related HMG-box family transcription factors) have been shown to act in consort to regulate pluripotency and to participate in a complex regulatory network, where they cross-activate and auto-activate their own promoters (Chew et al., 2005). The Oct4-Sox2 complex has been proven to bind to the Nanog promoter, as well (Rodda et al., 2005). Interestingly, it seems like Nanog is dispensible for inducing pluripotency, or lies downstream of Oct4 and Sox2, as it is not among the 4 genes, which were used for the generation of iPSCs (Takahashi and Yamanaka, 2006).

Although all these genes are important for the maintenance of pluripotency and are therefore considered as ES cell markers, it is important to note that they are not expressed only in the ICM in the short span of time when embryonic stem cells are isolated. Oct4 expression is also maintained in the epiblast and persists in primordial germ cells throughout development. Similarly to Oct4, Sox2 is first expressed in the blastomeres of the 4-cell stage embryo and persists in the ICM and then epiblast (Avilion et al., 2003; Chew et al., 2005). Nanog transcript first appears in the ICM of the morula prior to blastocyst formation (Mitsui et al., 2003; Chambers et al., 2003). It seems like Nanog is switched off after implantation, but then reappears in the proximal epiblast at about E6.0 (Avilion et al., 2003).

1.6.1.4 Other types of stem cells

To illustrate the difference between pluripotent stem cells (ESCs and iPSCs) and other types of stem cells, a short overview of the latter is also given. Another class of stem cells are the adult or tissue-specific stem cells. They are found in already formed organs in the adult organism and are believed to function in the body as its natural mechanism to constantly repair itself. Interest in these cells grows and together with research and the number of reports, the notion that almost every organ contains stem cells is also becoming increasingly popular. Similarly to a pluripotent stem cell, a single (clonal) adult stem cell can both self-renew and differentiate to multiple lineages usually associated to the organ it came from (reviewed by

Weissman, 2000; Gage, 2000). Though unlike pluripotent stem cells, adult stem cells cannot make all cells of the body, but only a very limited number of cells types.

The discovery of stem cells, which are able to replenish tissues, dates back to the 1960s when experiments with radiational ablation of bone marrow cells in mice were performed (McCulloch and Till, 1960; Till and McCulloch; 1961; Siminovitch et al., 1963; Becker et al., 1963; Till et al., 1964). Till et al. (1964) were the first to describe some of the basic processes related to haematopoietic stem cells (HSCs). Since then, stem cells in various organs have been reported. Some of the more prominent studies include - intestinal, skin, neural, uterine, mesenchymal and haematopoietic cells (reviewed by Gage, 2000; Weissman, 2000; Barker et al., 2010). Scientists still disagree about the true stemness of some proposed types of adult stem cells, for example, putative kidney stem cells.

The classes of stem cells are not even limited to embryonic and adult stem cells. It has been found that stem cells are present in extraembryonic tissues and compartments. For example, umbilical cord blood stem cells are found in the placenta after a baby is born (reviewed by Dovat and Feig, 1997). Although, they are isolated from extraembryonic tissue, and indeed from a very unique source, they have been characterised as hematopoietic stem cells and other abilities that they have been suggested to possess remain disputable. Amniotic fluid stem cells have also been discovered and their properties are also of a large scientific interest (Prusa et al., 2003; Prusa et al., 2004; Tsai et al., 2005).

In summary, over time, there have been multiple discoveries that many types of explanted cells have the ability to replenish themselves, which has increased the hopes that potential cell-based therapies for regeneration of diseased tissue might be possible. The fact that the differentiation abilities of adult cells are limited has made ESCs a very attractive source for obtaining virtually unlimited numbers of the necessary tissue-specific differentiated cells. The discovery of iPS cells has also initiated numerous discussions about their regenerative potential. On one hand, their ESC-like pluripotency (and therefore wide differentiation potential)

makes them a highly attractive source of differentiated/progenitor cells. iPS cells have even demonstrated at least two advantages over ES cells - their derivation is not ethically controversial; and they are donor - specific, which makes them a potential advanced autologous therapeutic product that does not require immunosuppression. Still, the properties of induced pluripotency have not been fully characterised, so a direct substitution of ESCs with iPSs is not yet possible and proof-of-principle studies should be first performed with ES cells.

1.6.2 Embryonic stem cell differentiation to a renal lineage – a literature review

Unlike many other types of cells that have been produced *in vitro* from ES cells, the generation of kidney cells remains relatively refractory to directed differentiation. Spontaneous ES cell differentiation or the use of strictly defined protocols has efficiently generated other mature cells, for example, beating cardiomyocytes or mature neurons (van Laake et al, 2007 and Brüstle et al., 1997). Unlike these cells, which are recognisable by a beating activity or a very particular morphology (in a combination with molecular, histochemical and functional methods), renal cells are difficult to detect. Another level of complexity to recognising kidney cells is the lack of a single renal marker for committed progenitor cells. All these setbacks have made it very difficult to study the derivation of renal progenitors from ES cells and later - iPS cells. A few groups have used various differentiation methods or transplantation to look for mES cell-derived renal cells (Kim and Dressler, 2005; Steenhard et al, 2005; Kramer et al., 2006; Vigneau et al., 2007; Bruce et al, 2007; Morizane et al., 2009; Ross et al., 2009; Ren et al., 2010). An overview of these studies is given in Table 1.2.

Due to the difficulty of finding a single early kidney cell marker, these studies have frequently used a combination of genes to look at the mRNA profile of differentiated embryoid bodies on the basis of reverse transcription PCR. The limitation of this method is that it detects gene expression in a pool of cells rather than single cells and is therefore not indicative of the co-expression patterns of a combination of genes in individual cells. Furthermore, in the process of ESC differentiation in general,

pluripotency markers like Oct4, Nanog, AP, telomerase are progressively downregulated, while all genes specific for more differentiated states and specified populations of cells increase by default. When analysing the influence of chemicals on the differentiation potential of ES cells, usually a control (untreated) and an experimental (treated) groups are present (an untreated group has not always been provided). Noting a downregulation of pluripotency genes and upregulation of the gene of interest in the experimental sample, though, might have two interpretations. Indeed, more cells might have differentiated to the cell type of interest, but also - more cells might have differentiated in general. The latter possibility might mean that the provision of specific molecules might be responsible for speeding up the process of differentiation, rather than forcing cells down a certain lineage. Secondly, when looking for kidney cells, which cannot be traced by a single marker molecule, but require detection by a combination of genes, upregulation of two genes of interest in the sampled pool of cells does not directly mean that one population of cells co-expressing the genes exists; there might be two other distinct populations of cells which have upregulated either gene A or gene B. Only a few of these studies have tried to address the presence of non-kidney cells in the differentiated EBs by screening for a limited number of non-kidney related genes (Bruce et al., 2007; Vigneau et al., 2007; Mae et al., 2010). Furthermore, although scientists have revealed a lot of information about gene expression patterns in living organisms and their development, it is important to note that these patterns can be altered by *in vitro* manipulations. This might be especially relevant for ES cell differentiation, as during *ex vivo* procedures, these ICM-like cells do not receive the correct signals present in development. There have been no reports to disprove the possibility for cells being arrested at a partially programmed stage in their differentiation or expressing a combination of genes, which would not normally be seen in development, therefore, virtually creating a cell existing only *in vitro,* or possibly in malignancies, might not be impossible.

In addition to conventional differentiation by supplementation with small molecules and growth factors, transgenic lines have also been created to test for the *in vitro* nephrogenic potential of ES cells. Kobayashi et al. (2005) have genetically

engineered mESCs to express *Wnt4* before differentiating them via the EB method. They reported that the water transport transmembrane protein Aquaporin2 was upregulated when the transfected cells were treated with a combination of HGF and Activin A (Aquaporin2 is a water channel regulated by anti-diuretic hormone and is critical for water absorption in the kidney; Takata et al., 2008). Although, tubular structures were formed in teratomas, a very careful examination would be necessary to understand more closely what the properties of these tubules are.

Other growth factors have also been used for induction of renal genes in wild-type cells - a combination of activin A, bone morphogenetic protein 7 (BMP7), BMP4 and retinoic acid (Kim and Dressler, 2005); activin alone (Vigneau et al., 2007); BMP4 alone, both in serum and serum-free medium (Bruce et al., 2007) or the sequential or combinatorial use of three small molecules and retinoic acid (Mae et al., 2010). Kramer et al. (2006) have tested the intrinsic potential of ES cells to give rise to kidney cells spontaneously when differentiated via the EB method without the addition of growth factors.

Only quite recently were iPS cells tested for their ability to differentiate to renal cells (Morizane, 2009). Gene expression studies, based on PCR suggested that iPS cells have a potential very similar to ES cells, but exhibited attenuated expression of kidney markers. Recently, a few groups have reported work on differentiation of human ES cells to a renal lineage (Batchelder et al., 2009 and Dolt, personal communication), also with limited success.

Despite the fact that there have been several studies on the *in vitro* renogenic potential of ES cells, unfortunately the information obtained is still not thoroughly comprehensive and robust. These studies have not yet been expanded further in additional reports to clarify some of the mechanisms and processes of differentiation and improvements of already reported methods have not been suggested. Unlike other branches of directed differentiation, the renal lineage seems to be only in its dawn and many more studies are necessary. In order to solve some of the potential issues outlined earlier in this section, functional and histochemical techniques able to

Table 1.2 - ESC differentiation to renal cells - summary of literature

Reference	Method	Analysis	Authors' conclusions
Kramer et al., 2006	mESCs differentiated via the EB method	semi-quantitative reverse transcription PCR, immunocytochemistry	differentiated cells express early and late kidney markers
Kobayashi et al., 2005	Wnt4-transformed mESC were differentiated via the EB method and treatment with HGF and Activin A	reverse transcription PCR; quantitative PCR; western blot for Aqp2; immunocytochemistry for kidney markers; 3D assay for tubule formation	reported expression of Aqp2 by PCR, western blot and immuncitochemitry; expression of kidney-related markers; tubule formation in 3D culture
Steenhard et al.,2005	undifferentiated mESC injected into kidney rudiments	assessment of cell integration into kidney tubules by β-Gal+ and electron microscopy; immunohistochemistry of injected kidney rudiments for kidney markers	integrate into kidney structures as assessed by β-Gal, electron microscopy and adenovirus transfection with GFP; express kidney markers
Kim and Dressler, 2005	ROSA26 ESCs - derived EBs treated with a combination of retinoic acid, Activin A and Bmp7	western blotting and reverse transcription PCR of EB extracts; immunohistrochemistry of EBs; injection into kidney mouse rudiments	EBs upregulate kidney markers; EBs show co-expression of E-cadherin and Pax2 and respond to induction with spinal cord; EB-derived cells integrate into kidney rudiments
Bruce et al., 2007	mESC genetically modified to express kidney-specific Pax2 reporters were differentiated via EBs and treatment with Bmp2, 4 and 7	real-time PCR for kidney-specific genes, presence of reporter positivity in EBs; immunocytochemistry; FACS	upregulation of kidney markers over time and after some of the treatments; suggest a spontaneous kidney differentiation program in EBs grown in serum or serum-free conditions when supplemented with BMP4

Vigneau et al., 2007	ROSA26-Brachuyry-GFP mESCs were differentiated via the EB method, sorted for Brachyury, treated with Activin A and injected into kidney rudiments	FACS selection for Brachyury+ cells after treatment with Activin A; gene expression studies by reverse transcription PCR and immunohistochemitry of the resulting EBs; integration studies in kidney rudiments	upregulation of kidney progenitor genes after FACS selection and treatment with Activin A; decrease of neural-specific genes; incorporation of the derived cells into priximal tubules and ureteric buds of mouse kidney rudiments
Morizane et al., 2009	mESC and iPS were differentiated via the EB method, by the addition of Activin and in some cases other factors (Gremlin, Wnt4, Gdnf, Gdf11, LIF and BMP7	real-time PCR	upregulation of kidney genes after differentiation as detected by real-time PCR (Pax2, WT1, KSP, Nephrin, Ngn2)
Ross et al., 2009	eGFP-labelled mESC were examined for their ability to repopulate decellularise rat kidneys and differentiate to kidney cells	tracking the ability of cells to repopulate the decellularised organ and differentiate by microscopy; kidney gene expression by immunohistochemistry and real-time PCR	migration of cells and repopulation of the decellulrised matrix; positivity for Pax2 and Ksp-cadherin after long-term culture by immunohistochemistry and PCR
Ren et al., 2010	mESCs differentiated with the EB method by an initial treatment of retinoic acid and Activin A and a subseqent treatment with conditioned medium from ureteric buds	analysed by immunocytochemistry and FACS	ESC derived cells transition through mesoderm to give rise to cells expressing kidney markers
Mae et al., 2010	mESC differentiated by small molecules and retinoic acid	gene expression by reverse transcription and real-time PCR; immunocytochemistry	intermediate mesodermal markers were enhanced (Osr1);markers of other lineages downregulated; renal markers upregulated

detect marker co-expression in individual cells should be employed to study *in vitro* ESC differentiation to renal progenitors. Such an approach would help scientists circumvent at least one of the caveats of studying kidney development - or the frequent inconclusiveness and possible misinterpretations based on reverse transcription studies of mixed populations of cells. Single-cell and three dimensional studies of kidney structures would help confirm without any doubt that transplanted cells localise in renal tubules and very careful and stringent co-expression studiesand *in situ* hybridisation for multiple markers should confirm the identity of the cells in question.

As the results from *in vitro* differentiation studies need significantly more improvement, it might be necessary to approach the problem from two sides and add the dimension of developmental biology with a particular reference to ES cell differentiation. Up to now no developmental studies have been performed to directly translate to stem cell differentiation. Paradoxically, at the same time, almost all of the outlined studies have made use of information related to the normal processes of kidney development that would happen in embryogenesis - transition to primitive streak and mesoderm, acquisition of intermediate mesodermal properties and the influence of nephrogenic factors. This reveals that careful experiments with early embryos have to be performed to obtain some missing links in these areas. For example, it would be particularly interesting to address the following scientific problems: 1 – the timing of acquisition of renogenic potential in development; 2 - the position and characteristics of these early renocompetent cells; 3 – the question of whether a transition through mesoderm and intermediate mesoderm is required for differentiation or whether it is possible to generate kidney cells via alternative routes. Another more general, but fundamental, issue remains to be clarified as well. In spite of the existence of a number of publications reporting the differentiation of ES cells to a renal lineage, 5 years after the first reports, no improvements to these protocols were reported and the studies have not been taken further. Also, no attempts for the isolation and purification of ES cell - derived kidney cells have been reported. This thesis addresses some of these questions.

1.7 Perspectives

In this section, I would like to discuss briefly the possible impact of this scientific work by drawing the connections between two different scientific areas and add the additional aspect of their potential application in clinical practice. Some of the relationships between these three pivotal foci are illustrated in Figure 1.6. First, the interconnectedness between kidney development and ES cell biology is much more direct. For instance, experiments examining early kidney development in embryogenesis might provide important insight for improving ESC differentiation to kidney cells and vice versa – understanding early embryonic development and kidney development would pave the path to understanding how cells take lineage decisions and make fate commitments. Although, some information is available about the signals that might be involved in various steps (as described earlier in this chapter), it is still unknown whether kidney cells might be produced directly from ES

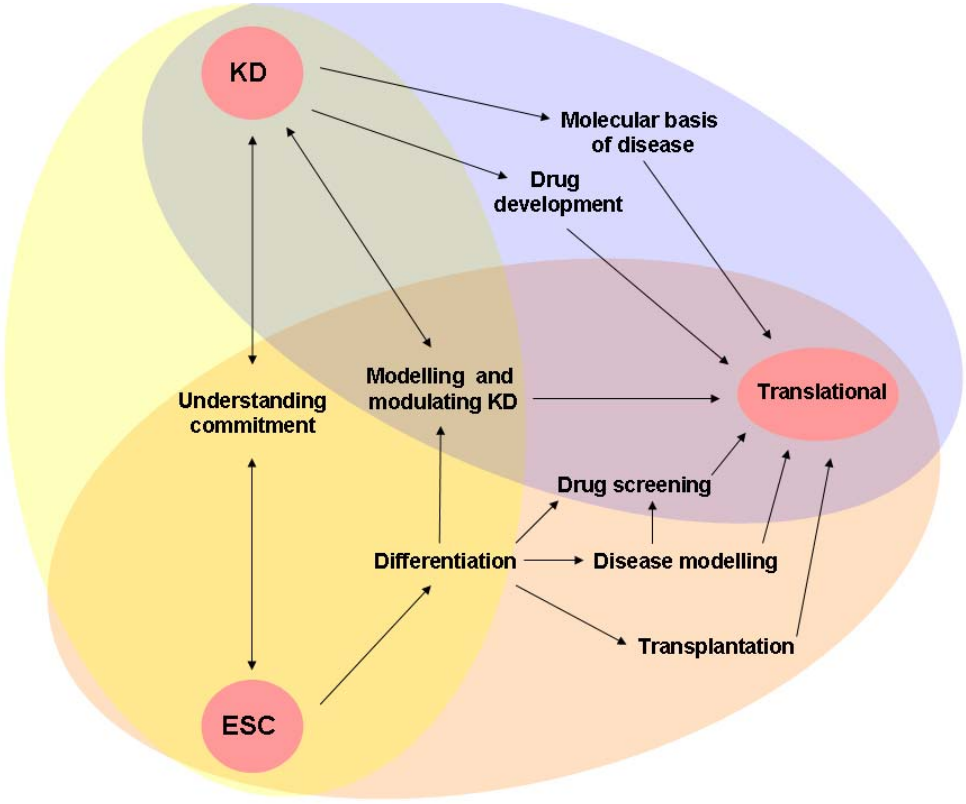

Figure 1.6 - Interconnectedness between embryonic stem cell research, kidney development and potential clinical applications
In yellow - connections between ES cell research and kidney development
In pink - potential applications of ES cell research to clinical studies
In blue - potential relevance of kidney development to clinical studies
Two-headed arrows denote a potential bidirectional transfer of information
KD - kidney development

cells and whether passing through developmental stages sequentially (for example, mesoderm and intermediate mesoderm) is indispensable or a sufficient condition in the process. Solving this question is of great significance to understanding kidney development, but even more so to understanding cell behaviour and specification *in vitro.* Evidence indicating that cells can leap across their developmental chronology of fates would lead to radical changes in the current concept of commitment. Understanding normal development is a prerequisite for understanding the cellular and molecular basis of disease, which then reflects into the development of methods for treatment. At the same time, if the knowledge accumulated by studying kidney development could be applied to generating ESC-derived renal cells the possibilities for clinical improvements will be highly increased. ESC-derived renal cells could be immediately used for large-scale drug screening experiments. In addition, the possibility to use iPS-derived renal cells would be even more exciting as this would allow screening of the influence on drugs on particular diseased renal cells in unlimited quantities. In addition to drug screening, ESC or iPSC-derived renal cells might prove useful in medical devices to improve the quality of life of patients on dialysis. As mentioned earlier in the chapter, the function of the kidneys is not only limited to excretion of urine. They are important in maintaining a healthy water-salt balance and are a part of the endocrine system producing essential hormones. Bioartificial hemofilters containing human proximal epithelial cells have already been designed to address this problem and clinical trials are underway (Humes et al., 1999; Humes et al. 2004). The possibility of using functional and responsive ESC- or iPSC-derived kidney cells could provide an unlimited number of proximal tubular cells for these devices.

In addition to their potential use for developmental studies, modelling disease, and drug screening, ESC- or iPSC-derived renal cells might find a place in cell replacement therapies to substitute for cells lost in damaged organs. Although this is not yet possible due to safety and ethical (in the case of ESCs) concerns, *in vitro*-produced cells might become a key part of regenerative medicine.

Chapter 2

Materials and methods

2.1 Mice and Mating

2.1.1 Mouse strains

All animals were maintained and sacrificed in compliance with the Animals (Scientific Procedures) Act (1986) and the appropriate Home Office guidelines on the Act. Animals were obtained from and maintained under the care of BRR, CIP, University of Edinburgh. CD1 mice were used for isolation of wild-type tissues. TgTP6.3 transgenic mice (Pratt et al., 2000) were used for isolation of GFP^+ tissues. These were a kind gift from Dr. Thomas Pratt, University of Edinburgh. TgTP6.3 mice express a Tau-GFP fusion protein under the CAG promoter and therefore show GFP-positivity at comparable levels in most cells and tissues.

Timed matings were carried out according to the standard for the animal facility procedures. Two females and one male were set up in a single cage in the evening and plugging was monitored on the following morning. The morning of discovery of the vaginal plugs was designated E0.5. Stock TgTP6.3 mice were kept in Individually Ventilated Cells (IVCs). Breeders were maintained in conventional cages.

2.1.2 Genotyping

CD1 wild type females and TgTP6.3 transgenic males were mated for the generation of GFP-positive embryos. As reported by Pratt et al. (2000), homozygosity of the transgene ($TgTP6.3^{+/+}$) leads to lethality in early embryonic development. Hemizygotes are GFP-positive and survive without any noticeable phenotypic differences from wild type (WT) mice. When breeders (hemizygotes for the transgene - $TgTP6.3^{+/-}$) were mated with WT female CD1s, the possible resulting phenotypes were only $TgTP6.3^{+/-}$ (GFP-positive) and $TgTP6.3^{-/-}$ (i.e.WT). In that case, it was possible to determine the genotype of pups born (ear clips) and embryos isolated for experiments by fluorescence microscopy for GFP-positivity (Figure 2.1).

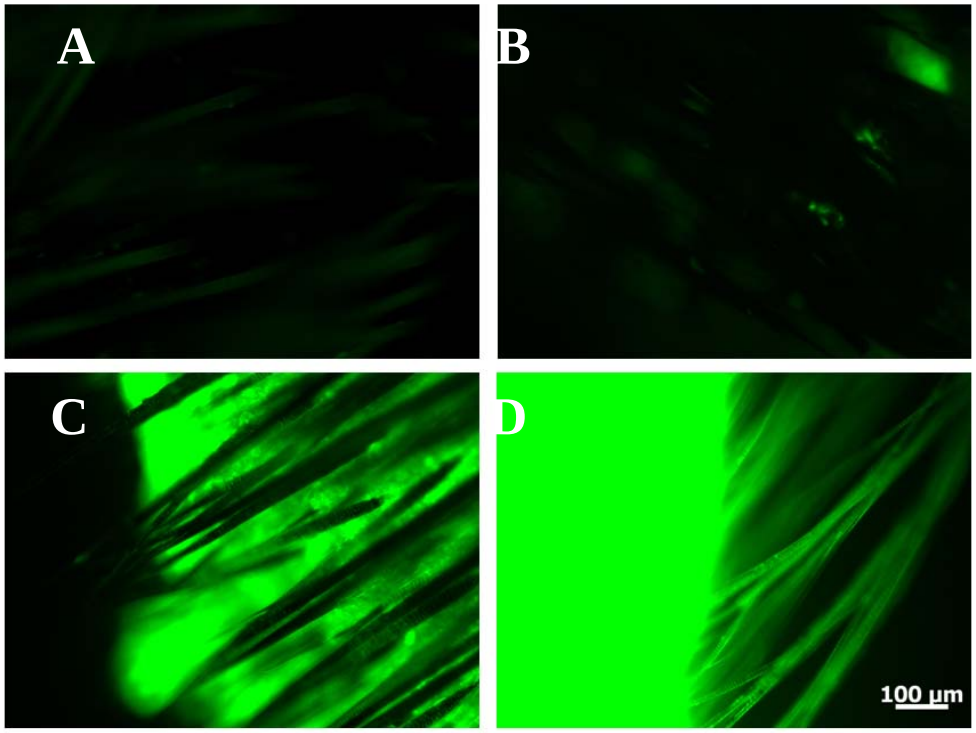

Figure 2.1 – Genotyping of tauGFP mice
A and B - ear clips of GFP-negative pups resulting from a cross between a WT female and a hemizygous for the transgene male showing no fluorescence. Fur is slightly autofluorescent; C and D - micrographs showing the easily distinguishable phenotype of hemizygous pups (with black and white coat, respectively A and B). All micrographs were taken at the same exposure time

2.2 Tissue culture

2.2.1 Isolation of E11.5 kidney rudiments

Embryos were removed from the mouse uteri with the help of forceps and a surgical blade. 25 gauge needles (BD Microlance) attached to 1mL syringes were used for all finer dissections. The embryos were decapitated and all tissues rostral to the developing hind limb buds were removed in one single incision with the needles. The caudal parts of the embryos were bisected along the midline to allow access to the kidney rudiments, located dorsally to the hind limb buds and WD. The rudiments were carefully dissected out and cultured in Complete Kidney Culture Medium (CKCM) consisting of Minimal Essential Medium (MEM) with non-essential amino acids (Sigma), 10% fetal calf serum (Biosera), 100units Penicillin and 100µg/mL Streptomycin (Sigma). All kidney cultures were kept at 37°C in a humidified incubator with 5% CO_2. Caudal parts that were not required for immediate use were

preserved in Bijoux bottles containing dissecting medium at 4ºC for up to 2 days (Davies, 2006).

2.2.2 Isolation of tissues from E10.5 embryos

The embryos were carefully removed from the uterus by an incision in the amniotic sac and decapitated. Caudal halves were collected for tissue dissection.
Before dissection, the bisected caudal parts were carefully examined to identify the correct stage of kidney development progression. Only embryos, which showed a slight enlargement of the Wolffian duct, but no formation of a UB invading the neighbouring uninduced MM were used for experiments.

2.2.3 Isolation of tissues from E9.5 embryos

Embryos were obtained by a quick scalpel incision cutting the uterus and amniotic sac. The embryos were teased out by gently squeezing the surrounding tissues with a pair of forceps. Embryos were examined and staged. E9.5 embryos from the same uterus were found in stages ranging from E9.0 to E10.25. Whenever possible, only embryos at Theiler stage 15 were selected for tissue harvesting. In this case, the number of somite pairs (21-29) and absence of hind limb buds were used for determining the stage. Due to the scarcity of embryos in some experiments, embryos with initiated hind limb buds, but without visibly formed metanephric anlagen (early Theiler stage 16) were used. Needles were used for embryo decapitation and the dissection of the nephrogenic region, shown on Fig. 2.2 by a red dotted line.

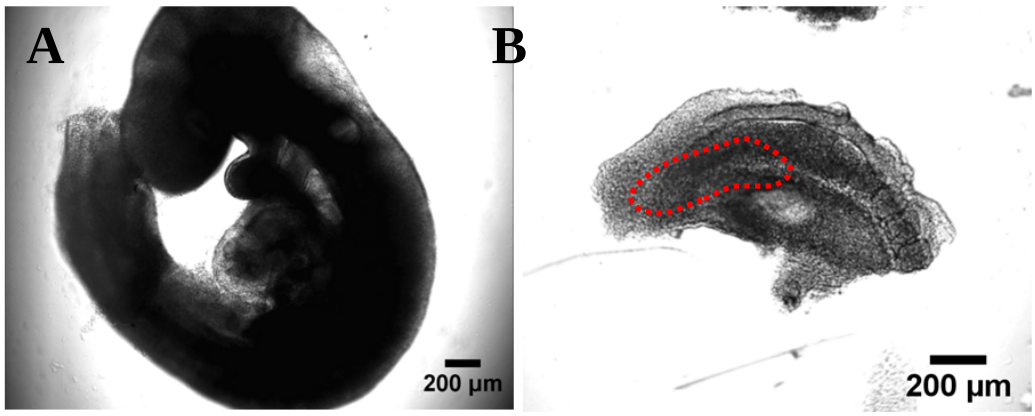

Figure 2.2 – Isolation of tissue from E9.5 embryos
A - a typical E9.5 mouse embryo: B - a micrograph of an E9.5 bisected caudal part, the tissue isolated for experiments has been showed by a red dotted line

2.2.4 Isolation of tissues from E8.5 embryos

The obtained mouse uterus was cut into pieces containing one implantation site each by forceps dissection. Embryos were obtained by a sufficiently large incision with a scalpel in the individual pieces of uterus. Only embryos at approximately Theiler stage 13 were selected for use in experiments. These typically contained 7-12 formed somite pairs and some showed initiated development of the mandibular component; neural tube closure had taken place only until the proximal part of the tail. An example is shown on Figure 2.3. The tissue dissected for experiments is indicated by a red dotted line. The incision to separate the caudal from the rostral part was always made after the last fully formed somite pair.

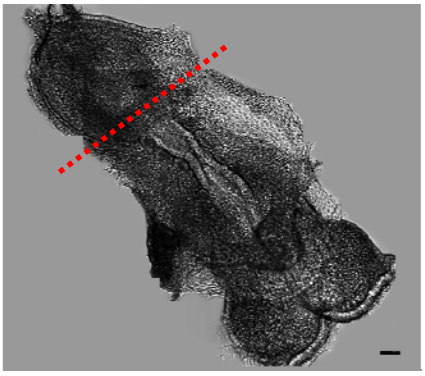

Figure 2.3 – Isolation of tissue from E8.5 embryos
A typical E8.5 mouse embryo; scale bar: 100µm

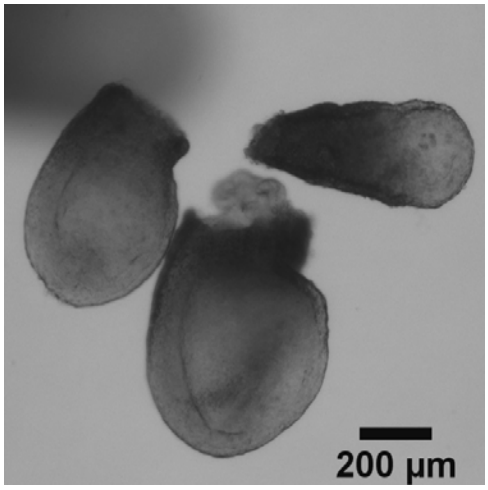

Figure 2.4 – Typical E7.5 embryos
Micrograph of E7.5 embryos isolated from the same uterus, showing different size and stage of development

2.2.5 Isolation of E7.5 embryos

The two uterine horns were separated and surrounding fat was removed. At this embryonic stage, the embryo implantation sites were still visible as distinct bulges on the uterus. They were segmented by forceps dissections and embryos were carefully extracted by opening the decidua from the implantation side. All extraembryonic tissues were removed and whole embryos were used for the experiments. Embryos obtained from the same uterus showed a great variation in size and development (Figure 2.4). Embryos selected for experiments had to fulfill the following criteria: 1 - were in the pre-somite stage and 2 - exhibited neural plate in the stage of head fold formation.

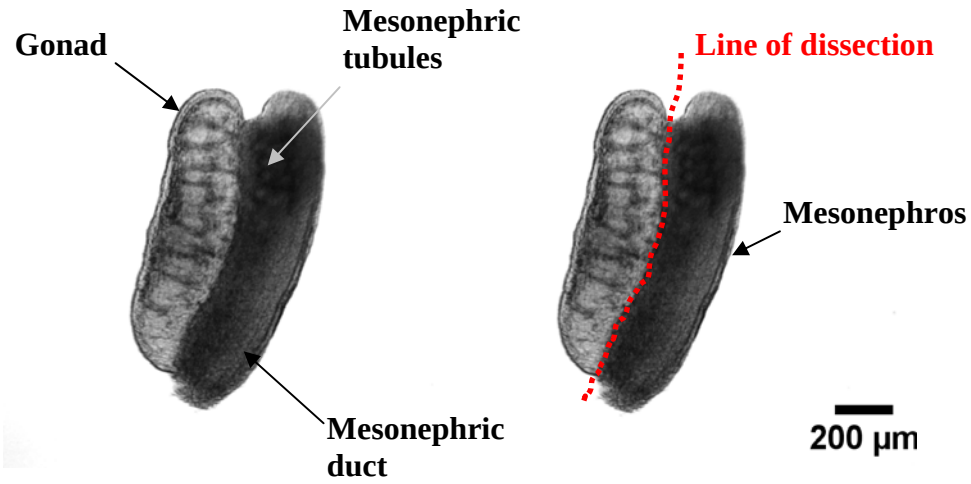

Figure 2.5 – Isolation of mesonephroi
Light micrographs of a gonad-mesonephros region from an E11.5 mouse embryo. The gonad, mesonepros, mesonephric tubules and mesonephric duct are shown by arrows. The red dotted line indicates the line of dissection to obtain only mesonephroi.

2.2.6 Isolation of mesonephroi from E11.5 mouse embryos

Embryos were obtained as described for E11.5 kidney rudiments. The embryos were sacrificed by decapitation. Tissues rostral to the forelimbs were removed, as well as tissues ventral to the fore- and hind-limb buds (inner organs), including the limb buds. The remaining portion of the trunk was bisected along the spinal cord, exposing the meta- and mesonephroi. The whole gonad-mesonephros region was dissected out, followed by removal of the gonad.

2.2.7 Isolation of spinal cord

E11.5 mouse embryos were used for the isolation of dorsal spinal cord. After sacrificing the embryos, caudal parts were kept for kidney isolation and the rest of the body was used for spinal cord isolation. First, the anterior limbs and viscera were removed. A thin dissecting needle was inserted in the anterior opening of the spinal canal and a second dissecting needle was used to rupture the dorsal spinal cord along the midline, by stroking movements along the first needle. The bisected spinal cord was opened to the side (as shown on Figure 2.6) and the clear parts (dorsal spinal cord) were excised leaving the ventral spinal cord and the somites.

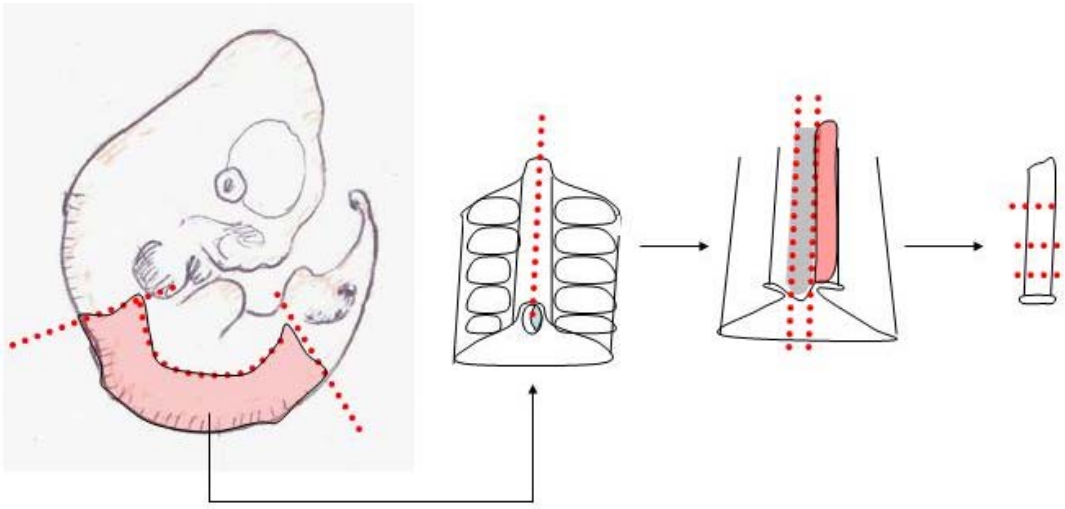

Figure 2.6 - Isolation of spinal cord
After sacrificing the embryos by decapitation, the caudal parts and viscera were removed leaving the dorsal portion of the trunk containing somites and spinal cord (as shown on the diagram). The dissected tissue was placed on its ventral side and by inserting a needle in the spinal canal, the dorsal spinal cord was cut along the midline. Unfolding it to the side allowed removal of a longitudinal piece of dorsal spinal cord

2.2.8 Tissue culture on filters

The obtained kidney rudiments or other tissues were cultured on sectioned 5µm isopore membrane filters (Millipore, Sigma) placed upon Trowell screens in CKCM (Davies, 2010).

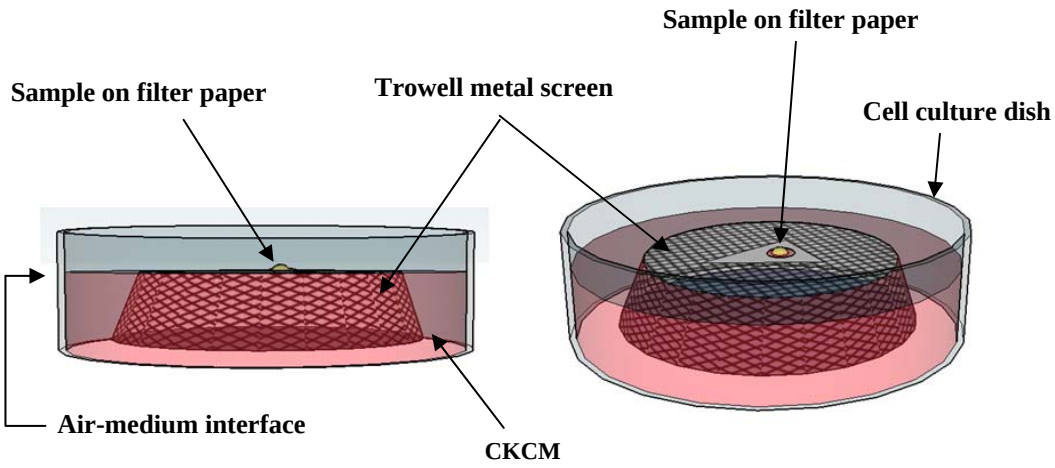

Figure 2.7 – Tissue culture setup
A diagrammatic representation of conventional tissue culture, showing a 3.5 cm cell culture dish with a sample cultured on a piece of polycarbonate filter placed on a Trowell metal screen at the medium-air interface

2.2.9 Co-culture of tissues and dorsal spinal cord

Tissues were harvested as described in previous sections and placed on filters. Long stripes of dorsal spinal cord were dissected as previously described and placed within physical contact with the sample, encircling it. Small square pieces of spinal cord were used for inducing isolated MMs.

2.2.10 Disaggregation of tissues into single cells

Tissues (e.g. E11.5 kidney rudiments or nephrogenic regions from earlier embryos) were obtained by a mechanical dissection in serum-free medium, as previously described. During long waiting periods, the samples were kept in dissecting medium at 37ºC and 5% CO_2 in a humidified incubator until used. Tissues were transferred to a 3.5cm dish with pre-warmed 1x Trypsin-EDTA solution (containing 0.25% Trypsin and 0.1% EDTA in Hank's Balanced Salt Solution) with the help of a flame-polished Pasteur pipette. The enzymatic treatment was carried out for 2min at 37ºC. The samples were collected with a glass Pasteur pipette and moved to a new tissue culture dish containing CKCM for 5 min to stop the trypsinisation. After being placed in a 1.5mL microcentrifuge tube, in 200µL of Advanced Dulbecco's Modified Eagle's Medium (DMEM), the clumped treated tissue was disaggregated by vigorous trituration until a single-cell suspension was obtained. An adjustment to this procedure was made for treating E7.5 embryos, where the incubation time in Trypsin-EDTA was increased to 3min.

2.2.11 Reconstruction of kidney-like rudiments from mixtures of single-cell suspensions

First, single cell suspensions were generated from either tissues or adherent cells and the numbers of cells were counted. In the case of adherent cells or disaggregated embryoid bodies, the cells were passed through a 40µm cell strainer to make sure that no clumps of attached cells were present, interfering with the production of fine chimerism with the kidney rudiment cells. Althought the 40µm strainer generates mainly single cells, occasional aggregates were also present. In most cases 100,000 embryonic kidney cells (host cells) were mixed with 10,000 or 15,000 test cells in a 0.5mL microcentrifuge or a PCR tube. The suspensions were mixed immediately

before centrifugation at 3,000rpm for 2min. The pellets were detached from the tubes by careful flushing with a 200µL pipettor set to 100µL and transferred to filter culture with a flame-polished glass Pasteur pipette. Pellets were cultured in CKCM supplemented with ROCK inhibitor (as described in section 2.5) for 24h and only CKCM thereafter.

2.3 Fixation and immunohistochemistry (IHC)

2.3.1 Methanol fixation

Tissues were fixed by replacing the culture medium with ice cold methanol (-20°C) by gentle pipetting and incubation for 10min at room temperature. Before immunostaining, the pieces of filter with rudiments immobilised on them were placed in Bijoux bottles with PBS. Two short washes with PBS were followed by a wash for 30min at RT. The PBS solution was then directly replaced with 400µL of primary antibody solution.

2.3.2 Paraformaldehyde fixation

Tissues were fixed by replacing the medium with 4% Paraformaldehyde (PFA) in PBS and incubated for 30min. The samples were then rinsed two-three times with PBS, left to wash in PBS for 30min and permeabilised with 0.1% Triton-X in PBS for 30min. Both incubations were performed at room temperature. The final solution was then replaced by primary antibody solution.

2.3.3 PFA-methanol co-fixation of pelleted cell mixes or tauGFP cells

Samples we fully immersed in PFA and incubated for 30min at room temperature. They were then rinsed 2 times with PBS and incubated in PBS at room temperature for another 30min. Tissues were post-fixed with ice-cold methanol for 10min and then stored in methanol at -20ºC in light-protected Bijoux bottles.

2.3.4 Immunostaining

Freshly fixed tissues or tissues stored in methanol at -20°C were stained as follows: the samples were rehydrated and washed in PBS for at least 30min prior to staining;

Table 2.1 – List of primary antibodies
A list of primary antibodies (used in different combinations for double- and triple - labeling experiments) with details about dilutions and purchasing information

Antibody	Company	Dilution	Catalogue No
mouse anti-human WT1 (monoclonal)	Dako	1:50	M3561
mouse anti-Calbindin (monoclonal)	Abcam	1:100	ab82812
rabbit anti-Laminin	Sigma	1:100	L9393-5mL
rabbit anti-Six2	Lifespan	1:200	LS-C10189
rabbit anti-Pax2 (polyclonal)	Covance	1:100	PRB-276P
mouse anti-E-cadherin	BD Trasduction Labs	1:100	610181
rabbit anti-Calbindin D-28K	Chemicon	1:100	AB 1778
goat anti-megalin (P-20) (polyclonal)	Santa Cruz	1:50	sc-16478
Mouse anti-Oct3/4	BD Biosciences	1:150	611202

Table 2.2 – List of secondary antibodies
A list of secondary antibodies (used in different combinations for double- and triple - labeling experiments) with details about dilutions and purchasing information

Antibody	Company	Dilution	Catalogue No
goat anti-mouse IgG - FITC	Sigma	1:100	F0257-2ml
goat anti-mouse IgG - TRITC	Sigma	1:100	T5393-1ml
goat anti-rabbit IgG - FITC	Sigma	1:100	F9887-.5ml
goat anti-rabbit IgG - TRITC	Sigma	1:100	T5268-1ml
donkey anti-mouse IgG - AlexaFluor 647	Invitrogen	1:100	A31571
goat anti-rabbit IgG - AlexaFluor 647	Molecular Probes	1:100	A21244
chicken anti-goat IgG-FITC	Santa Cruz	1:100	sc-2988
chicken anti-goat IgG-Rhodamine	Santa Cruz	1:100	sc-2860

primary antibody incubations were done at 4°C overnight, followed by 2 short washes in PBS and an incubation in PBS for 3-6h; samples were left in secondary antibody overnight at 4°C and washed for at least 1h at RT before mounting for microscopy. As the immune system in mouse embryos is not yet developed (reviewed by Landreth, 2002) there are no immunoglobulins and Fc receptors, which allows the use of mouse primary and secondary antibodies raised without non-specific staining or problems with background.

2.3.5 Antibody/lectin co-staining

Lectins were commercially available already conjugated to fluorophores and were therefore applied to samples together with secondary antibodies. All samples that were co-stained with antibodies and lectins were blocked with 1% milk (dried skimmed milk, Marvel) in PBS and reagents were diluted in the blocking solution.

Table 2.3 - List of fluorescently conjugated lectins used for IHC

Lectin	Company	Concentration	Catalogue No
DBA Lectin - FITC	Sigma	10µg/mL	L9142-1MG
DBA Lectin - TRITC	Sigma	10µg/mL	L9658-2MG
LTL Lectin - fluorescein	Vector	1:100	FL-1321

2.3.6 Oct4 staining of mouse ES cells

Oct4 staining of WT or tauGFP$^{+/-}$ ESC was performed as follows: cells seeded on cover slips were washed in PBS for 30-60min prior to staining; primary antibody (mouse anti-Oct3/4, BD Biosciences) was applied for 2h at RT; cells were rinsed with PBS 2x and incubated in PBS for a further 1h at RT; the cells were incubated in secondary antibody for 2h at RT, washed with PBS for 30-60min and the cover slips were mounted for microscopy, sealed with nail varnish and imaged.

2.3.7 Nuclear staining with DAPI

DAPI was obtained from Invitrogen, reconstituted to a stock concentration of 10.9mM and used at a final concentration of 300nM. For tissue counter-staining DAPI was applied together with the secondary antibody solution and incubated overnight at 4°C to allow for even penetration. Monolayers of cells were stained with DAPI for 5min at RT.

2.4 Cell culture

2.4.1 Counting cells

After disaggregation to single cells, the cells were resuspended in a known volume of medium and mixed well by pipetting. 10µL cell suspension were aspirated and mixed with 10µL Trypan Blue. 10µL of this mixture were applied onto a Neubauer counting chamber and 5 squares were counted. The number of cells per mL was calculated by averaging the number of cells obtained from the 5 squares, multiplied by the dilution factor (2) and the chamber factor (10,000).

2.4.2 Routine culture of mouse embryonic stem cells

Mouse embryonic stem cells (mESC) were kept in ESC medium (Advanced DMEM (12491-015, GIBCO), 10% ESC-grade fetal calf serum (PAA), 1000U/mL LIF, 2mM L-glutamine, 5µM 2-mercaptoethanol, 100U/mL Penicillin and 100µg/mL Streptomycin.

tauGFP$^{+/-}$ ESC were kept under Puromycin selection at all times, where ESC medium was supplemented with Puromycin (Sigma) to a final concentration of 2µg/mL. Oct4-GFP ESCs were cultured in medium, supplemented with 400µg/mL G418 (Sigma). ESC lines were cultured on gelatinised cover slips and supplied with fresh medium every 2 or 3 days.

2.4.3 Passaging of mouse embryonic stem cells

The adherent cells in 6-well plates were washed once with pre-warmed PBS and incubated in 1mL 1x Trypsin-EDTA solution for 5min at 37°C. The enzymatic treatment was stopped with 1mL ESC medium, the cells were collected, triturated to

generate a homogenous single cell suspension and centrifuged. The pellet was resuspended in 1-3mL of ESC medium, mixed well and a few droplets of cell suspension were added to freshly gelatinised 6-well plates containing 2mL ESC medium.

2.4.4 Thawing of cells

Vials were kept on ice after being removed from liquid nitrogen, until thawed rapidly by immersing their bottom half in a 37°C water bath for 1-2 min. The cell suspension was aspirated with a pipette containing 1mL normal culture medium, directly transferred to a 15mL conical tube and centrifuged at 1000rpm for 5min. The medium was removed, cells were resuspended in 2mL fresh culture medium and applied to gelatinised culture dishes.

2.4.5 Freezing of mouse cells

Cells were frozen in cryovials in 1mL Recovery cell-culture freezing medium (12648010, Invitrogen) or 1mL home-made medium containing 10% DMSO, 40% Advanced DMEM and 50% ES cell-grade serum. The cells were first enzymatically detached from the cell culture dishes, then centrifuged at 1000rpm for 5min, resuspended in freezing medium and placed in a -20°C freezer. After 1h, the cryovials were transferred to a -80°C freezer for 24h and stored in liquid nitrogen or at -80°C if needed for use within a couple of weeks.

2.4.6 Gelatinisation of culture dishes

0.1% sterile Gelatin from porcine skin (Fluka) in PBS was pipetted in culture dishes: 1mL for 3.5cm, 3.5mL for 6cm and 5mL for 10cm dishes and incubated for at least 15min at room temperature. The liquid was aspirated and replaced with cell culture medium right before adding cell suspension.

2.4.7 Depleting fibroblast-mESC co-cultures from fibroblasts

As mouse embryonic fibroblasts (MEFs) are significantly bigger and heavier than ESCs, they sediment at the bottom of the cell culture dish (and adhere to it) much more quickly than do stem cells allowing for separation. Upon trypsinisation, the

mixed suspension of MEFs and ESCs was pipetted in a fresh culture dish and left in an incubator for 45min – 1h. The medium (which contains mostly unattached stem cells) was aspirated and transferred to a gelatinised culture dish.

2.4.8 CellTracker staining of cells

Cells were either detached from cell culture dishes or obtained from primary tissue by dissection and trypsinisation, and pelleted by centrifugation at 1000rpm for 5min. The pellet was resuspended in 4μM CellTracker solution in dissecting medium and kept in an incubator at 37°C for 45min. Cells were harvested by centrifugation and washed two times with serum-free medium before finally resuspending them in CKCM for counting and use in experiments.

2.4.9 EB formation from mESC

ES cells were trypsinised and centrifuged at 1000rpm for 5min. The cells were resuspended, counted with a Neubauer chamber (as described), adjusted to the desired number of cells and plated on 10cm bacteriological-grade dishes in differentiation medium (DMEM (Sigma), 2mM L-Glutamine (Sigma), 1mM sodium Pyruvate (Sigma), 1x non-essential amino acids (Invitrogen) and 5μM 2-mercaptoethanol). Wherever indicated, the differentiation medium was supplemented with DMSO (control, as diluent) or DAPT. Medium was changed on day 3 of EB formation (to allow cells to aggregate) and every second day thereafter. EBs were used for either isolation of RNA and gene expression studies, or disaggregated into single cells for use in cell mixing experiments. In the latter case, the EB - derived single cell suspension was passed through a 40μm cell strainer to ensure that no clumps of cells were present, interfering with the experiment.

2.4.10 Monolayer differentiation of mESC

ESCs were harvested from adherent culture as previously described and counted with a Neubauer chamber. For differentiation 6 $x10^4$ cells/cm were plated in differentiation medium containing 4μM DAPT (γ-secretase inhibitor) or an equal amount of diluent (DMSO).

2.4.11 Culture of hESC

The cells were cultured on Matrigel-coated culture dishes or flasks in mTESR Basal medium containing 1x mTESR supplement (both from Stem Cell Technlogies). The cell culture containers were coated with Growth Factor Reduced Matrigel at a concentration of 328µg/mL (diluted in KO-DMEM, Invitrogen) for 1h at RT. For transfected hESC, G418, Fungizone and Penicillin/Streptomycin were also added to the culture medium. Fresh medium was supplied every day.

2.4.12 Passaging of hESC with Collagenase

Cells were washed once with PBS and incubated in Collagenase IV (Invitrogen), diluted to 200U/mL in KO-DMEM, for 5-10min at 37°C until the colonies started to lift around the edges. The Collagenase was the aspirated and cells washed once with PBS before being removed from the dish with a cell scraper and gently disaggregated by trituration. Human embryonic stem cells (hESC) were usually subcultured 1:2.

2.4.13 Freezing of hESC

Cells were detached from tissue culture flasks and dishes, as previously described, centrifuged at 1000rpm for 5min and resuspended in 1mL cold (4°C) Cryostor freezing medium (CS10, Biolife Solutions). The cell suspension was aliquoted into 1 or 1.5mL cryovials, which were then placed in a "Mr. Frosty" isopropanol cell freezer, loaded with isopropanol at 4°C, and left at 4°C for 10min, before being transferred to -80ºC.

2.5 Protein inhibitors

Protein inhibitors for treatment of kidney cultures, tissue cultures, adherent cells or EBs were supplied by directly diluting them in the respective culture medium at the desired concentrations. Y-27632 (Y0503, Sigma) was reconstituted in dH_2O to a stock concentration of 5mM and used at a concentration of 10µM. Glycyl-H1152 dihydrochloride (2485, Tocris) was reconstituted in dH_2O to a stock concentration of 5mM used at a concentration of 1.25µM. DAPT was reconstituted in DMSO and used at a final concentration of 4µM.

2.6 Molecular Biology

2.6.1 RNA extraction (spin column)

RNA from tissues and cells was extracted using the SV total RNA isolation system (Promega) according to the protocol supplied by the manufacturer. Several small modifications were made to improve the quantity of RNA isolated and to collect the sample at a higher concentration. These were as follows: at the lysis step, the sample was incubated for 5min at 70°C, not for 3min, as suggested by the manual; at the elution step, 100µL of nuclease-free water were used to collect the RNA from the spin column; furthermore, the resulting 100µL were reapplied to the spin column membrane, incubated for 5min and eluted a second time. The secondary eluate was stored at -80°C.

2.6.2 RNA extraction (TRIzol)

The RNA isolation was performed according to the manufacturer's instructions (Invitrogen). Centrifugations were performed at 4°C. At the final step, in some cases the ethanol needed more than 30min to evaporate.

2.6.3 Reverse transcription (cDNA synthesis) for semi-quantitative PCR

For semi-quantitative PCR, the concentrations of obtained total RNA were measured with a Spectrophotometer Ultrospec 4000 (Pharmacia Biotech), Nanodrop or Agilent. 200ng RNA from each sample were used for the synthesis of cDNA. One reaction (total volume 20µL) contained a final concentration of 10U/µL MLV Reverse Transcriptase (M170A, Promega), 1x MLV Buffer, 1U/µL rNasin RNAse inhibitor (N251A, Promega), 1mM dNTPs, 200nM Random Primers (C118A, Promega), 200ng DNA and nuclease-free water. After mixing, the reaction was incubated at 42°C for 1h, then 75°C for 8min, and the product was stored at -20°C for PCR.

Table 2.4 - Reagent list and concentrations for cDNA synthesis from isolated total RNA

Reagent	Stock concentration	Amount used [µL]	Final concentration
M-MLV Reverse transcriptase	200U/µL	1.0	10U/µL
M-MLV Reverse transcriptase	5x	4.0	1x
rRNasin RNase inhibitor	40U/µL	0.5	1U/µL
dNTPs	10mM	2.0	1mM
Random Primers	100µM	1.0	200nM
RNA	Varies	RNA adjusted with water, max 11.5µL combined	200ng
nuclease free water	Varies		Varies

In the cases where the obtained total RNA concentration was too low, it was necessary to combine several equivalent reactions into one. For example, in a 20µL reaction, the maximum possible amount of RNA and water combined is 11.5µL. If the RNA concentration in the original stock required a larger amount of solution than 11.5µL to be accommodated, all reagents in the reaction were multiplied by 2x, 3x, etc. to get a final RNA content of 200ng RNA. Respectively, 2x, 3x, etc times more cDNA mix was then used for PCR.

2.6.4 Primer design

Primers were designed with the online tool Primer3 version 0.4.0, located at http://frodo.wi.mit.edu/primer3/. The default settings of the program were used, together with the option "rodent mispriming library". mRNA information was obtained from NCBI Entrez Gene and the mRNA sequence was extracted in FASTA format from the "Genomic regions, transcripts and products" link. Primers with a melting temperature of about 60ºC and GC-content of 40 to 60% were selected. The

Table 2.5 – List of primers
A list of forward and reverse primers used for transcript detection of the respective genes, based on cDNA synthesis; the expected product size is also provided in base pairs

Gene	Forward Primer	Reverse primer	Product size [bp]
Oct4	CACGAGTGGAAAGCAACTCA	AGATGGTGGTCTGGCTGAAC	246
Nanog	AAGTACCTCAGCCTCCAGCA	GTGCTGAGCCCTTCTGAATC	163
Brachyury	CCGGTGCTGAAGGTAAATGT	CCTCCATTGAGCTTGTTGGT	248
Osr1	CTGCCCAACCTGTATGGTTT	GCGAGGCTTGGTCTTAAGTG	237
AFP	AAACATCCCACTTCCAGCAC	CTTCCGGAACAAACTGGGTA	218
AchE	CCTGGGTTTGAGGGTACTGA	GGTTCCCACTCGGTAGTTCA	234
αSMA	CTGACAGAGGCACCACTGAA	CATCTCCAGAGTCCAGCACA	160
GAPDH	AACTTTGGCATTGTGGAAGG	ACACATTGGGGGTAGGAACA	223

selected primers were checked for unspecific binding to undesired mRNA sequences and genomic DNA with BLASTn.

A list of primers for the experiments in this work is given in Table 2.5.

2.6.5 PCR for gene expression studies

For PCR, a master mix with all reagents was prepared and 24µL were aliquoted in each thin-walled PCR reaction tube. The PCR master mix was prepared as shown. GoTaq polymerase and green GoTaq buffer were obtained from Promega and the dNTP mix was purchased from Invitrogen. The following settings of the Thermal Cycler were used: step 1 - 4min denaturation at 94°C; step 2 - 60s at 94°C, 60s at 56 to 61°C, 90s at 72°C (depending on the optimal melting temperature for the primer pair) and step 3 - final elongation for 10min at 72°C. Step 2 was performed for 25-35 cycles and the reaction was kept at 4°C after completion. The whole product was loaded on a 1% agarose gel for analysis. A negative control was performed for every set of reactions to confirm the absence of contaminants in the reagents, where no cDNA was added to the reaction. Wherever necessary, a positive control was also performed.

Table 2.6 - Reagent list and concentrations for PCR

Component	1 reaction [µL]	Final concentration
GoTaq DNA polymerase	0.125	1.25U
5x GoTaq reaction buffer	5.00	1x
dNTPs	0.50	0.2mM
forward primer	1.00	1.0µM
reverse primer	1.00	1.0µM
cDNA	1.00	Varies
water	16.375	-
total	25.00	-

2.6.6 Agarose gel electrophoresis

1% gel was prepared with UltaPure agarose (Sigma) ant TAE buffer. GelRed (Biotium) was added for visualisation of DNA at a final concentration of 1x. The gel was set for 30min, wells loaded with the whole content of the PCR reaction and the electrophoresis was run in a BioRad chamber at 80 to 100V. The size of the fragments was determined on the basis of a 100bp DNA ladder (G210A, Promega) to confirm specificity of the product.10µL DNA ladder were mixed with 2µL Orange/Blue Loading Dye (Promega). The DNA was visualised with a UV transilluminator (UVP) and Visi Doc It Processor (UVP), and images were printed with a VideoGraphing printer (Sony, UP_890 CE). The images were digitalised by scanning.

2.6.7 DNA extraction from freshly isolated and cultured kidney rudiments

Dissected kidney rudiments were placed in a 1.5mL microcentrifuge tube and pelleted by centrifugation at 3000rpm for 2min. The medium was removed and replaced by lysis buffer. Cultured kidney rudiments were first removed from the

isopore membrane filters by gently detaching them with dissecting needles and then placed in lysis buffer.

DNA isolations were performed with a DNeasy Blood and Tissue kit (69504, Qiagen), according to the protocol provided by the manufacturer. Proteinase K (EO0491, Fermentas) was used for the protein degradation step. The 1.5mL microcentrifuge tubes with samples were incubated in a water-loaded heat block at 56ºC for 40min - 1h and vortexed every 20min to ensure effective proteolysis. When the solution was clear and no fragments or particles were visible on inspection, the following step of the protocol was performed. The optional step of RNase treatment was also performed. Ribonuclease A from bovine pancreas (R4642, Sigma) was used at the concentration suggested by the manufacturer. Incubation time was increased to 5-6 minutes at RT. The obtained DNA was eluted from the spin-column in 200µL buffer AE (provided by the manufacturer) and the elution was performed twice with a 5min incubation period on the spin-column membrane to increase DNA yield.

2.7 Microscopy

2.7.1 Preparation of samples for microscopy

Upon completion of IHC, the samples were washed in PBS for at least 1h at RT. For mounting tissue samples, two 22x22mm cover slips (VWR International) were glued with nail varnish at the two opposite sides of a 22x64mm large rectangular cover slip (VWR International) leaving a space in between. The former were used as spacers. Samples was transferred to dried cover slips and fully immersed in hard-set or conventional Vectashield before mounting them with a second 22x64mm cover slip and sealing them with nail varnish. All slides were labelled and stored in light-protected chambers at 4°C until imaged.

2.7.2 Microscopes

Images were taken with the equipment listed in Table 2.7.

Table 2.7 – List of microscopes
A comprehensive list of equipment used for fluorescence and light microscopy with details about imaging software

Microscope	Camera	Software
Zeiss Imager. A1	AxioCam MRm	AxioVision Rel 4.7
Zeiss Observer D1	AxioCam MRm	AxioVision Rel 4.7
Leica Ortholux II	Leica DC 350F	Leica IM50 v 1.20 Release 19
HUND Wetzlat Wilovert	MiniVid LW Scientific	IrfanView version 3.91 (pictures) amcap DirectShow Video Capture version 8.12 (video)
Zeiss Axioskop 2 FS mot confocal	Zeiss LSM 510	Zeiss LSM 510
Zeiss Axiovert confocal	Zeiss LSM 510	Zeiss LSM 510
Leica DMRE confocal	Leica TSC NT	Leica TSC NT

Table 2.8 – Fluorophores, lasers and excitation wavelengths
A table of excitation wavelengths and lasers used for imaging samples labelled with different fluorophores

Fluorophore	Excitation wavelength [nm]	Laser	Artificial colour of channel
Alexa Fluor 647	633	Helium Neon	dark blue
GFP FITC	488	Argon Crypton	green
TRITC Rhodamine	543	Helium Neon	red
DAPI	760	Ti:sapphire multiphoton	cyan

The excitation wavelengths for confocal microscopy were set as shown in Table 2.8, lasers and fluorophores have been used as indicated. A 40x Plan Neofluar oil-immersion lens was used for all confocal sections for counting cells.

2.7.3 Image processing

Image manipulations, including channel merges, image adjustments, measurements, quantification, counting, averaging, production of movies from stacks was done with the NIH program ImageJ version 1.43 with the MBF collection of plugins compiled by Tony Collins, both freely available from http://rsbweb.nih.gov/ij/download.html. Speckles on confocal sections were enhanced by the "smooth" function of the software, which replaces each pixel with the average of its 3x3 neighborhood.

Chapter 3

The development of a quantitative system for assessing cell renocompetence

3.1 Introduction

The aim of this chapter is to evaluate the possible methods for integrating test cells into kidney rudiments for functional quantitative studies to be applied in testing the renogenic potential of cells. Furthermore, it serves to clarify why the method of disaggregation and reaggregation of kidney rudiments has been selected for experiments in later chapters and to provide experimental evidence that the selected method is suitable for both qualitative and quantitative studies to assess the potential of different types and sources of cells to become part of kidney tubules. Figures resulting from this study, which are not essential for further chapters, were marked as supplementary and shown only for reference at the end of this thesis.

3.1.1 Why is it necessary to devise an assay for studying acquisition of renogenic capacity?

As discussed in Chapter 1, studying the acquisition of renogenic capacity in ES and early embryo cells is difficult, as no single robust marker for early kidney progenitors is available. ES cell studies have addressed this problem by using a combination of genes for reverse transcription PCR detection and injection of cells into kidney rudiments for visual analysis (Kim and Dressler, 2005; Steenhard et al, 2005; Kramer et al., 2006; Vigneau et al., 2007; Bruce et al, 2007). Although cell injection is a good method for qualitative assessment, it might pose limitations to quantitative studies due to possible variabilities of the procedure. At the same time performing only reverse transcription analysis does not give sufficient information about the identity of differentiated cells as it detects the expression profiles of the whole mixture of tested cells rather than that of a single cell. This is a serious limitation when using heterogeneous systems such as EBs or primary tissues consisting of many cell types, as it does not provide information for the co-expression of markers in a single cell. Therefore, for accurate analysis, a combined system that allows studying the functional abilities of cells to make kidney-like tubules and their gene expression on the basis of various markers is necessary.

First, the most suitable method for introducing the tested cells in a developing kidney rudiment to allow for analysis of the ability of the tested populations of cells to localise in forming kidney tubules had to be identified. In such a system, the tested cells would be exposed to the signals from the developing rudiment necessary for early metanephric development. This presents the additional advantage of using the embryonic kidney rudiment as a niche for providing the right differentiation signals potentially improving the process.

3.1.2 The importance of a quantitative system for introducing cells into kidney rudiments

As discussed in Chapter 1, the development of functional systems for studying the renogenic potential of various types of cells, such as different types of stem, progenitor or adult cells, is essential. In addition to the possibility of screening different cells, there is a necessity for screening the same type of cells, for example embryonic stem cells, but after treatments with different combinations of factors and molecules. The non-quantitative version of the disaggregation-reaggregation method gives a great opportunity to screen cells and treatments on the basis of the presence or absence of the ability of certain cells to integrate in re-forming ureteric bud structures and nephrons and their marker expression patterns. Once populations of cells with renogenic capabilities have been identified, a quantitative method would allow for comparing the efficiency of different treatments or abilities of different cell types to contribute to the structure of developing organotypic kidney cultures.

3.1.3 The ideal assay for studying renogenic potential

The ideal assay for the purposes detailed above would offer a repeatable method for introducing the same number of cells in kidney rudiments (1), a homogeneous distribution of the test cells (2), and their accurate quantification (3). The technique would optimally allow for the integration of cells in both the developing nephrons and the extending ureteric bud (4). It should offer a possibility to incorporate a high-resolution detection by confocal microscopy (5) and allow the assessment of multiple cell markers simultaneously (6).

One of the most important tools in this assay would be an extremely robust method for tracing cells (7). The danger of tracer transfer and other requirements for good cell and lineage markers have been discussed elsewhere (McLaren, 1976; West, 1984; MacKay et al., 2005). The 6 most important conditions for an ideal marker have been presented in a contemporary perspective by MacKay et al. (2005), who have suggested that such markers should be:

- retained within cells
- not transferred between cells
- widely expressed
- easy to detect in fresh and fixed material
- stable and expressed uniformly throughout development
- and developmentally neutral.

In the following sections several different approaches for cell delivery have been discussed to determine which one would fit the seven criteria for a good assay most closely.

3.1.4 Methods for introducing test cells into developing kidney rudiments

3.1.4.1 Microinjection

A method for introducing exogenous cells into a tissue could be a direct injection of cells into the region of interest. This technique has been used in the first studies reporting the injection of cells into the mouse blastocyst (Gardner, 1968; Papaioannou et al., 1975). Microinjection of cells has also been used for cell delivery into embryonic kidney rudiments (Steenhard et al., 2005; Kim and Dressler, 2005). Vigneau et al. (2007) have microinjected EB-derived cells into both explanted embryonic kidney rudiments and the kidneys of live newborn mice. The latter method is reported to generate a high number of ESC-derived cells integrated into renal tubules over long-term grafting and would therefore be an attractive approach for studying the potential of cells to differentiate to renal cells. Nevertheless, a quantitative assessment of cells integrating in various kidney compartments will be

more difficult due to large amount of tissue to be screened (an adult kidney versus an embryonic kidney).

Preliminary studies were performed as a part of this thesis to test the possibility of injecting cells in E11.5 kidney rudiments manually, by conventional or mouth-pipetting. Kidneys often developed poorly due to the damage or did not show kidney localisation of the injected cells (results not shown). Occasionally, labelled cells were detected in the treated rudiments, but they were localised only at the injection site. The viability of these cells was not confirmed as pilot studies showed that the injection procedure was very difficult to reproduce.

Labelled MMs were also tested for their ability to integrate into developing kidney rudiments, without injection. The labelled MMs and a single kidney rudiment were placed in a hanging droplet for 24h to allow adhesion and cultured in the conventional kidney culture system thereafter. Results showed that MM cells were unable to invade the kidney and therefore failed to enter nephrons (Supplementary Figures 1 and 2). Inducing mechanical injury to the kidney rudiments before incubation with labelled MMs in a hanging droplet did not improve the results (Supplementary Figure 3). None of these approaches showed promising results for providing a convenient and reproducible method for introducing test cells into kidney rudiments.

3.1.4.2 Intravenous injection of cells

Another possible method for delivery of cells into kidneys is injecting the cells systemically. Various groups have reported success with this method, for example, for the introduction of mesenchymal stem cells (MSC) and amniotic fluid stem cells (AFSCs) into the kidneys of adult mice after injury (Morigi et al., 2004; Herrera et al., 2007; Hauser et al., 2010). Importantly, Herrera et al. (2007) have reported that the process of stem cell homing to the kidney after injury might be due to the presence of the surface molecule CD44 in MSCs. It is known that the proteoglycan CD44 is a substrate for hyaluronate (Aruffo et al., 1990), which is upregulated in kidneys subjected to ischemic injury (Johnsson et al., 1996). Studies with anti-CD44

blocking antibodies show that cells lacking this extracellular molecule stopped migration of MSCs to glycerol-injured kidneys. CD44 expression was also reported in AFSCs (Hauser et al., 2010). The extensive evidence suggesting that stem cell homing to injured kidneys is CD44 - mediated is a significant limitation to assessing the properties of primary cells, which are non-homogeneous populations and might lack the expression of CD44. For this reason, the method of systemic injection of cells in mouse models of kidney injury did not provide a convenient tool for the intended studies.

3.1.4.3 Disaggregation of kidney rudiments to single cells and reformation of kidney structures in culture

There have been already many proofs-of-principle for disaggregation and reaggregation of tissues. It has been reported that various cell or tissue explants can be dissociated and reaggregated to form organotypic cultures - retina (Watanabe and Raff, 1990; Bytyqi et al., 2007), aorta-gonad-mesonephros region (Sheridan et al., 2009), thyroid (Bell et al., 1984), skin (Bell et al., 1983), pancreatic islets (Halban et al., 1987; Matta et al, 1994), liver (Takezawa et al., 2000; Mizumoto et al., 2008) etc. The MM of kidney rudiments has also been disaggregated and its ability to reform a limited number of nephrons has been shown (Auerbach and Grobstein, 1958). Very recently, Unbekandt and Davies (2010) reported a high-efficiency method that allows the disaggregation of whole E11.5 kidney rudiments (both MM and UB) to single cells by enzymatic treatment. The suspension of single embryonic kidney cells can be pelleted and the pellet cultured in complete kidney culture medium (CKCM) supplemented by ROCK inhibitor (ROCKi) for the first 24h and only CKCM thereafter (as described in Chapter 2). When the pelleted embryonic kidney cells are cultured for 4 days or more, they form structures typical of developing kidney rudiments. Fragments of UB are formed throughout the pellet, as can be seen on Figure 3.1.1. In developing kidney rudiments, Calbindin is a marker for the ureteric bud (Mounier et al., 1987; McIntosh et al., 1986; Brun et al., 1987; Liu et al., 1993; Davies, 1994). The cells also retain their competence to respond to nephron-inductive signals and nephrons form, as visualised by the component of basal lamina, Laminin (see Figure 3.1.1 and Unbekandt and Davies, 2010). As reported by the

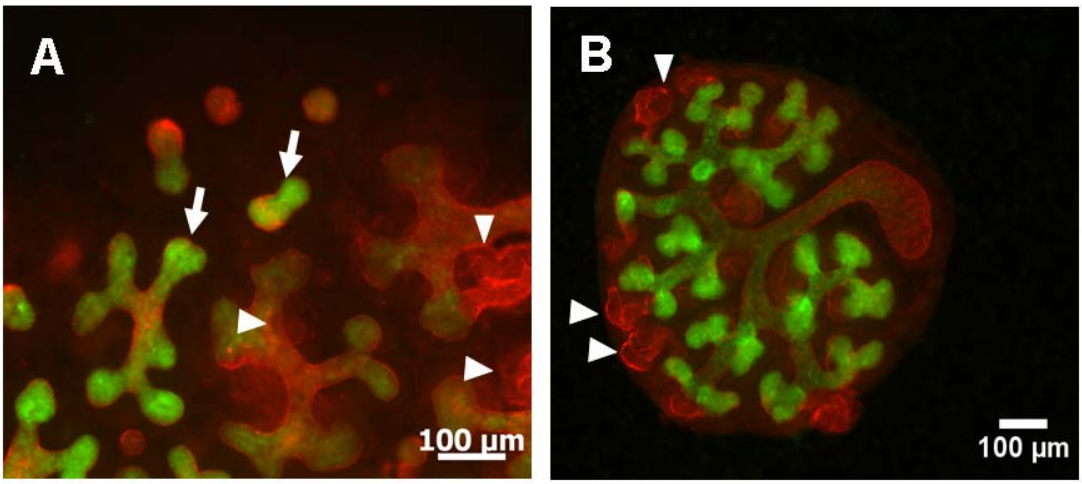

Figure 3.1.1 – Comparison between reaggregated and conventional kidney cultures
A - reaggregated embryonic kidney cells after 3 days of culture showing formation of UB fragments (arrows) and induction of nephrons (arrowheads); B - an embryonic kidney rudiment, explanted at E11.5 and cultured for 4 days, showing a continuous collecting duct system and nephrons positioned mainly at the periphery of the rudiment; green - Calbindin, red - Laminin

authors and confirmed by my experiments (see results section), the procedure is very robust, as development of structures takes place in every properly executed experiment. Also, the major benefit of using this system is the presence of a single cell suspension stage, which is extremely convenient for homogeneously mixing other populations of cells with embryonic kidney cells without the need for injection. Importantly, it also allows for the integration of cells in both the developing nephrons and the extending ureteric bud. Preliminary studies in this thesis and the authors' report have shown that the disaggregation-reaggregation system might be extremely suitable for cell mixing experiments.

3.1.5 Possible sources of error in a quantitative application of the disaggregation system

A system for quantification of integrated cells would require that a known number of cells be mixed with kidney cells in a known proportion. Although, these cells might have different properties and therefore show different potential to integrate into kidney structures, or a lack of such ability, we would expect to find a comparable number of cells localising in reaggregated kidney rudiments after repetition of the same procedure. At the same time, the reaggregation method is technically

demanding and experiments and preliminary tests have shown that various steps in the procedure might introduce a significant bias into potential attempts for quantification. Based on preliminary studies, the factors that could contribute to variation were identified and detailed in the following sections.

3.1.5.1 The developmental stage of the mouse embryos

For the reaggregation system, kidney rudiments are explanted from a significant number of embryos at an approximate embryonic age - E11.5. Although timed matings deliver embryos at approximately the desired stage, they do not always maintain the precision necessary for some mixing experiments (Downs and Davies, 1993). There is a lot of variation between embryos coming from the same uterus and there might be an even larger gap in the development of embryos coming from two or more uteri in experiments requiring a large number of rudiments. In this context, kidney rudiments have two main attributes with the potential to influence the outcome of experiments - the size of the rudiments themselves and the developmental maturity of both UB and MM cells. The size difference between rudiments can be corrected for by counting the number of cells after disaggregation and by always using the same number of host and disaggregated cells for quantitative studies. The differentiation state of UB and MM cells presents a more subtle challenge, as it cannot be corrected for. In the initial stages of kidney development, the cascade of reciprocal inductive signals between the MM and UB brings about very rapid changes in the “potency” of cells - UB cells start do divide rapidly and UBs to branch, while the MM undergoes MET to form nephrons. Cells that have already been initiated to progress through these differentiation processes might have the ability to recover from disaggregation more quickly as they have already been “induced” or committed to develop and might thus form larger structures more quickly. This will not be relevant to reconstituting tissues from a single population of cells, but might have a certain impact when two or more populations of cells are mixed. For example, in our case, where the two populations of WT and tauGFP cells are being mixed, more mature WT cells might result in more WT structures being reformed biasing the proportion of WT/tauGFP cells in structures, in comparison to the theoretical expectation. Also less developed cells might show an initial lag phase

necessary for their induction, before they could start to participate in morphogenetic processes.

3.1.5.2 Preservation of tissues

It is a routine procedure to preserve caudal parts of E11.5 embryos for several days in Minimal Essential Medium at 4°C, after sacrificing the embryos (Davies, 2006). Although, no significant differences were reported when the tissue was used within 48h in whole kidney rudiments, a bias in experiments with disaggregated cells could not be excluded. Preserved cells could be either more sensitive to enzymatic treatment or have a decreased response to ROCKi - mediated survival. Also, preserved tissues might have a normal potential, but might also undergo an initial lagging phase of recovery from cold storage before starting to develop normally.

3.1.5.3 Counting errors

For cell mixing experiments cells were counted before mixing at the single-cell stage to ensure accurate proportions of cells before pelleting. Counting with a Neubauer chamber in solution of Trypan blue contains bias at several levels. The more obvious potential source of error is counting the number of cells itself. Counting only one cell more results in a difference of 20,000 cells per mL of cell suspension. This comes from the fact that the average number of cells counted per square is multiplied by the dilution factor (2 in that case) and the chamber factor (determined by the volume accommodating cell suspension in the chamber) - 10,000. So, for one more counted cell this gives:

1x 2 x 10,000 = 20,000

The second source of error is also related to the enzymatic treatment, in combination with calculating the numbers of available cells. Trypan blue is a dye, which is taken up by dead or dying cells and allows excluding them from the count. In some cases cells might show an attenuated stress response, thus apoptosing after having been counted.

3.1.5.4 Pipetting error

Pipetting error might occur when aliquoting the counted cells for pelleting. This could lead to a significant error, especially in the tested cells, as the cell suspension used for mixing was often in volumes close to 20µL. In this case, a pipetting error of only 2µL would actually mean a whole 10% of the target cell number.

3.1.5.5 Pelleting efficiency

Due to their size, shape and weight, different cell populations might have different pelleting rates (might apply to both UB cells versus MM cells, which come from the same organ rudiment and "host" cells versus tested cells, which might come from different tissues and might belong to earlier or later stages of development). Pelleting is also dependent on the centrifuge tubes, as experience has shown that different types and brands lead to different results (observations, data not shown). In general, after centrifugation, some cells, together with cell debris, are always left out of the pellet and form a characteristic vertical trail of cells, which can be traced from the pellet to the hinge of the tube. This can lead to variation between samples as none of the cells in the trail will be transferred with the pellet. If a certain cell type shows a higher tendency to localise in this thin strip of excluded cells, a minor bias for a certain cell type would occur.

3.1.5.6 Placing the pellet in culture

Some cells are frequently lost in the process of placing the pellet on top of a slice of polycarbonate filter. Sometimes, a small portion of the pellet might break off.

3.1.5.7 Repelleting

When during the procedure the pellets completely break apart, cells have to be resuspended and re-pelleted, in the process of which cells might be lost.

3.1.5.8 Shape and size of the pellet

In the case of thicker pellets, the positioning of certain cell types might be biased. Although the same procedure is followed every time, sometimes the experiments resulted in a smaller pellet, a very small pellet (which cannot be transferred) or even

no pellet at all. In the former case, the ratio of host-tested cells should still be preserved, but this has not been tested separately. In the latter two cases, this does not affect these experiments in particular (as they never reach being placed into culture), but is indicative that there might be another unknown (and therefore unpredictable) factor influencing pellet formation.

3.1.6 Final comments

In this section, the characteristics of an ideal quantitative assay and the possible sources of error have been identified. On the basis of this information, sets of experiments could be designed to test the robustness of the disaggregation-reaggregation system and detect whether these errors would allow for using it quantitatively to assess renocompetence in different cell populations. These are presented in the following section. First, two cell labeling methods have been tested. Next, an experimental setup for quantitative analysis was designed and two approaches of quantitative assessment were compared. Finally, the potential differences between labelled and unlabelled cells were addressed.

To develop a method for quantification of cells potentially integrating in renal epithelia, as a proof-of-principle, it would be necessary to test how cells already proven to have this ability behave in the reaggregation system. This control population of cells should have the same mixing properties as embryonic kidney cells. For this reason labelled and unlabelled embryonic kidney cells from E11.5 rudiments were used for all experiments presented in this chapter.

3.2 Results

3.2.1 CellTracker Green is not a suitable staining reagent for quantification of cells in mixed-cell organotypic cultures

Preliminary studies were performed to investigate whether embryonic kidney cells stained with the commercially available dye CellTracker Green will be traceable in cell-mixing experiments.

E11.5 kidney rudiments were isolated, disaggregated and stained with CellTracker, as described in the Materials and Methods chapter. Stained and non-stained cells were mixed in a ratio 1:1 (50% of all cells in the mixture were green). Pellets were cultured for 5 days, which is the maximum recommended incubation time for CellTracker-stained cells and, co-fixed with PFA and Methanol (as described). Samples were stained to visualise tubular structures and imaged.

Micrographs indicated a relatively weak and non-uniform CellTracker staining (Figure 3.2.1, A and C). Green cells were found in both ureteric buds and nephrons (arrowheads), but their identification was very difficult, as is obvious from the images. Non-epithelialised cells in the interstitium also showed a weak staining, but counting numbers of cells with certainty was not possible. Interestingly, in some cases CellTracker-positive cells in UBs showed a weaker Calbindin staining indicating that the dye might be toxic to cells or interfere with their normal development and gene expression (Figure 3.2.1, A and C, marked by stars).

As exemplified by Figure 3.2.1, it was not possible to determine the percentage of green cells in the mix. These observations, together with the difficulty to treat cells with the dye before every experiment, and the limitation of incubating stained samples in culture for only 5 days, makes CellTracker an unattractive tool for quantitative studies with the reaggregation system.

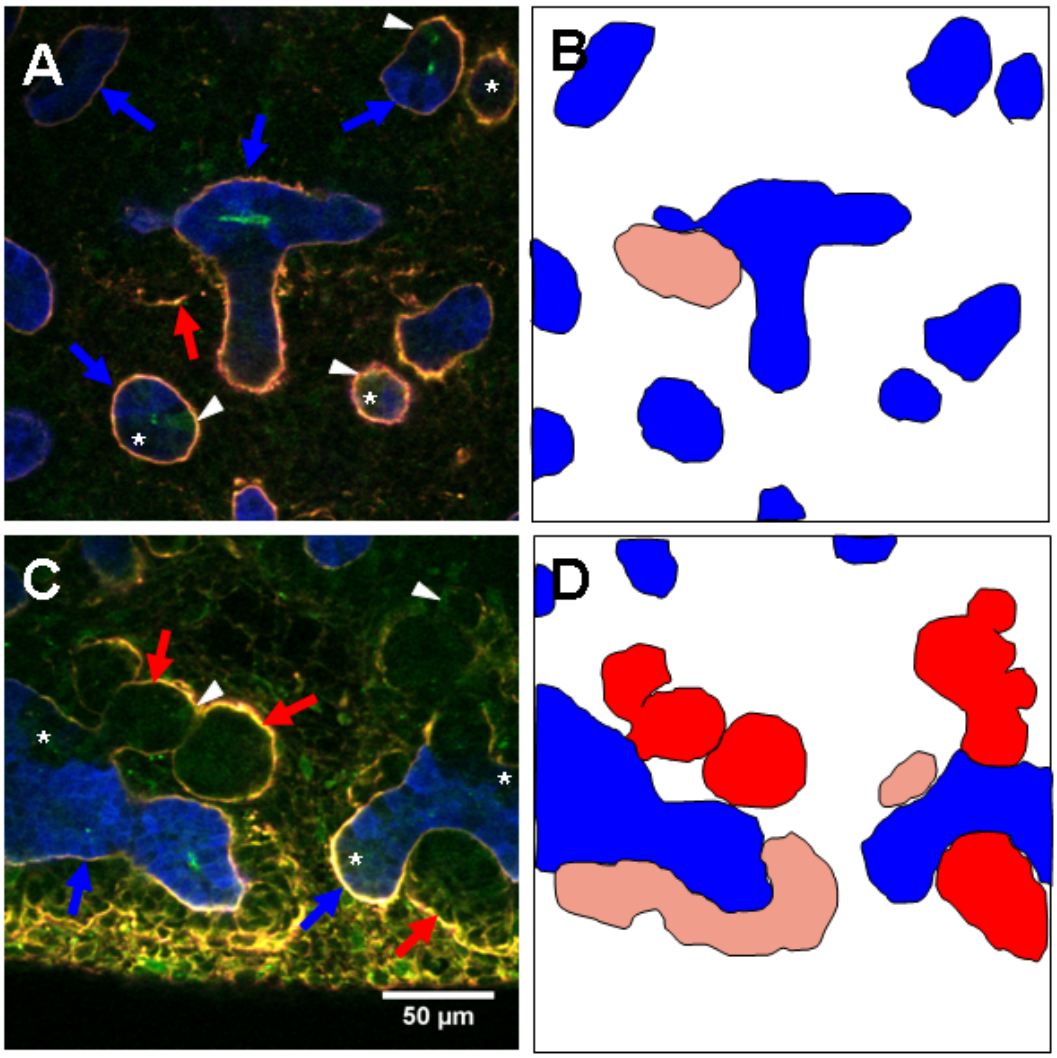

Figure 3.2.1 – Reaggregated organotypic rudiments containing CellTracker-stained E11.5 embryonic kidney cells
A and C - reaggregated embryonic kidney cells after 5 days of culture showing formation of UB fragments (blue arrows) and induction of nephrons (red arrows); stars indicate regions of the UB, which do not express (or express lower levels of) Calbindin, possibly as a result of the CellTracker treatment; B and D - schematic representations of the micrographs given in A and C, showing UB structures in blue, nephrons in red, and the condensing mesenchyme in pink;
green - CellTracker Green-labelled E11.5 kidney cells, red - Laminin, blue – Calbindin; the mixes contain 50% CellTracker-labelled cells

3.2.2 Characterisation of kidneys explanted from TgTP6.3$^{tauGFP+/tauGFP-}$ mice

As the quality of the CellTracker staining was not sufficiently high for the intended experiments, another method for tracing cells had to be sought. It was predicted that using genetically, rather than transiently, labelled cells would allow for a much better

cell traceability. In addition, the possibility of culturing cell mixes for longer periods of time would maximise the number of structures formed and hence reveal more about the potential for cell integration. Therefore, tissues from mice expressing GFP in virtually all of their cells were tested, as described below.

TgTP6.3$^{tauGFP+/tauGFP-}$ transgenic mice were kindly provided by Thomas Pratt, Centre for Integrative Physiology, University of Edinburgh. The transgene consisted of a tau-GFP fusion and puromycin resistance gene, linked by an internal ribosome entry site (IRES). The expression of both was driven by a human cytomegalovirus immediate early enhancer (HCMVIEE), coupled to the chicken β-actin promoter and first intron (Figure 3.2.2, A). Mice hemizygous for the transgene exhibit GFP fluorescence in all of their tissues, while homozygous mice die early in embryonic development (Pratt et al., 2000; MacKay et al., 2005). Upon mating, TgTP6.3$^{tauGFP+/tauGFP-}$ males crossed with wild type (WT) CD1 females would generate only WT embryos and hemizygotes (viable), Figure 3.2.2, B. By fluorescence microscopy it was determined that indeed approximately 50% of all embryos resulting from the matings carried the transgene.

Next, experiments to test whether transgenic freshly isolated unfixed tissues can be identified by fluorescence microscopy were performed. For embryonic kidney cell isolation, caudal parts and E11.5 kidney rudiments were dissected as described in the Materials and Methods section. GFP expression was detected by fluorescence microscopy of freshly isolated living tissue. tauGFP-positive kidney rudiments were clearly distinguishable from non-transgenic ones by their bright green fluorescence. All transgenic kidneys were very highly fluorescent (Figure 3.2.2, E and F), while WT rudiments were clearly negative for GFP (Figure 3.2.2, C). Even after increasing the exposure time for imaging WT kidneys 20 times above original levels, WT and transgenic kidneys were still clearly distinguishable (compare Figure 3.2.2, D taken at 884ms with Figure 3.2.2, E and F, taken at 43ms) allowing for a rapid and accurate microscopy-based determination of genotype.

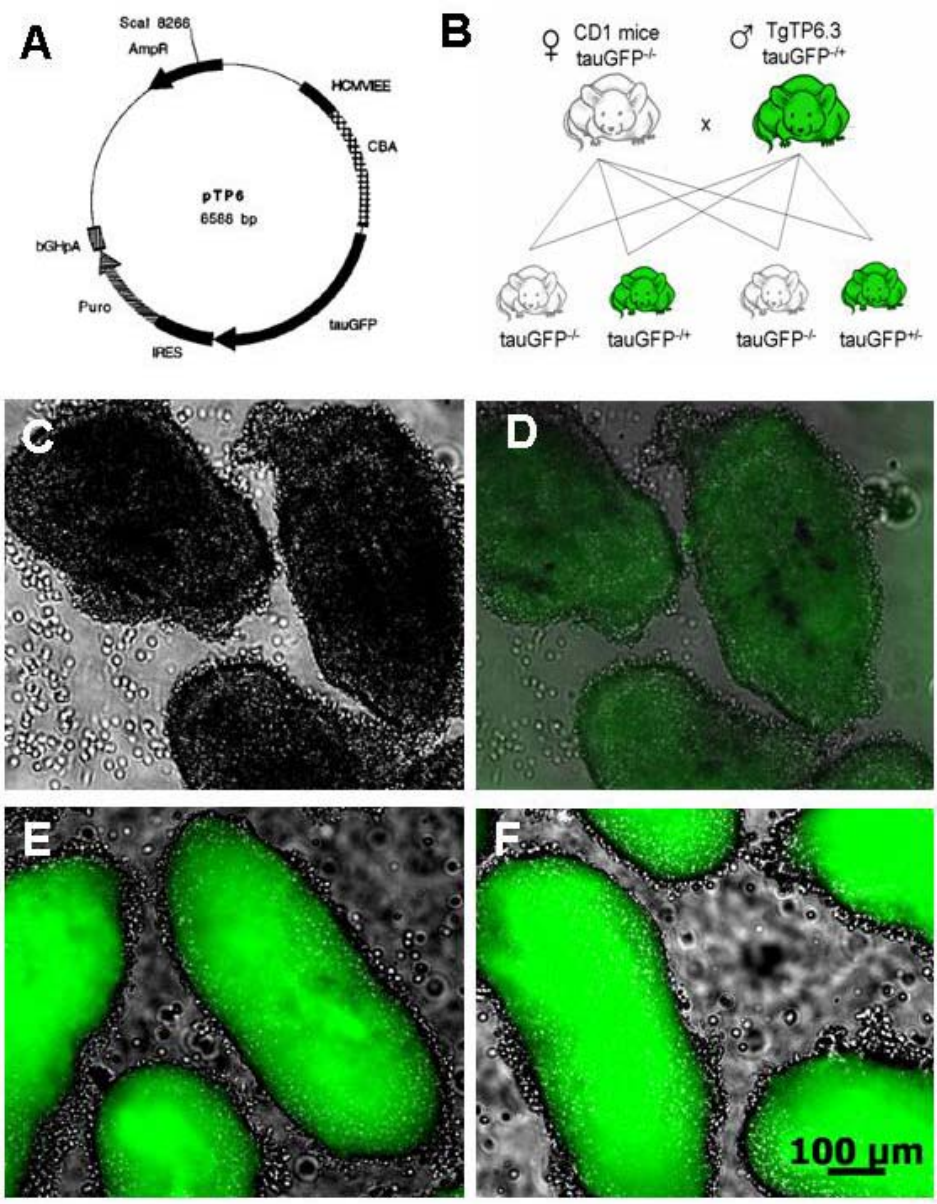

Figure 3.2.2 - Characterisation of GFP expression in TgTP6.3$^{tauGFP+/tauGFP-}$ transgenic mice:
A - a schematic representation of the pTP6.3 construct used for transfection of mouse ES cells and generation of transgenic animals (from Pratt et al., 2000). The construct encodes a tau-GFP fusion and puromycin resistance gene, linked by an internal ribosome entry site (IRES). The expression of both is driven by a human cytomegalovirus immediate early enhancer (HCMVIEE), coupled to the chicken β-actin promoter and first intron; B - illustration of matings between wild-type CD1 females and TgTP6.3 males for the generation of tauGFP+ embryos for experiments. 50% of resulting conceptuses are expected to be transgenic; C - bright-field and GFP fluorescence merge of micrographs of wild type kidney rudiments. Fluorescence channel exposure time 43ms; D - bright-field and GFP fluorescence merge of micrographs of wild type kidney rudiments. GFP channel was captured at 884ms; E and F - bright-field and GFP fluorescence merges of micrographs of wild type kidney rudiments, 43ms; GFP in green

3.2.3 Cells from TgTP6.3$^{tauGFP+/tauGFP-}$ embryonic kidneys show some variation in fluorescence intensity

After successfully verifying the accuracy of transgenic kidney rudiment identification based on fluorescence microscopy, it was necessary to observe mouse kidney rudiments derived from tauGFP+ animals at a cellular level to monitor the differences of GFP-positivity in different types of kidney cells. At E11.5, there are only two or three main types of cells in a developing embryonic kidney - the cells of the UB, the uninduced MM and potentially some induced MM cells. Monitoring only those three cell types, especially before the epithelialisation of nephrons had taken place, does not give useful information about the variability of GFP fluorescence between cell types. For this reason, kidney explants from a later embryonic stage were used for characterisation. E14.5 rudiments were dissected as described for E11.5 rudiments and disaggregated by incubation with 1x Trypsin-EDTA for 5min at 37°C. Cells were plated on 22x22mm cover slips in 6-well plates and fixed with 4% PFA after 24h of culture to let the cells attach.

Microscopic observations of 3 samples, obtained from 5 pairs of plated kidney cells, showed that GFP fluorescence levels were sufficient for detection in all observed cells (Figure 3.2.3, B, C and D). At the same exposure time, control cells obtained from WT E14.5 kidneys did not exhibit any autofluorescence and were virtually undetectable. (Figure 3.2.3, A).

In the cell, the function of the protein tau is to stabilise microtubules and it is therefore localised cytoplasmically (Weingarten et al., 1975). Similarly to the native protein, the tau-GFP fusion protein has also been detected in the cytoplasm and is excluded from the nucleus (Pratt et al, 2000). During cell division, the GFP signal is detected co-localising with the mitotic machinery, suggesting that fusion protein localised as reported for endogenous tau (Pratt et al., 2000; Weingarten et al., 1975).

Although cells were detectable in all cases, the observed primary E14.5 kidney cells had somewhat different fluorescence levels (figure 3.2.3, B, C, D). For example, Figure 3.2.3, C shows phenotypically similar epithelial cells showing lower

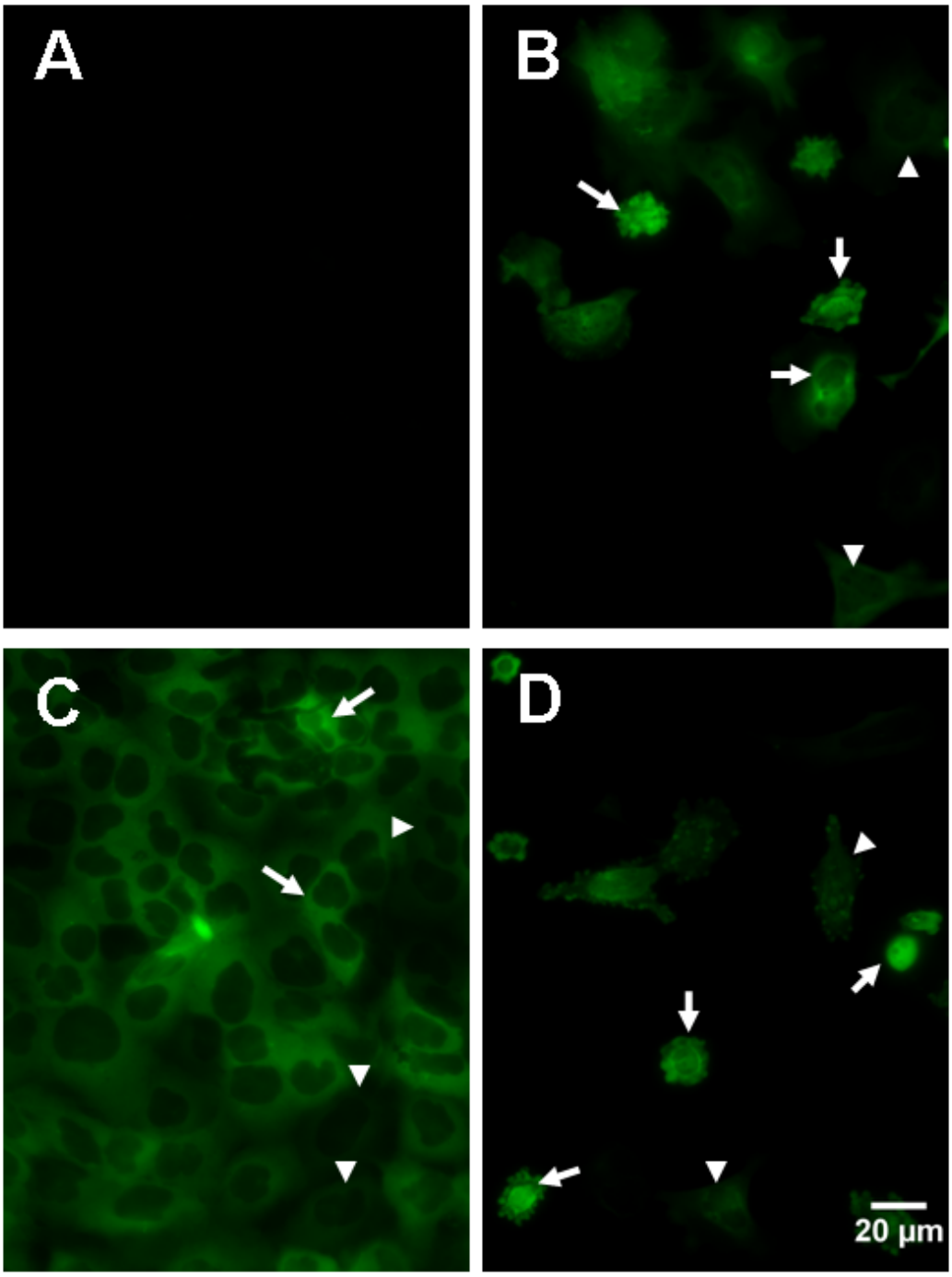

Figure 3.2.3: Characterisation of GFP fluorescence in transgenic kidney cells.
A - control showing wild-type kidney cells derived from wild-type E14.5 embryos; B, C and D - tauGFP expression of E14.5 kidney cells derived from TgTP6.3$^{tauGFP+/tauGFP-}$ transgenic embryos; B and D - show kidney cells with several different morphologies, which express high (arrows) or lower (arrowheads) levels of tauGFP; C - shows differences in GFP intensity between cells with a similar morphology. Arrows point at examples of brighter cells, while arrowheads indicate cells with lower levels of GFP; GFP in green

(arrowheads) or higher (arrows) levels of GFP fluorescence. Differences in fluorescence levels were detected both between morphologically similar and morphologically different embryonic kidney cells.

3.2.4 tauGFP cells are easily detectable in cell disaggregation-reaggregation experiments

WT and genetically labelled with tauGFP kidney cells were mixed and pellets of reaggregating organotypic cultures were prepared. After 6 days of culture, the pellets were fixed and stained for Laminin, Calbindin and DAPI to investigate detectability of tauGFP cells. GFP-positive cells could be clearly seen in the three renal compartments - nephrons (arrowheads, Figure 3.2.4), ureteric bud reaggregates (arrows, figure 3.2.4) and the interstitium (the regions surrounding renal epithelia, green cells not indicated). As integration into renal epithelia rather than the interstitium will be the focus of the following chapters, the presence of cells in the interstitium was not extensively examined.

This preliminary analysis of tau-GFP kidney cells confirmed that genetic marking of cells is significantly superior to using the transient label CellTracker (compare to images on Figure 3.2.1). In addition, cell mixing experiments with CellTracker - stained cells suggested that carry-over of dye is possible and label transfer from grafted cells to host cells might occur (unpublished data, Davies lab; Supplementary Figure 4). This is also inconsistent with the requirements that have been suggested for good cell and lineage markers described in the introduction of this chapter (McLaren, 1976; West, 1984; MacKay et al., 2005). In contrast to CellTracker, the tauGFP-tagged primary cells seemed to fulfil all conditions with the only limitation of variable fluorescence in some cells. The variation of fluorescence between different types of cells might anyway be unavoidable due to the different cell sizes, shapes and function. On the basis of the tests performed, it could be concluded that tauGFP-tagged cells are an excellent and very suitable tool for cell mixing experiments with embryonic kidney cells.

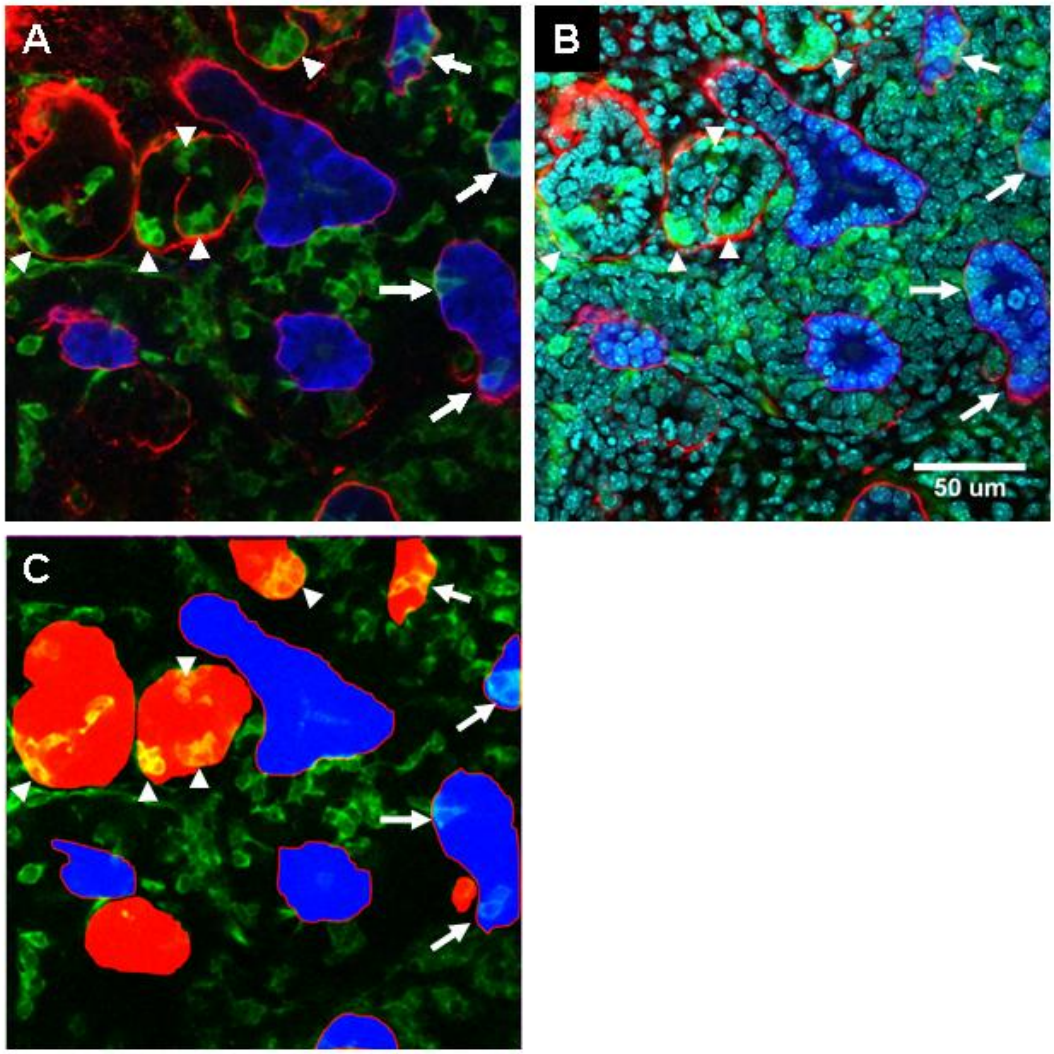

Figure 3.2.4 - Disaggregated E11.5 mouse kidney rudiments containing a mixture of WT and tauGFP+ cells, shown after reaggregation and a 6-day culture
A – tauGFP+ cells (GFP, green) were easily detectable by confocal microscopy when integrated into the structure of both nephrons (Laminin, red) and UBs (Calbindin, blue). They were also well-visible in the interstitium (space around renal epithelia); B – the same confocal section as in A, showing nuclear DAPI staining in cyan, in addition to Calbindin (blue), Laminin (red) and GFP (green); C – a schematised version of the micrograph in A, outlining the nephrons in red and ureteric buds in blue, surrounded by red. GFP+ cells are clearly visible when integrated in both types of structures, as well as when localising in the interstitium.
Arrowheads show GFP+ cells integrating in nephrons. Arrows show GFP+ cells integrating in UBs.

3.2.5 Quantitative studies and a comparison between two methods of analysis for assessing the integration of control GFP-tagged cells provide proof that experiments are robust and repeatable

After a robust method for tracking integrating cells was found, the possibilities for a quantitative use of the disaggregation-reaggregation system had to be tested. For quantitative studies, E11.5 WT embryonic kidneys cells were used as host cells, and tauGFP+ E11.5 kidney cells as control test cells. For every experiment, a defined ratio of green/non-green cells was used for assessment. At the single cell suspension step, the numbers of cells in both suspensions were counted and 15,000 tauGFP+ cells were added to 100,000 WT kidney cells for the formation of pellets. This is a ratio of 1:7.67 tauGFP: WT cells, which is respectively 13 and 87 percent. Assuming that WT and tauGFP+ cells behave in the same way, after 6 days of culture, we would expect to see a proportional rate of integration in the three early renal compartments - UB, nephrons and stroma and comparable results between different experiments.

Pellets for quantification were prepared and treated, as follows. After centrifugation, the pellets were cultured in CKCM supplemented with 1.25μM ROCKi. The medium was replaced with conventional CKCM after 24h to remove the inhibitor. Pellets were grown for 6 days and co-fixed with PFA and methanol. Samples were triply stained for the UB-maker Calbindin, the component of the basal lamina - Laminin, and DAPI for nuclei. As previously demonstrated, Calbindin appears as a uniform staining throughout the cell. Laminin is detected in the basal laminae of both UB structures and nephrons and therefore appears as an outline of both UB structures and nephrons. Therefore, when analysing images of kidneys, a Calbindin+ Laminin+ epithelial structure was identified as a UB, while a Calbindin- Laminin+ - as a nephron.

The integrated cells were detected by GFP expression. Assessing the numbers of cells in the renal compartments was performed on the basis of the DAPI staining.

In addition to a repeatable and robust procedure for producing pellets containing the same number of GFP+ cells, an appropriate and statistically relevant method had to be designed for acquisition and assessment of the data. A common procedure for data collection and analysis was therefore devised to screen organotypic cultures rapidly and accurately by confocal microscopy. At least 6 pellets resulting from at least 3 separate experiments obtained by reaggregation-disaggregation were analysed by confocal microscopy. For each experiment, multiple kidney rudiments were isolated and disaggregated to obtain enough cells for the generation of cell mixes. For each pellet, 15 confocal micrographs were made, each showing a single confocal section. The areas of sample to be micrographed were selected by visual inspection of the Laminin staining, which is only indicative of the presence of structures, but gives no information about the presence or localisation of tauGFP+ cells. Areas containing any structures were selected at random. It was necessary to control for micrographing areas containing kidney epithelial structures, as otherwise, no useful information for the integration of these into test cells would have been extracted.

Only 10 of the 15 confocal sections were used for cell counting analysis. It was noticed that thicker pellets are more difficult to stain in their central areas in comparison to peripheral ones. That is why 5 of the 10 sections taken were used as spares, in case the quality of some images was not sufficient for quantification.

In the test stainings, penetration problems were more apparent in the DAPI channel, where nuclei in the core of the pellets were almost indistinguishable. Including DAPI in the secondary antibody mix for an overnight incubation, rather than at the end of the staining process, improved the outcome sufficiently for cell counting.

Two methods were devised for screening the pellets for integrating tauGFP+ cells. Method 1 used for analysis assesses the percentage of green cells (tauGFP+ cells) localising in each of the three different embryonic kidney compartments - UB, nephrons and stroma. For this purpose, the following were counted in 60 confocal sections:

- the total number of cells on a section which includes the number of WT cells and tauGFP+ cells - **TC**
- the total number of green cells on a section - **TGC**
- the total number of all cells localising in all UB structures on a section - **UBC**
- the number of green cells localising in UBs on the same section - **GCUB**
- the total number of all cells localising in all nephrons on a section - **CN**
- the number of green cells localising in nephrons on the same section - **GCN**

The total number of stromal cells (**TSC**) has been calculated by subtracting the number of cells in nephrons and UBs (**CN + UBC**) from the total number of cells (**TC**).

TSC = TC - (CN + UBC)

The total number of green cells in the stroma (**GCS**) has been calculated by subtracting the green cells in UBs and nephrons (**GCUB + GCN**) from the total number of green cells on the section (**TGC**).

GSC = TGC - (GCUB + GCN)

Cell integration was assessed according to the criteria described below. Nuclei were counted on the basis of DAPI staining. A structure was identified as a UB fragment when it was both Calbindin+ and Laminin+. A second supporting criterion was used in addition due to differences in staining intensity of UBs, which made the identification of some UB fragments difficult. Unlike nephrons, which have a more complex morphology, the UB normally consists of a single-layered epithelium with regularly arranged cells. Observing the positioning of nuclei on the basis of DAPI staining therefore gives additional information about the identity of the structure. In a nephron, the basal lamina component - Laminin marks the basal (outer) side of the nephron. At the same time no Calbindin expression is observed. A Laminin+ Calbindin- structure was assigned a nephronal identity. A morphological criterion for identification of nephrons was also used in addition to the histochemical information

- nephrons appear much more convoluted, may appear multilayered and contain cells with different nuclear shapes and sizes.

On the basis of these counts, the following proportions were calculated:

- the percentage of cells in UB that are green
- the percentage of cells in nephrons that are green

First, the issue of calculating the minimum number of sections necessary for accurate analysis was addressed, by plotting the trend of the mean number of green cells and the mean standard deviation for every additional section count. The running mean of total green cells and the running standard deviation were analysed for 40 separate sections. As can be seen on Figure 3.2.5, the running mean fluctuates severely in the initial counts, up to 7 sections counted, then decreases to about 170 cells per section at section 30 and maintains a relatively constant level thereafter. A similar effect was noticed for the running standard deviation, which is high in the first few counts, but then decreases and starts maintaining a constant level. On the basis of this analysis, it could be concluded that counting 30 sections per experiment gives a sufficient level of accuracy for the quantitative analysis of integrating cells.

Second, it was determined whether a minimum of three biological replicates was sufficient for accurate data representation of the proportion of green cells integrating in nephrons and UBs. The results are shown for each one of three separate experiments, as well as after pooling all counts (Figure 3.2.6 A, B and C). The values shown are the GFP+ cells localised in UBs or nephrons, as a percentage of the total number of cells in either type of renal epithelia. The data is presented as 95% confidence intervals for the mean number of cells localising into either UBs or nephrons ± the margin of error in percent. The normal theory approximation of a confidence interval of a proportion was used. It is known as the Wald interval and defined by:

$$\hat{\pi} \pm z\sqrt{\hat{\pi}(1-\hat{\pi})/n} \qquad (1)$$

(Wald and Wolfowitz, 1939) where $\hat{\pi}$ is the proportion of successes in a Bernoulli trials process, estimated by the statistical sample. Z is the $z_{1-\alpha/2}$ quantile or the 1-α/2 percentile of a standard normal distribution and n is the sample size. For a 95% confidence interval $\alpha = 0.05$, so $z_{1-\alpha/2} = 1.96$.

The analysis of 90 sections obtained from three separate experiments for cells localising into either UBs or nephrons showed that the efficiency of integration in these two compartments can vary between experiments (Figure 3.2.6, A, B and C). Integration in UBs ranged from 17.23 ± 0.91% to 30.92 ± 1.23% in the three

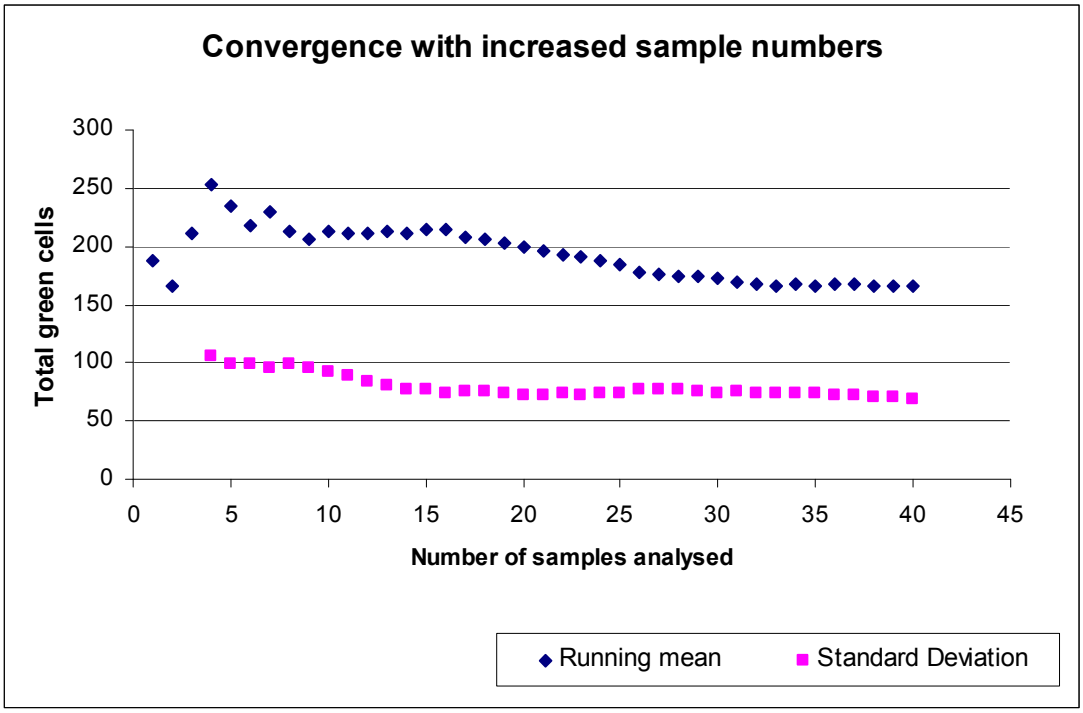

Figure 3.2.5 - Determining the minimum number of sections necessary for accurate cell quantification by examining the behaviour of the running mean and running standard deviation

This analysis was based on reaggregated pellets containing approximately 13% tauGFP+ cells mixed with WT cells. Pellets were cultured for 6 days, fixed and stained for counting of green cells. The mean number of green cells and the mean standard deviation for every additional section count are shown on the graph. The running mean of total green cells per section and the running standard deviation were analysed for 40 separate sections. The running means (blue diamonds) fluctuate severely in the initial counts, up to 7 sections counted, then decrease to about 170 cells per section at section 30, and maintain a relatively constant level thereafter. A similar effect was noticed when plotting the running standard deviation, which is high in the first few counts, but then decreases and also starts to maintain a constant level. After section 30, additional measurements did not change the trend of the running mean or running standard deviation, which indicated the minimum number of sections required for quantification.

different experiments, while integration in nephrons ranged from 11.86 ± 0.96% to 19.41 ± 0.62%. Pooling the data for all three experiments resulted in obtaining very similar efficiencies of integration - 22.78 ± 0.50% for UB cells and 19.41 ± 0.52% for nephron cells (Figure 3.2.6, A, B and C, pooled). A two-tailed student's t-test for these populations showed that the difference in efficiencies of integration is not significant ($p = 0.25$). These results suggest that for standardised quantitative studies, pooling the results from at least three separate experiments is sufficient for decreasing the experimental error of the variation in different biological samples.

In addition, it was interesting to observe that presenting the data as an average of the GFP+ cells integrating in both types of renal epithelia resulted in correcting the proportions of cells - the same percentage of green cells was calculated for all three individual experiments (Figure 3.2.6, D). In addition, comparing the graphs on Figure 3.2.6, A and B, it can be noticed that the mean percentage of green cells in UB decreases from Experiment A to Experiment C, while the mean percentage of green cells integrating in nephrons increases proportionally at the same time. The average of both types of renal epithelia approximates 21% in all experiments (Experiment 1, Experiment 2 and Experiment 3), as well as in the pooled data set (Figure 3.2.6, D). As the proportion of total GFP+ cells in both types of renal epithelia seems to be constant in all three experiments, the variation of green cells in nephrons versus ureteric buds, seems to be due to variation in the homogeneity of cells in the starting populations used for mixing. More precisely, it is possible that the 15,000 green cells mixed into Experiment 1 contained more UB cells than the 15, 000 cells mixed into Experiment 3. Therefore, the variation that is observed is not due to an error in the method of analysis, but is due to the natural variation of cells in the starting population. On the contrary, these results suggest that the combination of experimental method and method of analysis gives an accurate, but also a sensitive, representation of small differences in the starting populations of cells. These results suggest that the quantification method is indeed a very useful tool for comparing two populations of cells with very similar renogenic potentials.

The similar integration rates of GFP+ cells, together with the recurrent percentage of green cells integrating in renal epithelia in individual experiments was a good indication that in spite of the large variance that can occur between different experiments, a sufficiently large number of samples and repeats makes this method a robust way for comparing the integration potential of different types of cells. In particular, the results in this chapter have identified that analysing at least three separate experiments (biological replicates) with three technical replicates each, 10 sections each, gives an excellent basis for comparing the ability of cells to integrate into renal epithelia.

Furthermore, an alternative method for analysis was applied to confirm the results obtained by Method 1. Instead of calculating percentages of cells, the number of cells per unit area of a certain renal compartment was used as an indicator. 60 sections were analysed by both methods to allow for comparable results. For quantifying the proportion of cells in each compartment that are green, analysis was performed as described for Method 1. For assessing the number of green cells per unit area, the following were calculated for the same set of data:

- the number of green cells localising in nephrons per unit area
- the number of green cells localising in UBs per unit area
- the number of green cells localising in the stroma per unit area (the number of green cells in the stroma was calculated by subtracting the green cells in nephrons and UB from the counted total number of green cells on a section; the area of stroma was quantified by subtracting the area of nephrons and buds on the confocal section from the total area of kidney tissue captured on the same section)
- the total number of green cells on a section per unit area (in this instance, the total area taken up by the reaggregated kidney rudiment on a section)

A

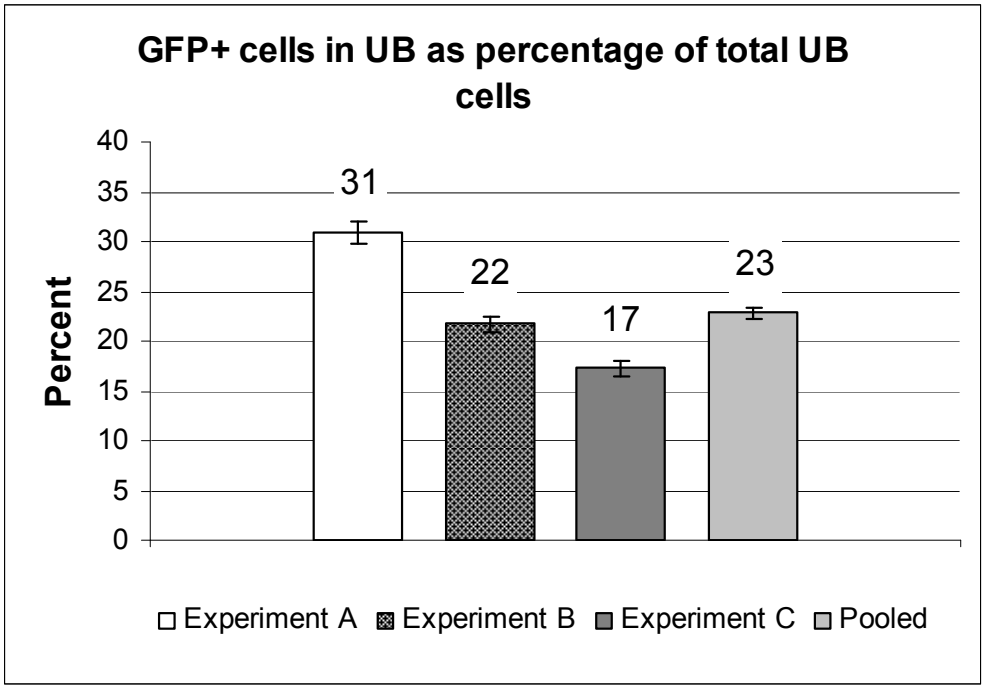
GFP+ cells in UB as percentage of total UB cells
Percent
40
35
30
25
20
15
10
5
0
31
22
17
23
Experiment A
Experiment B
Experiment C
Pooled

B

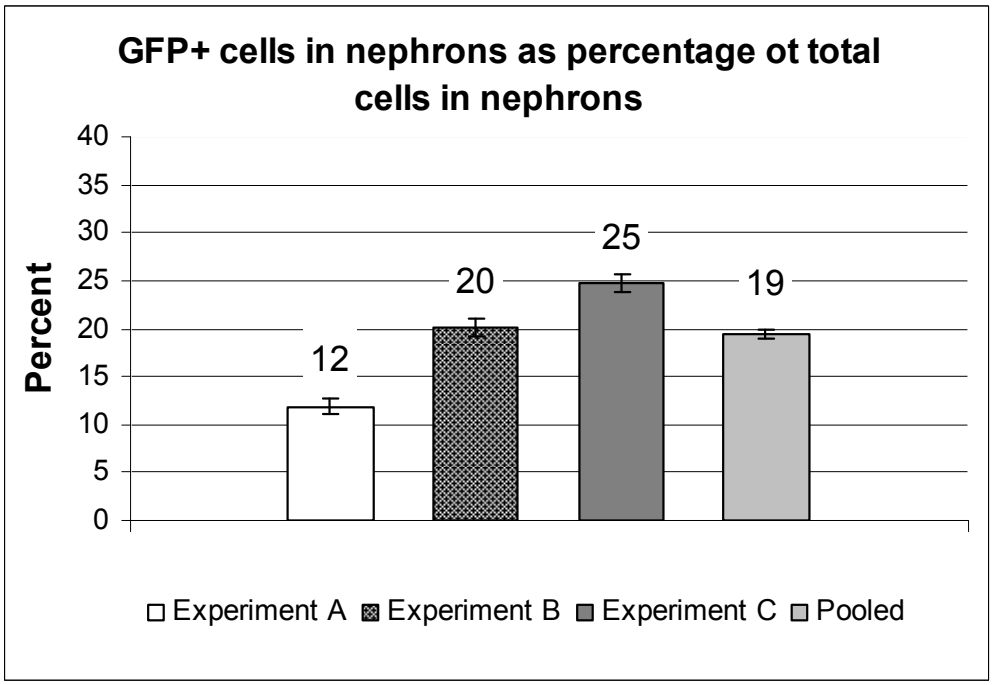
GFP+ cells in nephrons as percentage ot total cells in nephrons
Percent
40
35
30
25
20
15
10
5
0
12
20
25
19
Experiment A
Experiment B
Experiment C
Pooled

C

	GFP+ cells in UB [percent of total UB cells ± margin of error]	GFP+ cells in nephrons [percentage of total cells in nephrons ± margin of error]
Experiment A	30.92 ± 1.23	11.86 ± 0.96
Experiment B	21.71 ± 0.95	20.17 ± 1.04
Experiment C	17.23 ± 0.91	24.79 ± 1.15
Pooled data	22.78 ± 0.59	19.41 ± 0.62

D

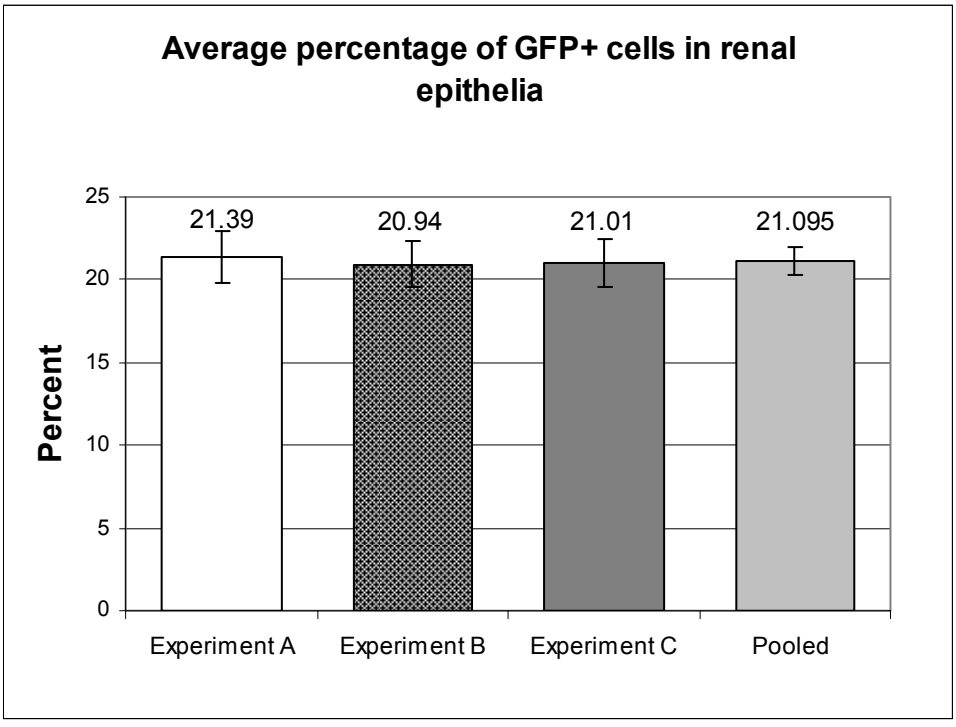

Figure 3.2.6: Quantification of the percentage of GFP+ cells integrating in renal epithelia
A - illustrates the GFP+ cells localising in UB structures as a percentage of total UB cells; Experiment A showed that 30.91±1.03% of all UB cells were green, expressed as a percentage of total cells ± the margin of error as calculated for a 95% confidence interval; 21.71±0.80% of all UB cells in Experiment 2 were green in comparison with 17.23±0.77% in Experiment C. The average percentage of UB cells that were GFP+ was calculated by pooling all data and was 22.78±0.50%.

B - illustrates the GFP+ cells localising in nephrons as a percentage of the total number of cells in nephrons; Integration of GFP+ cells in Experiment A is 11.86±0.80%, Experiment B - 20.17±0.87% and Experiment C - 24.79±0.97%. The pooled data shows integration 19.41±0.52% when calculated for all data sets. The percentages in both A and B rounded to a whole number are shown above each bar.

C - A table summarising the values obtained from counting experiments, represented as a percentage of cells in two types of renal epithelia that are GFP-positive ± the margin of error based on a 95% confidence interval experiments are shown separately and as a pooled set of data

D - the bar chart shows the integration of green cells in both types of renal epithelia (nephrons and UBs), collectively without discriminating for a particular type. The data sets for the bar chart were generated by averaging the data from A and B. The margins of error were calculated by following the rules for error propagation after mathematical operations on the basis of the values from A and B. The percentages of cells integrating in renal epithelia in experiment A, B and C, as well as the pooled data from all experiments, are shown above the bars.

Area measurements were made on the basis of visual inspection of Calbindin and Laminin staining (as previously described) and manual selection of the relevant areas in ImageJ. To avoid scaling errors, the results were obtained in pixels from the raw data. As the number of green cells per pixel gave a very small and inconvenient for representation value, the data was therefore converted to cells per kilopixel (1000 pixels = 1 kilopixel). It must also be noted that the error for Method 1, which was previously given as a 95% confidence interval has now been converted to SEM for two reasons - the data were given as a proportion, not in percent; to be able to compare the analyses obtained by Method 1 and Method 2 (measuring cells per unit area doesn't result in a binomial distribution as it is not a "yes/no" event). As calculating the proportions of green cells required division of measured values, mathematical operations were used to calculate the propagation of uncertainty, while obtaining these values.

A comparison between the two methods for data analysis of integration is shown in Figure 3.2.7 A, B and C. As can be seen from the bar graphs and table, both methods show extremely similar results. For simplicity in describing the comparison between the two methods, the value obtained by dividing the number of green cells per renal compartment by the total number of cells in the same compartment (for Method 1) or by the area of the compartment in kilopixels (for Method 2) will be referred to as Integration Coefficient. The values used to generate Figure 3.2.7 A and B are given in Figure 3.2.7. It can be seen that in both methods, very similar proportions of GFP+ cells were observed in nephrons (0.14 ± 0.02 for Method 1 and 0.13 ± 0.01 for Method 2) and the stroma (0.18 ± 0.01 and 0.17 ± 0.01). Although for UB cells, the mean Integration Coefficient for Method 1 was slightly higher than the value obtained for Method 2 (0.29 ± 0.04 versus respectively 0.22 ± 0.03) that difference was still accommodated for by taking into account the standard errors. The cumulative Integration Coefficients for all renal compartments taken together were essentially the same - Method 1 showed tauGFP+ cell integration of 0.19 ± 0.01, while Method 2 indicated a number of 0.18 ± 0.01. This analysis provides proof that both the experimental approach allowed an estimation of the ability of cells to integrate into renal epithelia, but also that the analysis methods provided for a good

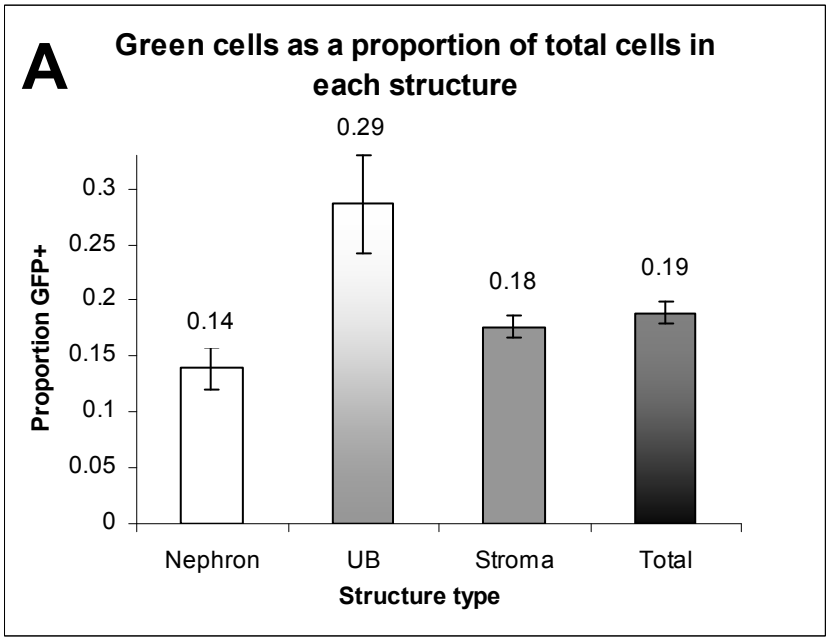

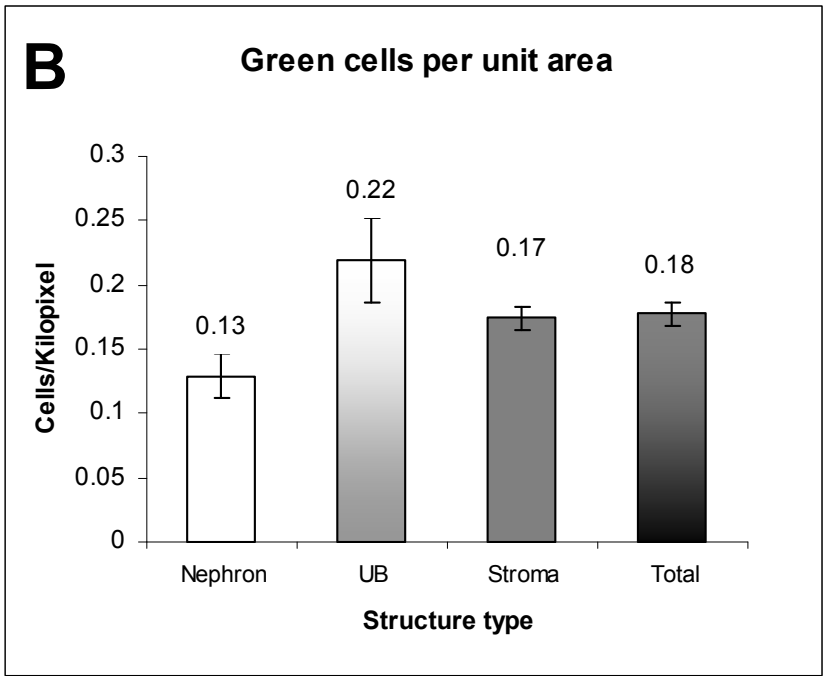

	Integration Coefficient Method 1 ± SEM	Integration Coefficient Method 2 ± SEM
Nephron	0.14 ± 0.02	0.13 ± 0.02
UB	0.29 ± 0.04	0.22 ± 0.03
Stroma	0.18 ± 0.01	0.17 ± 0.01
Total	0.19 ± 0.01	0.18 ± 0.01

Figure 3.2.7 - Comparison of two methods for analysis of cell integration

A - shows analysis Method 1, based on estimating the proportion of cells green cells in each compartment (by dividing the number of GFP+ cells by the number of GFP- cells in each compartment).
B - the same set of data analysed by Method 2, which measures the average number of green cells found in a particular compartment per unit area. Values are shown as the number of cells per kilopixel area of the confocal section.

C - illustrates the raw data for generating the bar graphs in A and B and compares the integration coefficients of Method 1 and Method 2. The integration coefficient of Method 1 was formed by calculating the proportion of green cells (from total cells) in a compartment. The integration coefficient in Method 2 is the number of green cells per kilopixel area of the respective renal compartment. Error bars were calculated by following the mathematical operations for propagation of uncertainty based on the SEM.

and accurate interpretation of the results. It was concluded that using either method for quantitative studies would offer an accurate method for assessment of the integration potential of different types of cells.

3.2.6 Quantification studies could not reject the possibility that the tauGFP+ cell population might grow faster than the WT population

After having considered the suitability of the disaggregation-reaggregation system for quantitative studies and compared two possible methods for data analysis, I investigated whether the experimentally obtained values correspond to the theoretical numbers of cells expected to be found in renal structures. As previously mentioned, 15,000 GFP+ cells were mixed with 100,000 WT cells for pelleting. Therefore, we would expect the pellets to contain about 13% of GFP+ cells. By Method 1 it was determined that 18.90 ± 0.32% of all cells in pellets were green. This is 5.90% ± 0.32% more green cells than expected. As even the largest error calculated for a 95% confidence interval could not accommodate the difference, it either came from uncertainty that wasn't accounted for or the observation was not a random event. If the increased numbers of cells were not observed by chance, the possible reasons could be - tauGFP cells proliferate faster than WT cells; fewer tauGFP undergo cell death in embryonic kidney development; tauGFP cells survive manipulations and enzymatic treatment better; tauGFP cells respond more to treatment with ROCKi, which inhibits cell death. To address whether there are such differences between WT and tauGFP cells, a protocol for monitoring the change of cell numbers was devised. Although cells are largely different in size, shape and protein content, their DNA content should be the same for all types of cells. Therefore, the amount of DNA extracted from a population of cells could serve as an indicator of relative cell number. This method was employed to detect whether tauGFP cell numbers increased more than WT cell numbers, as described below.

An equal number of tauGFP+ and WT kidneys was isolated from E11.5 mouse embryos. Half of the freshly isolated rudiments were used for immediate DNA isolation (time point 0) and the other half - after 6 days of culture. To minimise variability between the pools of rudiments used at the two different time points, the

pair of kidneys isolated from the same embryo was always divided between the two groups. Quantifying the amount of DNA in the starting culture would allow correcting for cell number differences between the two tested populations at the beginning of each experiment.

The second half of isolated kidneys was cultured for 6 days in a conventional culture system, as consistent for the mixed-cell pellets characterised earlier in this chapter. The DNA content in the second half of rudiments was quantified after 6 days of culture. Dividing the DNA content at D6 by the value from D0 would provide information about the relative increase in cell number after 6 days of culture or how many times the population has increased from D0 to D6. As the growth of a whole population of cells is a balance of cell proliferation and cell death, such a comparison will provide insight only about the cumulative effect of both, which will be referred to as "growth". As cell proliferation and cell death were not a particular focus of this thesis, they were not pursued individually.

The results of 5 independent experiments are summarised on Figure 3.2.8. Figure 3.2.8, A shows a comparison between the increases of the DNA content in wild type (extracted from CD1 mice) kidneys and tauGFP+ kidneys. From the bar chart we see that the population of cells in the CD1 pool has increased 2.62 times from D0 to D6, while the population of cells in the tauGFP pool has increased 3.09 times. The data given are averages on the basis of 5 individual experiments. Error bars are standard errors of the mean (SEM). Although, tauGFP cells indeed showed a higher increase in cell number, it was found that this difference was not significant. A two-tailed student's t-test assuming unequal variance gave a p value of 0.43. Even if we postulate that it is not possible to measure a higher than the real DNA concentration at any point and therefore perform a one-tailed student's t-test, the p value drops only to 0.22, once again failing to reject the null hypothesis. Although the data from these experiments did not show a significant difference in the relative growth of WT and tauGFP+ rudiments, it was interesting to observe that the value for tauGFP cells was consistently higher than that of WT cells in all five separate experiments (Figure 3.2.8, B). In addition, Figure 3.2.8, B demonstrates that the increase in DNA content between cultured CD1 and tauGFP kidneys was significant in two of the five

experiments performed. This suggests that the number of experiments performed might not have been sufficient to pinpoint potential differences in population growth. A second method for analysis was used to test whether different treatments of data give the same results. Rather than comparing the times increase in DNA concentration, the change of DNA concentration, or Δ[DNA], was expressed as the difference of the DNA concentration at D6 and the DNA concentration at D0. The main specificity about using this approach is that the number of kidneys used in each experiment was also taken into account to calculate Δ [DNA] per kidney, unlike in the first method. For the first method, expressing the results per kidney does not change the result as the ratios of [D6]/[D0] for one kidney or all kidneys remains the same as an equal number of kidneys were used at both time points and the components cancel each other. The results obtained using the second approach, recapitulated the initial analysis. TauGFP+ kidney cells showed a larger difference of DNA content between D6 and D0 (the average increase observed per kidney was 536ng, in comparison to CD1 cells (384ng). Although, the difference was quite large, a student's t-test showed that it was not significant. Similarly to the previous approach, looking at every experiment separately, demonstrated that tauGFP tissues generated a higher concentration of DNA from the same number of rudiments.

Two other independent studies also showed that there was a larger increase in tauGFP cells, as compared to wild-type cells. In the first test, numbers of cells were counted, instead of quantifying DNA. Cell counts were performed with a standard Neubauer chamber. To correct for inaccuracies in pipetting and counting, each sample was pipetted onto the counting chamber 4 individual times and the same pipetting was counted thrice. The increase of cells from D0 to D6 was expressed as a ratio of the number of cells at D6 divided by the number of cells at D0 (similarly to the DNA quantification experiments). These cell counts showed a once again higher proportion of tauGFP+ cells in comparison to WT cells (Figure 3.2.9). The final difference between the cell numbers obtained from CD1 and tauGFP kidneys was significant when analysed with a two-tailed student's t-test assuming unequal variance ($p<<0.01$). These results could not be treated as conclusive as only one experiment was performed.

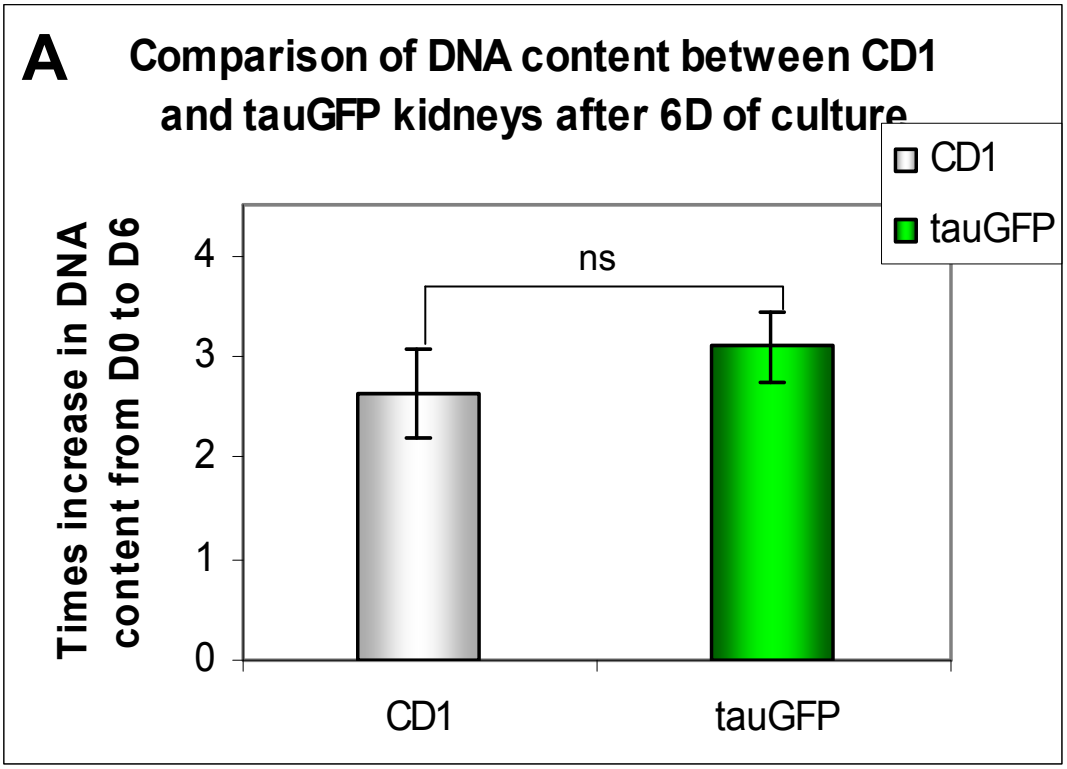
A
Comparison of DNA content between CD1 and tauGFP kidneys after 6D of culture
CD1
tauGFP
Times increase in DNA content from D0 to D6
4
3
2
1
0
ns
CD1
tauGFP

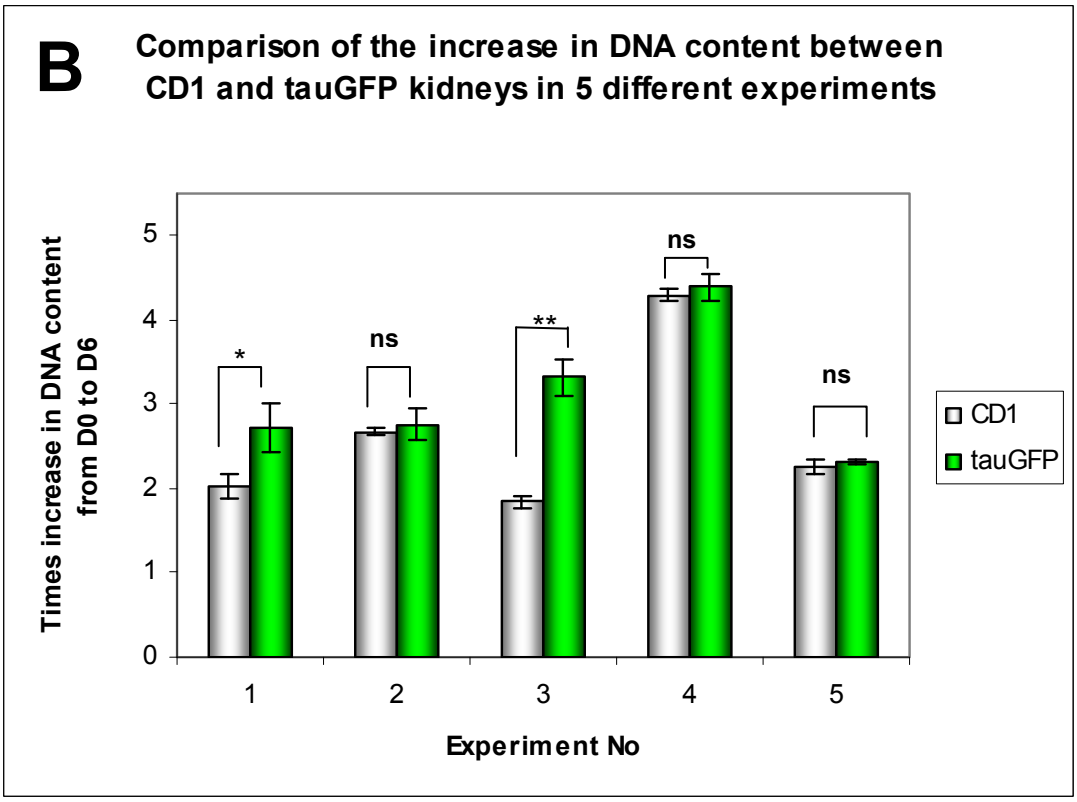
B
Comparison of the increase in DNA content between CD1 and tauGFP kidneys in 5 different experiments
Times increase in DNA content from D0 to D6
5
4
3
2
1
0
*
ns
**
ns
ns
1
2
3
4
5
Experiment No
CD1
tauGFP

Figure 3.2.8 - Comparison of the DNA content of CD1 and tauGFP embryonic kidneys after 6 days of culture

A - shows the times increase of the DNA content of both types of kidneys from D0 to D6. The data is based on 5 separate experiments. The DNA content measured on the basis of DNA extraction from all right kidneys of embryos at D6. Differences in the starting concentration of DNA were corrected for by an initial quantification of the DNA content of all left kidneys at D0. The error bars are standard deviation. The difference between CD1 and tauGFP kidneys is non-standard on the basis of a two-tailed unpaired student's t-test.

B - Shows the results obtained from all 5 individual experiments separately. 2 out of the 5 experiments showed a significant difference between the increase in DNA concentrations of tauGFP and CD1 kidneys. Bars are standard deviation. Ns - non-standard; * = $p < 0.05$; ** = $p < 0.01$

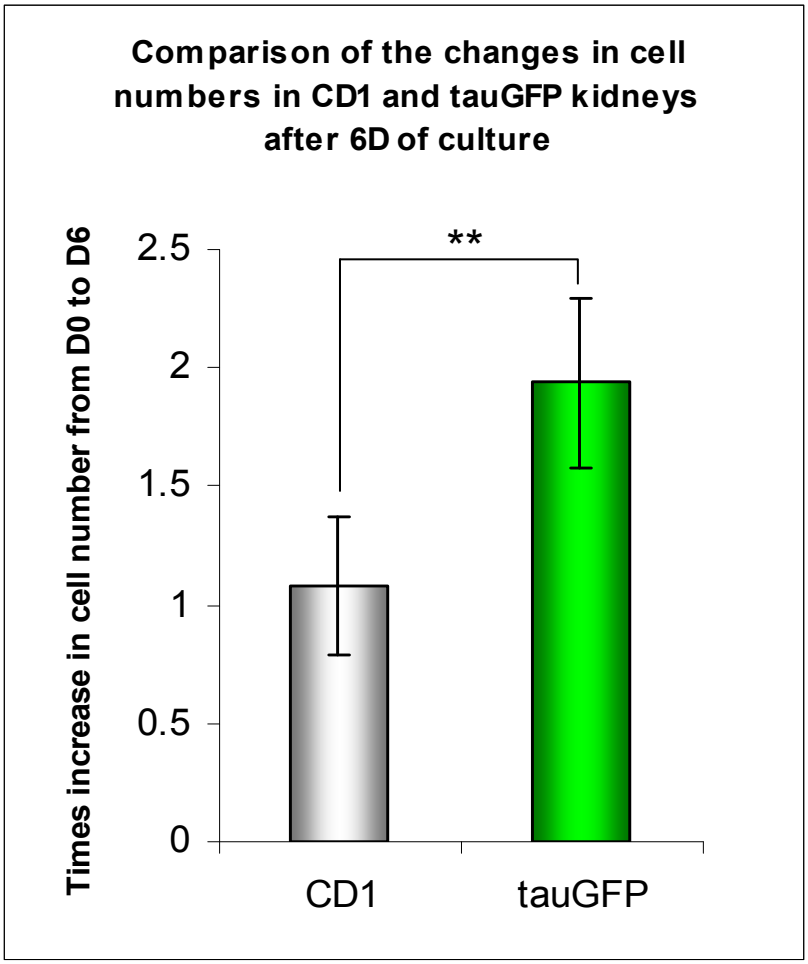

Figure 3.2.9 - A comparison of the increase in cells numbers of CD1 and tauGFP kidney cells after disaggregation, reaggregation and 6D culture
The number of CD1 cells increased 1.08 times, while the number of tauGFP cells increased 1.93 times. Cells were counted three times in 4 separate pipettings both at D0 and at D6. The error bars show standard deviation. Significance was estimate with an unpaired student's t-test assuming unequal variance ($p = 0.003$).

Similar results were obtained when DNA was isolated from cultured pellets made from the same number of tauGFP+ and tauGFP- cells. DNA yield for GFP+ cells was higher after 6 days of culture. 2.21µg DNA were obtained from CD1pellets, while 2.85µg were calculated for tauGFP pellets. Only one experiment was performed.

The results from all experiments studying the possibility for differences between WT and tauGFP kidneys were not conclusive, but the possibility for such a difference

could also not be rejected on the basis of the experimental analysis performed. On the contrary - results suggested that designing methods to decrease variation and performing a large number of experiments might demonstrate the existence of a potential difference between the two types of rudiments. A separate study would be needed to address this issue for obtaining more conclusive data. Importantly, this study has shown that there are either no significant differences in the growth of WT and tauGFP cell populations or the latter grow faster. This suggests that the detection of tauGFP cells will not be lost in experiments due to an overgrowth by WT cells.

3.3 Summary and discussion

In this chapter, I have described the development and testing of tools improving the available methods for studying kidney development and the renogenic potential of different types of cells. I have developed a robust quantitative method for assessing the potential of cells on the basis of their ability to contribute to the structure of developing ureteric buds and forming nephrons. In this section, I will shortly discuss, how the developed method satisfies the 7 conditions for a good assay for studying the renogenic potential of cells, on the basis of the experimental results from section 3.2.

First, the identification of a good method for tracking cells after mixing them with embryonic kidney cells has been described. In these studies, the use of tauGFP+ mouse embryos for cell extraction and mixing studies has proven significantly better than transient labeling methods such as CellTracker. Some of the disadvantages of transient labelling are that the label is diluted out with cell divisions, which significantly decreases the permissible culture time of experiments. In addition, experiments have shown that although CellTracker labelling indeed worked robustly every time (based on microscopic verification after each staining procedure), at the end of the culture time the intensity of staining differed between experiments (results presented in Chapter 5). The staining of control embryonic kidney cells with CellTracker generated images, in which labelled cells were extremely difficult to distinguish. These micrographs would be very difficult to interpret in qualitative

studies and will not be useful at all for quantifying integrating cells. In contrast, the use of genetically labelled cells largely improved the quality of the images produced and made the detection of cells much easier. It fulfilled all 6 requirements for a good marker for cells, as described in section 3.1.3. The only limitation that could be detected was the slight variation of fluorescence levels between some cells. In later quantitative experiments including cell counts, it was determined that this does not have an impact on cell detectability. Then, the other criteria for a good assay, discussed in section 3.1.3 were tested. As required, it was determined that in control conditions the disaggregation-reaggregation system allowed for the integration of cells in both UB and nephrons (condition 4). It worked well in combination with confocal microscopy (condition 5) and allowed the assessment of at least two markers simultaneously, as demonstrated by Calbindin/Laminin co-staining (condition 6). Quantitative studies also confirmed that this method was suitable for introduction of a defined number of cells, a homogenous distribution of the tested cells and counts resulted in useful quantitative data (conditions 1, 2 and 3).

Several limitations of the disaggregation-reaggregation system have also been identified. Experimental analysis showed that the proportion of cells integrating in the three early kidney compartments - nephrons, UBs and stroma, varied significantly between experiments. Experiments suggested that this was due to varying proportions of cells in the starting populations. Furthermore, quantitative data demonstrated that this problem can be solved by performing a sufficient number of biological repeats. Another limitation of the assay was that the experimental percentage of tauGFP cells found in renal epithelia was higher than the theoretical value. As previously mentioned, tauGFP+ cells express a tau-GFP fusion protein under the CAG promoter. Pratt et al. (2000) have reported that the tauGFP fusion protein is very clearly distinguishable in the process of neurons carrying the construct, in contrast to other cells carrying a construct for GFP only. This leads to the conclusion that the tauGFP fusion helps the reporter protein to be transported to the processes of neural cells and that the tau component is functional. Tau is a protein essential for and a major regulator of microtubule assembly (Weingarten et al, 1975). It acts by a physical contact with microtubules. This means that the tauGFP

fusion protein might play a role in providing additional stability to microtubules due to the existence of the GFP moiety, thereby providing increased protection to the cell in conditions of stress, such as enzymatic treatment. To detect such a possible difference between tauGFP and WT cells, additional experiments were performed. DNA quantification experiments were used as an approach to monitor the change of relative cell number and therefore as an indirect indicator of growth (defined as the balance of cell proliferation and cell death in a population of cells). Experiments based on DNA quantification of cultured kidneys of both types showed a higher average increase in DNA content for tauGFP+ kidneys, but this effect was not significant. Supporting experiments confirmed these results, although did not provide any statistically assessable data. Although this study did not identify the reason for the higher than expected percentage of tauGFP positive cells, it was very important in providing an independent check that tauGFP cells did not grow slower than WT cells. In cell mixing experiments, a higher proportion of tauGFP cells would not affect the final conclusions from experiments, as it has been shown to reappear consistently in all experiments. It is essential, though, that the percentage of integrating green cells was not lower than the theoretical value. Such an outcome would have introduced the danger of failing to detect small numbers of integrating tauGFP cells, thereby obtaining a completely negative result for the respective population.

Overall, experiments performed in this chapter determined that the embryonic kidney disaggregation-reaggregation system fulfills the criteria for a good assay system detailed in section 3.1.3 very well. Even though, several limitations of this method were detected, they could be circumvented by performing a sufficient number of repeats and careful analysis. The comparison of two methods of analysis of the quantifications showed extremely similar results suggesting that either one could be used for assessing the integration potential of different populations of cells, as convenient. The quantitative version of the disaggregation-reaggregation system therefore provides a robust method for studying the renogenic potential of cells.

Chapter 4

Undifferentiated embryonic stem cells form chimeric structures with renal epithelia, but do not express kidney markers in the disaggregation-reaggregation system

4.1 Introduction

As outlined in Chapter 1, one of the aims of this thesis is to investigate acquisition of renogenic potential by studying *in vitro* differentiation of embryonic stem cells to kidney cells. Once a good qualitative method has been established, the quantitative assay developed in Chapter 3 could be used to evaluate what proportion of the tested cells are able to contribute to the structure of renal epithelia. In the current chapter, I investigate one particular approach to ESC differentiation. This is to test whether the microenvironment of the developing kidney rudiment is sufficient to induce renal differentiation in ESCs. I will start by first establishing some criteria and definitions, as a tool to explain the results from mixing ES cells into organotypic cultures. Second, I will discuss the advantages of using the disaggregation-reaggregation system as a potential niche for differentiation (also in comparison to previously published studies). Next, I will present experimental evidence that, although ESCs placed in the environment of reaggregating embryonic kidney rudiments are able to form chimeric structures with native renal epithelia, they fail to express renal markers. Finally, I will discuss how these results could fit the information currently available in the literature.

4.1.1 Definitions for assessment of integration of test cells into reforming renal structures in reaggregated cultures

Before results from the cell reaggregation/ESC-integration experiments can be presented, the terminology used in future parts of this thesis has to be defined. These definitions are necessary to describe the different possible behaviours of test cells, after they have been mixed with embryonic kidney cells and mixed in organotypic cultures. It has previously been demonstrated (Unbekandt et al., 2010; Chapter 3 of this thesis) that control labelled embryonic kidney cells have the ability to integrate into all renal compartments indistinguishably from non-labelled cells. Therefore, the ability of test cells to integrate into the structure of reforming nephrons and UBs is one of several criteria for being able to classify the investigated cells as renal. A summary of the terms commonly used in this thesis to characterise the behaviour of grafted cells is given in Table 2.1.1. Column one of the table shows the term most

commonly used to refer to cells exhibiting the properties described in column 3. Column two provides phrases that can be used synonymously with the terms found in column 1.

4.1.2 Criteria for identifying cells as renal

Many of the limitations and difficulties in determining whether ES cells have differentiated into kidney cells or not, have been discussed in Chapter 1. They have been summarised here to provide support for selecting the criteria for renal cell determination given below.

Difficulties in the assessment of the derivation of kidney cells (in organotypic cultures):

- the lack of a robust marker for tracking the grafted cells, without any risk of transfer of the labelling reagent
- the lack of a single marker for the identification of kidney cells
- the existence of many different types of renal cells, which express different combinations of markers
- reverse transcription PCR is, by itself, inadequate in assessing gene expression in mixtures of cells, including embryoid bodies or organotypic cultures as it doesn't provide resolution to the single-cell level
- functional studies on the basis of soluble reagent incorporation are difficult to perform as other types of tubules with the properties to transport substances exist

These limitations have made it necessary to look for a good analytical approach to screen for the generation of renal cells critically and define the requirements that cells must fulfil in the context of mixed organotypic cultures, in order to be considered as renal cells. These criteria should not be used individually, but should be fulfilled in conjunction:

- the cells should be well-detectable
- they should be able to integrate into developing renal epithelia

Table 4.1.1 - Criteria for characterisation of ESC-derived cells grafted in developing kidney organotypic cultures

Term referring to test cells	Synonymous words/phrases	Properties of the test cells after integration in reaggregates
found/localised in the interstitium	found/localised outside renal tubules; dispersed	Unknown
form structures	-	- form assemblies of more than 5 cells - are enclosed by a basement membrane - display some degree of organisation
form chimeric structures with renal epithelia	form/are within physical contact with host renal epithelia; associate with renal epithelia; are (found) (in the structure of) renal epithelia	- form structures of more than 5 grafted cells - display some degree of organisation - are within physical contact with host renal epithelia - are enclosed by a basement membrane, continuous between grafted and host structures - do not form fine-grained chimeras, but rather segregate from host renal epithelia - may or may not express renal markers - may display a different morphology from renal cells
integrate into the structure of renal epithelia	localise into renal epithelia	- individual cells or many cells found into a physical contact with renal epithelia - enclosed by the same basal lamina as the host structure they are found in - have a morphology indistinguishable from renal cells - may or may not express renal markers
integrate into the structure of renal epithelia and express renal markers	-	- as above, but express renal markers

- potentially renal cells integrated into the structure of developing renal epithelia should have a morphology indistinguishable from the surrounding host kidney tubular cells on the basis of several sub-criteria – overall morphology, shape, size, position in the native tubule with respect to neighbouring cells, consistent positioning of the nucleus with respect to the positioning of neighbouring nuclei
- should co-express at least two kidney markers with sub-criteria – to express these markers in the correct cellular compartments, to co-express a marker combination consistent with the literature, should express these markers as above to match the location/function of the respective cells (for example, if a cell is found in a tubule, it should express tubular, but not stromal markers).

After the tools necessary for testing the usefulness of using the kidney rudiment as a microenvironment for differentiation of ESCs to renal cells had been established, it was possible to proceed to description and analysis of the experimental results. In the following chapter section, tauGFP ESCs were first characterised for GFP expression, the ability to maintain in an undifferentiated state and the ability to give rise to cells from the three germ layers before their renogenic ability was examined.

4.1.3 Advantages of using the kidney disaggregation-reaggregation method as an alternative approach to explanted kidney rudiments to provide a microenvironment for differentiation of embryonic stem cells

Unlike many other cell types, which can routinely be produced from ES cells, methods for generating kidney cells are still in the first steps of their development. This being the case, the efforts for devising defined conditions for ES cell differentiation should first be focussed on finding one sufficiently effective method for generation of kidney cells, rather than many less efficient ones.

Experiments studying aggregation of ES cells and cleavage-stage tetraploid embryos (Nagy et al., 1990; Nagy et al., 1993) have shown that, when re-introduced into

foster mothers and left to develop to term, embryonic stem cells are capable of generating all cells and tissues of the body. In contrast, in entirely *in vitro* conditions where no re-implantation is involved, the cells no longer receive the right signals to guide them to form a normally developing embryo. Still ESCs differentiate to a multitude of cell types, which includes mesodermal cells, spontaneously (Martin, 1981; Li et al., 1998). By the same token, it could be hypothesised that ESCs would behave the same way after being mixed with embryonic kidney cells in the disaggregation-reaggregation system. Once they have differentiated spontaneously to mesoderm or intermediate mesoderm, they could potentially acquire the ability to respond to the signals from the kidney microenvironment and progress to make renal cells (Figure 4.1.1). Furthermore, the reaggregation system has the important advantage of starting structure formation from a single-cell suspension. This allows for an additional criterion to assess the differentiation process on the basis of the cells' abilities to integrate into the structure of developing renal epithelia and orient themselves correctly with respect to neighbouring kidney cells. The small size of the organotypic cultures, as well as the existence of already available methods for three-dimensional analysis of at least two different markers in addition to GFP, make this system a promising approach for studying the *in vitro* generation of kidney cells.

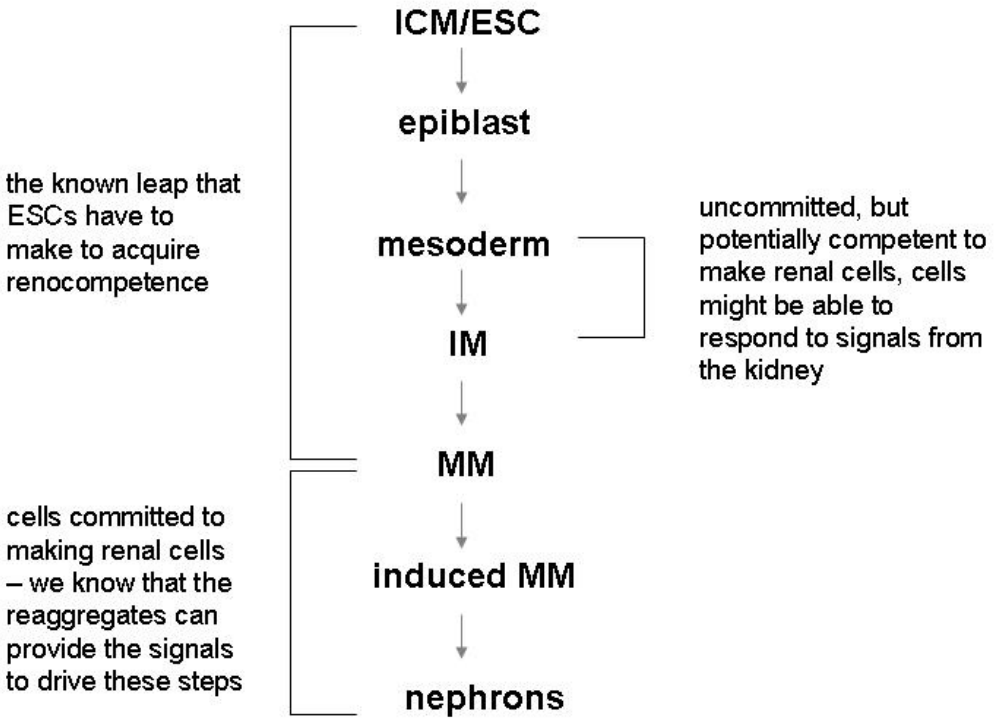

Table 4.1.1 - The developmental steps from inner cell mass (ESC) to renal cells
ICM - inner cell mass; IM - intermediate mesoderm; MM - metanephric mesenchyme

Up to now, there has been only one study that reported testing the ability of totally undifferentiated cells to respond to the signals provided by the microenvironment of a developing kidney (Steenhard et al., 2005). The authors reported that injection of mouse ROSA26 ES cells into E13 mouse kidney rudiments resulted in the formation of tubular-like structures within 5 days. These cells also seemed to express markers associated with renal cells such as WT1 and α_1 Na+/K+ ATPase, and were able to bind *Lotus tetragonolobus* lectin. First, the results presented in this study suggested that use of the microenvironment of a developing kidney rudiment for the differentiation of ES cells might hold some promise as a method of directed differentiation. Second, it also provided valuable insight into the limitations of the method of injection and into potential ways to improve the results of similar experiments. One of the important findings that Steenhard et al., (2005) reported about the ESC-derived structures was that they did not observe any chimeric structures between the ROSA26 ES-derived cells and native kidney cells. The ability of ESC-derived cells to form chimeric structures with native kidney cells would be one of a few important criteria, which would contribute to the identification of these tubules as kidney tubules, both in normal development and in *in vitro* systems. This comes from our knowledge that in development dispersed MM cells aggregate to form renal vesicles, which develop into nephrons (Grobstein, 1955) and that disaggregated embryonic kidney cells reaggregate to form individual UB structures and nephrons (Unbekandt and Davies, 2010). Furthermore, if the potential of such cells to be used in cell replacement therapies in the future has to be considered, they would be useful for replacing lost kidney cells only if they possess the ability to form chimeric structures with them to replace cells that have been lost. With regard to these limitations of the currently available methods, it was concluded that the disaggregation-reaggregation culture system gives an excellent possibility to obtain more information about the ability of ES cells to respond to signals from the microenvironment of a kidney to differentiate to renal cells. Performing the experiments with E11.5 kidney rudiments rather than E13 ones would give ESC-derived cells a better chance to demonstrate whether they could integrate into host kidney structures and allow for better analysis of the properties of these cells. Combined with the possibilities to study simultaneously the co-expression of several

markers in three dimensions, the described approach provides an extremely valuable tool for studying the potential of ES cells to generate renal cells *in vitro* in response to signals from the microenvironment.

4.2 Results

4.2.1 Optimisation of ES cell culture conditions

To make sure that no contaminant cells were present in mixing experiments with kidney cells, all embryonic stem cell lines worked with and described in this chapter were depleted of mouse embryonic fibroblast feeder cells. To find the best conditions for culture of feeder-free ES cells, wild-type control E14 cells were plated in three different conditions: gelatinised tissue culture plates, where gelatine was washed 2 times before cell plating; on gelatinised tissue culture plates where the gelatine was only aspirated after coating (without washes); and on gelatinised, ethanol-sterilised 22x22mm glass cover slips placed in the wells of 6-well tissue culture plates.

24h after seeding, the morphology of cells in the three different conditions was assessed by light microscopy. 5 wells per setup were characterised morphologically and all examined wells showed consistent results. In the wells where gelatine was washed with PBS prior to seeding cells, more flat cells were observed in comparison to the other two setups. This made controlling for unusually high percentages of differentiating cells very difficult due to the presence of flatter ES cells (Figure 4.2.1, A, B and C, arrows). In the sample where gelatine was not washed after coating, the flat cells decreased at the expense of more three dimensional colonies with light halos around them (as characteristic for mouse ES cells cultures on fibroblasts). ES cells on gelatinised glass cover slips were almost entirely three-dimensional and almost no flat cells were observed (Figure 4.2.1, G, H and I). This provided: 1- a good, morphology-based approach for controlling the cultures visually for unusually increased numbers of flattening cells; and 2 - a convenient tool for fixing and staining cells for fluorescence microscopy, where cells would be already attached to cover slips and could be mounted on glass slides for better imaging. Due to these advantages, cells were routinely cultured without a feeder layer on gelatinised cover

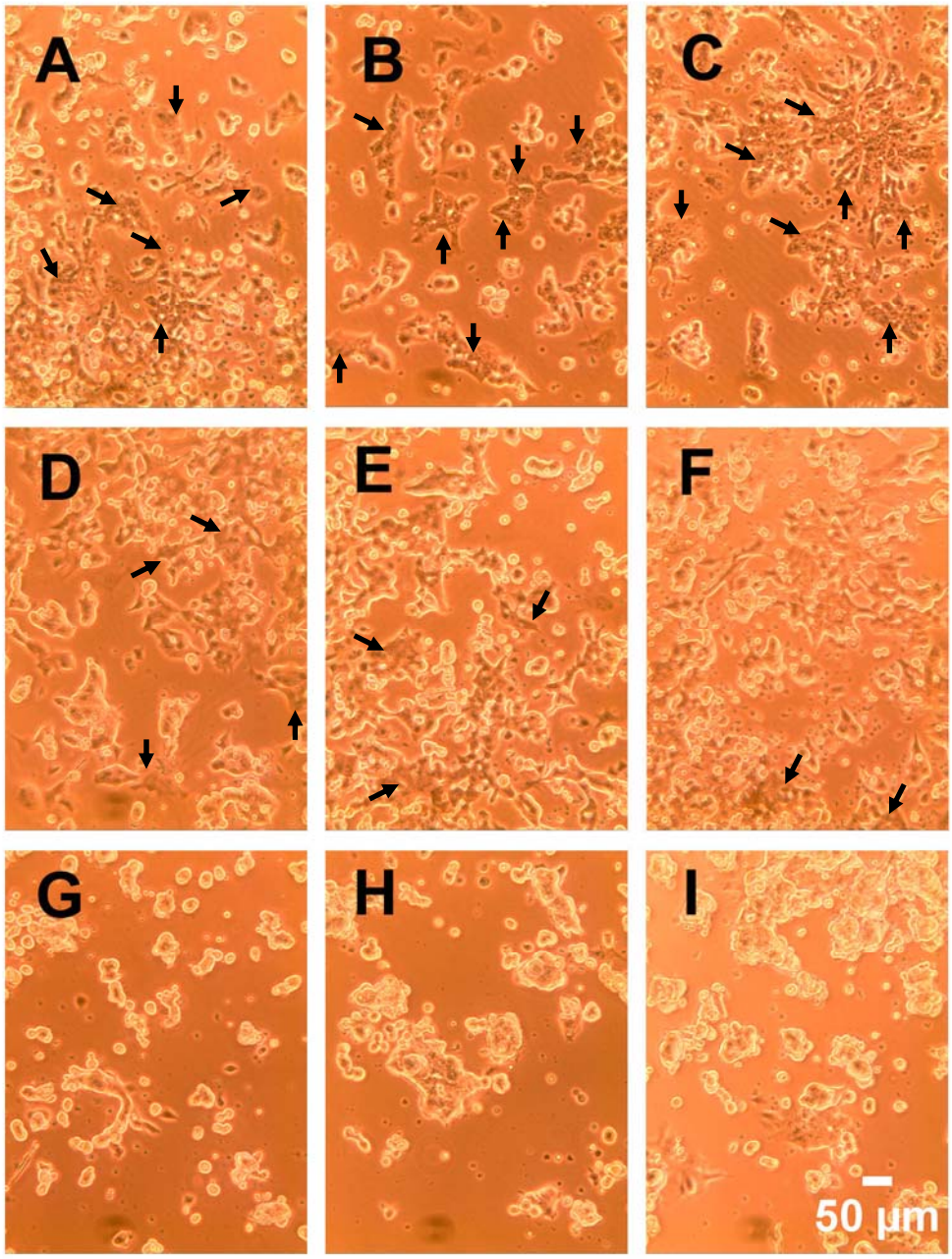

Figure 4.2.1 - The influence of substrates on the morphology of ESCs in culture
A, B, C – ESCs cultured on gelatinised cell culture dishes, where the gelatine was washed twice with PBS before seeding; D, E, F – ESCs cultured on gelatinised cell culture dishes, where the gelatin was not washed with PBS before plating the cells; G, H, I – ESCs cultured on conventional gelatinised glass cover slips.
The three columns contain representative images for three different wells (overall 5 wells per setup were examined). Arrows indicate ES cells with flatter morphology.

slips, which were not washed with PBS after treatment.

Furthermore, a simple test was used to check whether the flat cells described in the paragraphs above (as shown on Figure 4.2.1, A, B and C) were the result of differentiation or whether they were an alternative morphology of still-pluripotent cells. For this purpose, flatter cells, cultured directly on the cell culture dish where gelatine was washed twice, were detached enzymatically and plated on gelatinised cover slips. The morphology of the cells after replating was indistinguishable from the cells shown on Figure 4.2.1, G, H and I indicating that the cells were not differentiating, but displayed different morphology when seeded on different substrates.

4.2.2 Characterisation of tauGFP+ mouse embryonic stem cells

4.2.2.1 tauGFP ES cells maintain transgene expression under selection and conditions favouring pluripotency

tauGFP mouse embryonic stem cells were kindly provided by Dr. Jane Quinn, University of Edinburgh. The same line of embryonic stem cells had also been used for the production of the tauGFP mice characterised in the Materials and Methods Chapter and previous chapters (Pratt et al., 2000). These cells were cultured under continuous Puromycin selection to maintain selective pressure for the randomly inserted construct (construct, as shown on Figure 3.2.2, A). For using these cells to test differentiation to a renal lineage on the basis of mixing them in the cell disaggregation-reaggregation system described in Chapter 3, they first had to be characterised for GFP fluorescence, pluripotency and differentiation potential.

Both control E14 ES cells (parent line) and tauGFP ES cells were plated at a low density on gelatinised glass cover slips, incubated for 24h to let them attach and fixed with PFA and methanol. They were then stained with DAPI to visualise the nuclei and mounted for microscopy. Micrographs of the control and GFP+ populations were taken at the same exposure times.

The control E14 ESCs did not show any autofluorescence and were clearly

distinguishable from the tauGFP-tagged cells (Figure 4.2.2, A). As with the tauGFP kidney cells shown in Chapter 3, some differences in the intensity of GFP expression were observed (Figure 4.2.2, A-E). There were very intensely labelled with GFP cells (Figure 4.2.2, B) referred to as strongly positive cells. There were also cells, which exhibited a weaker GFP-fluorescence, termed "positive" (Figure 4.2.2, C, arrows). These were very clearly distinguishable from control cells, but had a weaker fluorescence intensity than strongly positive cells. Two other types of cells were also observed in the labelled population of cells – weakly positive cells and negative cells. The weakly positive cells had very low levels of fluorescence and were difficult to distinguish from control cells (Figure 4.2.2, D, arrow). Negative cells were not at all distinguishable from control cells and did not exhibit any detectable florescence (Figure 4.2.2, E, arrow).

Too many weakly positive or negative cells could interfere with cell mixing experiments. To determine whether this was the case, the numbers of cells in different categories were quantified on the basis of 10 randomly taken fluorescence micrographs. Total cells were counted on the basis of DAPI staining. The results were presented as a percentage of the total number of cells ± the margin of error calculated for a 95% confidence interval. As can be seen on Figure 4.2.2, F and G, the percentage of cells that did not express the tauGFP fusion protein was very low. 98.70 ± 0.61% were found to express detectable levels of the protein, while only 1.30 ± 0.61% were determined as negative. Such a small fraction of negative cells could not affect the results of cell mixing experiments.

The distribution of the counted cells into the categories: strongly positive, positive, weakly positive and negative was also compared (Figure 4.2.2, H and I). Cell counts allowed concluding that strongly positive and positive for tauGFP cells were most frequent in the culture, representing respectively 76.74 ± 2.20% and 19.15 ± 2.05 of total cells. The difficult to detect weakly positive cells accounted for only 2.80 ± 0.88% of the total population. These results confirmed that even if weakly positive cells were undetectable in organotypic cultures, this would not affect the data analysis of the experiments.

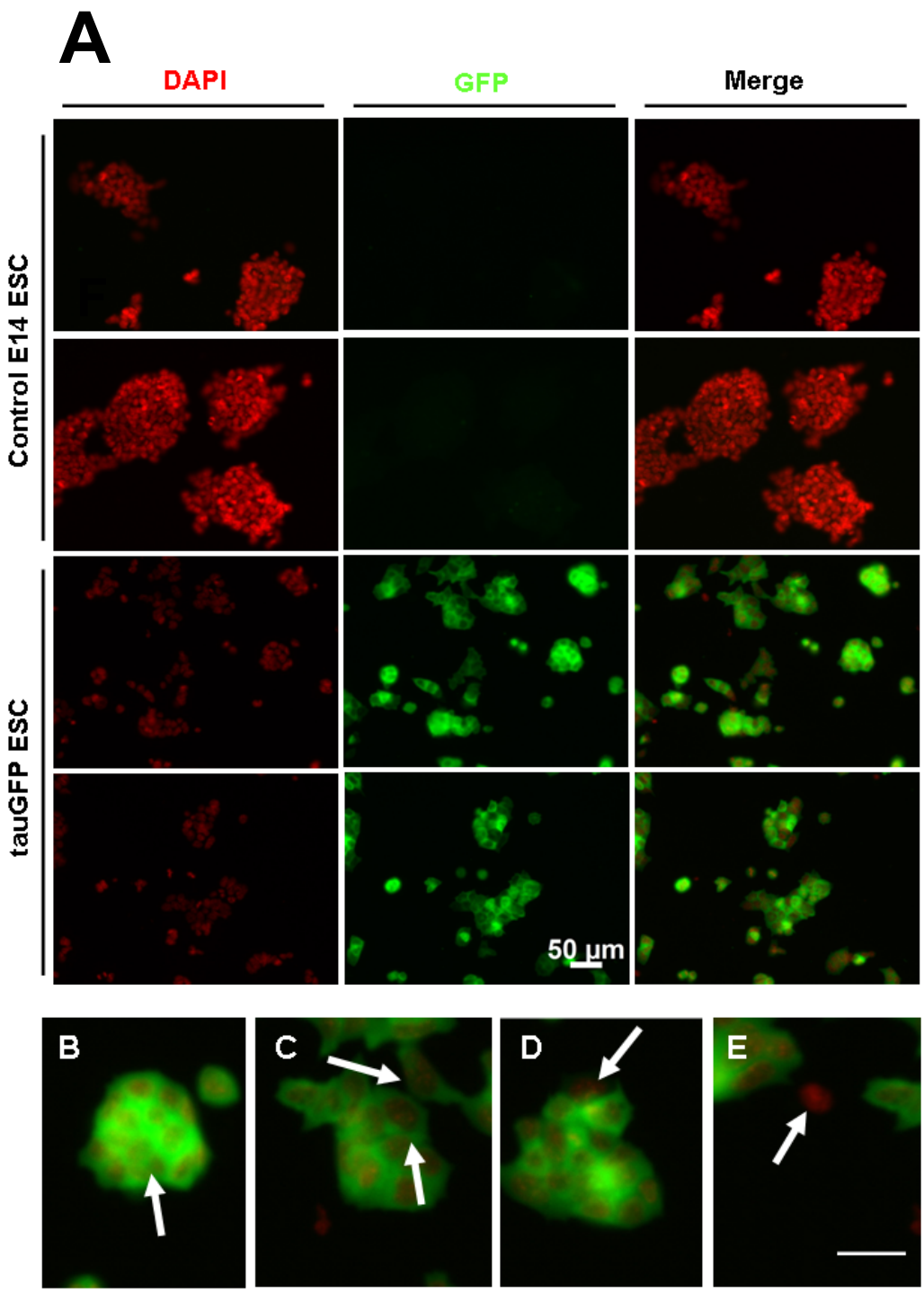
A
DAPI
GFP
Merge
Control E14 ESC
tauGFP ESC
50 µm
B
C
D
E

F

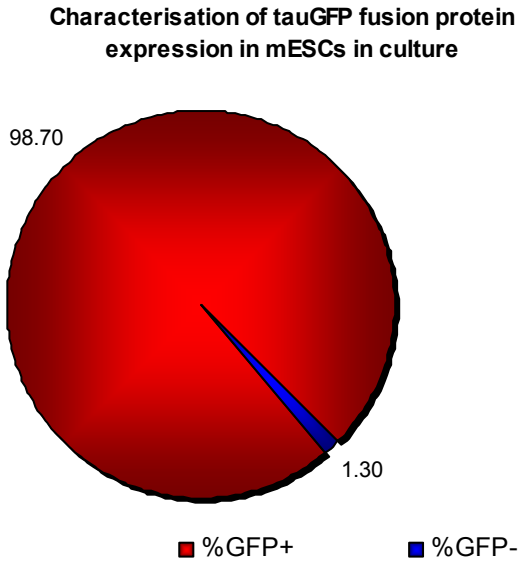
Characterisation of tauGFP fusion protein expression in mESCs in culture
98.70
1.30
%GFP+
%GFP-

G

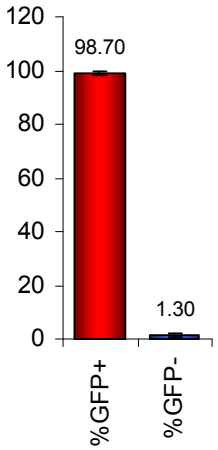
120
100
80
60
40
20
0
98.70
1.30
%GFP+
%GFP-

H

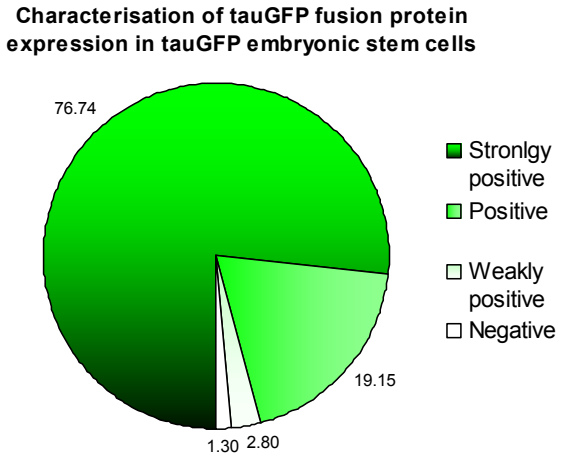
Characterisation of tauGFP fusion protein expression in tauGFP embryonic stem cells
76.74
19.15
1.30
2.80
Stronlgy positive
Positive
Weakly positive
Negative

I

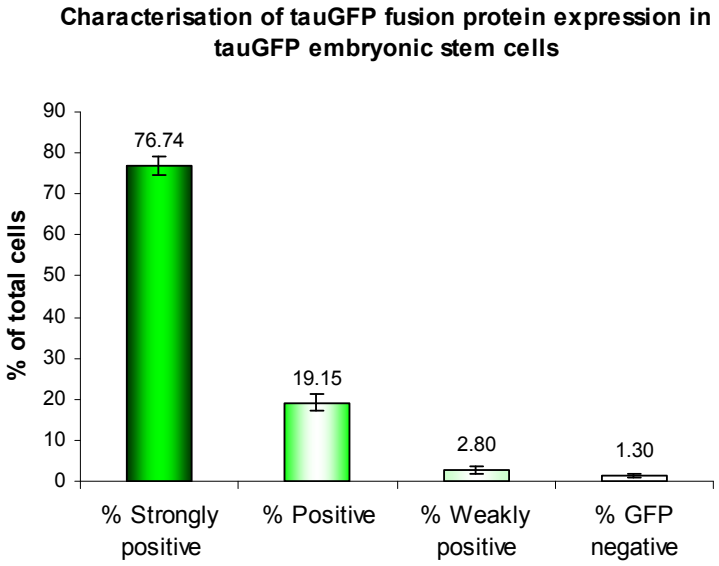
Characterisation of tauGFP fusion protein expression in tauGFP embryonic stem cells
% of total cells
90
80
70
60
50
40
30
20
10
0
76.74
19.15
2.80
1.30
% Strongly positive
% Positive
% Weakly positive
% GFP negative

Figure 4.2.2 - Characterisation of tauGFP ESC
A - Micrographs showing tauGFP expression in the transgenic ES cell line and lack of GFP expression and autofluorescence in the parent E14 ES cell line at the same exposure time; B, C, D, E – details of tauGFP+ cells illustrating the different fluorescence intensities of transgenic cells, as defined in the text; B – strongly positive cells (arrow); C – positive cells (arrows); D – weakly positive cells (arrow); E – negative cell (arrow); F – pie chart showing the proportion of tauGFP+ and negative cells in the culture; G – bar graph showing the percentages of tauGFP+ and negative cells, error bars are SEM; H – pie chart showing the proportions of cells with different fluorescence intensities in the culture; I – bar graph showing the percentage distribution of cells with different intensities in the culture, error bars are SEM.

4.2.2.2 tauGFP ES cells retain expression of the GFP fusion protein at least 15 days after removal of selective pressure

Although, the quantification of tauGFP expressing cells demonstrated that expression of the fluorescence protein is maintained very well under selection and in conditions favouring pluripotency, it was also important to note that Puromycin would have to be removed in mixing experiments with wild-type kidney cells. Removal of selection in these experiments could significantly decrease the percentage of tauGFP positive cells over the course of the experiment, thereby rendering the grafted cells undetectable. Therefore, GFP fluorescence after a long-term differentiation culture in the absence of Puromycin had to be tested, as well.

For this purpose, EBs from tauGFP and control E14 cells were formed and kept in suspension culture for 15 days. EBs were then stained with DAPI, sandwiched between two cover slips and imaged for nuclei and GFP fluorescence. The micrographs showed that due to the complex morphology of embryoid bodies it was not possible to quantify the number of GFP positive cells (Figure 4.2.3). The greatest difficulty was to assess the number of nuclei on the section, as cell death that naturally occurring during the morphogenetic processes in EBs made it very difficult to distinguish debris (possibly random fragments of nucleic acid) from nuclei (Figure 4.2.3). Although this experiment did not generate any quantitative data, it was sufficient to show that GFP positive cells were still maintained even after 15 days of EB culture under conditions lacking selection, which was much longer than the timescale of cell mixing experiments.

4.2.2.3 tauGFP ES cells express the pluripotency marker Oct4

For examining the potential of ES cells to produce kidney cells *in vitro* it was next necessary to confirm that the starting population of cells to be used in cell mixing experiments contained mainly undifferentiated cells. Screening for the pluripotency marker Oct4 would also allow determining whether the tauGFP ES cell line, produced by a genetic modification expressed this marker as expected. For these

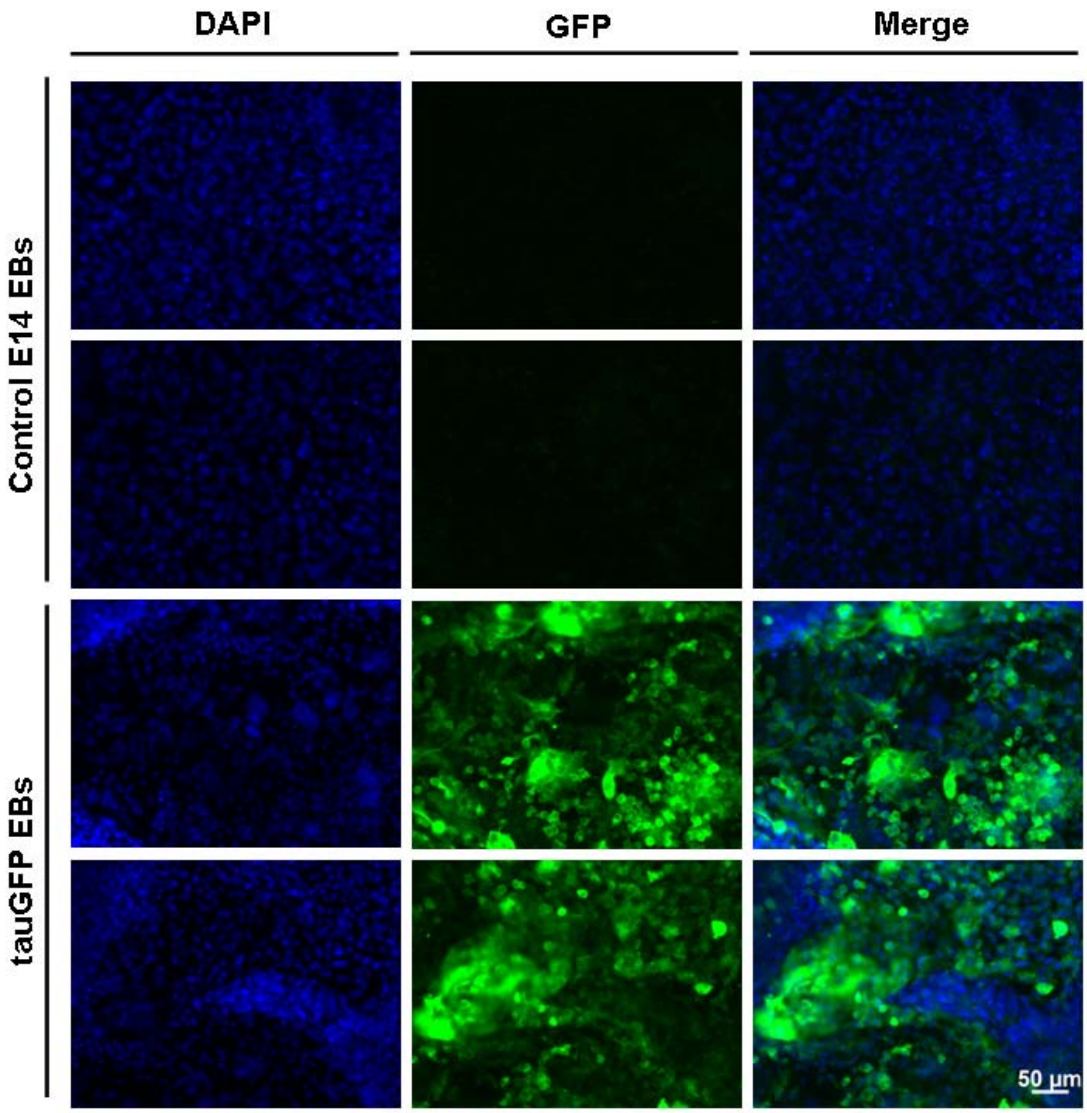

Figure 4.2.3 - GFP expression of tauGFP EBs, 15 days after culture in Puromycin-free medium
Control E14 EBs shown in row 1 and 2 do not show GFP fluorescence when micrographed at the same exposure time as used for imaging tauGFP cells. The nuclear staining for DAPI shows that cells are present in the EBs. Images of tauGFP EBs (rows 3 and 4) show that GFP fluorescence is retained even after a 15 day culture in Puromycin-free conditions. These images also illustrate the complexity of maturing EBs containing regions with cellular debris, which made quantification of the GFP+ cells extremely difficult.

purposes, control E14 and tauGFP ES cells were seeded at a low density on gelatinised glass cover slips, incubated for 24h to attach and fixed with PFA, followed by methanol. The fixed cells were stained for Oct4 and DAPI. Figure 4.2.4 shows representative images of the staining for both secondary antibody controls and samples. Although, the controls for both types of cells show relatively high background fluorescence, a comparison to the Oct4-stained samples revealed that the staining was clearly distinguishable from negative cells. As can be seen from Figure 4.2.4, background fluorescence is present fairly uniformly within the colony of cells, in contrast to the Oct4-stained cells, which showed a specific nuclear staining. Additionally, these experiments were used to confirm that Oct4 positive cells were also expressing tauGFP, as evident from the micrographs shown in Figure 4.2.2, 4th column with panels.

While acquiring images for Oct4 quantification studies, the DAPI channel was used for selection of areas containing high number of cells for counting. The selection of areas was done blindly with respect to Oct4 as this channel was not observed in the process. 10 different micrographs of cover slips seeded with cells were taken for both the control E14 cells and tauGFP cells. The Oct4 positive cells in the two groups were quantified as a percentage of the total number of cells, assessed by DAPI+ nuclei. The results were presented in Figure 4.2.2, B and C as proportions of negative and positive cells for E14 wild type cells and tauGFP ES cells. In the E14 populations, 94.9% of cells were found to be Oct4 positive compared to 96.3% of the tauGFP cells. The comparison between the two types of cells is shown in Figure 4.2.2, D indicating that an extremely high percentage of cells expressed Oct4, as expected from undifferentiated pluripotent cells. The two populations contained relatively the same proportion of positive cells, as shown by an unpaired student's t-test ($p=0.4$), as well as a low number of differentiated cells (E14 - 5.1%; tauGFP - 3.7%). On the basis of these studies it was concluded that tauGFP ES cells were maintained undifferentiated as compared to their parent population and as normally expected for embryonic stem cells.

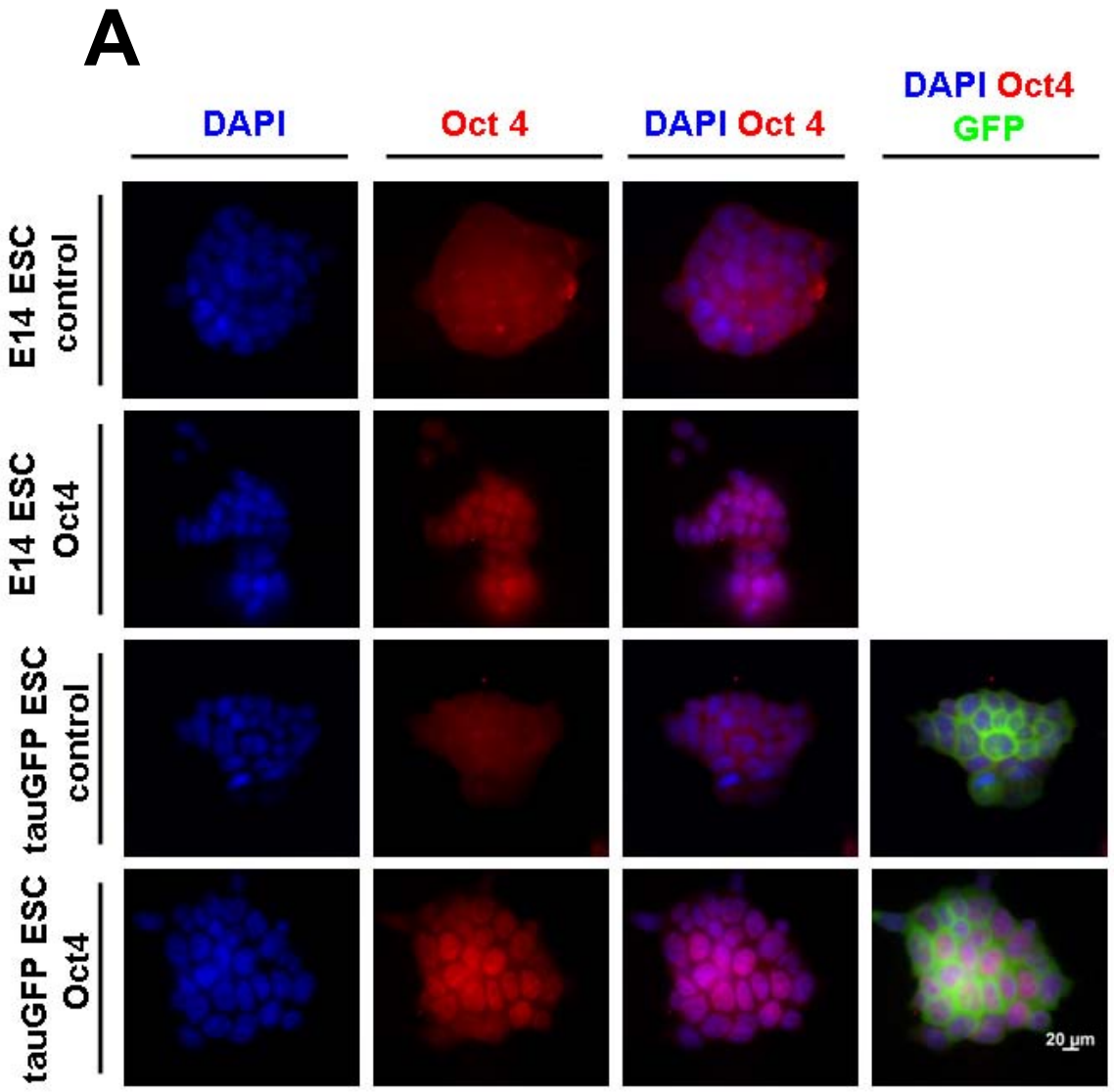
A
DAPI
Oct 4
DAPI Oct 4
DAPI Oct4
GFP
E14 ESC control
E14 ESC Oct4
tauGFP ESC control
tauGFP ESC Oct4
20 µm

B

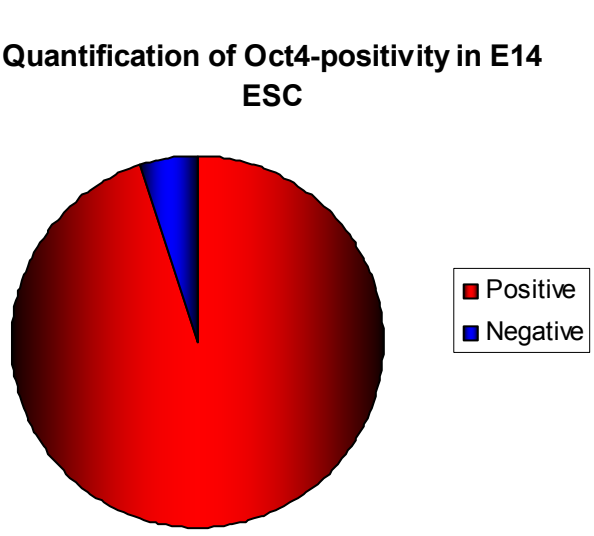
Quantification of Oct4-positivity in E14 ESC
Positive
Negative

C

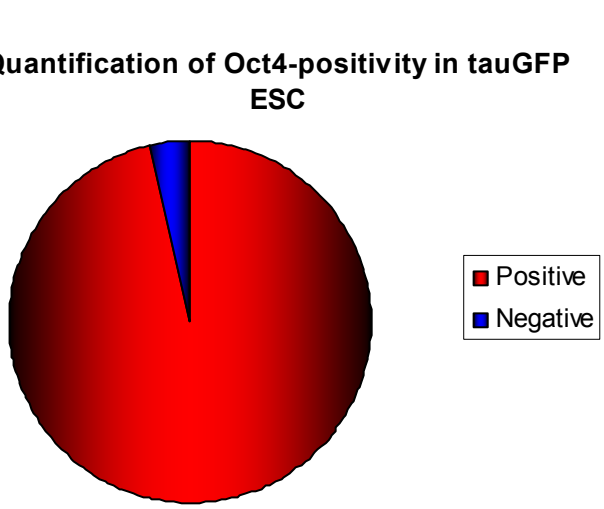
Quantification of Oct4-positivity in tauGFP ESC
Positive
Negative

D

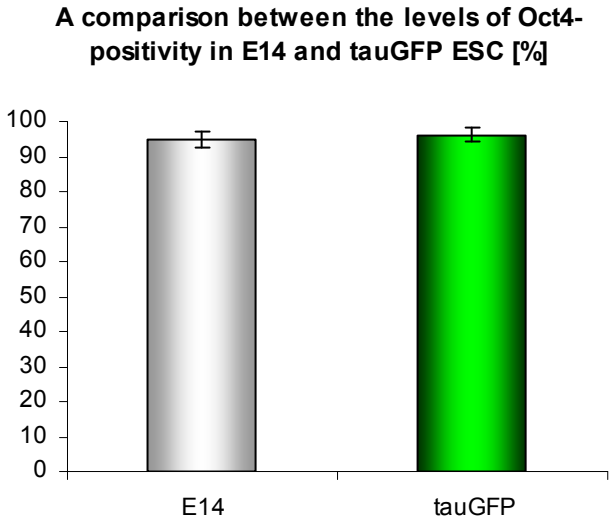
A comparison between the levels of Oct4-positivity in E14 and tauGFP ESC [%]
100
90
80
70
60
50
40
30
20
10
0
E14
tauGFP

Figure 4.2.4 - Characterisation Oct4 expression in tauGFP ESCs
A – Micrographs showing the expression of Oct4 and tauGFP in tauGFP ESCs and the parent E14 stem cell line. Although background in the Oct4 channel is high, the images clearly demonstrated that Oct4 staining (nuclear) is distinguishable from the non-specific staining (whole cell). tauGFP cells expressed both Oct4 and tauGFP robustly under conditions of pluripotency; DAPI (dark blue), Oct4 (red), tauGFP (green). B – a pie chart showing the proportion of Oct4 positivity in control E14 ESCs; C - a pie chart showing the proportion of Oct4 positivity in tauGFP ESCs; D – shows a comparison between the percentages of cell in E14 and tauGFP ES cell cultures expressing tauGFP, error bars represent the margin of error for a 95% confidence interval

4.2.2.4 tauGFP mouse ESCs can differentiate to the three germ layers

In addition to checking whether tauGFP cells expressed pluripotency markers, it was necessary to confirm that the genetically modified ES cell line had not lost its property to give rise to the three germ layers. In the design of this experiment it was taken into account that cells senesce with passages, which might limit their differentiation potential. Differentiation experiments were therefore performed at passage 50 - the latest passage that the cells were allowed to reach at any stage.

The potential of tauGFP ESCs to differentiate to the three germ layers was assessed by screening mRNA transcripts by cDNA synthesis and PCR amplification of the cDNA fragments. The three genes selected to show the presence of endodermal, mesodermal and ectodermal lineages and the respective references are shown in Figure 2.4.5, A. The tissues that these markers are most commonly associated with are also given.

For this set of experiments, embryoid bodies were formed from E14 and tauGFP embryonic stem cells and cultured for 14 days in a suspension culture. Embryoid bodies were harvested for RNA isolation and cDNA was synthesised for detection of gene-specific transcripts by PCR. For a positive control, RNA was isolated from whole E11.5 embryos. GAPDH was used as a loading control. The primer pairs used for these reactions are given in Table 2.5 of the Materials and Methods section of this thesis. The size of the bands resulting from cDNA synthesis and PCR amplification was assessed by running a DNA ladder and was compared to the expected values given in Table 2.5 to confirm that the reaction product was specific.

The presence or absence of a specific product for the genes of interest was assessed by a comparison between E14 undifferentiated ES cells, tauGFP undifferentiated ES cells and E14 and tauGFP cells differentiated by the embryoid body method. The results show that there is no expression of differentiation genes in both types of ES cells, as expected. Cell differentiation led to the upregulation of all three markers in embryoid bodies. This suggested that tauGFP ES cells were able to give rise to cells

A

Germ layer	Gene	Expressed in	Reference
endoderm	alphafetoprotein (AFP)	Hepatocytes	Abelev, 1971
mesoderm	α smooth muscle actin (α SMA)	smooth muscle	Schildmeyer et al., 2000
		cadiac myoblasts	Ruzicka et al., 1988; Sugi and Lough, 1992
		skeletal muscle	Sawtell and Lessard, 1989
ectoderm	Acetylcholine esterase (AChE)	Neuroectoderm	Ravin et al., 1952

B

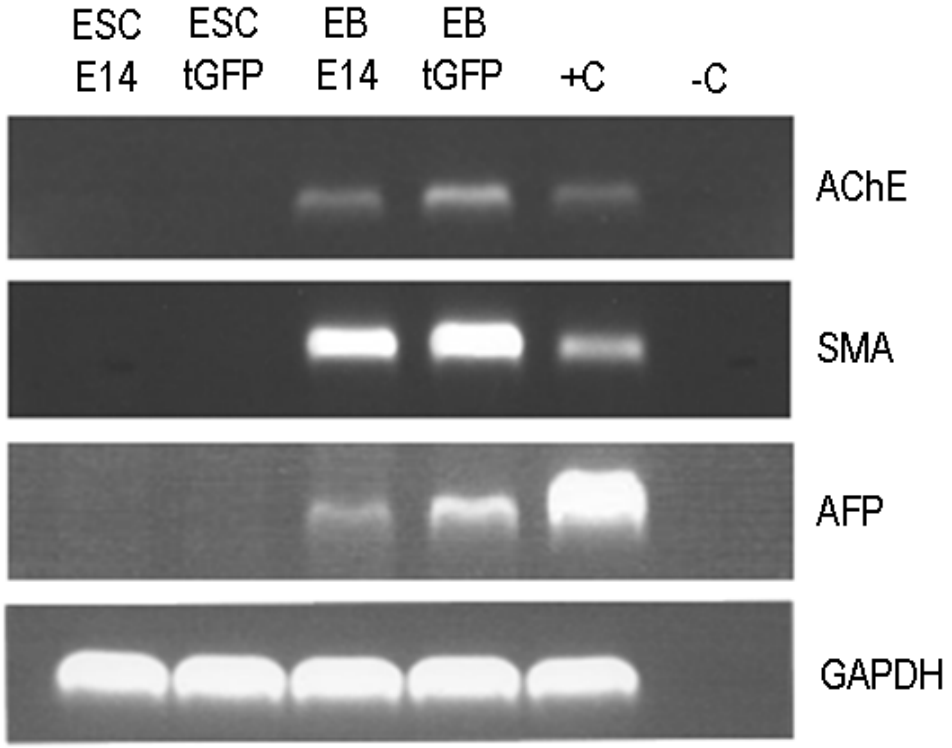

Figure 4.2.5 - Characterisation of the differentiation potential of tauGFP ES cells, as compared to control E14 ES cells
A – a table illustrating a selection of markers associated with the three germ layers with the respective references; B – PCR results showing the presence of transcript of all three tested genes in both control E14 and tauGFP ES cells. These results are based on reverse transcription of total RNA extracts. Both types of ES cells show no expression of the three markers when cultured in pluripotency conditions and presence of all three markers after being cultured as embryoid bodies for 14 days. –C (negative control) is water to detect unspecific products from contaminating DNA. +C (positive control) is based on cDNA prepared from a whole E11.5 embryo and shows the presence of all three tested genes, as expected.

from the three germ layers and behaved similarly to wild type E14 embryonic stem cells.

4.2.3 Undifferentiated mouse ES cells form chimeric structures with embryonic kidney cells

After it was confirmed that the tauGFP cells robustly express GFP under different conditions, express Oct4 under pluripotency conditions, and are able to differentiate into the three germ layers, their ability to respond to the signals of the microenvironment and differentiate to kidney cells in reaggregated organotypic kidney rudiments could be tested. For this purpose, tauGFP ES cells were made into a single cell suspension and extruded through a 40μm cell strainer, before mixing 15,000 ES cells with 100,000 embryonic E11.5 embryonic kidney cells for the formation of organotypic pellets. These experiments did not include a treatment with Y-27632 as reaggregates containing ESC are able to survive without ROCK inhibition. The ROCK inhibition step was omitted here to minimise the possible effects of the inhibitor on the differentiation potential of ESCs. The reaggregates containing ESCs were cultured for 7 days, and then fixed with 4% PFA and methanol. Epithelia were visualised by immunostaining for E-cadherin and tauGFP; ESC-derived cells - by their expression of GFP.

Confocal sections showed that tauGFP positive structures formed physical contacts with wild-type renal epithelia (Figure 4.2.6, white dotted lines). It was observed that tauGFP+ and wild type cells do not form fine-grained chimeras, but rather segregate into separate regions of the structures formed. Some of the tauGFP positive structures did not have a particular cellular organisation, but others rarely formed a single-layered epithelium with a lumen, as characteristic of renal tubules (Figure 4.2.6, G-I). Only from confocal micrographs, it was not clear whether these structures were formed just because they ended up next to each other by chance or whether a more complex process was involved. The former process would suggest that the number of contact points between tauGFP+ and tauGFP- epithelia on a confocal section would depend on the number of these structures. The more

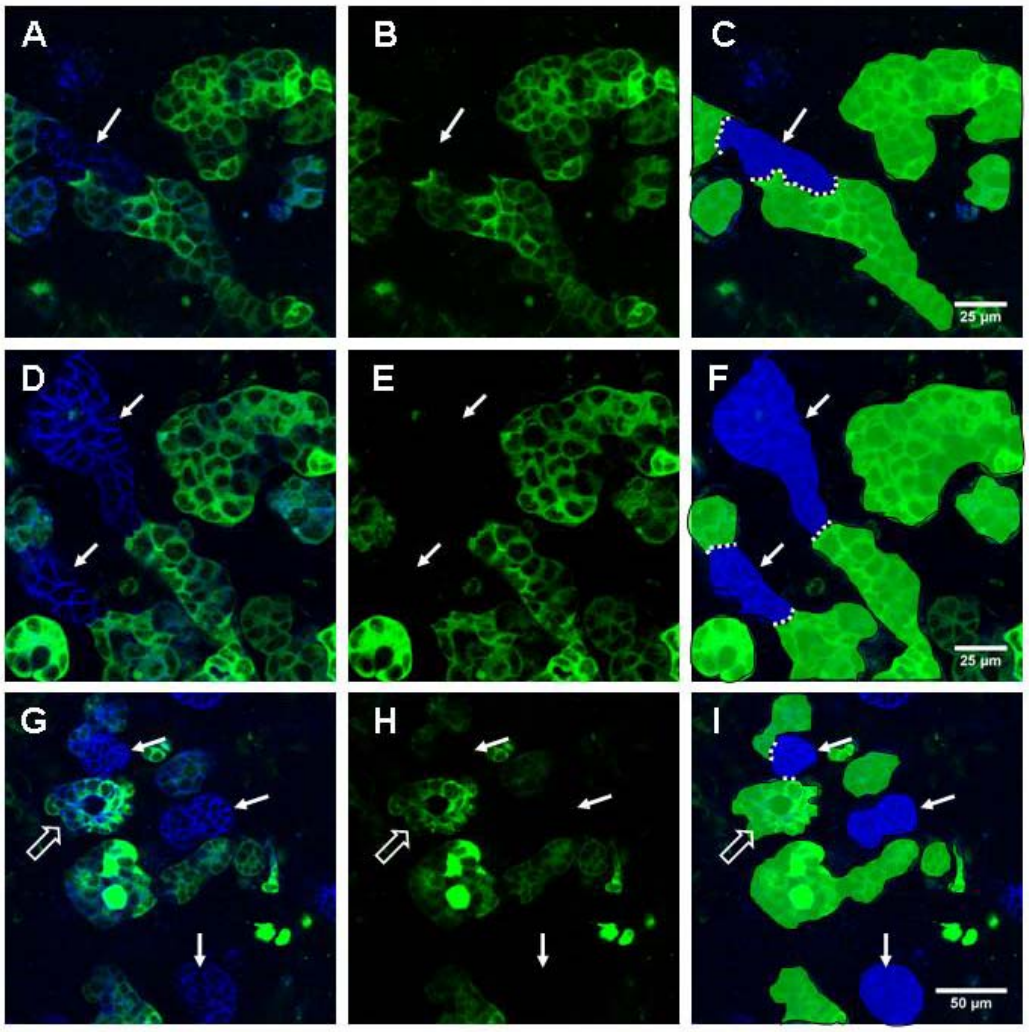

Figure 4.2.6 - Undifferentiated tauGFP ESCs show formation of chimeric structures when mixed with E11.5 mouse embryonic kidney cells and cultured as organotypic rudiments for 7 days
A, D and G show a double staining for E-cadherin (blue) and tauGFP (green); B, E and H show only the green channels of their respective panels A, D and G; C, F and I are a schematic version of the double stainings in A, D and G. Arrows indicate native kidney epithelia, which are E-cadherin+/tauGFP-. White dotted lines indicate the physical contacts between native kidney and tauGFP+ structures. The open arrows in G, H and I point at a tauGFP ESC-derived structure with a lumen.

structures, the more contact points. To test this, the number of both types of structures and the number of continuous contact points were quantified. The following criteria were used for quantification:

- structures had to be E-cadherin positive
- more than 5 adhering E-cadherin+ cells were counted as an epithelial structure (examples of structures, as counted, could be seen in the diagram in figure 4.2.6, C, F and I)
- the number of contact points between GFP- and GFP+ structures were counted (as shown by the dotted lines on Figure 4.2.6, C, F and I)

For example, in Figure 4.2.6, C, there would be 1 wild-type structure (blue), 5 GFP+ structures (green) and 2 contact points. Figure 4.2.7, A and B, summarises the results from 4 organotypic cultures. The bars represent the average number of wild type structures, tauGFP+ structures or contact points per confocal section. Error bars are standard errors of the mean. The results are presented individually in A and as an average of all organotypic cultures in B. One-way ANOVA confirmed that the differences between the individual cultures were not significant in any of the three measured categories. To check whether the number of contact points between WT and tauGFP structures was dependent only on the number of structures of both types present on one confocal section, the following experimental analysis was designed. First, a coefficient was needed to provide information about the ratio of both types of structures co-existing on the same section. For this, the number (№) of tauGFP structures on one section was divided by the number of WT structures on the same section (№ TauGFP+/№ WT structures). This coefficient was then plotted against the number of contact points (Figure 7.2.7, C). The linear regression curve is also shown. Correlation analysis was performed by calculating the Pearson product - moment correlation coefficient (r). r shows the linear dependence between two sets of measurements and gives a value between -1 and 1. Values close to 0 show a very weak correlation, while values close to ± 1 indicate a strong correlation (Fowler et al., 1998). The r determined was 0.08 and suggested that there was only a very weak correlation between the number of contact points and the numbers of WT and tauGFP+ structures co-existing on a confocal section. This suggests that contact points are not formed by WT and tauGFP structures just ending up next to one another, but by another mechanism, possibly involving active recognition between

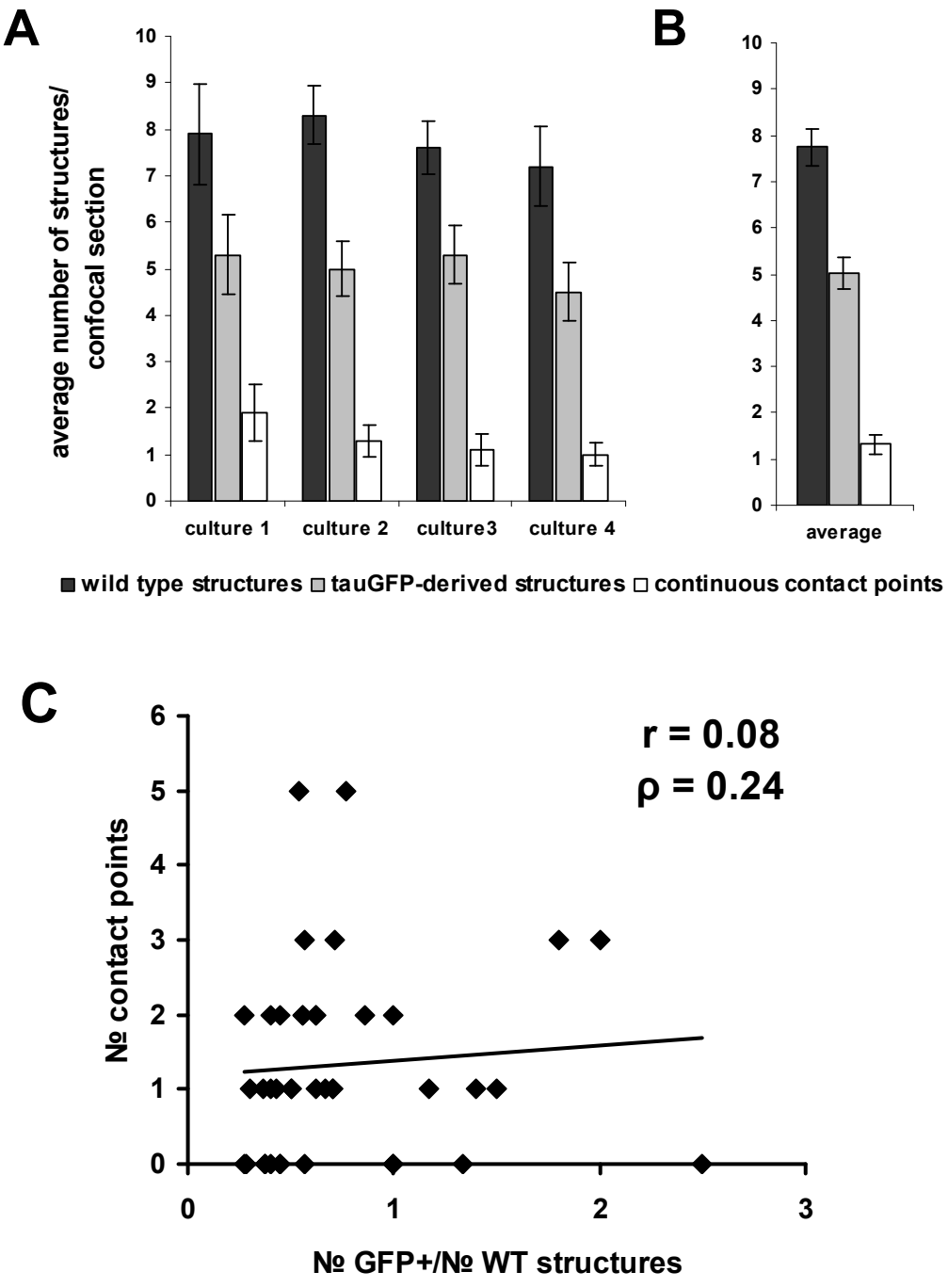

Figure 4.2.7 - Quantification of the fusion points between native and tauGFP-derived structures, as compared to the relative number of these structures
A – quantification of the number of three different types events in 4 organotypic cultures. These are based on counting tauGFP+, tauGFP- structures and adhesion points between the two in 10 confocal sections per sample. A one-way ANOVA showed that the differences between organotypic cultures for all three categories of counts were not significant
B - averages of all 4 experiments shown in A
C - analysis of correlation between the number of contact points and the numbers of tauGFP and WT structures co-existing on the same section; linear regression shown; r - Pearson coefficient for linear dependence; ρ - Spearman's coefficient for monotonically related variables

structures. Although, this test was very conclusive it had one disadvantage - that it measures only linear dependence. Since it was not known whether the dependence examined was linear or non-linear, these results were re-evaluated by a second method, which measures dependence of monotonically related variables, even if they are not linear. For this test, Spearman's rank correlation coefficient (ρ) was calculated and showed a value of 0.24 (for n=40, degrees of freedom=38) thereby confirming only a weak correlation between the variables.

4.2.4 tauGFP ESC-derived cells found in reaggregated kidney rudiments expressed the renal marker Pax2

To investigate whether the tauGFP ESC-derived cells found in chimeric structures of grafted and native kidney cells could be renal, organotypic pellets were stained for Pax2. As mentioned in Chapter 1, Pax2 is a marker of renal epithelia, but is also expressed in the nervous system (Dressler et al., 1990). Confocal micrographs revealed that some, but not all GFP-positive cells were positive for this marker (Figure 4.2.8). Co-localisation of green fluorescence and Pax2 staining could be clearly shown in some cells (as shown on Figure 4.2.8).

4.2.5 The Pax2/tauGFP double positive cells found in mixed organotypic cultures do not associate with renal epithelia and exhibit processes similar to neurites

To determine whether any of the observed Pax2 and GFP double positive cells localised into renal epithelia, cultured organotypic pellets were triply stained for E-cadherin, Pax2 and GFP. This screen identified two categories of tauGFP cells, which expressed Pax2:

- cells found in the interstitium, which were not associated with renal tubules
- epithelial cells found in chimeric and non-chimeric epithelial structures

Studies by confocal microscopy revealed that Pax2/tauGFP double positive cells of the first type, which localised in the interstitium did not express the epithelial marker E-cadherin, as would be expected from renal epithelia (Figure 4.2.9, A and C,

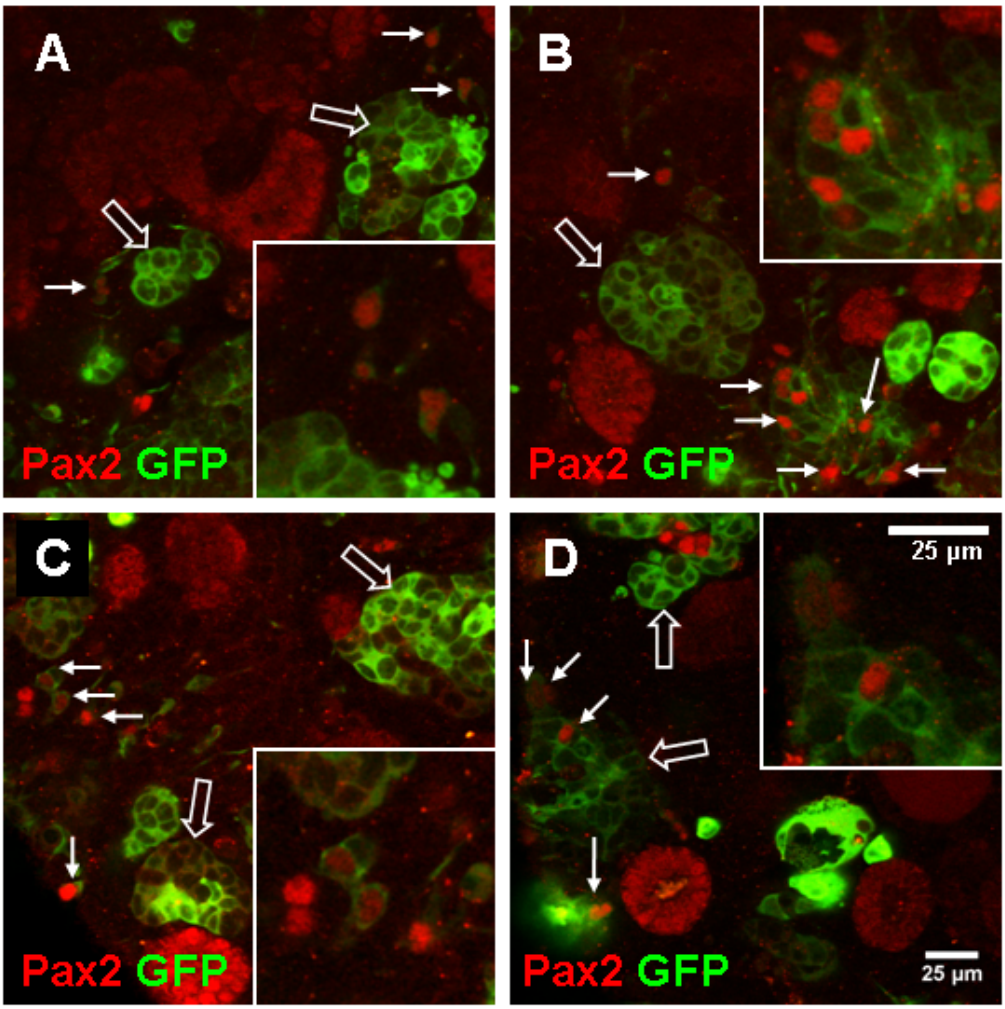

Figure 4.2.8 - Some tauGFP+ cells found in cultured organotypic pellets express the renal marker Pax2
A, B, C and D show representative images of 10-day organotypic cultures containing tauGFP ES cells. Open arrows indicate ES cell-derived structures negative for Pax2. Block arrows indicate cells and cell aggregates positive for Pax2. Details of tauGFP+/Pax2+ cells are shown in the magnified insets.

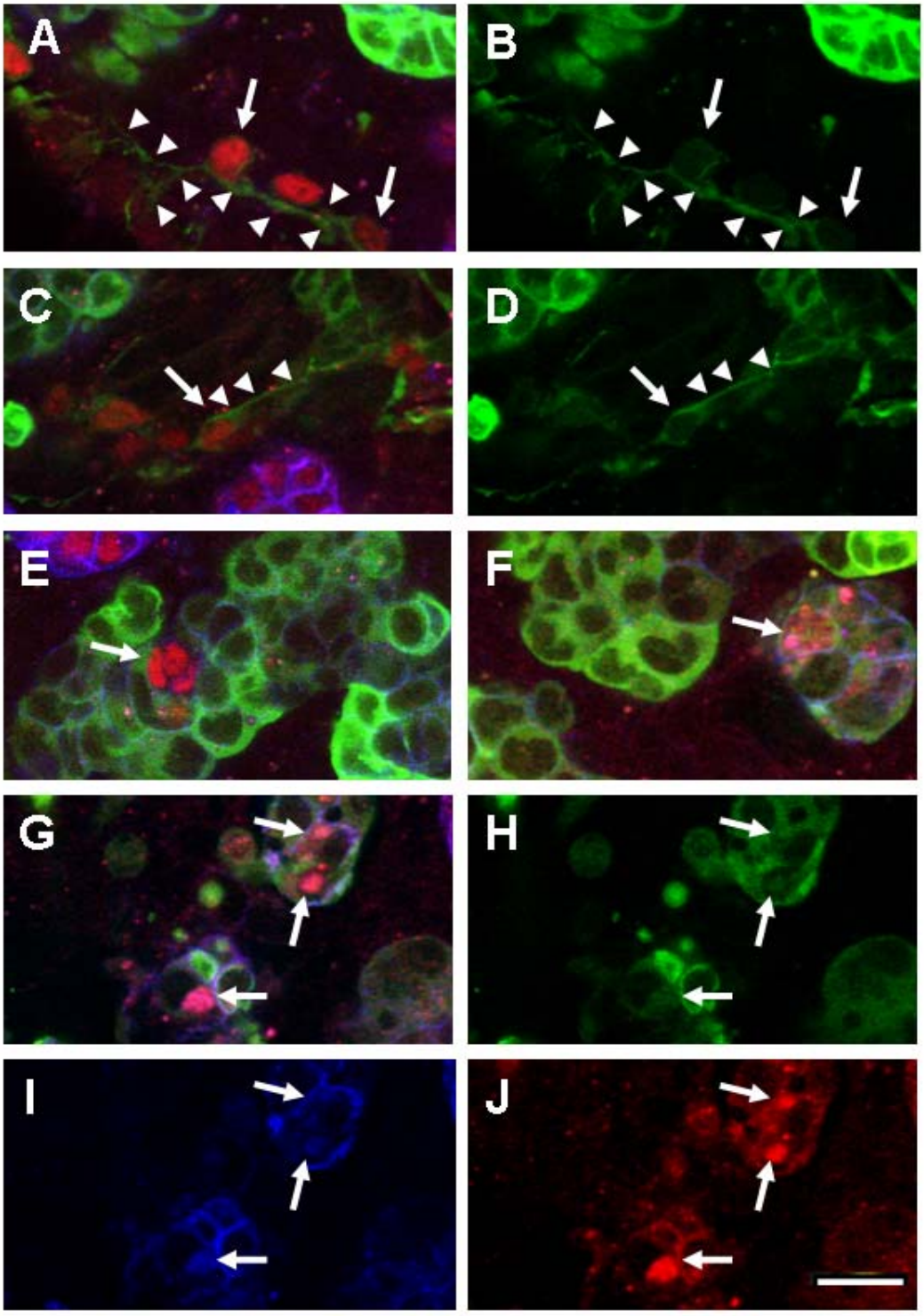
A
B
C
D
E
F
G
H
I
J

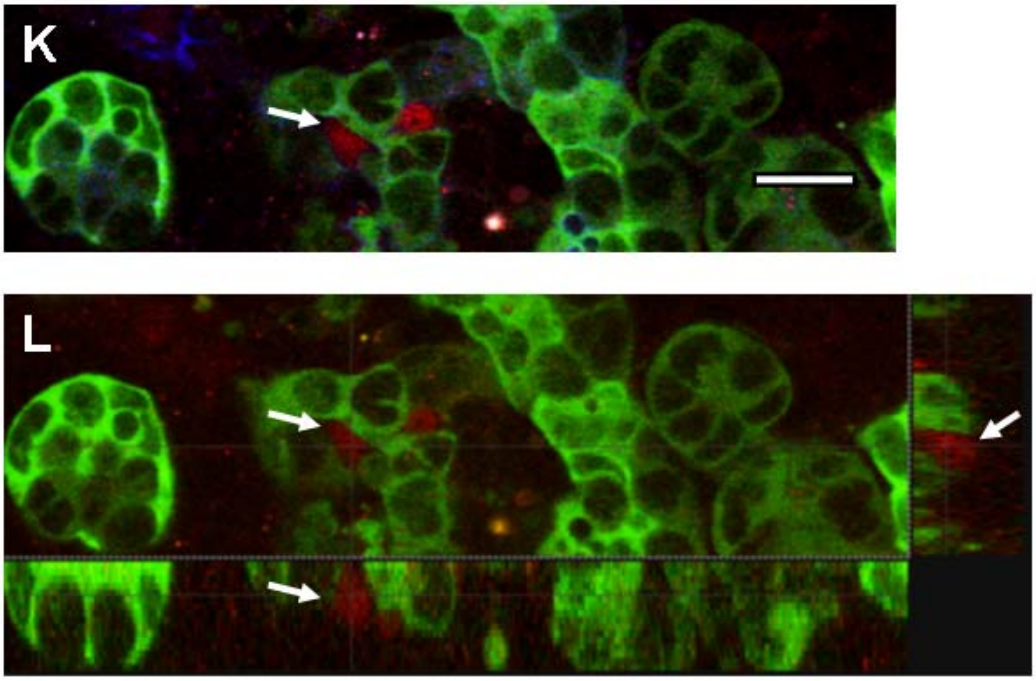

Figure 4.2.9 - Pax2+ cells derived from tauGFP ESCs do not co-express E-cadherin and show false positives
A – L – Pax2 (red), E-cadherin (dark blue), tauGFP (green); A and C show tauGFP+/Pax2+ cells (arrows) clearly exhibiting neural processes (arrowheads). Only GFP is shown in B and D; E – shows a small cluster of WT cells, which appear as tauGFP+/Pax2+ double positive cells (arrow); F – shows a cells with unhealthy morphology and signs of stress, which appear E-cadherin+/Pax2+; G – shows more examples of cells appearing double positive for E-cadherin and Pax2 (arrows). Examination of all acquisition channels separately reveals that Pax2 expression is false due to its presence in all other channel, which detect only non-nuclear markers H, I and J, arrows); K – shows another example of cells appearing doubly positive for E-cadherin and Pax2 (arrow); L – contains the same image as in K, but also includes three dimensional information showing that the Pax2+ nuclei are not surrounded by a layer of GFP+ cytoplasm indicating that these are intercalating WT cells (white arrows).

arrows). In addition, it was observed that in some cases these cells extended long processes very similar to neurites (Figure 4.2.9, A, B, C and D, arrowheads), detectable by the tauGFP reporter protein (Pratt et al., 2000).

A close examination of the second type of ESC-derived cells, which expressed both Pax2 and E-cadherin, revealed two major problems. First, some of these cells exhibited a dotty Pax2 staining, abnormal morphology and signs of stress (Figure 4.2.9, F and G). Examining individually the blue, red and green channels used to generate the overlay of a triply stained image, led to the observation that several events, which appeared to be Pax2 positive nuclei were present in all three channels. This, taking into account the different localisation of these markers (E-cadherin - on the plasma membrane; tauGFP - in the cytoplasm and Pax2 - in the nucleus) meant that this staining was artefactual. Together with the unusual morphology of the cells, this observation was very important in acknowledging the presence of false positive for Pax2 cells. The second problem with Pax2/tauGFP/E-cadherin triply positive cells was detected by extensive three dimensional studies of tauGFP structures containing Pax2 positive cells. Serial confocal sections of areas of interest, which contained putative triply positive cells, were made. The example shown in Figure 4.2.9, K and L, demonstrated that when examining cultures in two dimensions only, cells appeared Pax2/tauGFP positive. Studying the third dimension of these cells demonstrated that the Pax2 positive nuclei were not enveloped by a layer of tauGFP cytoplasm, which was a clear indication that these cells were tauGFP negative and therefore not ESC-derived.

In summary, on the basis of the information presented in this chapter up to this point, no ESC-derived cells could be identified as potentially being renal epithelia. Although detectable numbers of Pax2 positive cells were found in the interstitium, they did not have the ability to localise into renal epithelia and formed neurite-like extensions, which suggested that these could be Pax2 positive neural cells (Püschel et al., 1992; Cheng et al., 1998). The cells forming epithelial renal-like structures, which initially appeared triply positive for tauGFP, E-cadherin and Pax2, could in

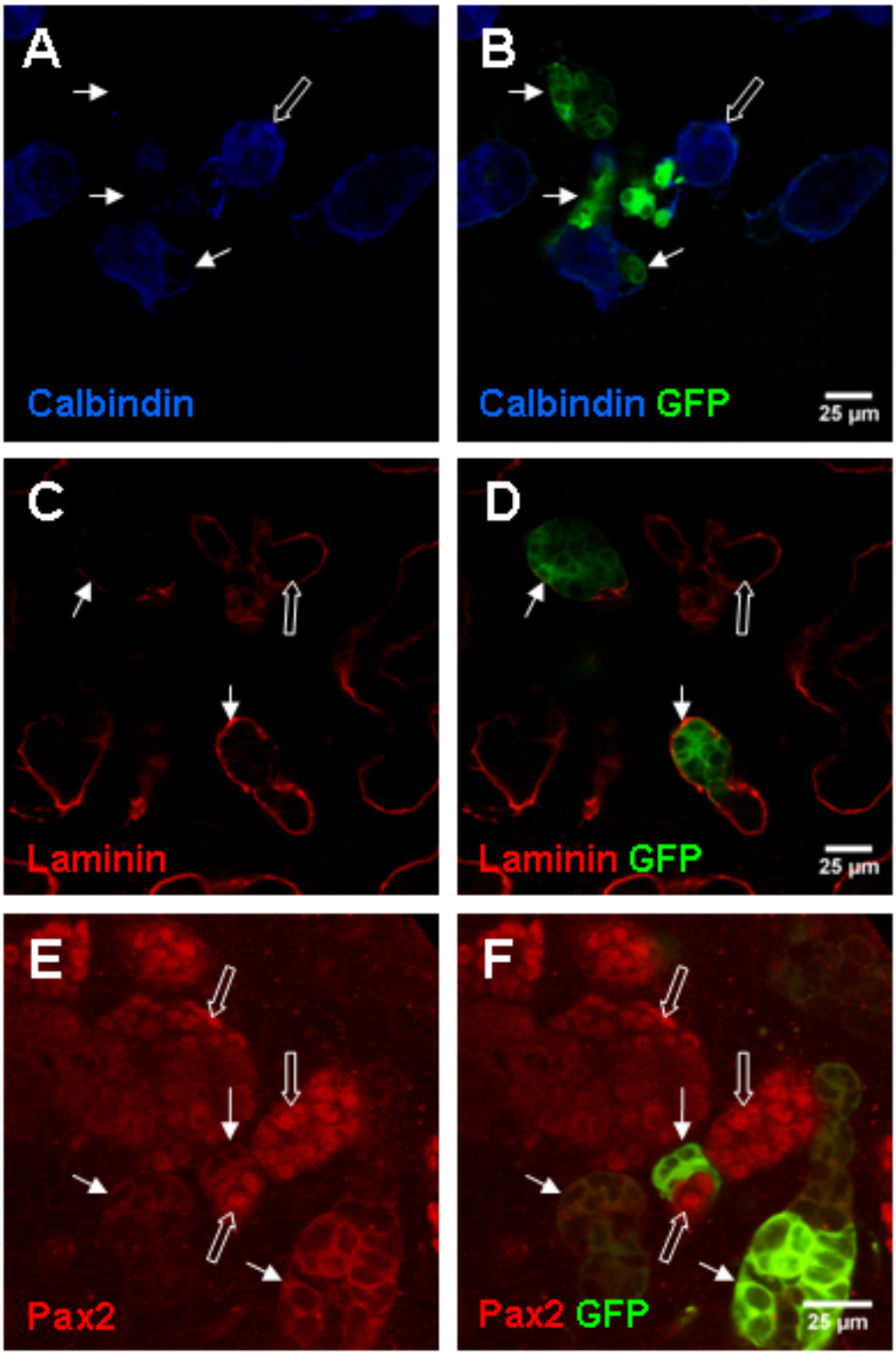
A
Calbindin
B
Calbindin GFP
25 µm
C
Laminin
D
Laminin GFP
25 µm
E
Pax2
F
Pax2 GFP
25 µm

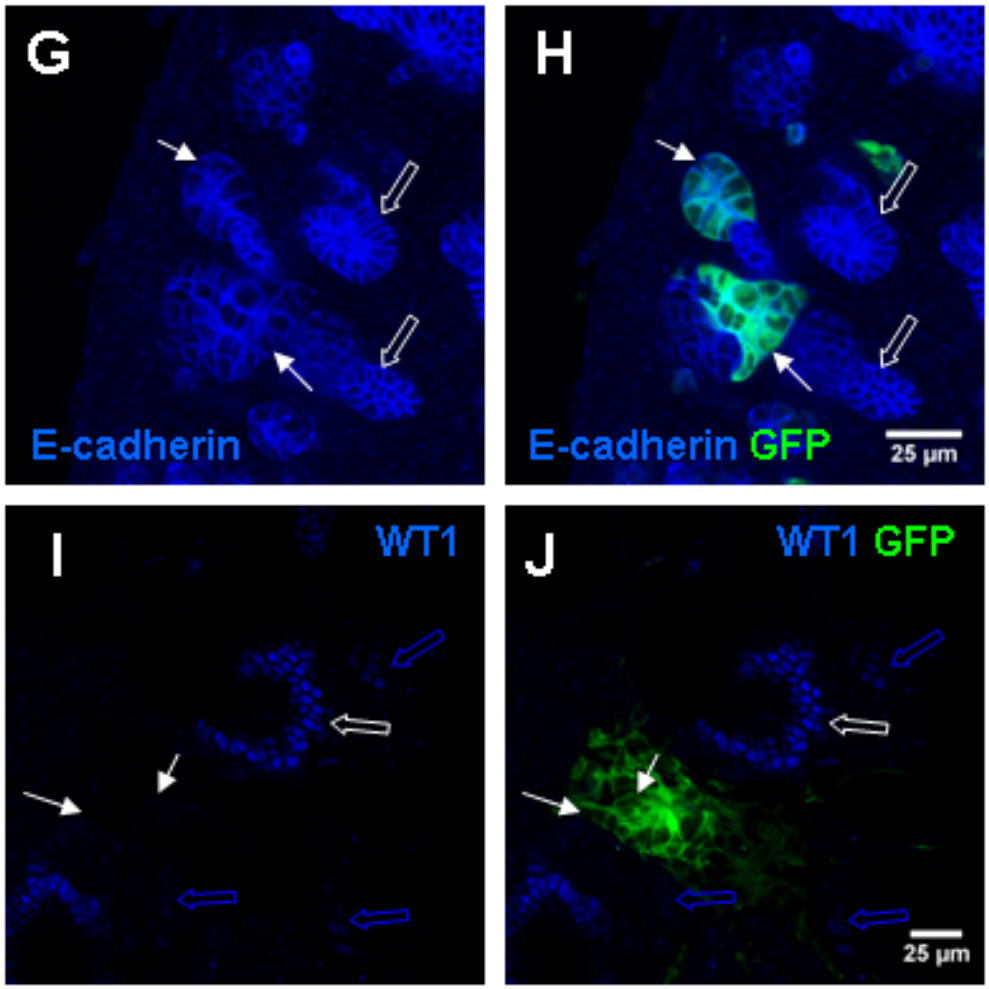

K

Protein	Present/absent	Details
Calbindin	-	not detected in any cells
Laminin	+ (+)	expressed in the tauGFP part of chimeric structures and stand-alone epithelial structures; not expressed by single cells in the interstitium or other cell clusters
Pax2	+ (-)	not expressed by cells in epithelial structures forming chimeras with renal tubules; expressed by stand-alone cells in the interstitium, frequently exhibiting neurites
E-cadherin	+ (+)	expressed by cells forming chimeric structured with renal epithelia and some stand alone structures; not expressed by other single cells and cell clusters in the interstitium
Wt1	-	not detected in any cells

L

	Calbindin	Laminin	Pax 2	E-cadherin	Wt1
Calbindin	-	-	n/a	n/a	n/a
Laminin	-	+	n/a	n/a	n/a
Pax 2	n/a	n/a	+	-	n/a
E-cadherin	n/a	n/a	-	+	n/a
Wt1	n/a	n/a	n/a	n/a	-

Figure 4.2.10 - Marker expression of tauGFP cells cultured in organotypic pellets
A, C, E, G and I show individual markers; B, D, F, H and J show markers and tauGFP expression; A and B – Calbindin (blue) is expressed by WT structures, but not by tauGFP+ structures; C and D – Laminin (red) is expressed by both tauGFP+ and tauGFP- structures; E and F – Pax2 (red) is expressed by WT structures, but not by tauGFP+ epithelial structures; G and H - E-cadherin (blue) is expressed by both WT and tauGFP+ structures; I and J – Wt1 (blue) is not expressed by tauGFP+ structures, but expressed strongly (white open arrow) and weakly (blue open arrow) by WT cells.
Open arrows indicate WT structures; white block arrows indicate tauGFP ESC-derived structures
K – is a summary of the overall marker expression of tauGFP ESC-derived cells found in organotypic cultures. A plus or a minus denotes whether any tauGFP+ cells express or do not express the respective marker. A plus or a minus in brackets gives information about whether this marker expression was consistent with markers of the respective renal compartment. More information about the expression patters is also provided
L – shows a summary of all immunohistochemical data obtained from tauGFP ESCs grafted in organotypic cultures. Red boxes indicate combinations of markers, which if co-expressed by the same cells would be a strong indication for the presence of ESC-derived renal cells.

all examined cases be classed as false positives or could be shown lacking tauGFP expression.

4.2.6 Further marker expression studies confirmed that the ESC-derived structures did not express the combination of markers normally present in developing renal structures

The gene expression profile of the tauGFP ES cell-derived cells present in organotypic cultures was characterised for the following 5 markers individually and in combinations of two at a time. The markers examined were Calbindin, Laminin, Pax2, E-cadherin and Wt1. Representative images for all genes were shown in Figure 4.2.10, A-J. The data was summarised in Figures 4.2.10, K and L. In the tables shown in Figure 4.2.10, K and L, a minus indicates that the marker examined was not detected by IHC in any tauGFP positive cells (i.e. the grafted ESC-derived cells) in any of the samples. A protein was marked as present (by a plus sign), when exogenous (tauGFP+) cells in the organotypic cultures were positive for this marker. Then, for all positive markers, the expression in the currect renal compartment was assessed. The result was indicated by a plus or a minus in backets on Figure 4.2.10, K. For example, "+ (-)" would indicate that tauGFP cells express this marker, but that positive cells did not localise into the correct compartments. These details were also provided in the last column of the table in Figure 4.2.10, K. The latter figure shows that only 3 out of the 5 genes tested were expressed by tauGFP+ cells and that only 2 of these were seen in the correct compartment. More importantly, a further assessment based on co-localisation studies (a summary is provided in Figure 4.2.10, L) confirmed that none of these cells fulfilled the requirement for co-expression of two or more kidney markers. In Figure 4.2.10, L, a red box indicates combinations of markers, which (if expressed by the same cell) would be a strong indication for this cell to be a kidney cell. Although, this summary shows that the tauGFP cells were positive for the genes of interest in some cases, they were never seen to express both markers of interest at the same time. No evidence was found that the cells forming chimeric structures with native renal epithelia could be renal cells.

4.2.7 Organotypic pellets contained undifferentiated cells after 6 days of culture

4.2.7.1 Mixtures of embryonic kidney cells with Oct4-GFP cells revealed the presence of undifferentiated cells in the organotypic culture

Embryonic stem cells stably expressing GFP under the Oct4 promoter were a kind gift from Dr. Patricia Murray, University of Liverpool. 15,000 Oct4-GFP cells were mixed with 100,000 E11.5 embryonic kidney cells as previously described. 6-day organotypic pellets were fixed and stained for Calbindin and Laminin, as previously described. Oct4-GFP cells were detected by GFP fluorescence. Confocal

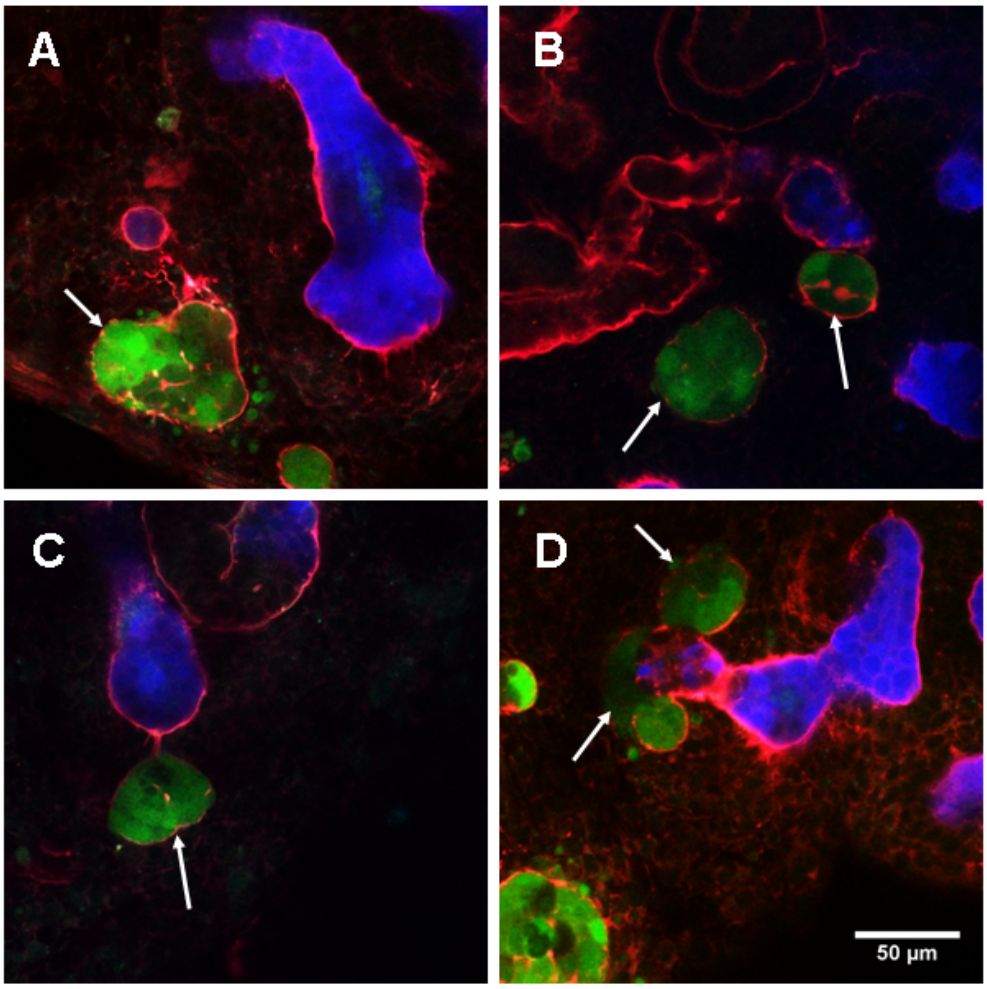

Figure 4.2.11 - Oct4-GFP ESCs grafted in ogranotypic cultures show that expression of Oct4 is maintained even after 6 days of organ culture
A – example of a Laminin-bound Oct4 positive structure (arrow); B – example of two Oct4-GFP expressing Laminin-bound structures, one of which in a close proximity to a renal tubule; C – example of an Oct4-GFP+ structure establishing a contact with a WT UB; D – Oct4+/Laminin+ structures have formed a chimeric structure with a renal tubule
Laminin (red), Calbindin (blue), Oct4-GFP (green)

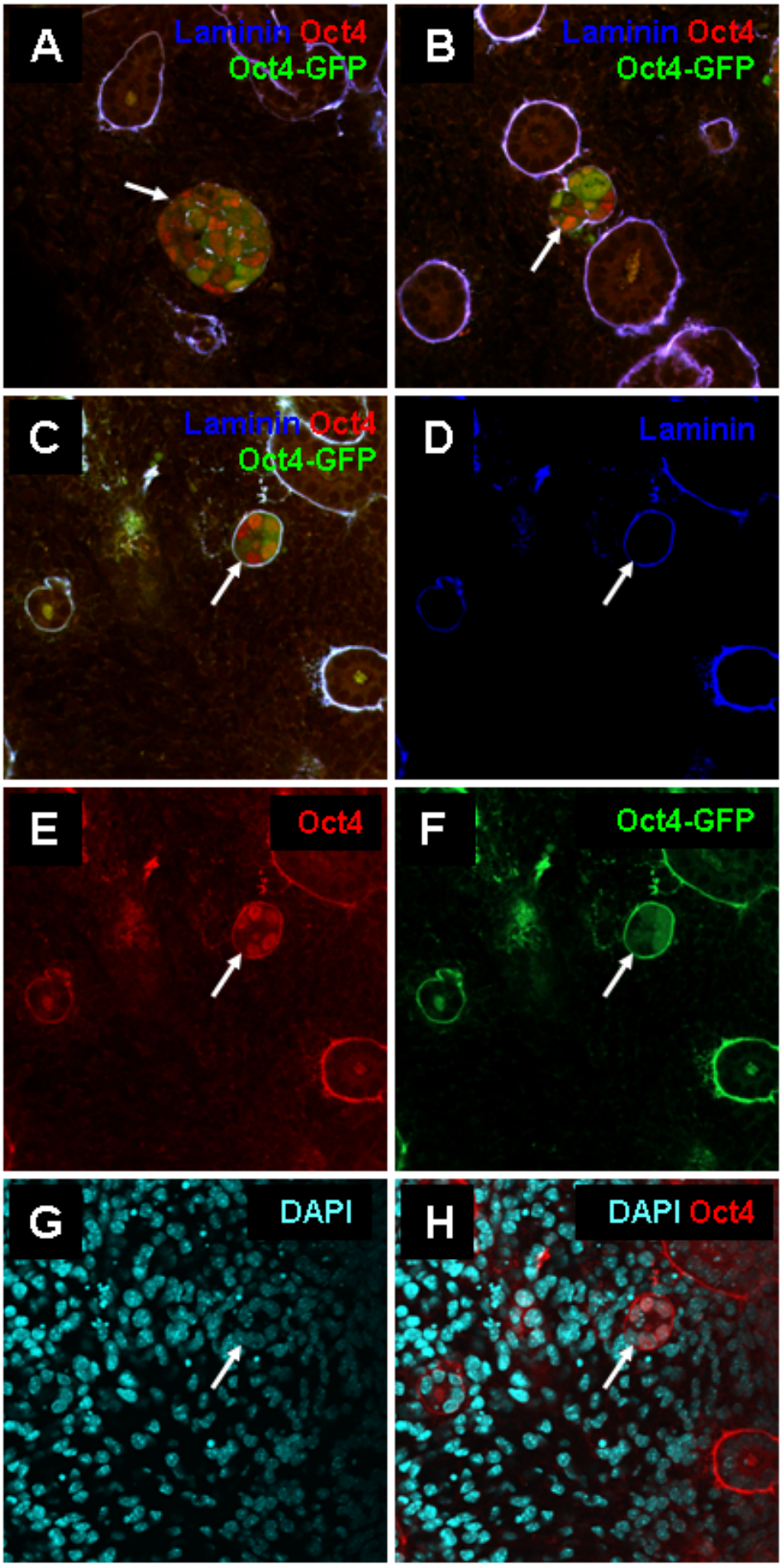
A
Laminin Oct4
Oct4-GFP
B
Laminin Oct4
Oct4-GFP
C
Laminin Oct4
Oct4-GFP
D
Laminin
E
Oct4
F
Oct4-GFP
G
DAPI
H
DAPI Oct4

Figure 4.2.12 - Immunohistochemistry for Oct4 confirms the specificity of Oct4-GFP expression and the presence of Oct4+ structures in organotypic pellets containing ESCs
A, B and C – examples of Laminin+ (blue) structures showing colocalisation of Oct4-GFP(green) and Oct4 antibody (red), arrows; D – Laminin expression of C (arrow); E – antibody detection of Oct4 of the sample shown in C (arrow); F - Oct4-GFP detection of the sample shown in C; G – DAPI (cyan) showing nuclear staining of C; H – DAPI (cyan) and Oct4 (red) showing the nuclear localisation of Oct4

microscopy revealed that GFP+ cells could be detected in the mixtures suggesting that undifferentiated cells could be still present even after 6 days of *in vitro* culture (Figure 4.2.11). Surprisingly, Oct4-GFP positive structures were observed to form chimeric structures with wild –type renal epithelia (Figure 4.2.11, D). This indicated that a differentiated state might not be required for the formation of chimeric structures, once again confirming that integration into renal epithelia does not provide sufficient evidence for renal differentiation and has to be used in conjunction with the co-expression of renal markers.

4.2.7.2 Immunohistochemistry for Oct4 showed co-localisation with Oct4-GFP and confirmed that the grafted cells expressed this pluripotency marker

As the Oct4-GFP transgenic line used in the experiments above had not been extensively characterised, the results obtained in the previous section had to be confirmed by immunohistochemistry for Oct4. For this reason, the organotypic cultures were co-stained for GFP, Oct4, Laminin and DAPI (Figure 4.2.12). Panels A, B and C of Figure 4.2.12 clearly showed that GFP fluorescence co-localised with nuclear Oct4, as detected by immunohistochemistry. The individual acquisition channels of the confocal section in panel C are shown in D, E and F. G shows DAPI staining for the same image and H – co-localisation between the nuclear stain and staining for the octamer-binding protein Oct4.

4.2.7.3 Oct4 positive cells express E-cadherin but not Pax2

In the previous section it has been shown that Oct4 positive cells can form chimeric structures with renal epithelia. To see whether these structures have similar expression profiles of relevant genes as the structures obtained with tauGFP ESCs, organotypic pellets containing Oct4-GFP ESC were stained for E-cadherin and Pax2. The Confocal micrographs produced from these cultures showed that Oct4-GFP+ structures indeed expressed E-cadherin and did not express the renal marker Pax2 (Figure 4.2.13, A-H). Open arrows indicate GFP+, stem-cell derived structures

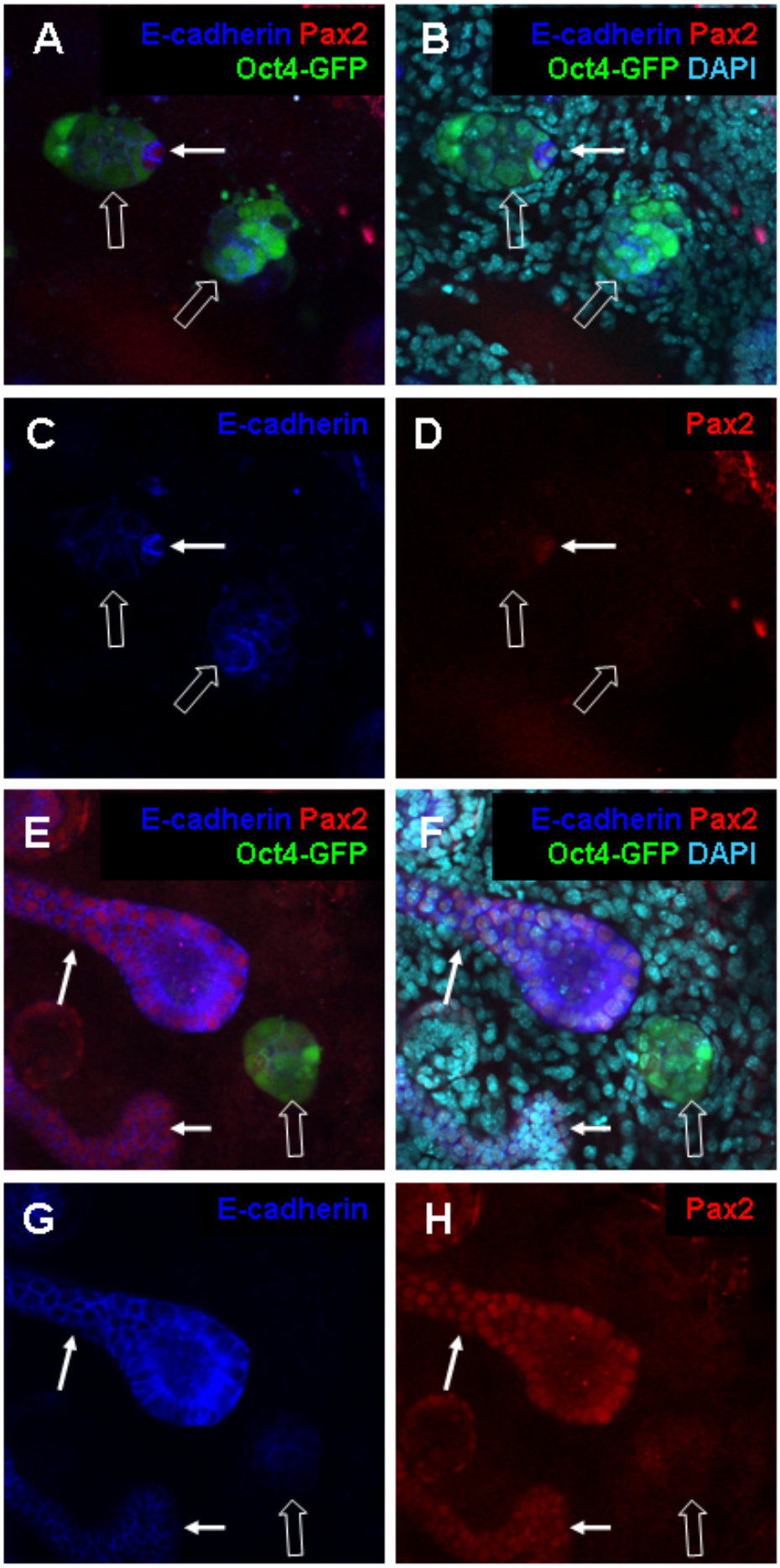
A
E-cadherin Pax2
Oct4-GFP
B
E-cadherin Pax2
Oct4-GFP DAPI
C
E-cadherin
D
Pax2
E
E-cadherin Pax2
Oct4-GFP
F
E-cadherin Pax2
Oct4-GFP DAPI
G
E-cadherin
H
Pax2

Figure 4.2.13 - ESCs grafted in reaggregated organotypic cultures co-express Oct4 and E-cadherin, but not Pax2
A and E – triple staining of organotypic cultures containing grafted cells showing that Oct4+ cells co-express E-cadherin and do not express Pax2; B and F – the same images in A and E, also showing nuclear staining for DAPI; C – E-cadherin staining of A; D – Pax2 staining of A; G – E-cadherin staining of E; H – Pax2 staining of E
arrow shows WT epithelia, open arrows show grafted cells

(E-cadherin+/Pax2-). White arrows indicate native renal epithelia, which co-express E-cadherin and Pax2. It should be noted that these images also show a chimeric structure between a GFP+/E-cadherin+/Pax2- structure and a native structure (Figure 4.2.13, A-D).

4.2.8 How are chimeric structures assembled?

The ability of kidney cells to form chimeric structures with exogenous cell types has previously not been reported. The results given in previous sections of this chapter provided evidence that the tauGFP positive cells forming chimeric structures with native renal epithelia did not possess renal characteristics. In such a case, it was interesting to investigate the mechanisms by which these structures were formed. Several possibilities for this process exist:

- cells directly assemble into chimeric structures at the single cell stage
- cells first form either native or host structures, which based on proximity to each other simply adhere (as examined in section 4.2.3)
- cells first form either native or host structures, which then fuse to each other as a result of recognition mechanisms (non-random, regulated)

Studying multiple serial confocal sections of reaggregated kidneys acquired for all of the studies throughout this chapter located pairs of tauGFP positive and tauGFP negative structures in close proximity to each other. In some cases, thin Laminin-positive extensions were seen connecting two individual structures (as in Figure 4.2.11, C). This was in support of the data presented in section 4.2.3 suggesting that a form of recognition mechanism between the two types of cells might be involved. Figure 4.2.14 shows what looks like a more advanced stage of the same phenomenon. The serial confocal sections (Figure 4.2.14, A-C, E-G) show how a unilayered strip of cells invade a tauGFP+ structure. Although the mechanisms of this process could not be identified, it was also demonstrated that both structures were positive for the epithelial adhesion molecule E-cadherin (Figure 4.2.14, D).

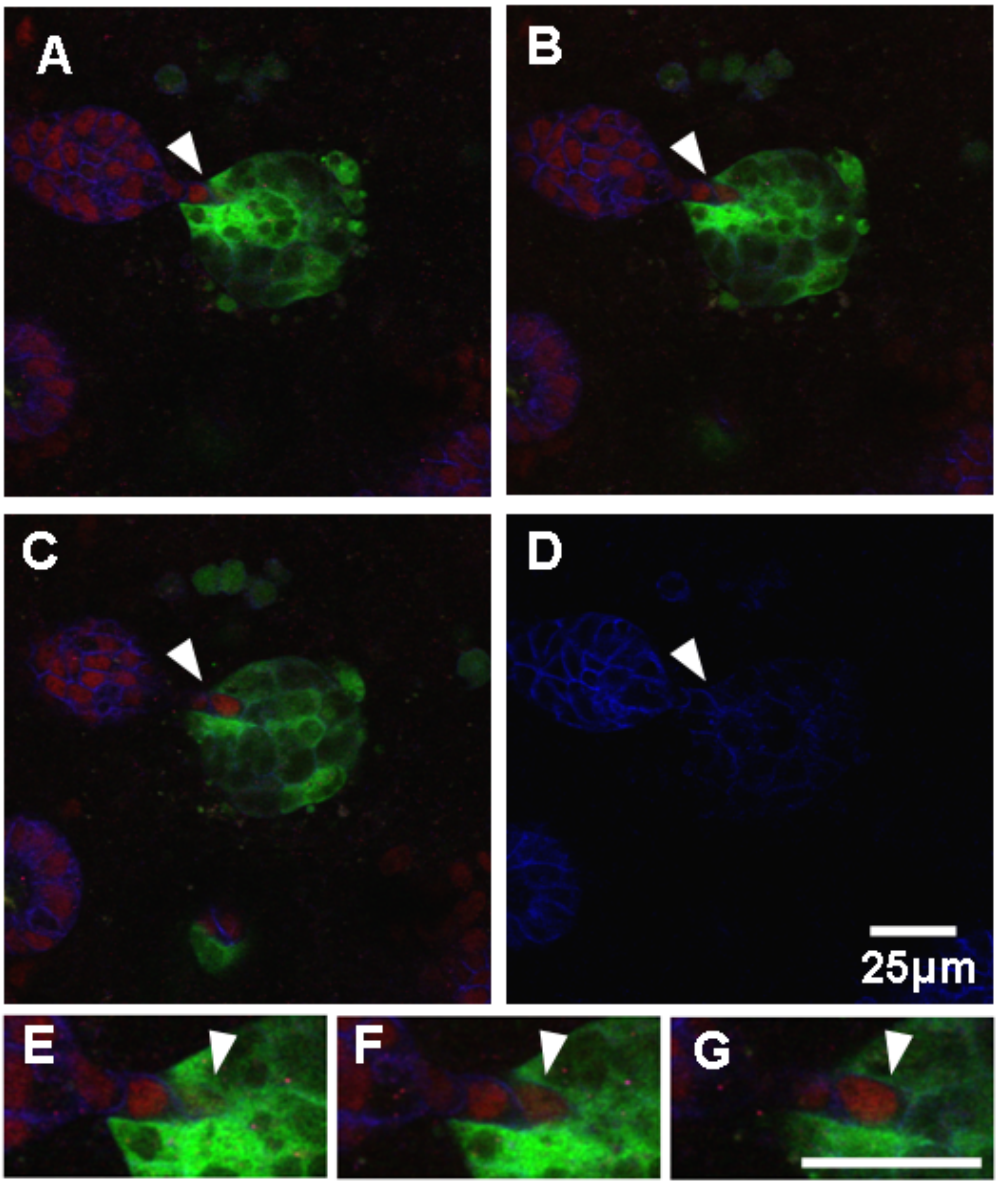

Figure 4.2.14 -Three dimensional imaging of tauGFP+ and WT epithelia, in the process of forming a chimeric structure
A, B and C – show serial confocal sections of the same epithelial structures, exhibiting a tauGFP ESC-derived component and a WT component. A string of WT cells can be seen intercalating between the cells of an entirely tauGFP ESC-derived structure
D – shows that both structures express E-cadherin; E, F and G – are magnified versions of A, B and C
E-cadherin(blue), Pax2 (red), tauGFP (green)

4.2.9 Pilot studies suggest that genetically labelled with GFP human embryonic stem cells behave similarly to mouse ES cells when placed in mixed organotypic cultures

4.2.9.1 Generation of human ES cells constitutively expressing GFP under the CMV promoter

As previously discussed, transient labelling methods show serious limitations for use in the organotypic pellet culture method. For this reason a stably expressing GFP hESC line had to be created for testing the renogenic potential of human ES cells. These experiments were done with the kind support and in the lab of Dr. Paul de Sousa, University of Edinburgh.

RCM1 human embryonic stem cells at P78 were treated with 10μM ROCK inhibitor Y-27632 for 3h before detachment from the cell culture plates. Cells were counted and collected in aliquots of 10^{-7} cells. 1 aliquot was resuspended in 1mL chilled PBS

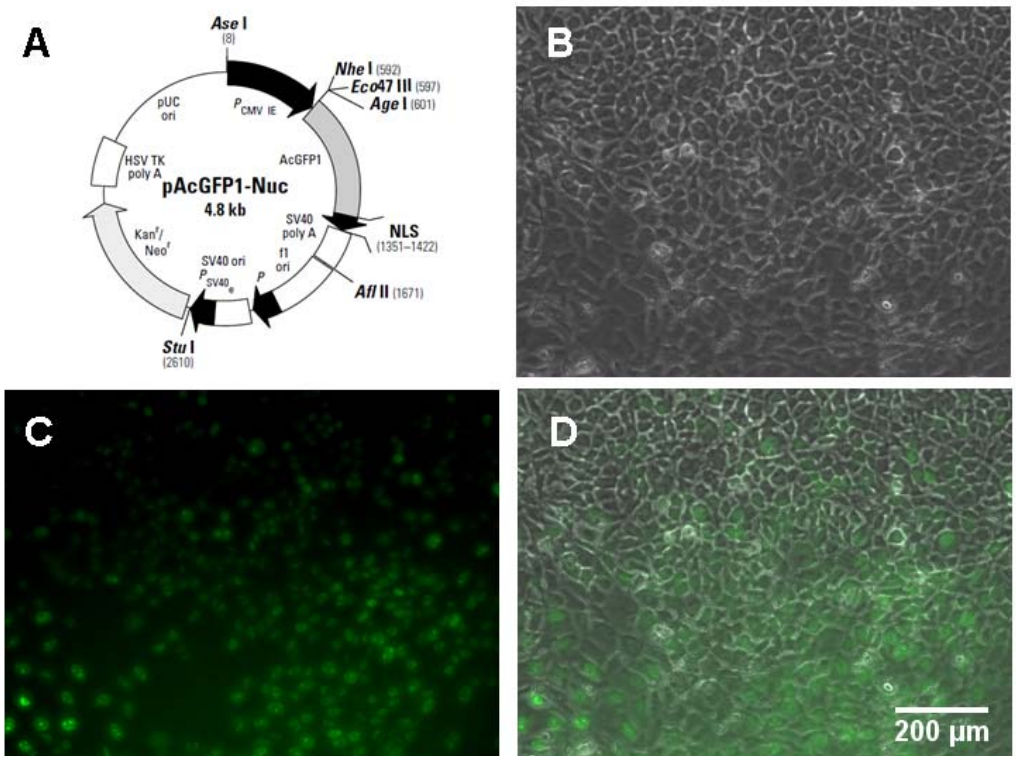

Figure 4.2.15 - Generation of a human embryonic stem cell line constitutively expressing nuclear GFP under the CMV promoter
A – diagram of the plasmid used for the generation of a transgenic hESC line; B – light micrograph showing a colony of undifferentiated RCM1 hESC; C – RCM1 hESC express nuclear GFP after transfection with pAcGFP1-Nuc plasmid; D – merge of B and C

only (negative control) and 3 were each resuspended in 1mL chilled PBS containing 50µg linearised with ApaII pAcGFP1-Nuc plasmid (Figure 4.2.15, A; Clonetech). The control and transfections were electroporated at 200µF, 340V (Biorad Gene Pulser) and plated on freshly coated with Matrigel 10cm cell culture dishes. Antibiotic selection with 200µg/mL G418 was started 2 days after plating. All plates were monitored for colony formation and growth over three weeks. In the control sample, colonies appeared and increased in size, but disappeared completely about two weeks of starting the antibiotic selection. In the transfected samples, colonies remained viable and showed a continuous growth. The transfected colonies were checked for GFP expression by fluorescence microscopy and 18 GFP colonies were picked in sets of 6 during weeks 3 and 4 after selection. Picking of colonies was carried out in sterile conditions, manually, by collagenisation and scraping with a 200µL pipettor. All clones were cultured as described in section 2.4 for routine culture of hESC.

4.2.9.2 GFP-tagged hESCs form chimeric structures with renal epithelia

To select lines, which might be suitable for mixing in organotypic cultures, the selected clones were examined for chimerism (the presence of both GFP+ and GFP- cells in the same clonal line) and fluorescence intensity. The line showing least chimerism and brightest fluorescence was selected for use in cell mixing experiments (Figure 4.2.15, B, C and D).

To avoid human cells disrupting the normal development of reaggregates (as they are considerable larger than mouse cells) 10,000 (rather than15,000 as in most reaggregates) of the selected clone RCM1 pAcGFP1-Nuc hESCs were mixed with 100,000 embryonic kidney cells and cultured as previously described for 6 days. The pellets were fixed with 4% PFA and permeabilised by methanol, before staining them for DAPI, Calbindin and Laminin.

Confocal micrographs revealed that the nuclear fluorescence of the genetically labelled hESCs could be detected in the organotypic pellets (Figure 4.2.16, A-F), although not all human cells were GFP positive. This was evident by the presence of

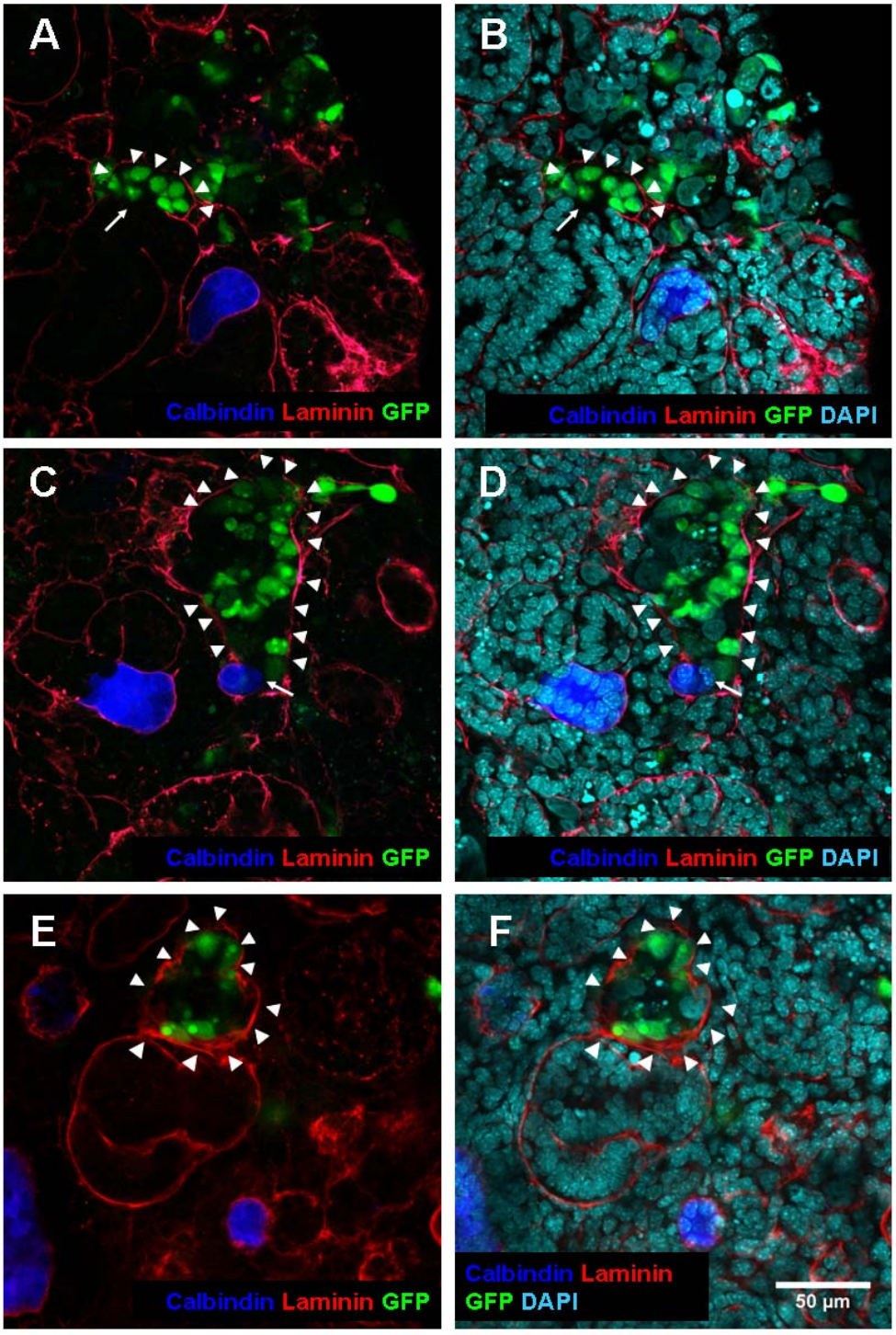
A
Calbindin Laminin GFP
B
Calbindin Laminin GFP DAPI
C
Calbindin Laminin GFP
D
Calbindin Laminin GFP DAPI
E
Calbindin Laminin GFP
F
Calbindin Laminin
GFP DAPI
50 µm

G

mESC	hESC
form Laminin - bound structures	form Laminin - bound structures
form chimeric structures with renal epithelia	form chimeric structures with renal epithelia
negative for Calbindin	negative for Calbindin
have small nuclei, which stain intensely with DAPI and show chromocentres	have large faintly stained with DAPI nuclei lacking chromocentres

Figure 4.2.16 - hESCs behave similarly to mESCs when mixed with embryonic kidney cells and cultured in organotypic pellets for 6 days
A and B, C and D, and E and F – show that hESCs form Laminin-bound structures when grafted in reaggregated organotypic pellets (arrowheads); A and B – show a chimeric structure formed by a WT nephron and human cells; C and D – show a hESC-derived and a WT UB enclosed by a continuous Laminin staining (arrow)
G – compares the observations made for human and mouse ESCs after grafting in kidney organotypic pellets

nuclei considerably bigger than these of mouse embryonic kidney cells, which stained for DAPI more weakly and lacked chromocentres (Moser et al., 1975). Similarly to mouse ES cells they were also seen in Laminin-bound structures (Figure 4.2.16, A-F), which in some cases formed chimeras with mouse renal epithelia (Figure 4.2.16, A-D). The major similarities and differences between mouse and human ES cells were summarised in Figure 4.2.16, G. As these were only pilot studies the hESC-derived cells were not characterised for marker expression and it was therefore unclear whether some cells remained pluripotent similarly to mESCs. Further studies would be necessary to investigate the behaviour of hESCs grafted in organotypic cultures.

4.3 Summary and discussion

In this chapter, I examined the potential of undifferentiated cells to differentiate to renal cells as a response to the signals from the kidney microenvironment, which in development is sufficient to support the growth kidney rudiments *in vitro.* The initial characterisation of constitutively expressing GFP mouse embryonic stem cells showed that these cells behaved indistinguishably from their parent ES cell line – E14. In conditions favouring pluripotency, the tauGFP ES cell line showed a normal expression of the pluripotency marker Oct4, combined with a robust expression of tauGFP in more than 95% of the cells in culture. No correlation was observed between Oct4 and tauGFP expression. The transgenic cells continued to express GFP on the long-term after withdrawal of Puromycin selection (EB experiments). tauGFP ES cells could also form embryoid bodies normally and were able to give rise to cells from the three germ layers. Since no abnormal changes could be detected in these cells, they could be used to study the differentiation potential of ES cells to renal cells after integration in reaggregated organotypic pellets. In the initial experiments, tauGFP ES cells showed promise for the generation of renal cells as they were observed to give rise to chimeric structures with renal epithelia. Further characterisation showed that these structures did not adequately fulfil the requirements for renal cells set out in the beginning of this chapter. First of all, although some ESC-derived structures showed the formation of a lumen, most of

them gave rise to tubular-like structures lacking a lumen, with a morphology and positional orientation very different from this of renal tubular epithelial cells. Only this information was insufficient to determine whether the cells could be renal or not, as they could have been in an immature stage still having to orient themselves properly and organise into continuous tubular structures. Examination of these structures for the expression of kidney markers and combination of kidney markers revealed that there was no evidence that these cells were renal. First, although ESC-derived Pax2 positive cells were indeed present in the developing organotypic cultures, they were not found in kidney tubules and were not expressing the epithelial marker E-cadherin. At least some of them could be identified as neural derivatives, as in addition to their Pax2 positivity, they exhibited the extension of neurites. Furthermore, artefacts, which looked like Pax2 positive tauGFP cells integrating in renal epithelia were detected in regions exhibiting unhealthy morphology. It was likely that some differentiating ESC-derived cells were not able to survive in the microenvironment of a kidney rudiment and underwent cell death, which created structures resembling Pax2+ nuclei. These were identifiable by exhibiting fluorescence of nuclear appearance in other fluorescence channels. Additionally, native Pax+/E-cadherin+ renal cells intercalating in tauGFP+ structures, created false positives when examined only in two dimensions. The finding that tauGFP-derived cells were positive for Laminin was inconclusive, as many non-kidney types of cells also express this marker. The co-localisation studies revealed that no Laminin+/Calbindin+ or E-cadherin+/Pax2+ cells could be detected in any of the examined experiments, which strongly suggested that no kidney cells were produced in the pellets. It cannot be completely excluded that undetectably low numbers of ESC-derived kidney cells were present in the reaggregated organotypic pellets, but no evidence was found to support this possibility. Importantly, Oct4 staining of cultured for 6 days organotypic pellets led to the discovery, that even after 6 days of culture, Oct4+ cells were still present in the organotypic cultures. This was not surprising as ES cells can be detected in differentiation cultures lacking pluripotency - supporting factors even after 10-15 days of culture (Chapter 5). What was more surprising was that Oct4+ cells were also able to engage in cross-talk with native renal structures and exhibit chimerism with wild-type renal epithelia. More detailed

marker expression studies detected that Oct4+ cells were also positive for E-cadherin, as normal for ES cells (Mummery et al., 1990).

These results were not completely consistent with the study of Steenhard et al. (2005) who reported that a renal differentiation program took place in ESCs after they had been subjected to the signals of a kidney microenvironment for 5 days. Although, their study did not provide evidence that Oct4 expression had completely disappeared in the injected in kidney rudiments ROSA26 ES cells after 5 days of culture, the presence of a detectable number of Oct4 positive structures in the experiments described in this chapter suggested that 6 (and even less so - 5) days were not a sufficient period for a complete stem cell differentiation. The high number of tauGFP ESC-derived structures forming chimeric structures with native renal epithelia in reaggregated organotypic cultures is highly reminiscent of the "striking" number of ROSA26 ESC – derived structures identified as renal by Steenhard et al. (2005). The current chapter also presented evidence that Oct4 expressing cells can form Laminin-bound structures resembling renal vesicles, very similar to the ones observed by the authors. All this evidence suggests that a revision of the study of Steenhard et al. (2005) where samples of injected cells could also be stained for Oct4, might provide valuable additional information about the ESC-derived cells. But even if the existence of ESC-derived structures in the experiments described by Steenhard et al. (2005) could potentially be explained, at least to some extent, by the presence of isolated Oct4-positive structures, the marker expression that they have reported still does not fit this hypothesis. Here, it would be valuable to once again refer to the limitations of cell tracking and the danger of false positives in organotypic cultures. The authors have based most of their immunohistochemical analysis on sections stained for β-galactosidase, which is less sensitive than using GFP in cell mixing experiments, as no individual cells can be seen clearly. This chapter has also provided evidence for the necessity of an extremely robust detection method with a single-cell level resolution, which also allows for a three-dimensional characterisation, due to at least two different types of sources of false positive for renal markers staining of ESC-derived cells. Although the authors have presented an indeed careful examination of marker expression, importantly, additional data from

the Davies lab suggests that developing nephrons might have a way of taking up debris from dead neighbouring cells to generate a third type of false positive, in which long portions of nephrons appear positive for the cell label (unpublished data, Supplementary Figure 4).

Of course, the limitation of using a single cell line for experiments should also be mentioned. It could not be excluded that although the tauGFP ESC line used in this thesis did not show any obvious differences from normally behaving mESCs by *in vitro* characterisation, it might have had a limited renogenic potential. Although a second ESC line (the Oct4-GFP ESCs) was used in the experiments and showed consistent results, it does not allow the detection of cells which could have formed renal tubules, as Oct4 expression in these cells should have been switched off.

Furthermore, it is interesting to discuss that all structures localising into renal epithelia were also positive for E-cadherin. This observation suggested that E-cadherin - associated cellular processes or E-cadherin itself could play an important role in the formation of chimeric structures. Very little is known about the process of how forming nephrons fuse to the ureteric bud (Georgas et al., 2009; reviewed by Gilbert, 2000). Working with treated in various ways or genetically modified embryonic stem cells might contribute to elucidating this process. As the data provided by the current study suggested a putative role for E-cadherin in the formation of chimeric structures, this could first be confirmed by knockout experiments and second – potentially transferred to studying whether E-cadherin has a role as a regulator of kidney development, especially in the fusion of renal vesicles to the UB. Cadherin-6 has already been implicated in this process (Mah et al., 2000). In Cadherin-6 mutants a significant number of renal vesicles fail to fuse with the UB and therefore fail to form functional nephrons. Similar experiments with abolishing only E-cadherin or both cadherins simultaneously could help clarify that further. It has already been reported that a stable transfection of *Snail*, which is a negative regulator of E-cadherin, is able to transform MDCK cells to a more mesenchymal phenotype (Cano et al., 2000).

Furthermore, studies combining the use of embryonic stem cells, which show an ability to produce fusions with renal epithelia, with studies in the *in vitro* disaggregation-reaggregation system could provide a valuable tool to dissect the timing and various steps of the process. Currently, evidence in the literature shows some disagreement about whether this process happens very early in renal vesicle formation (Bard et al., 2001) or later, at the late renal vesicle stage (Georgas et al., 2009). In addition, both of the studies acknowledge the possible existence of a multistep process, which initiates this fusion – first, the formation of an intimate contact between the RV and the UB; second, the degradation of basal lamina between the two; and third – the formation of a continuous epithelium with a lumen. These problems could also be addressed by an ES cell - based *in vitro* system, which offers the advantages of easy genetic manipulation.

Detailed confocal micrographs in the three dimensions presented in this chapter have captured the interactions between several pairs of tauGFP+ and native kidney structures. It would be therefore interesting to investigate, whether such fusion events could be following a mechanism similar to the one described by Samakovlis et al. (1996) for the tracheal development in Drosophila. The authors detail a process in which two tubes, which will fuse, establish a connection with each other on the basis of two single cells coming from the two different tubes, which extend protrusions to recognise each other.

Finally, although based on pilot studies with human embryonic stem cells, the data presented in this chapter suggested that human embryonic stem cells might behave similarly to mouse cells after being placed in the microenvironment of a developing embryonic kidney. These initial studies were discontinued due to several reasons. First, the mixing properties between mouse and human cells have not been extensively characterised and the known differences between the two types of cells pose an additional challenge to the interpretation of results. Also, as the pilot experiments with human cells did not show any advantages over the use of mouse cells, the latter system would be more suitable for further investigations, due to the better molecular tools already available.

Chapter 5

Inhibition of Notch signalling in mESC does not improve differentiation to kidney cells in the disaggregation-reaggregation system

5.1 Introduction

In the previous chapter, I showed that in embryonic kidney disaggregation-reaggregation experiments, undifferentiated mouse ES cells were able to associate with, and form chimeric structures with, renal epithelia, but failed to integrate into renal structures and to express normal kidney markers. On the basis of this finding, I hypothesised that pre-differentiation of ES cells might improve the renogenic abilities of these cells by first priming them to commit to a mesodermal lineage. Evidence in the literature suggested that Notch inhibition promotes the differentiation of ESCs to mesoderm at the expense of ectoderm (section 5.1.1). The studies described in this chapter evaluate whether Notch inhibition in differentiation cultures would be beneficial for generating ESC-derived renal cells. I will start this chapter by describing the motivation for the experiments herein in context of the published literature. Then, I will concisely review the mechanisms and players in the Notch signalling pathway and provide a few examples of how Notch signalling regulates developmental processes. I will then present pilot work suggesting that Notch inhibition does not positively affect renal differentiation.

5.1.1 The role of Notch inhibition in the differentiation of mouse embryonic stem cells

There are two possible ways for ESCs to obtain a renal identity. The first possibility is that they follow the normal processes that happen during development to become first mesoderm, then intermediate mesoderm and finally commit to the nephrogenic lineage (please refer to Figure 4.1.1 in the previous chapter and Chapter 1). The second way for obtaining kidney cells could be through developmental leaps, which would omit the intermediate stages and transit directly to a kidney fate via steps that are normally not present in development. The former possibility suggests that successful differentiation methods would have to take embryonic stem cells through the stages of normal development, in the process of which the desired lineage would have to be directed at each step at which cells normally make a “lineage choice”. In the case of trying to generate kidney cells, following the idea that cells have to follow the stepwise developmental pathway (epiblast, mesoderm, intermediate

mesoderm), would suggest that increasing the number of cells, which commit to a mesodermal lineage in a differentiation culture, could also increase the chances for obtaining kidney cells. For this reason, a method for the directed differentiation to mesoderm was sought.

A literature search identified a report that demonstrated Notch signalling in embryonic stem cells to be essential for some lineage fate choices. Lowell et al. (2006) discovered that the release of the Notch intracellular domain (NICD), activated genes favouring the differentiation of ESCs to a neural lineage. Conversely, inhibition of γ-secretase (which is necessary for Notch signalling activation) blocks most of the differentiation to neural cells and favours other lineages, especially mesoderm. This information was supported by other literature sources. Nemir et al. (2006) showed that inactivation of Notch1 enhanced the differentiation of ESC to cardiomyocytes, which are also of a mesodermal lineage. In addition, they concluded that Notch signalling influences the cell fate decision between mesodermal and neuroectodermal lineages, which is consistent with the previously presented data about the role of Notch signalling in development (see section 5.1.3). Schroeder et al (2006) also report that activation of Notch signalling inhibits the generation of Flk1+ mesodermal cells from ESCs. Information about the effects of Notch inhibition on the differentiation of mouse ES cells to renal precursors was lacking, but based on evidence in the literature, this approach might be useful for discovering a method for directed differentiation to renal cells, based on the evidence that it favours mesoderm specification.

5.1.2 The Notch pathway - discovery and mechanism

Notch signalling is a way of communication between two or more neighbouring cells, based on receptor-ligand interactions. This is a conserved mechanism for modulating the cell's response to developmental signals and controlling cell fate, which is based on amplification and consolidation of molecular differences between cells (Artavanis-Tsakonas et al., 1999; Fleming et al., 1998).

The first reference to Notch found in the literature was made by John Dexter in 1914, who described a mutant fly with notched wings. On the basis of Mendelian genetics, Dexter also determined that the mutation was caused by "a dominant sex-linked factor lethal when homozygous". A later reference to Notch was made by Morgan and Bridges (1916), summarizing Dexter's results and taking them further by Bridges' mapping the position of this factor to 2.6 on the X chromosome (Morgan and Bridges, 1916; Bridges, 1917). Mohr (1919) also encountered this phenotype in his experiments. He extensively described a fly mutant phenotype called "notch", characterised by a serration at the ends of the wings.

The importance of Notch for developmental processes became clear later when experiments in developing fly larvae demonstrated that lethal loss-of-function mutations of Notch produce a "neurogenic" phenotype, in which endoderm and mesoderm are absent, or almost absent, and have been substituted for a proliferating ectoderm with the characteristics of an early nervous system (Poulson, 1937). These results also suggested that the mutated factor is necessary in gastrulation, for the normal specification of the three germ layers.

NOTCH is a transmembrane receptor, which localises at the cell surface as a heterodimer resulting from an intracellular cleavage at site 1 (S1) of the protein in the trans-Golgi network (Blaumueller et al. 1997). Although flies have only one Notch receptor and *C. elegans* - two (which act redundantly) (Fitzgerald et al., 1993), mammals have four Notch paralogs (reviewed by Kopan and Ilagan, 2009) that could be either redundant or display unique functions (Krebs et al., 2003; Cheng et al., 2007). Notch proteins (Notch1, Notch2, Notch3, and Notch4) contain epidermal growth factor (EGF)-like repeats (Wharton et al., 1985; Kidd et al., 1986), which are followed by negative regulatory regions (NRR), consisting of three cysteine-rich Lin 12-Notch repeats (LNR). The intracellular region of Notch contains multiple functional domains - an RBPjκ-association module (RAM), seven ankyrin repeats (ANK domain), NLS (nuclear localisation sequences) and a PEST (proline, glutamate, serine and threonine-rich) domain, which regulates the stability of Notch intracellular domain (reviewed by Kopan and Ilagan, 2009).

Notch signalling is initiated by an interaction between Notch receptors and their ligands (Figure 5.1.1), which in mammals are the transmembrane proteins Jagged1, Jagged2, Delta1, Delta3 and Delta4 (Lindsell et al., 1995; Shawber et al., 1996; Bettenhausen et al.,1995; Dunwoodie et al., 1997; Shutter et al., 2000). On binding, the Notch receptor is activated by a series of proteolytic cleavages, which is initiated by ADAM (A disintegrin and metalloproteinase) (Qi et al, 1999). The enzyme cleaves Notch at site 2 (S2), which is deeply buried in the NRR (Figure 5.1.1). The initial release of the Notch ectodomain, creates a membrane-tethered intermediate - NeXT (Notch extracellular truncation), which acts as a substrate for γ-secretase (a multicomponent intramembrane-cleaving protease, I-CLiP) (de Strooper et al., 1999; Ray et al., 1999; reviewed by Wolfe and Kopan, 2004). This final cleavage at site 3 (S3) fully releases NICD for translocation to the nucleus, where it interacts with the sequence-specific DNA-binding protein CSL (also known as CBF1or RBPjκ and a homologue of the Drosophila suppressor of hairless Su(H)) (reviewed by Lai, 2004) via its RAM domain. Fortini and Artavanis-Tsakonas (1994) have observed a direct protein-protein interaction between NCID and the transcription factor CSL. After translocation to the nucleus the CSL-containing co-repressor complex is displaced by a CSL and NICD-containing co-activator complex, which mediates the activation of Notch target genes. In the absence of NICD, the co-repressor complex actively represses Notch target genes (reviewed by Lai, 2004). Components of the Notch signalling pathway or events resulting from Notch-mediated gene activation interact and cross-talk with other pathways, which then exert a cooperative effect on cell fate. For example, activated Notch signalling has been associated with an effect on histone acetyltransferases (HATs), SMADs, NFκB, HIF1α, *Hes* and many others (reviewed by Kopan and Ilagan, 2009; Jarriault et al., 1998). As the focus of this section is to give information about the general principles of Notch signalling, rather than provide a complete review about the complex regulatory networks involved in transcriptional activation and repression. As a summary, a snapshot of some important players is given in Figure 5.1.2.

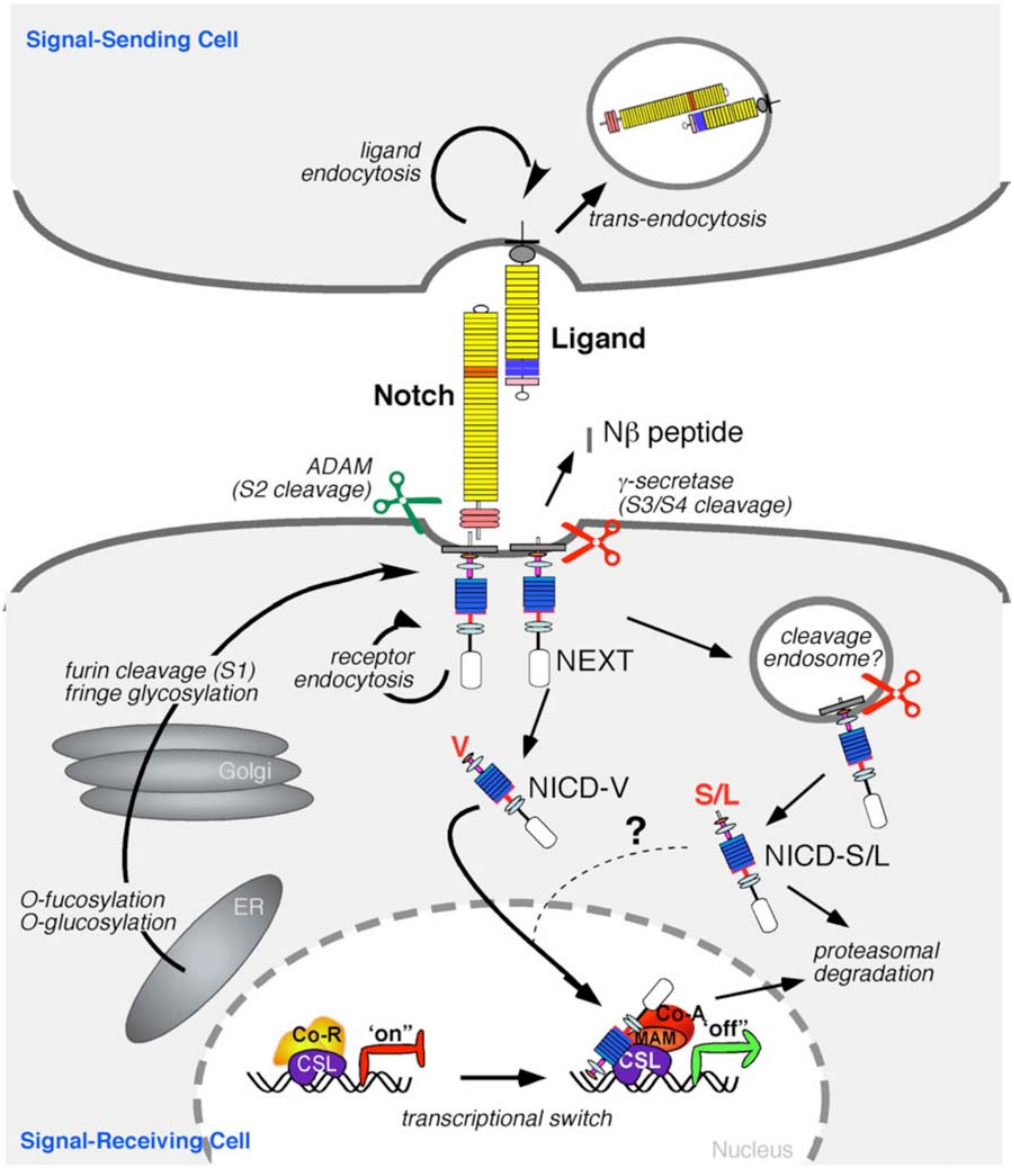

Figure 5.1.1 - General principle of Notch signalling activation (from Kopan and Ilagan, 2009)
After polypeptide synthesis, the Notch receptor undergoes post-translational modifications in the ER and is cleaved in the Golgi to form a heterodimeric protein trafficked to the cell surface. When the Notch extracellular domain establishes a contact with its ligand a cleavage by ADAM at S2 is initiated followed by a cleavage of the resulting intermediate (NEXT) at S3, which finally releases NICD. NICD is then translocated to the nucleus where it associates with other co-activators and CSL, thereby replacing CSL-associated co-repressors and activating transcription.

Component & Function	*Drosophila*	*Caenorhabditis elegans*	Mammals
Receptor	Notch	LIN-12, GLP-1	Notch 1–4
Ligand			
DSL/DOS	Delta, Serrate		Dll1, Jagged1 and 2
DSL-only		APX-1, LAG-2, ARG-2, DSL1–7	Dll3 and 4
DOS Co-ligands		DOS1–3, OSM7, 11	DLK-1, DLK-2/EGFL9
Non-canonical			DNER, MAGP-1 and 2, F3/Contactin1, NB-3/Contactin6
Nuclear Effectors			
CSL DNA-binding transcription factor	Su(H)	LAG-1	RBPjκ/CBF-1
Transcriptional Co-activator	Mastermind	LAG-3	MAML1–3
Transcriptional Co-repressors	Hairless, SMRTR		Mint/Sharp/SPEN, NCoR/SMRT, KyoT2
Receptor Proteolysis			
Furin convertase (S1 cleavage)	?	?	PC5/6, Furin
metalloprotease (S2 cleavage)	Kuzbanian, Kuzbanian-like, TACE	SUP-17/Kuzbanian, ADM-4/TACE	ADAM10/Kuzbanian, ADAM17/TACE
γ-secretase (S3/S4 cleavage)	Presenilin, Nicastrin, APH-1, PEN-2	SEL-12, APH-1, APH-2, PEN-2	Presenilin 1 and 2, Nicastrin, APH-1a–c, PEN-2
Glycosyltransferase modifiers			
O-fucosyl-transferase	OFUT-1	OFUT-1	POFUT-1
O-glucosyl-transferase	RUMI		
β1,3-GlcNAc-transferase	Fringe		Lunatic, Manic & Radical Fringe
Endosomal Sorting/ Membrane Trafficking Regulators			
Ring Finger E3 Ubiquitin ligase (ligand endocytosis)	Mindbomb 1–2, Neuralized	Y47D3A.22	Mindbomb, Skeletrophin, Neuralized 1–2
Ring Finger E3 Ubiquitin ligase (receptor endocytosis)	Deltex		Deltex 1–4
HECT Domain E3 Ubiquitin ligase (receptor endocytosis)	Nedd4, Su(Dx)	WWP-1	Nedd4, Itch/AIP4
Negative regulator	Numb		Numb, Numb-like, ACBD3
Neuralized Inhibitors	Bearded, Tom, M4		
Other endocytic modifiers	sanpodo		
NICD Degradation			
F-Box Ubiquitin ligase	Archipelago	SEL-10	Fbw-7/SEL-10
Canonical Target bHLH Repressor Genes	E(spl)	REF-1	HES/ESR/HEY

Figure 5.1.2 - Core components of the Notch signalling pathways (from Kopan and Ilagan, 2009)
This table gives information about the different components of the Notch signalling pathway in different species.

5.1.3 The role of the Notch pathway in development and self-renewal

Notch signalling is a mechanism of controlling cell fate decisions on the basis of local cell interactions. The mechanisms, which drive cell fate decisions are lateral specification (lateral inhibition) or lateral induction (Greenwald, 2005). One example of a lateral specification event involves a cell fate decision between an anchor cell (AC) and a ventral uterine precursor cell (VU) in early gonadogenesis in *C. elegans* hermaphrodites (Seydoux and Greenwald, 1989). This process starts with two equivalent cells, which can both become either an AC or a VU. Initially, both cells express LIN12 (Notch) and LAG2 (Delta). An initial stochastic event in expression levels results in one cell (the presumptive, but uncommitted AC) producing enough ligand to activate lin12 in the receiving cell. From this point onwards, *lin12* expression becomes restricted to the presumptive VU and *lag2* expression becomes restricted to the presumptive AC (Wilkinson et al., 1994). Importantly, the authors have identified that the essential step in this process is an auto-regulatory feedback, which amplifies and stabilises the initial stochastic event. *lin-12* activity promotes expression of *lin12* and represses *lag2* (Wilkinson et al., 1994). This has explained how a small balance shift of gene expression could lead to a profound effect on cell determination. These experiments have also demonstrated that cells committed to a certain fate inhibit their neighbours from adopting the same fate (hence "lateral inhibition"). Another example of a lateral specification event is the epidermis of *Drosophila,* where cells take the lineage decision between neural precursors or

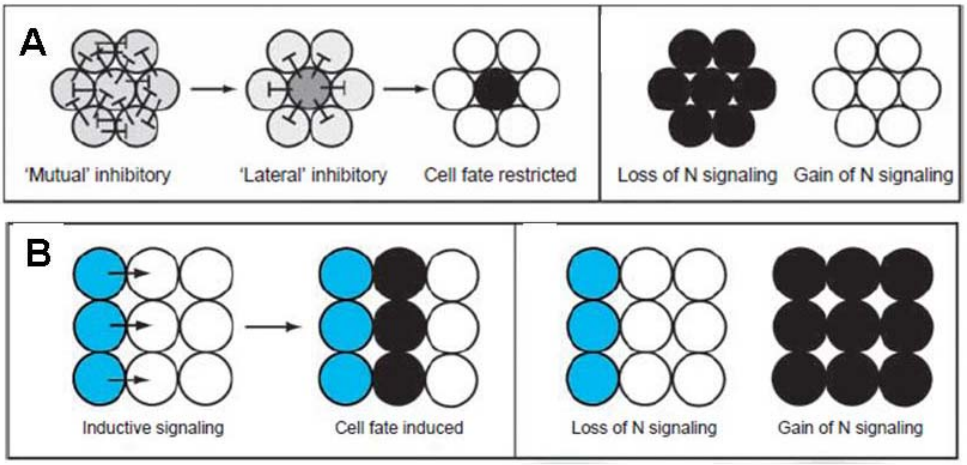

Figure 5.1.3 - Notch signalling in lateral inhibition and lateral induction
Modified after Lai, 2004

epidermal cells (Heitzler and Simpson, 1991). The authors have reported that cells produce neural precursors when neighbouring cells have a higher level of Notch activity and epidermal precursors if they have a lower Notch activity. They have concluded that cell fate choice is taken on the basis of competition between cells.

In contrast, it has been shown that Notch can positively regulate Jagged1 via "lateral induction" (Daudet and Lewis, 2005; Hartman et al., 2010). Daudet and Lewis (2005) have investigated this in inner ear morphogenesis. In mammalian inner ear morphogenesis, the prosensory specification defines regions of the otic epithelium, which will give rise to the six separate inner ear organs essential for hearing and balance. Electroporation of NICD-IRES-GFP resulted in the formation of ectopic sensory patches. Daudet and Lewis (2005) have shown that activation of Notch within hair sensory patches represses hair cell differentiation, but at the same time positively regulates Serrate1. In a positive feedback loop Serrate1 induces and perpetuates Serrate1 in neighbouring cells leading to a mechanism of lateral induction.

Artavanis-Tsakonas et al. (1999) have classified the Notch-Delta - mediated interactions between cells into three different types. The first one involves communication between equivalent cells. This type of interaction was discussed in the example of VU/AC cell specification in *C. elegans*. The second and third types, involve interactions between non-equivalent cells. In these, one of the cells is subjected to an internal or external bias, which is then stabilised by Notch-Delta signalling to result in a specific cell fate choice. The differentiation of the sensory organ precursors (SOP) of the peripheral nervous system in *Drosophila* is an example of an interaction involving a factor intrinsic to one of the cells. The SOPs divide ones to produce two cells (IIa and IIb), which divide a second time to give rise to the 4 cells of the socket, hair, neuron and sheath (Frise et al., 1996). During the first division, the membrane-associated Numb protein (antagonist of Notch activity) is asymmetrically segregated. Thus, only one cell receives Numb. In this cell, Notch signal transduction will be prevented and it will be specified as IIb, while the cell with active Notch signalling will be specified as IIa (Frise et al., 1996). An example,

of non-equivalent cells regulated by extrinsic signals is found in the development of the *Drosophila* compound eye where the cell fate of the R3 and R4 photoreceptor precursors are specified on the basis of a concentration gradient of Wingless emanating from the poles of the eye disc, which is then stabilised by Notch-Delta interactions (Fanto and Mlodzik, 1999; Yang et al., 2002)

In short, Notch signalling is necessary for cell fate choice at multiple steps of normal and postnatal development. The broad range of processes that Notch signalling regulates includes inhibition or induction of differentiation, binary cell fate decisions and, border formation, proliferation, apoptosis, and tumorigenesis (reviewed by Wilson and Radtke, 2006). In addition to its important role for cell specification and morphogenesis in development, it has also been implicated in *in vitro* systems. Since it has been shown that inhibition of Notch activity favours the formation of mesoderm in ES cell differentiation cultures, the pilot work described in the following section will investigate whether Notch repression might be useful for renal differentiation.

5.2 Results

5.2.1 Inhibition of Notch signalling in embryoid bodies does not improve renal differentiation

To test whether Notch inhibition in differentiating embryoid bodies will improve the differentiation of ESCs to renal cells on the basis of increasing the proportion of ESC-derived mesodermal cells, the ability of Notch-inhibitor treated EB-derived cells to integrate into developing renal epithelia in the disaggregation-reaggregation system was examined.

Embryoid bodies were formed from tauGFP ESCs over 2 days by plating the single cell suspension in non-adherent bacterial Petri dishes. $6x10^6$ cells were used per 10cm dish. The cells were cultured in DMEM supplemented with 10% FBS, 100U/mL Penicillin and 100µg/mL Streptomycin, 2mM L-Glutamine, 1mM Sodium Pyruvate, 1x non-essential amino acids and 5µM 2-mercaptoethanol. For differentiation, EBs were cultured in 35µM γ-secretase inhibitor DAPT. The control

pool of EBs was supplemented with an equivalent volume of DMSO (vehicle for DAPT). After 12 days of culture in suspension (11 days in DAPT or vehicle), the embryoid bodies were harvested and disaggregated into single cells by enzymatic treatment. As embryoid bodies proved very difficult to disaggregate, the cell suspension was passed through a 40µm cell strainer to make sure that no clumps of cells were present in the mixture. 15,000 control and DAPT-treated EB cells were mixed with 100,000 embryonic kidney cells, pelleted and cultured for 24h in ROCK inhibitor, as previously described for the formation of organotypic cultures. Experiments were cultured in CKCM for further 6 days after the removal of ROCK inhibitor. They were then fixed with PFA and post-fixed with ice cold methanol. The resulting pellets were stained and prepared for confocal microscopy.

In two independent experiments, microscopic images of immunostained pellets showed no integration of ESC-derived cells into renal structures in either the control sample or the DAPT-treated sample (Figure 5.2.1, A and B). On rare occasions cells were seen associated with renal epithelia, but formed structures distinct from nephrons or UBs. Observations showed that overall there were less tauGFP+ cells in the pellets at the end of the experiment than what was observed for undifferentiated ESCs in Chapter 4. This was not examined quantitatively.

The measurement of RNA with the Agilent Bioanalyzer is based on traditional electrophoretic assays, which have been transferred to a chip format. Charged molecules, like RNA, are electrophoretically mobilised by a voltage gradient, which separates them by size, aided by a sieving polymer matrix (Agilent 2100 Bioanalyzer, user manual, available at: http://www.chem.agilent.com/Library/usermanuals/Public/G2946-90004_Vespucci_UG_eBook_(SecPack).pdf). The advantage of this method is the presence of a number of internal controls, which help assess concentrations accurately, and provide detailed information about the integrity of the RNA based on an analysis of the ribosomal units and on the entire electrophoretic trace of the whole sample. Figure 5.2.2 shows the comparison between the three methods for RNA quantification. Samples are numbered as follows:

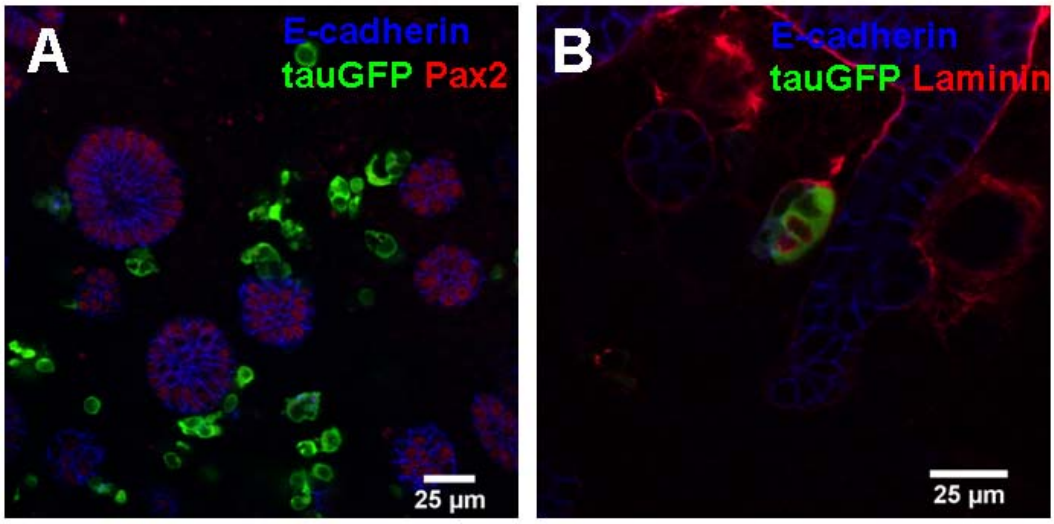

Figure 5.2.1 - Cells from EBs differentiated with or without the addition of DAPT do not integrate into the structure of renal epithelia
A - vehicle (DMSO)-treated EB cells mixed with kidney cells do not localise into the structure of renal epithelia. Pax2 (red) stains the nuclei of renal epithelia; B - DAPT-treated EBs found in proximity, but not integrated into renal epithelia. E-cadherin (blue) expression is stronger in UBs and weaker in nephrons; EB-derived cells are in green

1 - ESC RNA

2 - EB RNA at day 4 of culture (control)

3 - EB RNA at day 4 of culture (EBs supplemented with DAPT)

4 - EB RNA at day 6 of culture (control)

5 - EB RNA at day 6 of culture (EBs supplemented with DAPT)

6 - EB RNA at day 8 of culture (control)

7 - EB RNA at day 8 of culture (EBs supplemented with DAPT)

8 - EB RNA at day 15 of culture (control)

9 - EB RNA at day 15 of culture (EBs supplemented with DAPT)

Samples 5 and 6 were not measured with a conventional spectrophotometer for technical reasons. The general observation from all three types of measurements was that the readouts were comparable. It was observed that the NanoDrop and the Spectrophotometer almost always gave readouts higher than the Agilent Bioanalyzer. Although, the measurements made with the spectrophotometer were very similar to the rest, it had one major disadvantage - the large volume needed for spectrophotometric analysis caused a huge loss of valuable RNA, needed for cDNA synthesis. For this reason, this method was not considered any further. On the basis

of the results presented in this section, it was concluded that the NanoDrop was as efficient as the Agilent for RNA quantification. For reasons of convenience and cost, the Nanodrop was selected for all future measurements.

For the semi-quantitative gene expression studies, 200ng of RNA from all samples were used for first-strand synthesis. PCR was performed as described in the Materials and Methods chapter. The product was run on gel electrophoresis. Images of gels were collected as printouts and digitalised by scanning. GAPDH data was used for correcting experimental errors of DNA quantification and loading. Measurements were performed with the NIH software ImageJ. The band with lowest intensity for GAPDH product (sample 8) was given a value of 1.00 and all other bands were assigned a value according to their intensity as compared to the basal band. The area of all bands for each gene was counted as 100% and the percentage of a single band, representing one sample, was determined. The percentage value for

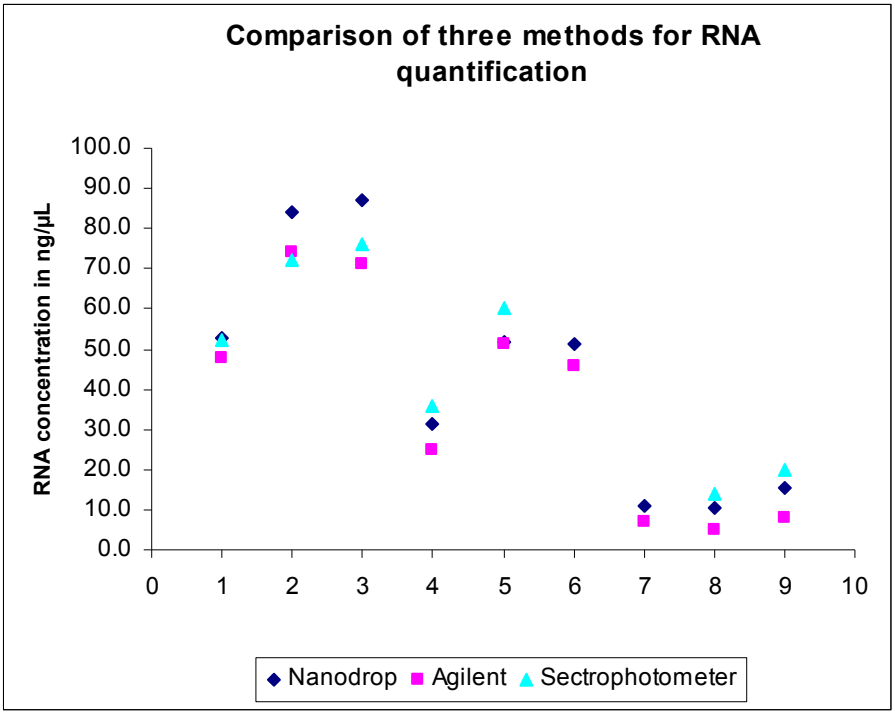

Figure 5.2.2 - A comparison of three methods for RNA quantification.
Overall, the three methods showed comparable measurements. The Nanodrop and spectrophotometer seemed to overestimate the concentration of nucleic acid in comparison to the measurements obtained with the Agilent Bioanalyzer. Samples 6 and 7 could not be measured with a spectrophotometer. Sample are labelled, as follows: 1 - ESC RNA, 2 - EB RNA at day 4 of culture (control), 3 - EB RNA at day 4 of culture (EBs supplemented with DAPT), 4 - EB RNA at day 6 of culture (control), 5 - EB RNA at day 6 of culture (EBs supplemented with DAPT), 6 - EB RNA at day 8 of culture (control), 7 - EB RNA at day 8 of culture (EBs supplemented with DAPT), 8 - EB RNA at day 15 of culture (control), 9 - EB RNA at day 15 of culture (EBs supplemented with DAPT)

each band was then divided by its corresponding coefficient obtained from the GAPDH quantification. These values were then plotted as graphs to illustrate the change of gene expression over time (Figure 5.2.3, A, B, C, D and E). The original data is shown in Figure 5.2.3, F.

5.2.2 Expression of the intermediate mesodermal marker Osr1 is not enhanced by DAPT treatment of embryoid bodies

As no EB-derived cells, both treated and untreated, were detected in renal epithelia, gene expression studies were performed to monitor whether embryoid bodies had a normal gene expression profile and whether there was a detectable difference of gene expression between the control and the sample incubated with Notch inhibitor. For this purpose, in an experiment performed as described in the previous section, EBs were cultured with either DMSO or DAPT and harvested at different time points for RNA isolation. The RNA was extracted immediately after sampling the EB suspensions by using a column-based RNA isolation kit (Promega), as described in the Materials and Methods section. RNA was stored at -80°C for the synthesis of cDNA. Before cDNA could be synthesised, the concentration of isolated RNAs had to be accurately determined to make sure that the same amount of RNA would be used for cDNA synthesis for comparing relative levels of gene expression.
To validate RNA quantification measurements, several methods for RNA quantification were compared. These included using a NanoDrop, a conventional spectrophotometer, and the novel-technology of Agilent Bioanalyzer 2100.
With the progression of differentiation, we expect a downregulation of pluripotency genes, such as *Oct4* and *Nanog* (Scholer et al., 1990; Chambers et al., 2003). As can be seen on Figure 5.2.3, A and B, the data were consistent with these expectations. Expression of Oct4 decreased first and is brought to almost 0 at day 15 of differentiation. Brachyury (T), which has been detected in the mesoderm of developing embryos, peaked at day 6. That is 2 days later than what has been found in some reports (Pearson et al., 2008; Bruce et al., 2007), but consistent with others (for example, Nemir et al., 2006). In normal development, the mesoderm expresses Brachyury only transiently and after a peak its expression decreases with the progression of development (Wilkinson et al., 1990). Consistently, in *in vitro*

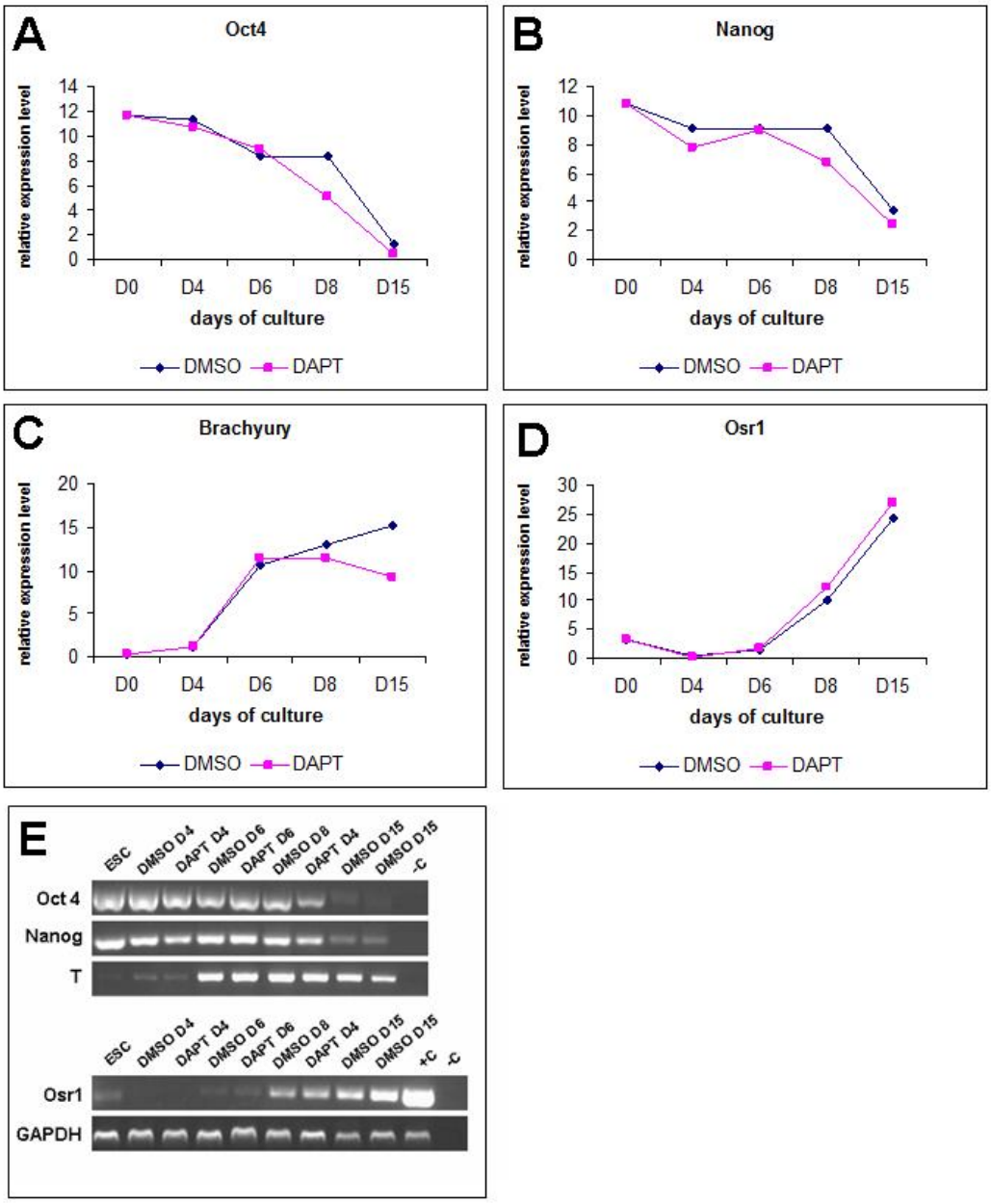

Figure 5.2.3 Gene expression analysis of control and DAPT-treated differentiating embryoid bodies
A and B - relative Oct4 and Nanog expression after correction for GAPDH levels. Oct4 and Nanog levels decrease from day 0 to day 15. The levels of pluripotency genes seem to decrease slightly faster in treated samples, as compared to the controls; C and D - comparison of the relative expression of T (Brachyury) and Osr1 in control and DAPT-treated samples; E - the original data from gel electrophoresis of the PCR product, which detects the relative levels of mRNA for the tested genes. The positive control for Oct4, Nanog and T is contained within the experiment and a separate such was not performed. The positive control for detection of Osr1 was done on the basis of RNA extracted from whole E11.5 embryos.
In A, B, C and D, each line shows data from a single experiment, which is why there are no error bars seen in the diagrams.

differentiation systems Brachyury should start to decrease with the maturation of cells (as seen on Figure 5.2.3, C). The earlier decline of Brachyury expression suggested that the DAPT-treated EBs might differentiate faster than the control ones. On the other hand, the fact that Brachyury gene expression did not at all decline in the control sample by day 15, was unusual. Osr1, the marker for intermediate mesoderm, which is expressed by multipotent kidney progenitors (Mugford et al., 2008), started to be expressed at day4 and was highly upregulated after day 6. Its presence indicated that differentiation was taking place in the EBs. The levels of Osr1 in the control and DAPT were similar. From the gene expression analysis data, it was clear that EBs performed as expected by downregulating pluripotency genes and upregulating markers for different stages of differentiation in the normal sequence. The gene expression levels between the control and DAPT-treated sample were very similar, but the latter progressed through the sequence of losing Oct4 and Nanog expression, going through a peak of Brachyury expression and gaining Osr1 expression slightly faster. The only noticeable difference between control and sample was in the detected mRNA levels of Brachyury, which remained higher in the control sample indicating attenuated differentiation (Figure 5.2.3, panel C).

5.2.3 DAPT treatment shows an efficient inhibition of the Notch signalling pathway

As DAPT treatment produced an inconclusive result for *Brachyury* (mesoderm) and showed neither an upregulation of *Osr1* nor an increase of renal integration, compared to controls, it was necessary to verify that the γ-secretase inhibitor was functioning as expected and that it efficiently blocked Notch signalling. On the basis of information found in the literature, a functional assay to test the effect of DAPT was designed. Cheng and Kopan (2005) reported that Notch signalling is essential for developing embryonic kidneys. They demonstrated that a lack of Notch activity leads to severe abnormalities in maturing renal compartments. They reported that Notch signalling is essential for proximal tubule and podocyte formation at the stage where S-shaped bodies are formed. To verify that the DAPT inhibitor was active, kidney rudiments were isolated from E11.5 mice and pooled. Half of them were cultured in medium containing 5μM DAPT, the other half - in medium containing vehicle

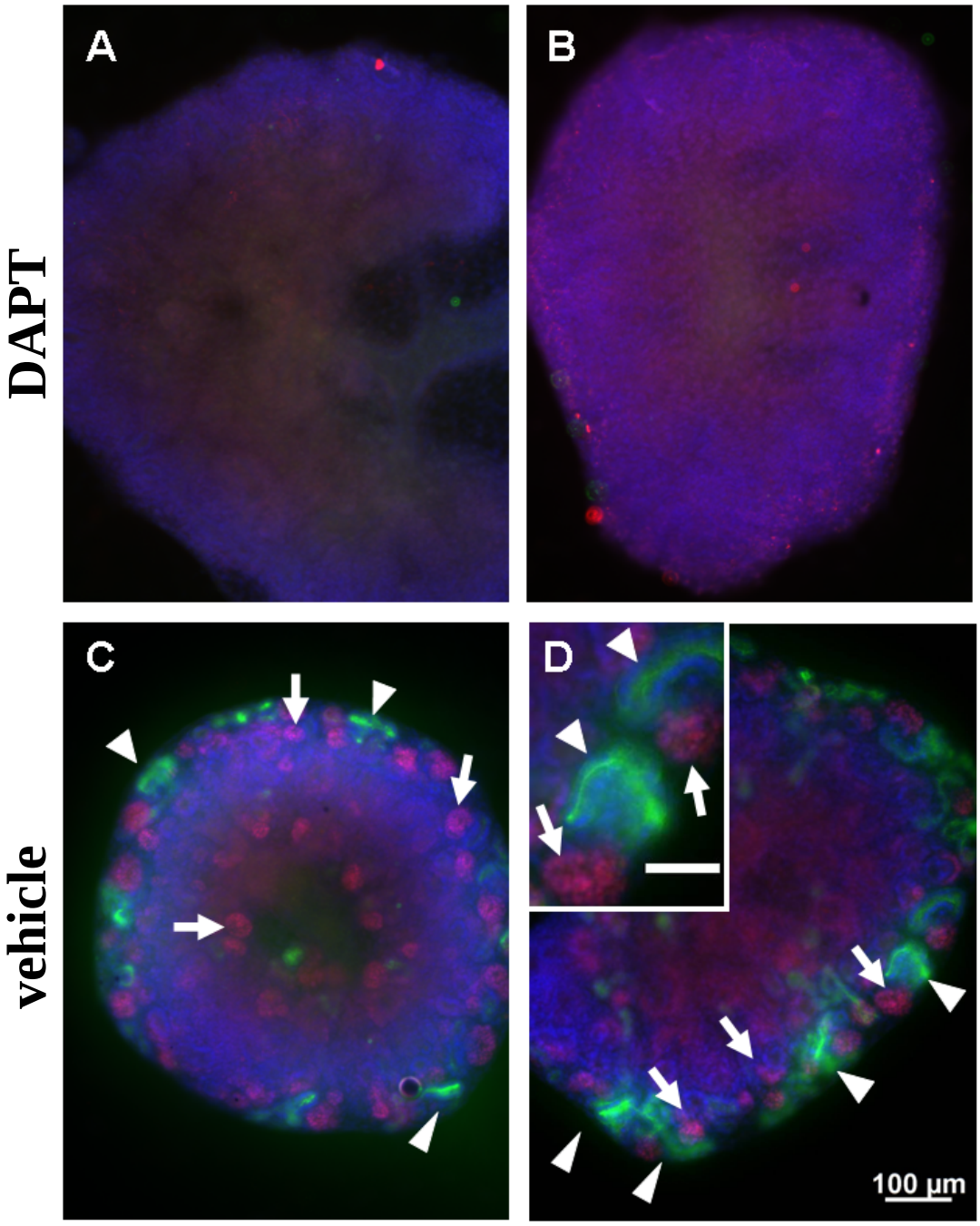

Figure 5.2.4 - Treatment of E11.5 embryonic kidneys with DAPT resulted in a loss of the proximal tubular segment and presumptive podocytes
A and B - (treated with DAPT samples) kidneys isolated from E11.5 kidney rudiments, cultured in 5µM DAPT for 5 days did not show presence of the proximal tubular marker LTL (in green). The high levels of expression of Wt1 (red) in characteristic crescents normally present in the presumptive podocytes, was also lacking. C and D - (untreated samples) control images of kidneys treated with an equal volume of DMSO (vehicle for DAPT) show normal LTL (green, arrowheads) and Wt1 (red, arrows) expression; inset in D is a magnification of a fragment of D showing luminal LTL and nuclear Wt1. Bar in inset - 50µm; DAPI is in blue

(DMSO). After 5 days in culture, the kidney rudiments were fixed and stained with Lotus tetragonolobus lectin (LTL), which is a marker of the proximal tubule (Laitinen et al., 1987), and for the podocyte marker WT1 (Mundlos et al., 1993; Grubb et al, 1994). The results undoubtedly confirmed the absence of the proximal tubular segment of the nephron, as shown on Figure 5.2.4. LTL staining was absolutely absent in the DAPT sample (Figure 5.2.4, A and B) and present, as expected, in the control (Figure 5.2.4, C and D). The success of this experiment was remarkable as the development of the proximal tubule was blocked in 100% of the treated samples (10 out of 10 cultured kidneys). These results were also confirmed by the staining for Wt1 with the same efficiency. As described in the introduction chapter, Wt1 is expressed at low levels in the induced MM and at high levels in the glomerular podocytes (Grubb et al, 1994; Cheng et al., 2003; Schedl and Hastie, 2000). Wt1 staining of the DAPT-treated embryonic kidneys showed a lack of $Wt1^{high}$ cells forming characteristic crescents of glomerular podocytes, though these were present in the vehicle control, Figure 5.2.4, C and D. This result was completely consistent with the data published by Cheng et al. (2003), who demonstrated that developing embryonic kidneys lacking γ-secretase activity for more than three days irreversibly lose their potential to form podocytes. These experiments therefore confirmed that the batch of DAPT used in ESC differentiation experiments was working normally.

5.2.4 Monolayer differentiation of ES cell cultures supplemented with DAPT does not improve the generation of cells integrating in renal structures

The differentiation strategy described in previous chapters was devised on the basis of published data reporting that inhibition of Notch signalling favours the generation of mesoderm from ESCs. This data was generated by EB-based differentiation of ES cells. Lowell et al. (2006) have reported successful mesoderm derivation in a monolayer cell differentiation system. This alternative approach was also tested based on the experimental conditions described in this paper.

For monolayer differentiation tauGFP ESCs were enzymatically disaggregated to produce a single cell suspension. $1x10^4$ cells per cm^2 were seeded in differentiation medium (DMEM with 2mM L-Glutamine, 1mM sodium Pyruvate, 1x non-essential amino acids and 5µM 2-mercaptoethanol with 10% FBS) supplemented with 4µM DAPT or the respective amount of vehicle (DMSO). Cells were incubated in these conditions for 4 days, then disaggregated enzymatically, passed though a 40µm cell strainer, counted and mixed with embryonic kidney cells. 15,000 ESC-derived cells were mixed with 100,000 kidney cells. The formed pellets were then cultured for 24h in medium supplemented with ROCK inhibitor and a further 3 days in CKCM. A staining of the pellets for Calbindin and Laminin showed that the localisation of treated cells into renal epithelia had not improved. On very rare occasions, patches of GFP positive cells could be seen either in a close proximity to renal tubules possibly initiating contact with renal tubules, or in already formed chimeric structures (Figure 5.2.5, A, C, D). These structures were negative for the UB marker Calbindin and could not be identified as UBs. Although the structures were Laminin-bound, they did not display the cellular organisation and size typical of nephron cells. The same observations were made in the DAPT-treated cells and the vehicle control, which confirmed that the inhibitor treatment did not improve differentiation. The adhering structures were very similar to the ones observed when undifferentiated ES cells were mixed with kidney cells, suggesting that undifferentiated cells might be remaining in the organotypic cultures. The PCR data presented on Figure 5.2.5 strongly supports this hypothesis as efficient Oct4 downregulation was achieved at about day 15 after LIF withdrawal, which is almost double the time used for monolayer differentiation combined with pellet culture. No cells in any of the 4 pellets examined seemed to integrate appropriately in the structure of developing renal epithelia. In comparison to EB differentiation, monolayer differentiation did not improve the generation of cells having properties to mix with renal epithelia and even seemed to favour the survival and presence of undifferentiated cells.

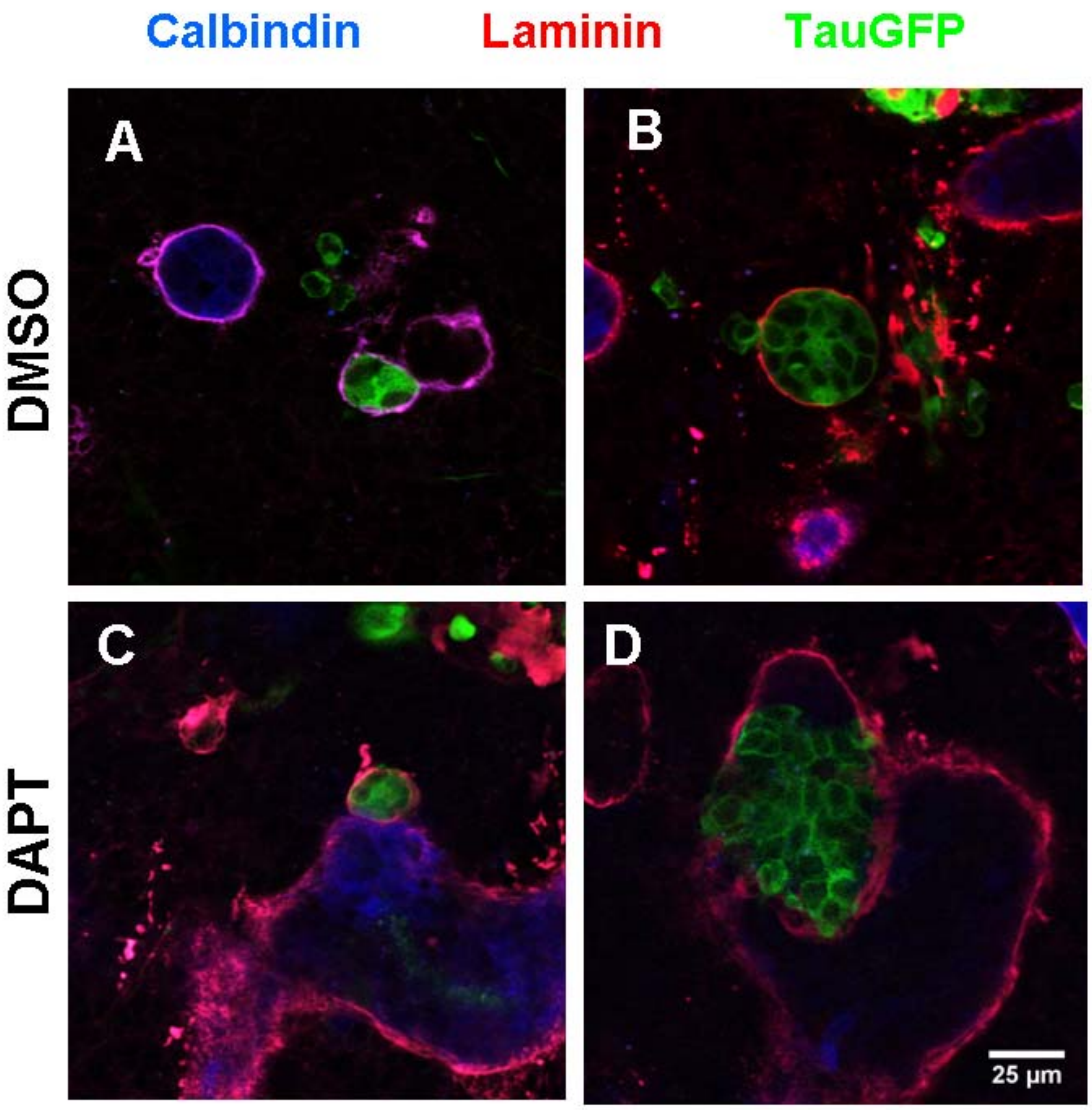

Figure 5.2.5 - Monolayer differentiation of DAPT-treated and control tauGFP+ cells
1x104 tauGFP cells per cm 2 were plated in differentiation medium supplemented with 4µM DAPT or an equivalent volume of vehicle. The cells were predifferentiated in these conditions for 4 days, then detached from the cell culture dishes. 15,000 ESC-derived cells were mixed with 100,000 embryonic kidney cells for the generation of organotypic reaggregates. Pellets were cultured for further 4 days, fixed and stained for Laminin (red) and Calbindin (blue). TauGFP cells were detected by their expression of GFP (green).
A and B - control cells formed Laminin-bound structures, which on rare occasions associated with renal epithelia, but did not integrate in their structure.
C and D - DAPT-treated cells were also seen in Laminin-bound structures, comparable to the ones seen in the control samples, did not show a normal renal morphology and also did not integrate into the structure of renal epithelia.

5.3 Summary and discussion

In Chapter 4, the ability of undifferentiated mESC to give rise to kidney cells after mixing in reaggregated organotypic cultures was assessed. As this strategy did not result in the generation of kidney cells, a pre-treatment of the cells was evaluated in the current chapter. The differentiation strategy used in this chapter was based on blocking Notch signalling to increase the formation of mesoderm. Screening results showed that two different methods for ES cell differentiation, embryoid bodies and monolayers, did not successfully generate cells that can integrate into renal tubules. At the same time, it could be concluded that this effect was not due to a lack of activity, or presence of a decreased activity of DAPT, as kidney culture experiments confirmed that the inhibitor blocked Notch signalling efficiently. This also indicated that the unsuccessful differentiation of ESCs to renal cells cannot be attributed to a lack of Notch inhibition, but rather to the inefficiency of this method in generating ESC-derived renal cells. On the basis of this result, it could be concluded that in the conditions used, blocking Notch does not lead to improving the differentiation of ES cells to kidney cells.

Before considering the semi-quantitative reverse-transcription PCR data, it is important to mention that as the results presented here are based on only one experiment, they cannot be treated as completely conclusive, but rather - as guidelines. Reverse transcription analysis showed that the transcript levels of *Oct4*, Nanog and *Osr1* were very similar in the control and DAPT-treated samples. Although, the DAPT-treated EBs seemed to downregulate *Oct4* and *Nanog* and upregulate *Osr1* slightly faster than control EBs, it could not be determined whether this small difference was statistically significant. The only obvious difference in the tested gene expression profiles of treated and untreated samples was in the expression of *Brachyury* at day 8 and day 15 of EB culture. After similar expression levels until day 6, control EBs continued upregulating Brachyury until day 15, while expression levels started decreasing in the DAPT-treated sample. In mouse embryonic development *Brachyury* expression peaks at E8.5-E9.5 and starts to be downregulated thereafter (Wilkinson et al., 1990). A similar expression pattern has

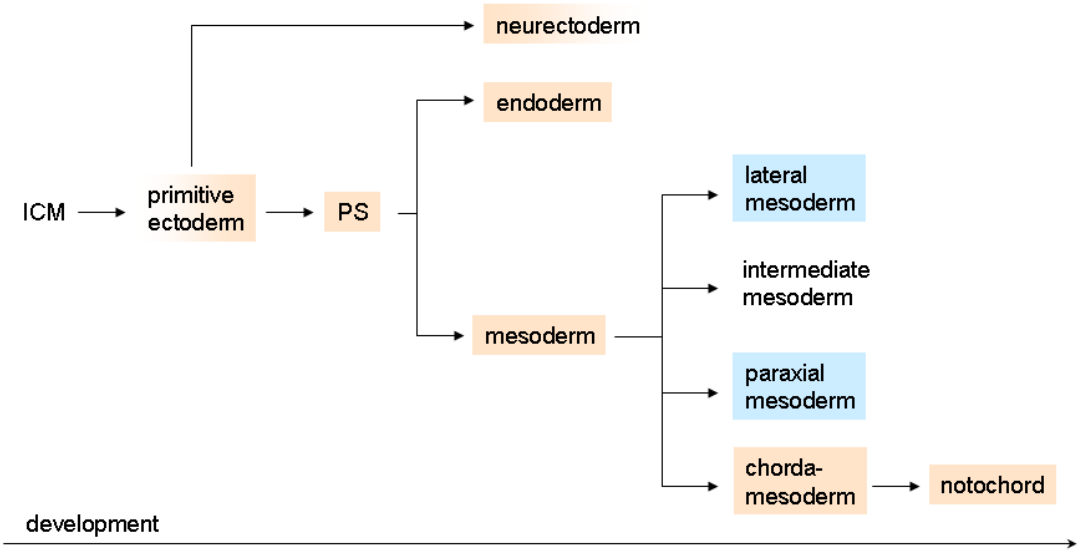

Figure 5.3.1 - Brachyury expression in early embryo development
Pink indicates Brachyury expression; blue indicates a lack of Brachyury expression; white - not reported; PS - primitive streak

been observed in *in vitro* differentiation systems (Nemir et al., 2006; Pearson et al., 2008). The DAPT-treated sample behaved consistently with these reports, unlike the control samples. To explain this, the expression patterns of *Brachyury* in development had to be more closely examined. Importantly, *Brachyury* is very often incorrectly referred to as a mesodermal marker. First, *Brachyury* transcripts have been detected before the onset of primitive-streak formation when the mesoderm has not yet formed (Thomas and Beddington, 1996). In addition, in early gastrulation, transcripts are found in the primitive ectoderm next to the primitive streak, which consists of cells destined to delaminate and form both mesoderm and definitive endoderm (Wilkinson et al., 1990). Expression has been shown in hindgut endoderm and neurectoderm (Inman et al., 2006). Furthermore, *Brachyury* is not only expressed by the notochord, but its expression there persists until very late developmental stages. Transcripts have been detected in mouse embryos even at E17.5, restricted to repeated clusters of cells along the spinal cord (Wilkinson et al., 1990). Interpreting the data from reverse-transcription PCR in the context of this information was very difficult. On one hand, the continuous increase in Brachyury transcript in the control sample could be an attenuated peak of mesendoderm formation. In this case, the earlier peak in the DAPT-treated sample could indicate a better (quicker) differentiation to mesendoderm. In combination with the observation that the relative levels of *Osr1* in both samples were similar, that could mean that although

mesendoderm was enhanced, intermediate mesoderm was not. This interpretation fits well with the report of Nemir et al (2006) who showed that deactivation of Notch signalling leads to an increased efficiency in generating ESC-derived cardiomyocytes (which are of mesodermal origin). In another interpretation, the *Brachyury* expression graph at D15 could be seen not as an attenuation of expression, but as a higher level of expression as compared to DAPT-treatment. At the same time, it has been reported that Notch inhibition favours mesoderm at the expense of ectoderm (Nemir er al., 2005; Lowell et al., 2006). Since, Brachyury is also expressed by some neurectodermal cells (Inman et al., 2006) this could mean that Notch inhibition functions to deplete the Brachyury+ neurectodermal cells in DAPT-treated, but not in control samples. Overall, the most relevant observation that Osr1 expression did not change after DAPT-treatment remains. Together with the data from reaggregated pellets, this suggested that Notch inhibition did not show any evidence for enhancing renal differentiation of mESCs.

Chapter 6

The intermediate mesoderm contains renocompetent cells

6.1 Introduction

In the previous two chapters, two strategies for the differentiation of ESCs to renal cells were tested. First, ESCs were exposed to the microenvironment of a developing embryonic kidney to see whether undifferentiated ES cells have the potential to respond to the signals from the environment and differentiate to renal cells. Second, a strategy of Notch signalling inhibition was employed with the purpose of improving the results obtained with undifferentiated ES cells. These experiments were based on reports showing that inhibition of Notch in ES cells leads to increase in the proportion of cells characteristic of a mesodermal lineage after differentiation. Neither strategy showed satisfactory results in producing kidney cells, as defined by the criteria described in Chapter 4 for obtaining cells with the potential to integrate in renal epithelia indistinguishably from kidney cells and express kidney markers. From these experiments it became clear that the methods tested were not useful for producing ESC-derived renal cells *in vitro*. It was then logical to address the question of how far, in developmental states, is an ES cell separated from the first type of cell that meets the criteria for renocompetence defined in Chapter 4.

One of the central gaps in knowledge that was observed while performing the studies described in this thesis was the lack of experimental evidence about the earliest cell lineage or cell type in mouse embryo development, which was able to give rise to kidney cells either on its own or when exposed to renogenic signals *in vitro*. Some reports have investigated similar problems in amphibian gastrulae (Holtfreter, 1944; Toivonen and Saxen, 1955), but it would be inappropriate to translate this information directly to mammalian systems, due to the extensive cell plasticity that amphibians possess. Unlike mouse work, transplantation studies with early amphibian gastrulae have shown that almost any part of them would be able to generate nephric tubules when grafted to the appropriate region of another embryo (Holtfreter, 1933; reviewed by Saxen, 1987). Attention has also been given to determination and cell commitment rather than acquisition of competence. For example, Sariola et al. (2003) summarised that after determination the MM “is committed to nephrogenesis and is thus genetically programmed to respond to

inductive cues from the ureteric bud and so ready to give rise to the range of cell types that characterise the kidney". Although, it seems like most people support the hypothesis that once formed the MM is already committed, the possibility of cells being competent to give rise to kidney cells outside the embryo without them being terminally committed and the timing of the acquisition of this competence, are not well understood.

Commitment defines the stage at which certain cells significantly decrease their plasticity to form other lineages and can essentially produce only more specified cells of the same lineage and in some cases retain multipotency to persist as organ-resident stem cells. The purpose of this chapter is not to address commitment (which has also already been temporally defined for the metanephros), but to address acquisition of competence or investigate when in development cells acquire the ability to give rise to renal cells independently of embryo development (Figure 6.1.1). First, this information will help pinpoint the size of the leap that embryonic stem cells would have to make in order to acquire the ability (competence) to respond to external signals promoting a renal fate (such as the ones found in the

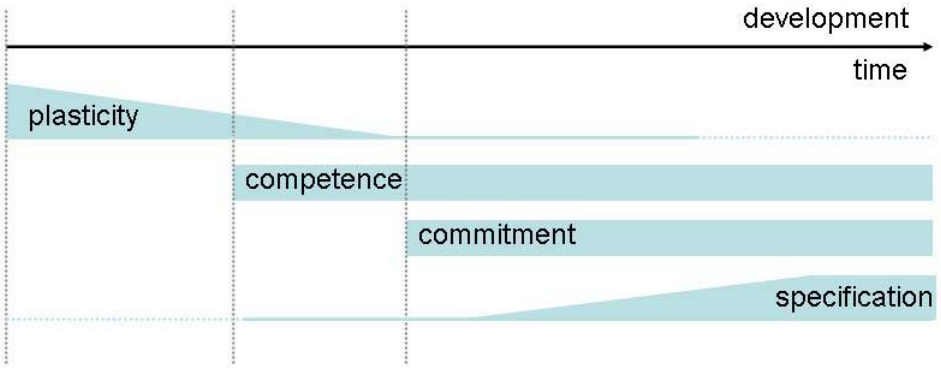

Figure 6.1.1 – Diagram illustrating the concepts of plasticity, competence, commitment and specification in the context of renal development
This diagram illustrates that development starts with cells possessing the highest plasticity or the ability to give rise to cells with different fates. At a certain moment in development, the potential for generating kidney cells in given conditions (without the complete set of signals and events present in development) is acquired. Such competent cells might have both the potential to give rise to kidney cells, but when placed in different conditions might show a potential to generate other cell types, as well. With development, all, or a subset of the competent cells get specified to a renal fate and lose their ability to produce other lineages.
Dotted lines indicate that some cells in early embryonic development might be specified or that a fraction of cells retain some plasticity even in advanced developmental stages and/or after their completion (stem cells)

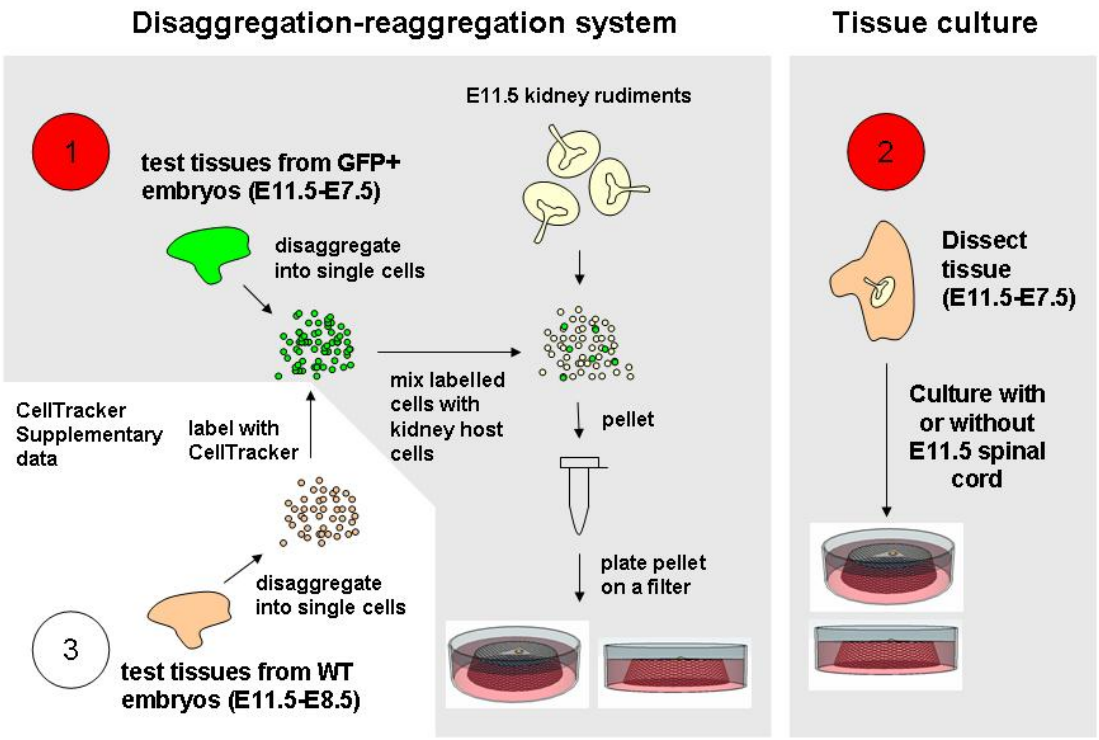

Figure 6.1.2 – A diagrammatic representation of methods for determining renocompetence used in this study
1 – the respective tissues from tauGFP+ embryos are isolated, disaggregated into single cells and mixed with disaggregated into single cells E11.5 embryonic kidney rudiments. Organotypic reaggregates are then re-formed by pelleting and cultured at the air-liquid interface on a polycarbonate filter
2 – conventional organ culture, in which structure formation is monitored after pieces of tissue are cultured at the air-liquid interface on a polycarbonate filer for several days
3 – the same as in 1, with the difference that wild type tissues stained with CellTracker are used instead of genetically labelled cells (data shown only on Supplementary Figure 7)

microenvironment of the embryonic kidney). Second, it will provide valuable information that will improve our understanding of kidney development and renal lineage specification. Third, combined with other studies, it could contribute to unravelling the principles of cell specification, in general.

To address the acquisition of renocompetence in mouse embryos, a strategy was devised to follow the ability of cells isolated from different embryonic stages to give rise to renal or renal-like cells and structures. Two assays were used for testing the renocompetence of cells (Figure 6.1.2). First, the kidney rudiment disaggregation-reaggregation approach was used as the main method for analysing the abilities of embryo-derived cells. The criteria for considering a test cell to be a renal cell in the disaggregation-reaggregation system have already been described in section 4.1.2 of

Chapter 4, for assessing ESC differentiation to renal cells. The same criteria are used here for testing the renocompetence of early embryo cells. The disaggregation-reaggregation assay was used as a primary method as it has the advantage of allowing the tested cells to be analysed at multiple levels. The ability of cells to integrate into renal tubules and orient themselves correctly with respect to neighbouring native kidney cells provides a functional test. At the same time, a combination of molecular markers can be studied to characterise these cells at the molecular level. Furthermore, this assay can also provide quantitative information (as demonstrated by Chapter 3). The second assay for studying the renogenic properties of early embryo tissues was traditional organ culture where tissue fragments are grown on a polycarbonate filter placed on a Trowell metal screen (Grobstein, 1953, Saxen et al., 1962). For the scientific questions to be addressed in this chapter, the tissue culture assay has two disadvantages. First, it does not provide as much information as the disaggregation-reaggregation system. Second, since it does not allow for a simultaneous assessment of cell integration, marker expression and morphology, when used only by itself, it would not provide conclusive results. One example of the latter is the lack of a possibility to mix labelled and unlabelled populations of cells, which means that the exact region of interest cannot be accurately mapped. Another example is that due to the lack of the appropriate external signals, complete UB development and nephrogenesis are not likely to take place, so only very rudimentary structures might be observed. At the same time, in spite of its disadvantages, tissue culture would be useful for providing an independent confirmation of the results obtained with the primary method. The robustness of the disaggregation-reaggregation system, supported by an independent check by a second very different method offers a very good tool for addressing the acquisition of renocompetence in early embryos. Disaggregation-reaggregation experiments with CellTracker-labelled tissue-derived embryonic cells (instead of tauGFP-labelled cells) have also been performed (Supplementary Figure 7). These results have not been presented here, as in other chapters and supplementary information (Chapter 4, Chapter 7, Supplementary Figure 4) it has been demonstrated that CellTracker is not a robust marker.

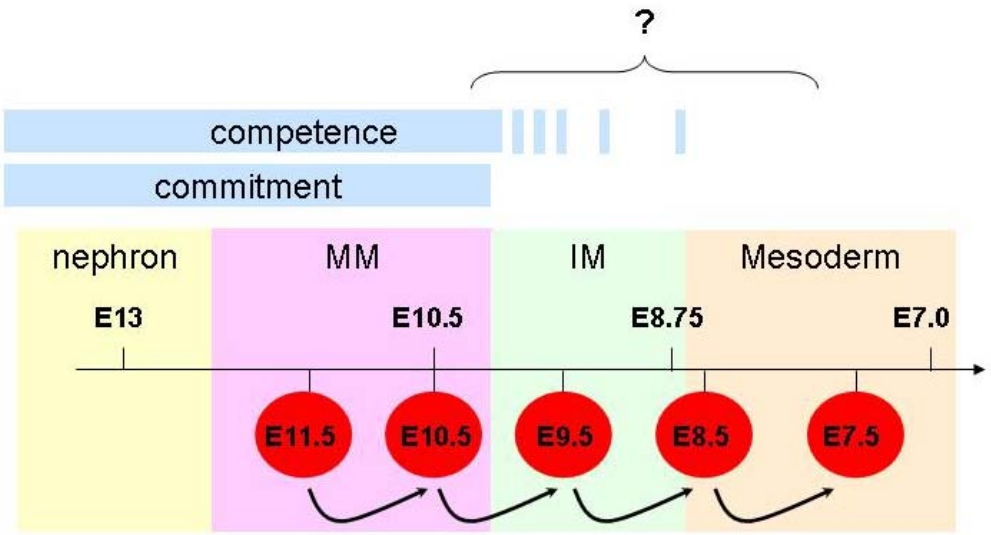

Figure 6.1.3 - A "backward" approach of addressing the acquisition of renocompetence in mouse embryo development
The backward approach works by an incremental decrease of the embryonic age of tested mouse embryos, First, metanephrogenic tissues from E11.5 are used. Embryo age is decreased by 1 embryonic day for every successful experiment until no successful integration/marker expression in the disaggregation-reaggregation system can be obtained. The yellow, pink, green and peach colour blocks help correlate the embryonic ages tested to the timing of mesoderm, intermediate mesoderm, MM, etc, formation. The blue strips address commitment and competence. Although it is known that the MM is competent to produce nephrons, it is not known whether the intermediate mesoderm (IM) or the mesoderm do so, as well.

All experiments presented up to this point of this thesis follow the normal course of embryonic development. For example, the differentiation of ESCs to mesoderm, intermediate mesoderm and kidney cells was followed. This chapter differs significantly from previous ones, as it adopts a "backward" approach to studying renogenic potential. In ESC experiments, a "forward" approach would be testing the cells at various time points of their differentiation, while they get more "mature". If *in vitro* differentiated to mesoderm cells had shown the potential to integrate into reaggregated kidney rudiments and expressed kidney markers it would have been concluded that the mesoderm present in embryo development before any intermediate mesoderm is formed already possessed renocompetence. In contrast, the experiments in this chapter work "backwards" by isolation of tissues from progressively younger embryos and testing them in the reaggregation system (Figure 6.1.3). The experiments start by using GFP+ E11.5 kidney rudiments as test cells. This serves as a positive control, as E11.5 rudiments are renocompetent and can contribute to the structure of other E11.5 kidney rudiments (shown in Chapter 3). The age of the test tissue is then incrementally decreased by 1 embryonic day (E10.5,

E9.5, E8.5, etc) at a time for every successful experiment (Figure 6.1.3). In this backward sequence, the first embryonic stage at which cells can no longer integrate into developing renal epithelia as previously described, will indicate that no renogenic competence is present at that stage. For example, if no integration is seen in E9.5 embryos, this would mean that E9.5 embryo cells are not yet competent to make kidney cells. The earliest renocompetent stage would then be one experimental step back, or in this example - E10.5. Unlike normal development, where the renogenic competence increases with increasing age (cells become more competent, while the embryo develops), in this approach, the renogenic competence will decrease with decreasing age (cells become less competent with each stepwise decrease of the embryonic age of the sample). The advantage of this "backward" approach is that it allows only one failed attempt of integration (the stage at which the cells would be too immature to give rise to kidney cells). The interval between the last successful integration (the youngest embryo stage, which contains renocompetent cells) and the first unsuccessful integration (the oldest embryo stage, which no longer contains renocompetent cells) will define the period in embryonic development when renocompetence is acquired. This is in contrast with "forward" approaches like ESC differentiation experiments, which can have many failed attempts of pinpointing the stage of acquisition of renogenic potential as many different treatments might not be useful for generating mesoderm, intermediate mesoderm, etc or as good markers for defining these populations are not available.

In order to evaluate the results from the "backwards" experiments, it was necessary to consider two factors – one, the exact location of tissue that was mechanically dissected for use in organ culture or cell mixing experiments; and two – the properties that these tissues have been reported to have in the literature (in correlation with the embryonic stage they have been isolated from). The staging of the embryos and the areas isolated have been described in the Materials and Methods Chapter of this thesis. To correlate the stage of kidney development with the embryonic age of mouse embryos, a literature search was performed. The results were given in Figure 6.1.4, A. As a whole, the key resources agreed in defining the timing of metanephros development. This, as detailed in Chapter 1, is one of the late

A

Developmental event	Embryonic day	Reference
One-stage egg	E0.0-E1.0	Kaufman, 2001
Two-cell stage	E1.0	Kaufman, 2001
4/16-cell stage (morula)	E2.0	Kaufman, 2001
Morula-blastocyst	E3.0	Kaufman, 2001
Blastocyst	E4.0	Kaufman, 2001
Blastocyst attachment	E4.5	Kaufman, 2001
Embryo implantation	E5.0	Kaufman, 2001
Mesoderm	E7.0	Downs and Davies, 1993
	E7.0	Kaufman, 2001
Presomite stage	E7.5	Kaufman, 2001
Intermediate mesoderm	E8.5	So and Danielian, 1999
	E9.0	Kaufman, 2001
Nephric duct	E8.0	Gilbert, 2000
	E8.5	Vetter and Gibley, 1966
	E9.0	Kaufman, 2001; Theiler, 1989
Pronephric anlage	E8.5	Vetter and Gibley, 1966
Pronephros	E8.0	Hoar, 1976
	E8.83	Vetter and Gibley, 1966
Mesonephric anlage	E9.5	Smith and MacKay, 1991
Mesonephros	E9.0	Vetter and Gibley, 1966
	E9.5	Hoar, 1976
	E10.0-E10.5	Kaufman, 2001
Metanephric anlage	E10.0	Vetter and Gibley, 1966
	E11.0-E11.5	Kaufman, 2001
Ureteric bud	E11.0	Hoar, 1976
	E11.0	Vetter and Gibley, 1966
	E11.0-E11.5	Kaufman, 2001
Metanephros	E11.0	Saxen, 1987
	E11.0	Vetter and Gibley, 1966
	E11.0-E11.5	Kaufman, 2001
Condensates	E12.5	Hoar, 1976
	E12.5	Vetter and Gibley, 1966
	E12.5-E13.0	Kaufman, 2001

B **The developmental ruler**

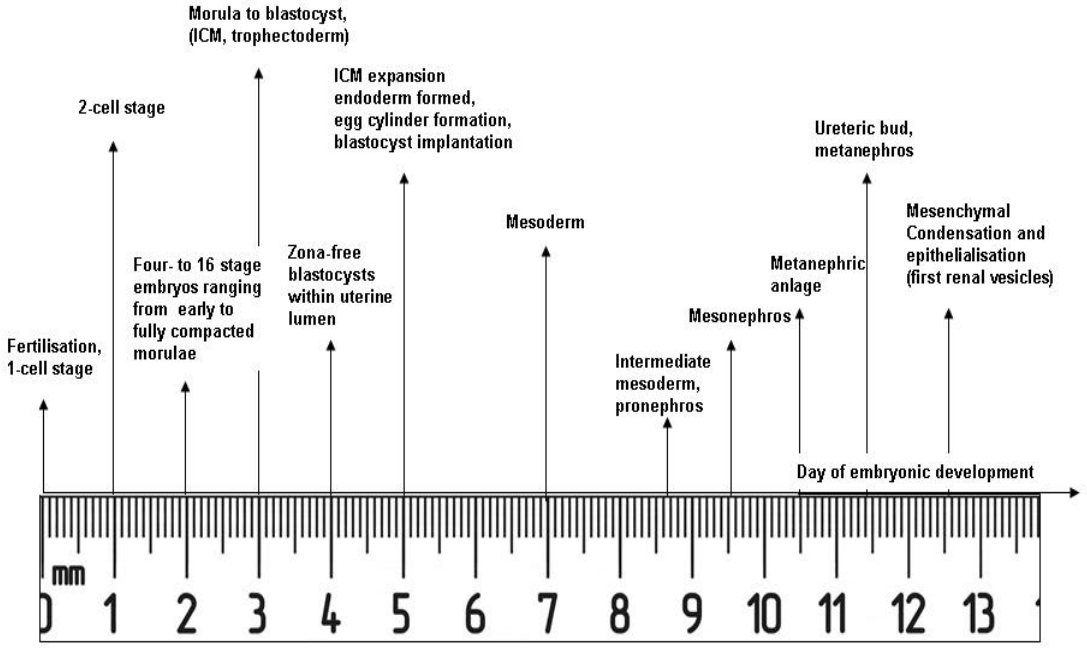

Figure 6.1.4 – A summary of developmental events relevant to kidney development
A – a table summarising information available from studies, which have examined the timing of structure/tissue/organ formation in mouse development. The data emphasises on the differences in reported timing, especially in the periods of most relevance to early kidney development (intermediate mesoderm, pronephros, mesonephros formation)
B – a schematic of important developmental events, plotted on a time line with the time of embryonic development shown as a ruler. For events, which were subject to disagreement in the examined reports the approximate median of the embryonic ages suggested was plotted

developmental events occurring in the organogenesis of the kidney and is preceded by the generation of the pronephros and mesonephros. It is important to note that the information available from the literature for the descriptions of the temporal occurrence of the metanephric anlage and all earlier stages, mesonephros, pronephros, nephrogenic cord and intermediate mesoderm, we more discordant (Figure 6.1.4, A). Although many of the mechanisms and genes involved in kidney development have now been identified, it seems like there has been less interest in describing the exact timing of these processes in the mouse. One of the few studies that correlates some stages of kidney development with the timing of embryo development was published by Vetter and Gibley (1966) and describes

morphogenetic processes in mesonephros and metanephros development. In his "Atlas of mouse development", Kaufman (2001) also provides information about the timing of structures appearing in the mouse. Hoar (1976) reviews the main events in the development of the gastrointestinal and urogenital systems with regard to time. These, together with other resources were used for the construction of a "map" and a table to match developmental events with the respective day of mouse embryo development, which will be referred to in further sections of this chapter. Figure 6.1.4, A and B do not describe certain major developmental events, as they have been made with relevance to kidney development only. Early stages of embryonic development have not been represented in detail on the diagram as they will not be relevant to the studies described in this chapter. For constructing the diagrammatic representation in Figure 6.1.4, B, the approximate medians of the developmental stages given in Figure 6.1.4, A were used.

In summary, two different tools will be used in this chapter to define the developmental stage at which renocompetence is acquired. The disaggregation-reaggregation assay will be used to test the cells at multiple levels, which can be summarised into three main categories - the ability of the cells to integrate into renal epithelia; the morphological properties of integrating cells; and the ability of integrating cells to express renal markers. These results will be presented together with the second assay, organ culture, which will provide an independent check for reaggregation experiments. First, only qualitative data will be presented. These experiments will demonstrate that cells from early embryos are able to integrate into developing nephrons and ureteric buds, and that tissue explants from the same embryo stages can form UB-like and nephron-like structures in culture. Next, quantitative data is going to be presented to follow how the numbers of cells able to integrate change with changing embryo age. In these quantitative experiments, labelled E11.5 kidney cells will be mixed with unlabelled E11.5 kidney cells as a control and the change of integration at different embryo stages will be followed by incrementally decreasing the age of the embryos used (E11.5, E10.5, E9.5, E8.5). Finally, the properties of these cells are going to be studied at the molecular level by immunohistochemistry for various markers.

6.2 Results

6.2.1 Early embryo cells integrate into renal epithelia in the kidney disaggregation-reaggregation assay

The screening for integration of cells in organotypic cultures was performed by using genetically labelled cells explanted from TgTP6.3 mice. Cells or tissues from these transgenic mice will be referred to as tauGFP+ for conciseness. Embryos harvested from mouse uteri were individually examined for GFP+ fluorescence and only GFP+ embryos were selected for further dissections. Tissues from E11.5, E10.5, E9.5 and E8.5 embryos were isolated as described in the Materials and Methods chapter. A summary of the tissues used is provided in Figure 6.2.1.

Embryonic stage	E11.5	E10.5	E9.5	E8.5	E7.5
Embryo development	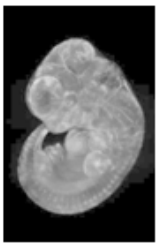	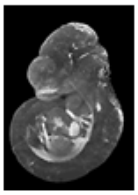			
Tissue isolated			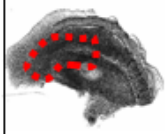		
Description of tissue isolated	E11.5 kidney rudiments	E10.5 metanephric anlagen with the neighbouring Wolffian duct	the future region of metanephros formation, possibly with nephric duct fragments	caudal halves, cut after the last formed somite pair	whole embryos

Figure 6.2.1 – Diagram of different embryonic stages and tissues used in this study
This diagram provides information about the embryo stages that were used in this study, as well as the tissues that have been isolated from each stage for the generation of single-cell suspensions for use in cell mixing experiments; images showing embryos at E11.5 and E10.5 were modified from the online atlas of mouse development available at http://www.emouseatlas.org, retrieved 11/2010

For cell mixing experiments the test tissues were disaggregated to single cells as previously described and mixed with disaggregated embryonic kidney cells from E11.5 rudiments. 15,000 labelled “test” cells were mixed with 100,000 E11.5 embryonic kidney cells. The reaggregated by centrifugation pellets were placed in organ culture and maintained for 6 days, before fixation with PFA and ice-cold methanol. The experiments were stained for Calbindin and Laminin. The grafted cells were detected by tauGFP fluorescence and all nuclei - by a staining for DAPI. For intact organ culture experiments (see Figure 6.1.2), tissues were isolated as above and cultured on a polycarbonate filter at the air-liquid interface. The samples were fixed with ice-cold methanol after 5 days of culture and stained for Calbindin and Laminin to detect possible kidney-like structures. The results obtained by both assays were presented according to the embryonic age of the tissue and the experimental method used starting with control E11.5 mixing experiments (Figure 6.2.2).

Image 6.2.2, A shows tauGFP+ cells from E11.5 kidney rudiments integrating in both nephrons (open arrow) and UB structures (block arrow). The labelled cells observed in renal epithelia were not distinguishable in their shape and orientation from native kidney cells (Figure 6.2.2, A). Most cells integrating in the UB were positive for the marker Calbindin (Figure 6.2.2, A, block arrow). The control studies of mixing labelled and unlabelled populations of E11.5 metanephric cells were confirmed by control organ culture (Figure 6.2.2, B). As expected, E11.5 embryonic kidney rudiments developed branched UBs (block arrow) and nephrons (open arrow) after 4 days in culture (Figure 6.2.2, B).

Similar results were obtained for the tissues isolated from the metanephrogenic regions of E10.5 embryos, which contained uninduced MM and the adjoining piece of WD (Figure 6.2.2, C and D). As demonstrated by Figure 6.2.2, C, tauGFP - labelled E10.5 cells were found integrating into both reformed UB structures (block arrows) and nephrons (open arrows). Tissue culture experiments indicated that when cultured with or without spinal cord, these metanephric anlagen formed UBs, which were able to branch, and nephrons (Figure 6.2.2, D, respectively open arrow and

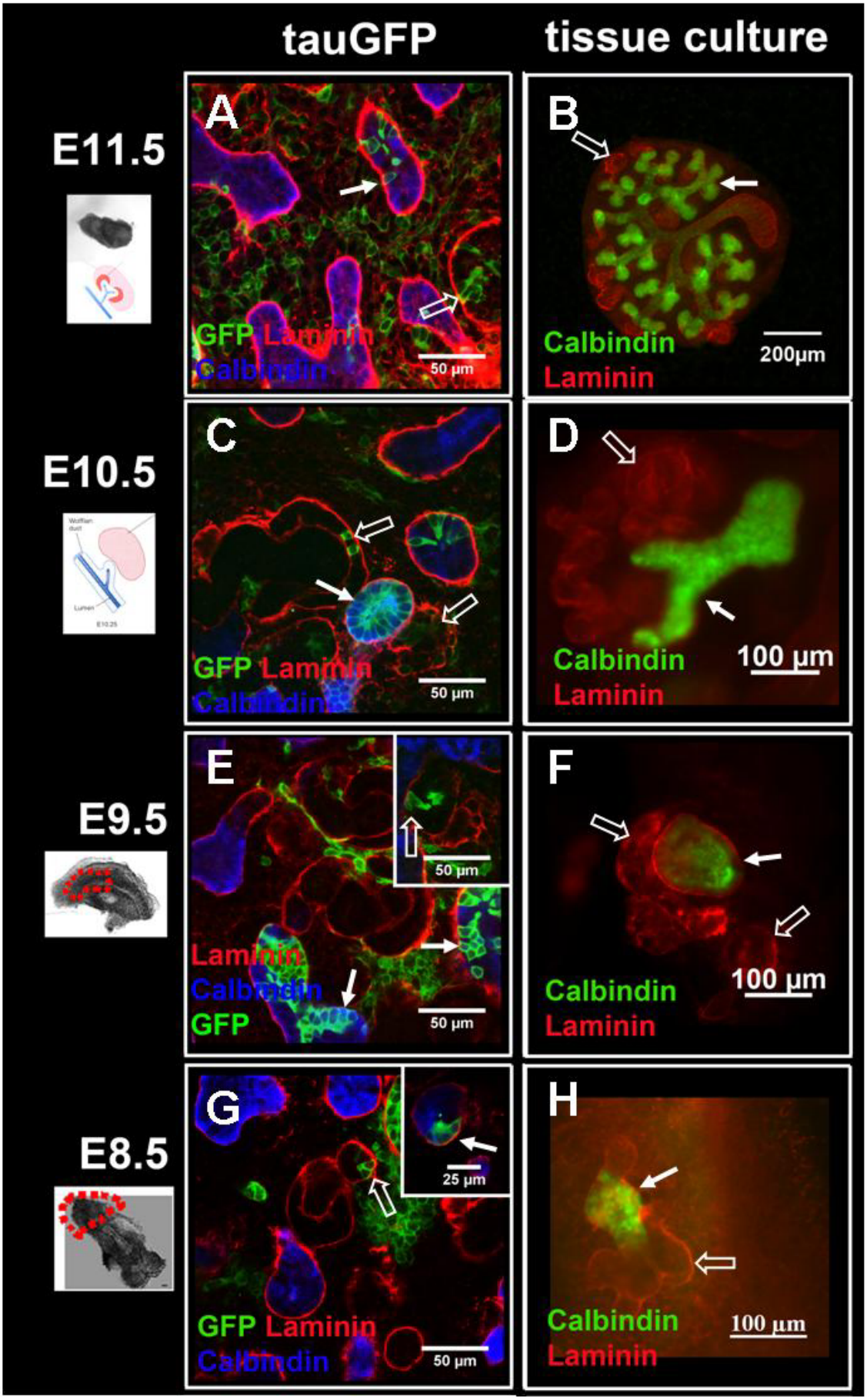
tauGFP
tissue culture
E11.5
E10.5
E9.5
E8.5
A
B
C
D
E
F
G
H
GFP Laminin
Calbindin
50 µm
Calbindin
Laminin
200µm
100 µm
Laminin
Calbindin
GFP
25 µm

Figure 6.2.2 – The ability of cells and tissues from different embryonic stages to contribute to integrate into renal epithelia and generate renal-like structures in organ culture

The respective embryonic stage is shown on the left; the isolated region was shown by a red dotted line if necessary; block arrows indicate cells integrating in UBs or forming Calbindin+ UB-like structures in the last column of images; open arrows indicate cells integrating in nephrons or the formation of nephron-like structures in the last column of images

A, C, E and G show that tauGFP+ cells from E11.5 metanephroi were able to integrate into both nephrons and UBs, where at least some of the integrating UB cells were Calbindin+; organ culture experiments in B, D, F and H show that the tissues isolated from different embryonic stages (as indicated in the diagrammatic panels on the left) for both UB-like and nephron-like structures; the ability of Calbindin + structures to branch disappeared in F and H.

block arrow). Although structures were formed, this observation suggested that at this stage, external signals for the complete development of branching UBs and nephrons might already be lacking.

No metanephros formation is seen in E9.5 embryos and even metanephric anlagen are not yet formed at this stage of embryonic development. Interestingly, cells isolated from the prospective metanephrogenic regions of these embryos were still able to integrate into either UBs (Figure 6.2.2, E, block arrow) or nephrons (Figure 6.2.2, E, inset, open arrow). Furthermore, a large proportion of the cells integrating in UBs were also positive for the marker Calbindin (Figure 6.2.2, E). Tissues cultured with the inducer spinal cord exhibited non-branched UB-like Calbindin+ structures, surrounded by tubular-like Laminin-bound structures (Figure 6.2.2, F, respectively block arrow and open arrows).

Cells with the ability to integrate into either UBs or nephrons were still present in tissues isolated from E8.5 experiments, as indicated by Figure 6.2.2, G, although these events were extremely rare. Some of the cells seen in UBs were positive for Calbindin (Figure 6.2.2, G, inset, block arrow). The cells found in nephrons were not distinguishable morphologically from normal nephron cells and seemed to have a consistent orientation with their neighbours to form a renal tubule with a lumen (Figure 6.2.2, G, open arrow). Culture of tissues isolated from the whole posterior part of embryos still showed the presence of Calbindin+ structures surrounded by Laminin-positive tubules (Figure 6.2.2, H, block arrow and open arrow respectively).

6.2.2 Cells from E7.5 embryos interfere with the normal development of reaggregated organotypic cultures

Reaggregated pellets were also prepared with cells isolated from an earlier embryonic stage. Since no metanephros, mesonephros, pronephros or their primordia are yet present in E7.5 embryos and the isolation of only mesoderm poses a serious limitation to the number of cells that could be used for experiments, whole embryos were disaggregated for mixing in the organotypic cultures. The renogenic capacity of tauGFP+ embryo-derived cells in the reaggregates was difficult to analyse, as the

reaggregated cultures grew abnormally in comparison to all previous cell mixing experiments (Figure 6.2.3 A-F). Pellets containing E7.5 cells, grown as previously described were unusually small and underdeveloped after 6 days in culture (Figure 6.2.3, C and D). To investigate whether this was due to an experimental error (such as expiry of any of the reagents used) or whether it was a real experimental result, the following test was performed. E11.5 kidney rudiments (which were used as "host" cells) were dissected, disaggregated into single cells and separated in two equivalent batches. One of the test tubes of cells was used for the generation of reaggregated organotypic cultures, which contained 115,000 embryonic kidney cells and no E7.5 embryo cells. The second test tube was used for the generation of organotypic cultures containing 115,000 cells, 100,000 of which were E11.5 embryonic kidney cells and 15,000 – tauGFP cells isolated from E7.5 embryos. These pellets were cultured for 6 days as described for reaggregated cultures in previous experiments. After 6 days, the difference between pellets lacking and containing E7.5 cells was discernible even by bright-field microscopy (Figure 6.2.3, A, B, C and D). Control pellets, which did not contain any E7.5 cells behaved as generally observed in cell mixing experiments – a large number of structures was present after 6 days of culture, the morphology of the pellets was healthy and the samples had greatly increased in size (Figure 6.3.2, A and B). On the other hand, pellets containing E7.5 cells were small, contained very few structures and showed signs of cell death, as can be seen on Figure 6.2.3, C and D. Although variation was observed in the survival rate of cells and the number of structures present, three independent experiments confirmed the general pattern trend of these results. The low number of structures was also confirmed when the pellets were stained for the markers Calbindin and Laminin (Figure 6.2.3, E and F). These results indicated that the unusual behaviour of pellets was not due to an adverse effect from any of the reagents or an error in preparation of the materials and that it was most probably due to the presence of E7.5 cells in the organotypic reaggregates.

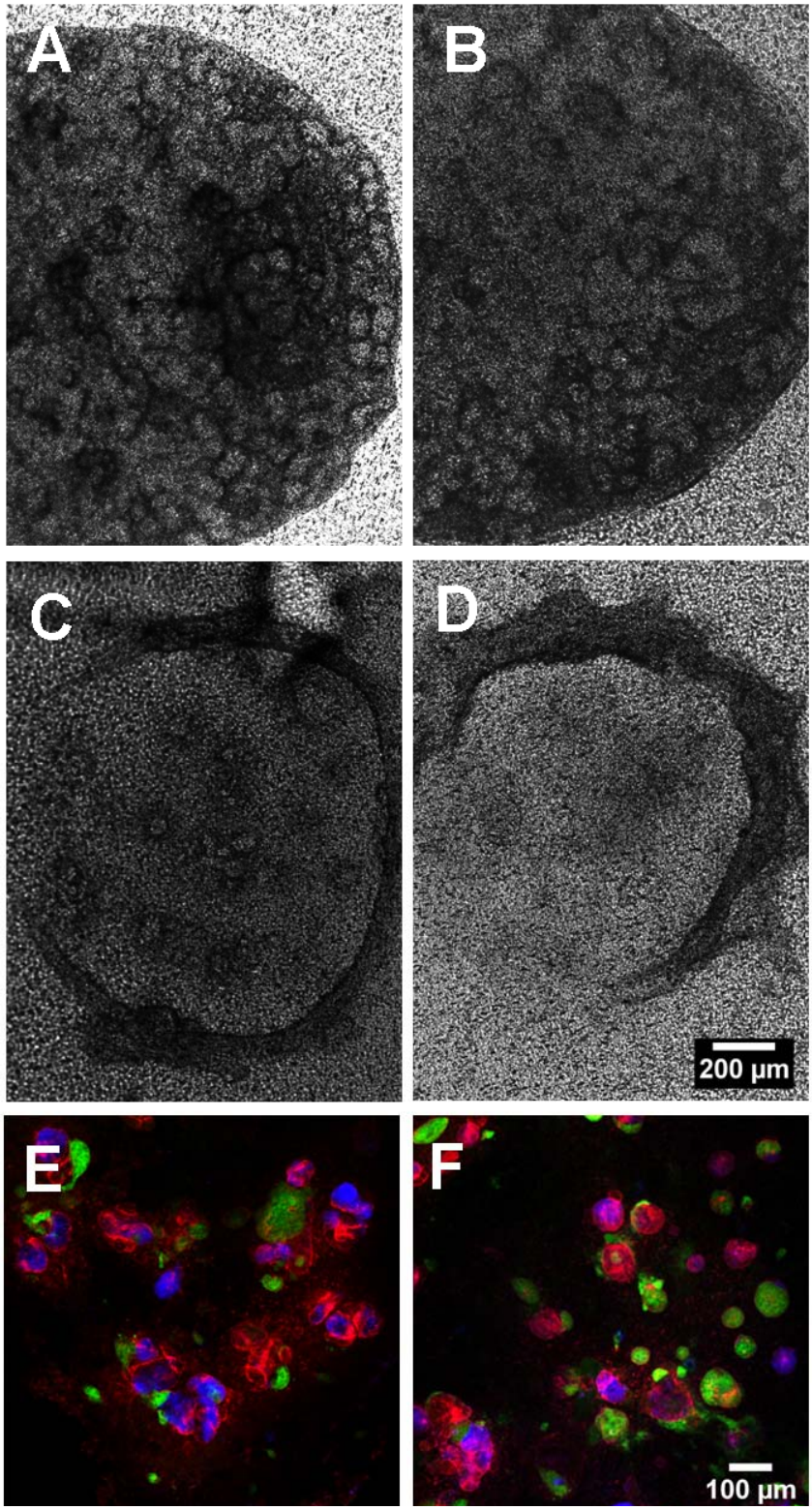

Figure 6.2.3 – Cells from E7.5 embryos interfere with the normal growth of reaggregated organotypic cultures
A and B – reaggregated pellets cultured for 6 days, exhibiting the formation of numerous structures (light, often round areas)
C and D – experiments performed with the same pool of reaggregated cells, but containing E7.5 tauGFP cells showed abnormal growth and degeneration after 6 days in culture; the difference between C and D also demonstrates the variation in the number of structures formed in these experiments (a few in C, but none in D)
E and F – reaggregates containing tauGFP+ E7.5 cells, stained for Calbindin (blue) and Laminin (red) also demonstrated that an abnormal number if structures was formed

6.2.3 Cells from E7.5 embryos might also be competent to integrate in developing renal epithelia

Although the results from E7.5 experiments could not be treated as conclusive due to the abnormal growth of the pellets, the samples, which contained some structures were fixed and stained for Calbindin and Laminin for examination. In many cases, the disaggregated E11.5 kidney cells had not developed normally (this will be discussed later in the text). Figures 6.2.4, A and C were a good representation of why these experiments were difficult to analyse. First, this confocal micrograph revealed that tauGFP+ cells can form chimeric structures with renal epithelia (arrows). At the same time, the borders between the Laminin-bound and Calbindin-positive part (UB) and the Laminin-bound and Calbindin-negative part (nephron) were not clear, as observed in normal reaggregates (for comparison see Figure 6.2.2). The Calbindin staining itself showed a strong mosaicism, which was not characteristic of normal ureteric buds. The dotted red and blue lines in Figure 6.2.4, A and B indicate unusually alternating Calbindin+ and Calbindin- areas. This did not allow determining which part of the renal epithelium was a nephron, UB, or possibly another unknown type of epithelium. Therefore, it was impossible to assess the ability of the mixed tauGFP+ E7.5 cells to contribute to kidney structures. In the few samples that could be examined, no tauGFP+ Calbindin+ cells were seen.

6.2.4 E7.5 tissues generate rudimentary tubular structures

Consistently with cell mixing experiments from later embryonic developmental stages, tissue culture experiments were also performed with E7.5 embryos. The tissues were isolated as previously described and co-cultured with spinal cord on a polycarbonate filter at the air-liquid interface for 5 days. The methanol-fixed tissues were stained for Calbindin and Laminin to look for the formation of rudimentary renal structures. Fluorescence micrographs showed that in some samples, there were Calbindin+ tubules connected to Laminin-bound and Calbindin-negative epithelia (Figure 6.2.5, A-D).

To illustrate the presence or absence of structures in cultured E7.5 embryos and characterise them for expression of Calbindin and Laminin, the observations of all

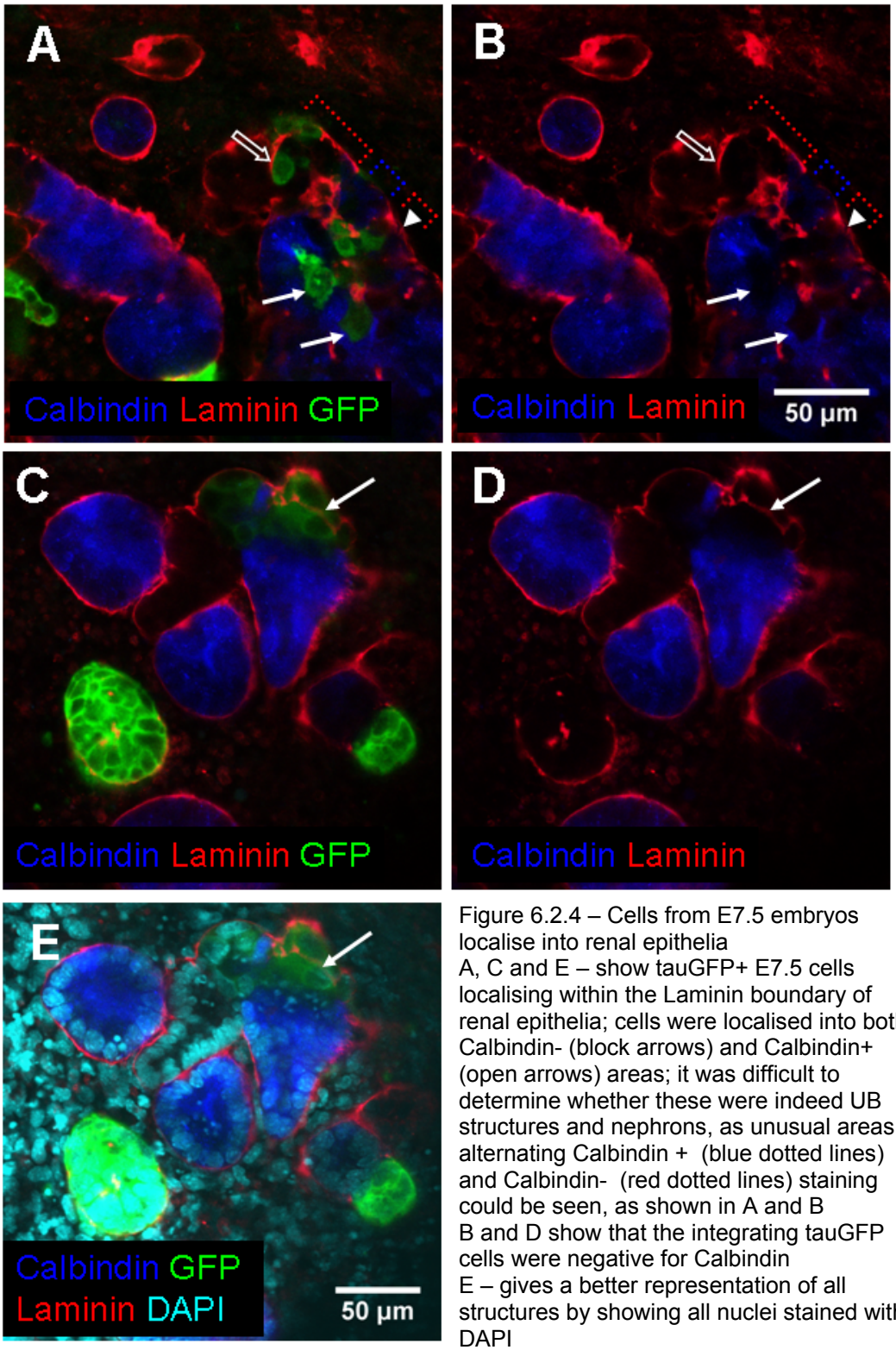

Figure 6.2.4 – Cells from E7.5 embryos localise into renal epithelia
A, C and E – show tauGFP+ E7.5 cells localising within the Laminin boundary of renal epithelia; cells were localised into both Calbindin- (block arrows) and Calbindin+ (open arrows) areas; it was difficult to determine whether these were indeed UB structures and nephrons, as unusual areas of alternating Calbindin + (blue dotted lines) and Calbindin- (red dotted lines) staining could be seen, as shown in A and B
B and D show that the integrating tauGFP cells were negative for Calbindin
E – gives a better representation of all structures by showing all nuclei stained with DAPI

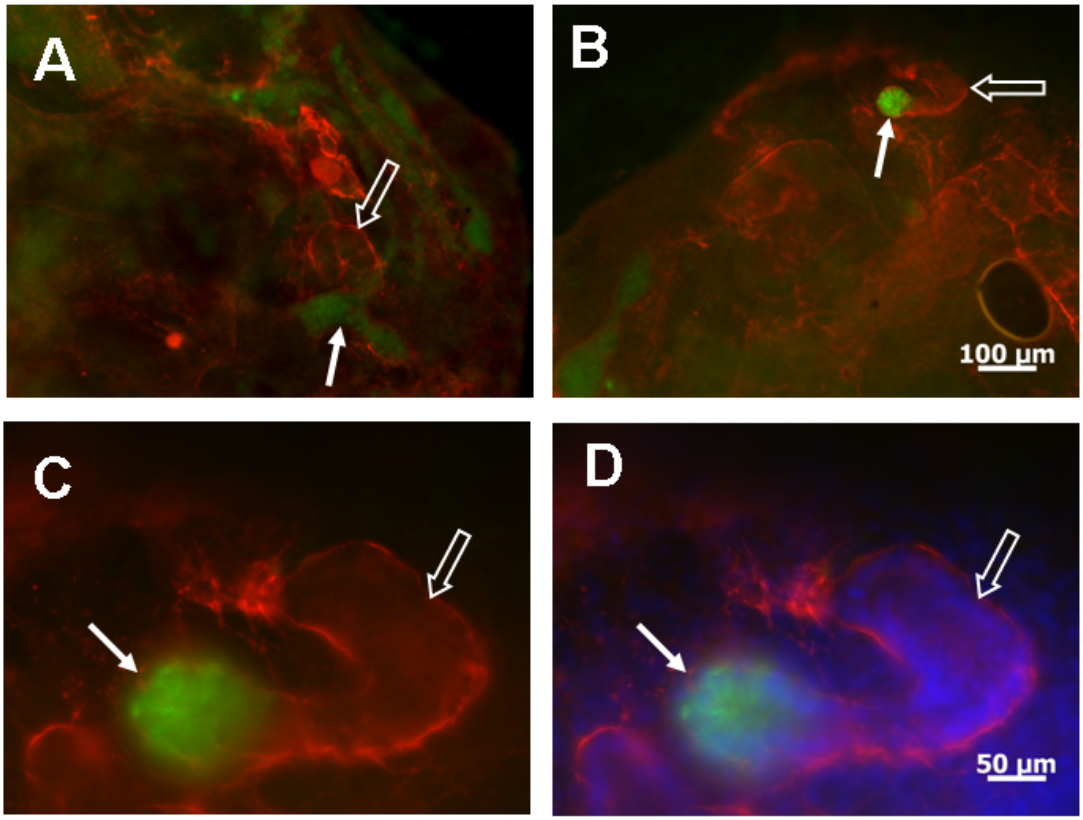

E

Sample Number	no SC				SC			
	Side 1		Side 2		Side 1		Side 2	
	C+ L+	C- L+	C+ L+	C- L+	C+ L+	C- L+	C+ L+	C- L+
1	-	-	-	-	-	-	-	-
2	-	-	-	-	-	-	-	-
3	-	-	-	-	+	+	-	-
4	+	+	+	-	-	-	-	-
5	+	-	+	-	-	-	-	-
6	+	-	+	+	n/a	n/a	n/a	n/a
7	-	-	-	-	n/a	n/a	n/a	n/a
8	-	-	-	-	n/a	n/a	n/a	n/a

Figure 6.2.5 – Cultures E7.5 embryos exhibit the ability to produce rudimentary kidney-like structures
A, B and C were stained for Calbindin (green) and Laminin (red)
D was stained for Calbindin (green), Laminin (red) and DAPI (cyan)
A and B are micrographs of two different embryos, showing Laminin+ Calbindin+ structures (block arrows) with associated Laminin+ Calbindin- tubules (open arrows)
C and D show a magnification of B
E – is a summary of the results of several tissue culture experiments, in which embryos were cultured either alone or together with spinal cord; SC denotes spinal cord; “side 1” was to the left of the midline with respect to the viewer, while “side 2” was to the right; “left” and “right” might not correspond to the real sides of the embryos, as their orientation after culture was not known; C and L denote Calbindin and Laminin; + or – denote positive or negative; n/a indicates that these experiments were not performed

	Integration tauGFP		Structure formation (culture of tissue fragments)	
Age	**UB**	**Nephron**	**UB**	**Nephron**
E11.5	yes	yes	yes	yes
E10.5	yes	yes	yes	yes
E9.5	yes	yes	yes	yes
E8.5	yes	yes	yes	yes
E7.5	inconclusive	inconclusive	yes	inconclusive

Figure 6.2.6 – Summary of the ability of cells or tissues from different embryo stages to integrate in renal tubules or form structures when cultured *in vitro*
A Calbindin+ Laminin+ structure was marked as a UB. A Calbindin- Laminin+ structure was marked as a nephron.

samples were presented in Figure 6.2.5, E. Since kidneys are paired organs, both sides of the embryo were examined for the presence of structures. “Side 1” and “Side 2” were used to describe whether the structures were seen on the left side or right side with respect to the viewer. This was done as it was important to document whether the two types of structures were both present at the same side of the embryo. Describing the sides with “left” and “right” was not possible for two reasons: 1 - it was not known whether the embryos were placed in culture on their dorsal or ventral side; and 2 – some embryos were misshapen after 5D in culture and rostral and caudal sides were also difficult to distinguish. “C” and “L” stand for Calbindin and Laminin. A plus or minus indicates presence or absence of the marker in a structure. SC stands for spinal cord, which was used as an inducer in some experiments (as indicated). The summary of data indicates that more structures were observed in the samples, which were not co-cultured with spinal cord. This might suggest that very high concentrations of signals emanating from spinal cord might be interfering with, rather than supporting renogenesis. This observation also provides support for the speculation that signals from E7.5 embryos could have interfered with normal reaggregation and development of the E11.5 kidney cells.

6.2.5 Quantitative characterisation of the ability of embryonic cells to integrate into renal structures

A summary of the renogenic capacity of cells derived from different stages of mouse embryonic development was given in Figure 6.2.6. Although, the experiments described in the previous sections of this chapter provided valuable information about the presence or absence of renogenic capacity in the different cell populations, they did not describe how this capacity decreases with the stepwise decrease in the age of embryos used for experiments. To characterise this, reaggregated organotypic pellets were set up and cultured as previously described. The numbers of cells integrating in nephrons and UBs were counted as detailed in Chapter 3 (Method 2). Calbindin and Laminin were used for distinguishing between the two renal compartments. The quantified data was expressed as integrating cells per megapixel of the screened confocal micrographs ± standard error of the mean. Significance was calculated by an unpaired student's t-test. The criteria for integration were applied, as described in Chapter 4. In short, cells were considered to integrate in UBs when they were seen in the structure of this renal compartment, expressed Calbindin and were morphologically indistinguishable from the surrounding cells. Cells were considered integrating in nephrons, if they fulfilled the criteria above, but were not Calbindin positive. The results were shown graphically in Figure 6.2.7, A - D, and numerically in Figure 6.2.7, E. Panels A and C present the data on a linear scale, while B and D – on a logarithmic scale.

From Figure 6.2.7, it becomes obvious that there was no significant difference in the ability of the isolated E11.5 and E10.5 cells to integrate into nephrons, but the difference for UBs was significant. The tauGFP+ cells integrating in UB decreased from 220 ± 33 to 140 ± 11 cells per megapixel between E11.5 and E10.6, while cells integrating in nephrons decreased from 130 ± 17 to 120 ± 10. One embryonic day earlier, the cells integrating into both compartments decreased significantly to 9.6 ± 4.0 (UB) and 5.3 ± 1.5 (nephrons) cells per megapixel. At E 8.5, cells integrating in both compartments could still be observed. The decrease from E9.5 for tauGFP+

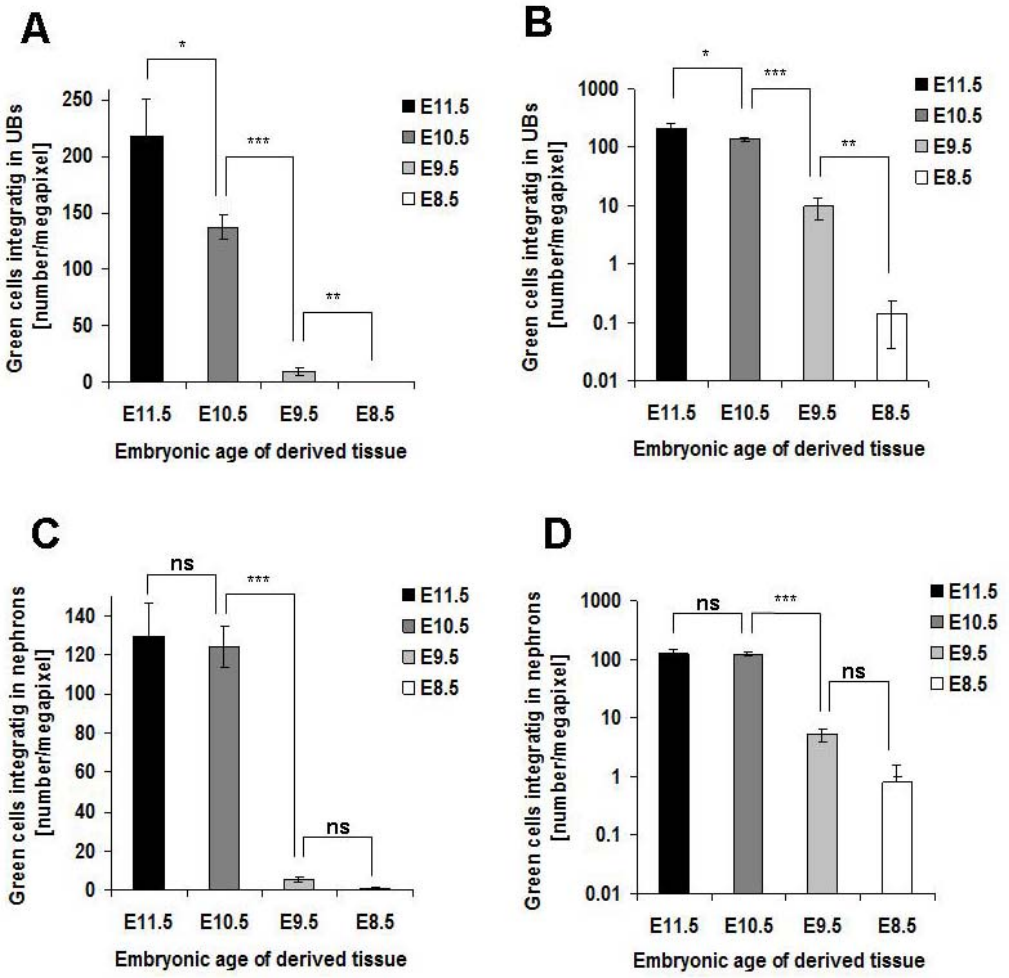

E

Age of source tissue	Green cells integrating in UB [per megapixel ± SEM]	Green cells integrating in nephrons [per megapixel ± SEM]
E11.5	220 ± 33	130 ± 17
E10.5	140 ± 11	120 ± 10
E9.5	9.6 ± 4.0	5.3 ± 1.5
E8.5	0.14 ± 0.11	0.81 ± 0.81

Figure 6.2.7 – Quantitative characterisation of the ability of early embryo cells to integrate into renal structures
All data is presented as the number of green cells integrating in nephrons or UBs per megapixel (1000000pixel = 1megapixel);
A and B present the integration of cells in UBs;
C and D present the integration in nephrons;
B and D display the data on the x-axis on a logarithmic scale as the presence of bars in the E8.5 samples is not well visible in A and C;
A and C present the same data as B and D, on a linear scale;
1000x1000 pixel = 230x230 µm
* $p<0.05$, ** $p<0.01$, *** $p<1x10^{-23}$
E - provides the numerical data used for the generation of the graphs in A-D. The values have been rounded to two significant figures.

cells found in UBs was significant, while that for cells found in nephrons was not. The cells quantified at this stage were 0.14 ± 0.11 and 0.81 ± 0.81 cells per megapixel respectively. Quantification of experiments with E7.5 embryos was not possible due to the morphological changes of the two "host" renal compartments.

6.2.6 Cells from E11.5 mesonephroi were able to integrate into renal epithelia

As mentioned in Chapter 1 of this thesis and in the introduction section of this chapter, the metanephros is not the only renal structure found in embryonic development. The development of the pronephros and mesonephros precedes the appearance of metanephrogenic primordia. Therefore, it could not be excluded that the cells of these organs could also be able to contribute to the structure of metanephric renal epithelia. This could mean that, potentially, in the qualitative and quantitative experiments described in previous sections, mesonephric cells could have integrated into metanephric renal epithelia. To test whether mesonephric cells had the capability to localise into metanephric structures, mesonephroi were isolated from tauGFP+ E11.5 embryos, disaggregated into single cells and mixed in the reaggregation system. The experiments were cultured for 6 days for consistency with all other experiments in this chapter, fixed, and stained for Calbindin and Laminin. Analysis by confocal microscopy revealed that mesonephric cells localised into both metanephric nephrons and metanephric UB structures (Figure 6.2.8). The morphology of the detected cells was also indistinguishable from metanephric renal epithelia at that level of microscopic analysis. Some, but not all of the cells integrating in ureteric buds were Calbindin-positive (Figure 6.2.8).

6.2.7 Early embryo cells mixed in reaggregated kidney rudiments do not express Oct4

Since experiments with embryonic stem cells have shown that a detectable number of cells remain Oct4 positive even after being cultured for 6 days in the disaggregation-reaggregation system. Although Oct4 is expressed by inner cell mass cells (and ESCs), it persists in certain types of cells in early embryogenesis. Oct4

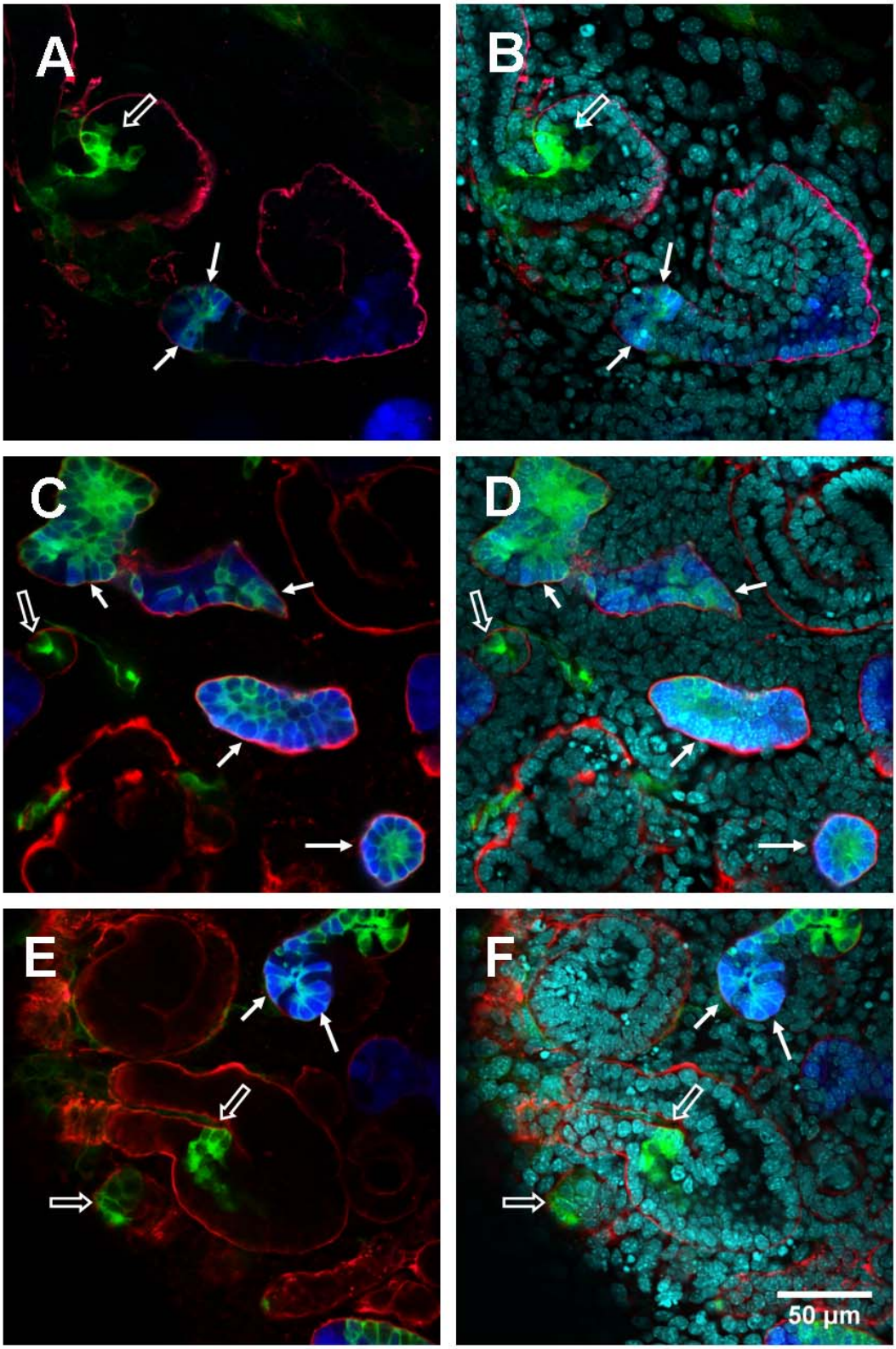

Figure 6.2.8 – Cells from E11.5 mesonephroi can integrate into developing renal epithelia
A-F – show that mesonephric cells integrating into both nephrons (open arrows) and UBs (block arrows); many cells integrating in UBs were positive for Calbindin
Calbindin (blue), Laminin (red), tauGFP (green), DAPI (cyan)

transcript has been detected at high levels in the neural ectoderm at E8.0 (Scholer et al., 1990). It was therefore interesting to check whether early embryo-derived Oct4+ cells could be found in the reaggregates and whether these integrated in renal epithelia. Since the earliest tissues used in organ disaggregation-reaggregation experiments (E7.5) caused abnormal development of reformed organotypic kidney rudiments, tissue from E8.5 caudal parts was used for performing these experiments. Single-cell suspensions were prepared as previously described and the resulting pellets were placed in a conventional organ culture system and cultured for 6 days. The fixed pellets were stained for Oct4. Laminin and DAPI were used to visualise the nuclei and the borders of renal epithelia.

Analysis by confocal microscopy did not identify any GFP+ Oct4+ in the reaggregates in both tauGFP+ cells found in renal tubules or the interstitium (Figure 6.2.9, A-F). In Figure 6.2.9, block arrows show that tauGFP+ structures were negative for GFP. Open arrows indicate artefacts, which looked similar to nuclear staining. These exhibited fluorescence in both the red and the red (blue) fluorescence channels, did not show colocalisation with DAPI or were much smaller than a normal nucleus, as indicated by the staining of neighbouring cells.

6.2.8 Marker expression analysis of tauGFP+ cells in the organotypic culture system

Next, it was necessary to determine whether tauGFP+ cells derived from early embryos expressed other renal markers in addition to Calbindin and Laminin, (which are quite wide-spread in epithelia) after integration in the disaggregation – reaggregation system. For screening for renal markers, it would be ideal to use tissues from the earliest stage that has shown a renogenic potential. This was identified as E8.5. Quantification experiments in section 6.2.5 of this chapter, however, suggested that too few cells with the potential to integrate were present at this stage and covering the scope of many different markers would not be possible due to the low prevalence of integrating cells. For that reason, E9.5 cells were used to characterise the properties of early embryo - derived tauGFP-tagged cells instead.

The disadvantage of studying renal markers in E9.5 embryos is that the information is not directly transferable to integrating E8.5 cells, as non-kidney cells have also shown the ability to localise into renal tubules. An example was presented in Chapter 4 of this thesis where ESC-derived cells were seen to form chimeric structures with renal epithelia, but failed to express renal markers. Integration is therefore not a sufficient condition for renal differentiation. Still, it should be noted that ESC-derived cells localising into renal tubules (which didn't express renal markers) were morphologically distinct from the neighbouring E11.5 embryonic kidney cells. This suggests that the criterion "morphology" can still be applied to E8.5 cells to obtain more information about what these cells are. Studying marker expression in E9.5 embryos is key in understanding whether cells isolated from an embryo stage, at which the intermediate mesoderm has not yet formed a metanephric blastema, are able to integrate, and also differentiate to the different kidney subtypes in the reaggregation system.

To address these questions, organotypic cultures were prepared as previously described for E9.5 tissues and cultured for 8 days (longer time was allowed for induction of marker expression in the tested cells). The experiments were stained for the following combinations of markers:

- Pax2 and WT1
- Megalin and E-cadherin.
- Six2 and E-cadherin

The expression patterns of these genes have been discussed in more detail in Chapter 1. In short, in the metanephros, Pax2 is expressed in the UB, the condensing mesenchyme, renal aggregates and nascent nephrons (Dressler et al., 1990); WT1 is expressed at low levels in the condensing mesenchyme and renal vesicle, and persists at high levels in the glomerular podocytes (Self et al., 2006; Pritchard-Jones et al., 1990); Megalin is a member of the low density lipoprotein receptors and transcript has been detected within the brush-border membrane of proximal tubular cells (Lundgren et al., 1997); E-cadherin expression is abundant in the distal tubule, but decreases significantly in the proximal tubule (Prozialek et al., 2004); Six2 is

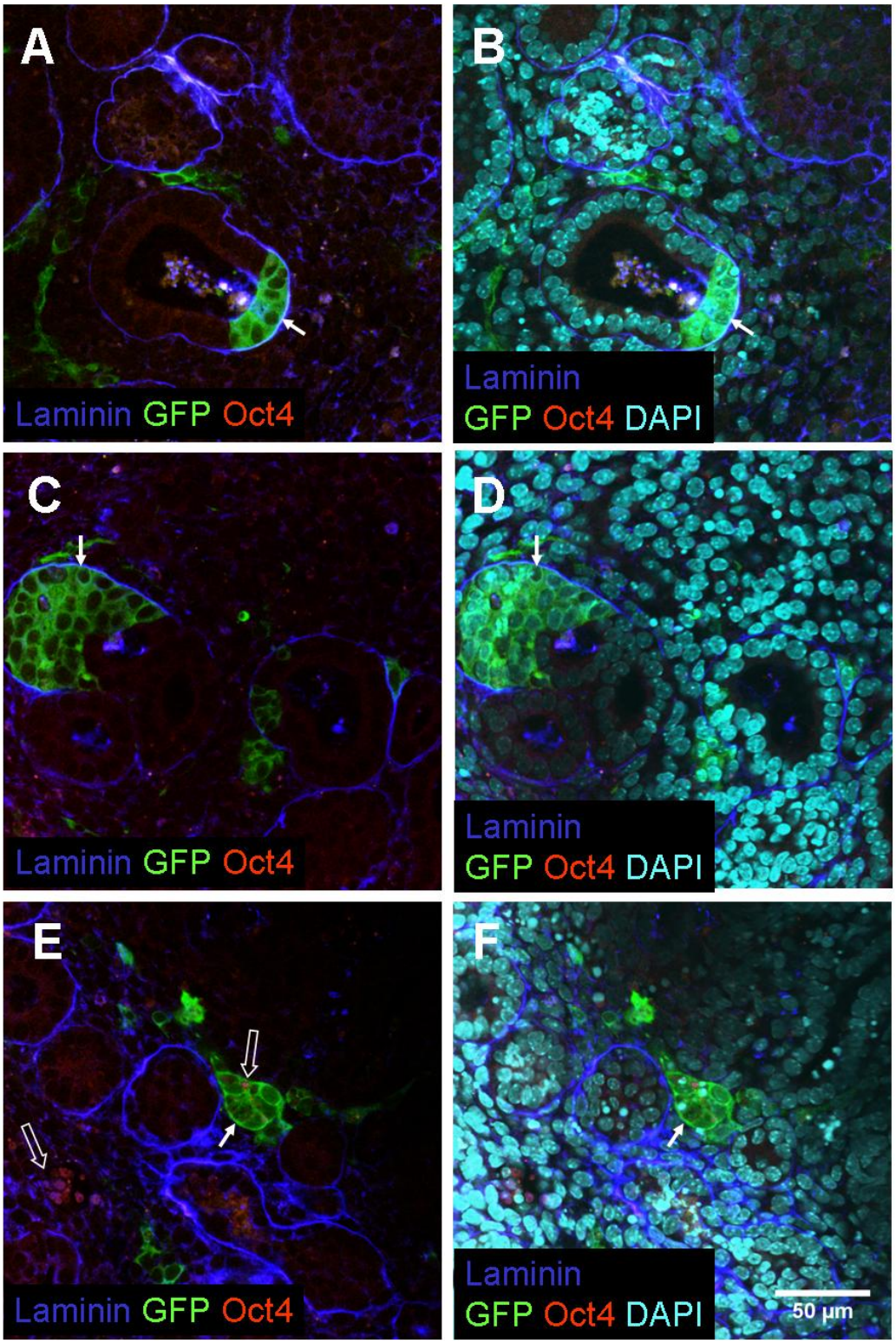

Figure 6.2.9 – Early embryo cells do not express Oct4 after 6 days in culture
A-F – images of organotypic cultures containing cells from the caudal parts of E8.5 emrbyos
A-D – tauGFP embryo cells localising into Laminin-bound structures do not express detectable levels of Oct4 (block arrows)
E and F – tauGFP cells, which did not localise into renal epithelia did not express detectable levels of Oct4 (block arrows); open arrows point at artefacts, which resembled Oct4+ nuclei, but were confirmed to show unspecific fluorescence in other fluorescence channels

expressed by the MM cells surrounding the UB tips (Self et al., 2006). It is also important to note that all of these genes are also expressed in other non-kidney tissues (discussed in Chapter 1).The Pax2 and WT1 staining allowed screening for tauGFP+ cells localising in the condensing mesenchyme and glomeruli, in addition to cells integrating into renal tubules. The wild-type kidney cells showed a normal expression of these markers – WT1 was highly expressed in glomerular podocytes and detected at a weaker level in the metanephric mesenchyme (Figure 6.2.10, A, B, C and D). Pax2 was expressed by the cap mesenchyme and in already formed renal tubules (Figure 6.2.10, A, B, C and D). Many wild-type cells were doubly positive for Pax2 and WT1 (Figure 6.2.10, C and D). These were largely found in the induced/condensing mesenchyme. Interestingly, some Pax2+ WT1+ cells were also observed in what appeared to be already formed tubules (Figure 6.2.10, E, F, G and H).

In tauGFP+ cells, the following four types of marker profiles were observed:

- tauGFP+ Pax2- WT1-
- tauGFP+ Pax2+ WT1-
- tauGFP+ Pax2- WT1+
- tauGFP+ Pax2+ WT+

The four types of cells above were also listed in an order of decreasing abundance. Most frequently seen were tauGFP+ Pax2- WT1- cells (Figure 6.2.10, A-D, block arrows). There was a detectable number of tauGFP+ Pax2+ WT1- (Figure 6.2.10, I and J, block arrows). These could be clearly seen integrating into already formed renal tubules and in the condensing mesenchyme (Figure 6.2.10, I and J, arrows). tauGFP+ Pax2- WT1+ cells were also present in the metanephric mesenchyme, but these were seen extremely rarely, sometimes in clusters of several cells (Figure 6.2.10, K-R, arrows). Only one occasion of tauGFP+ Pax2- WT1+ cells was detected in a glomerulus (n=3; Figure 6.2.10, W and X, arrows). tauGFP+ Pax2+ WT+ were extremely hard to detect and only a few occasions of these triply positive cells were seen in the experiments (n=3, Figure 6.2.10, S, T, U and V, arrows).

Megalin and E-cadherin staining identified E-cadherin+ tauGFP+ cells in renal tubules (Figure 6.2.11, A-D, arrows). A few tubules containing tauGFP+ cells were also positive for Megalin (Figure 6.2.11, A-D, block arrows). Micrographs also suggested that Megalin was specifically expressed by some tauGFP+ E-cadherin+ cells, as well as native proximal tubular cells, as in some cases the areas of positivity appeared to be on the luminal side of integrating tauGFP cells.

.

The Six2 and E-cadherin marker expression screening was more difficult to analyse as staining for Six2 was not as bright as the immunohistochemistry for other proteins. The properties of some tauGFP+ cells also contributed to the limitations as they seemed to be able to wrap around other cells thereby creating potential false positives. This could be more clearly demonstrated by the WT1 and Pax2 staining as the quality of these confocal images was superior. Figure 6.2.12, A and B, C and D show two serial confocal sections of an organotypic pellet containing E9.5 cells, stained for WT1 and Pax2. An arrow points at a cell, which shows an apparent expression of tauGFP, WT1 and Pax2. Looking at the neighbouring section showed the same WT1+ Pax2+ nucleus, which was not enveloped by a layer of tauGFP cytoplasm. Still, Six2+ cells could be observed in the reaggregates (Figure 6.2.12, E and F, arrows), although these events could be detected extremely rarely. Six2+ cells were negative for E-cadherin suggesting that these cells hadn't undergone MET (Figure 6.2.12, E and F, arrows).

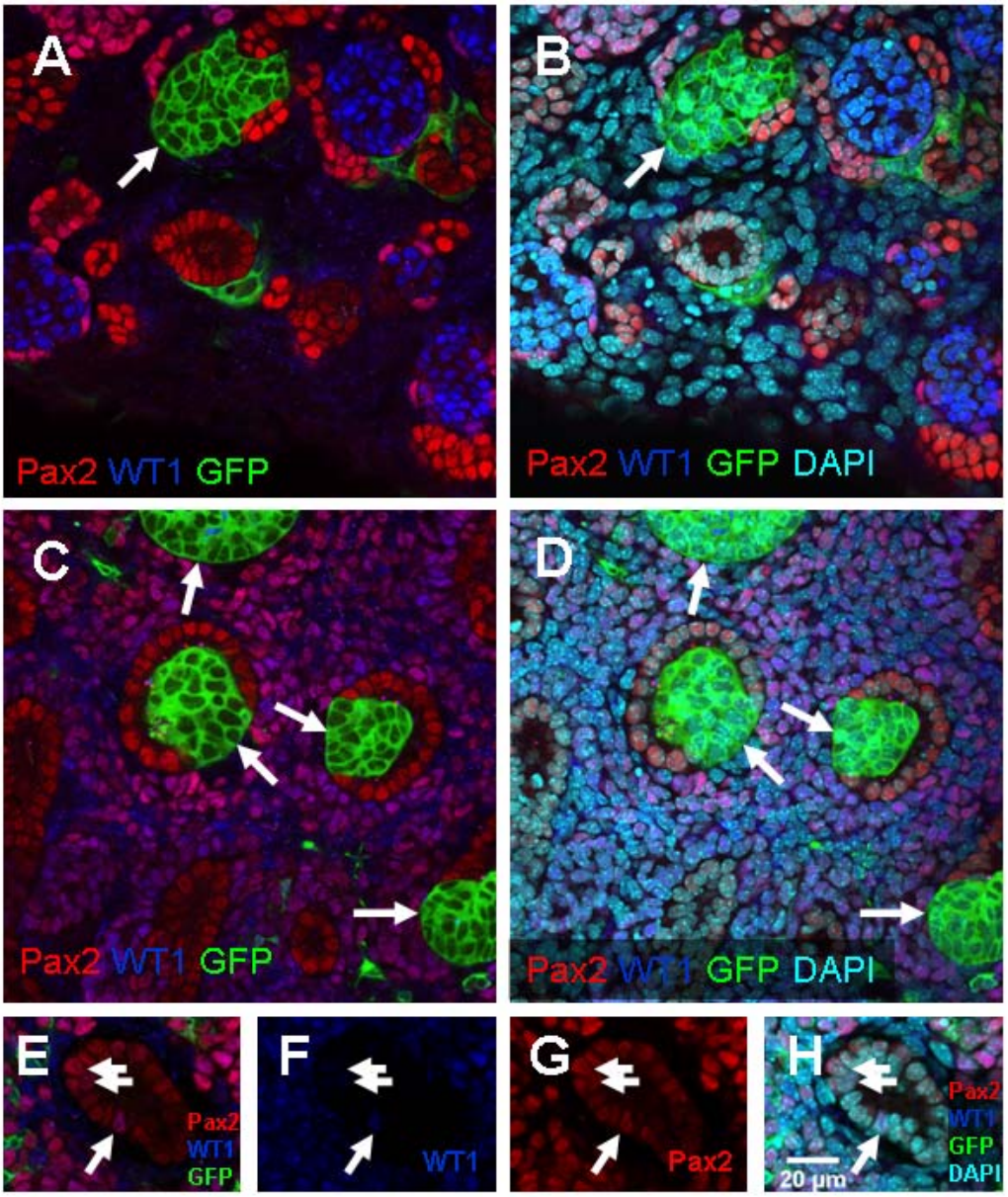
A
Pax2 WT1 GFP
B
Pax2 WT1 GFP DAPI
C
Pax2 WT1 GFP
D
Pax2 WT1 GFP DAPI
E
Pax2
WT1
GFP
F
WT1
G
Pax2
H
Pax2
WT1
GFP
DAPI
20 µm

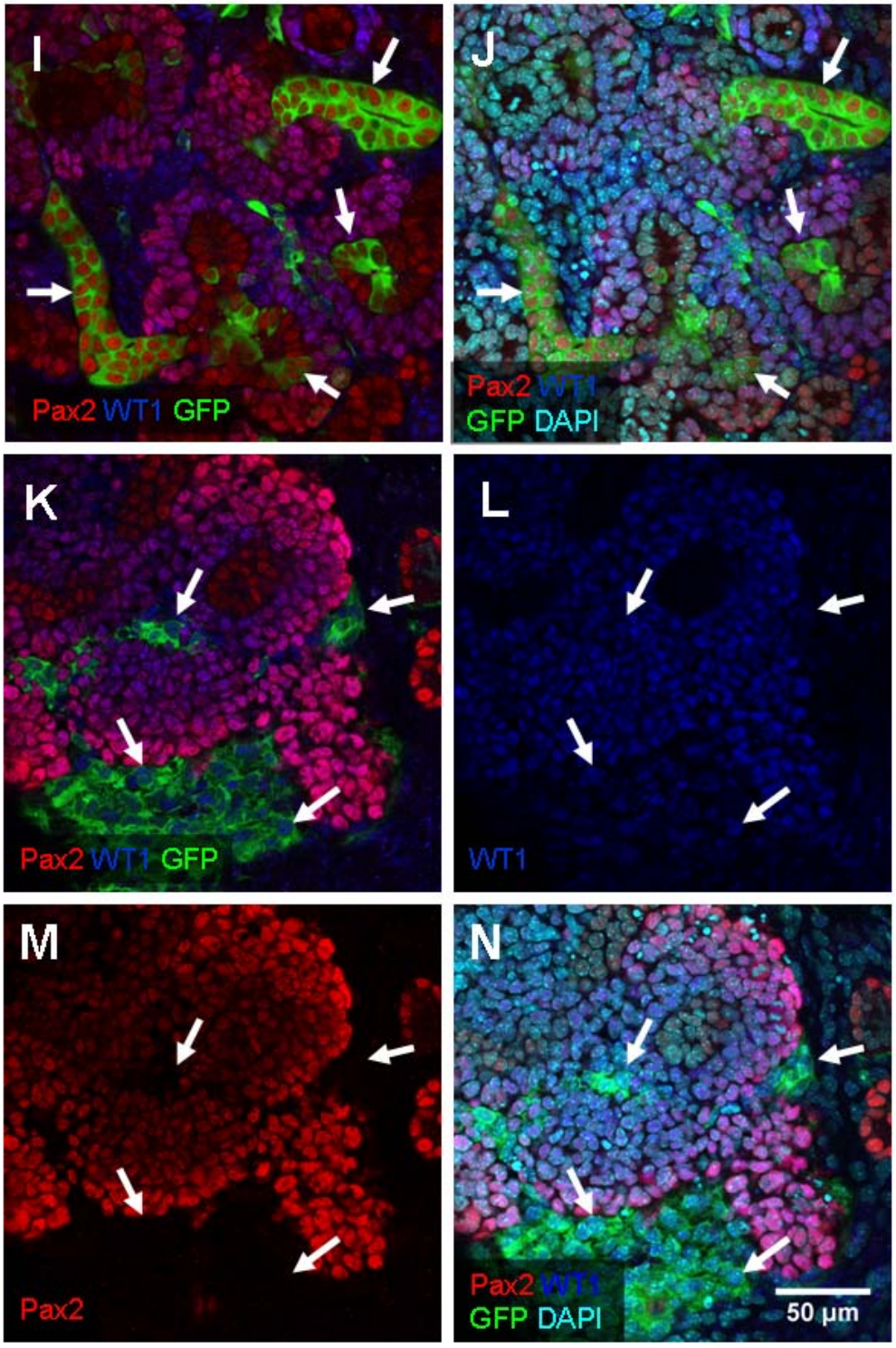
I
Pax2 WT1 GFP
J
Pax2 WT1
GFP DAPI
K
Pax2 WT1 GFP
L
WT1
M
Pax2
N
Pax2 WT1
GFP DAPI
50 µm

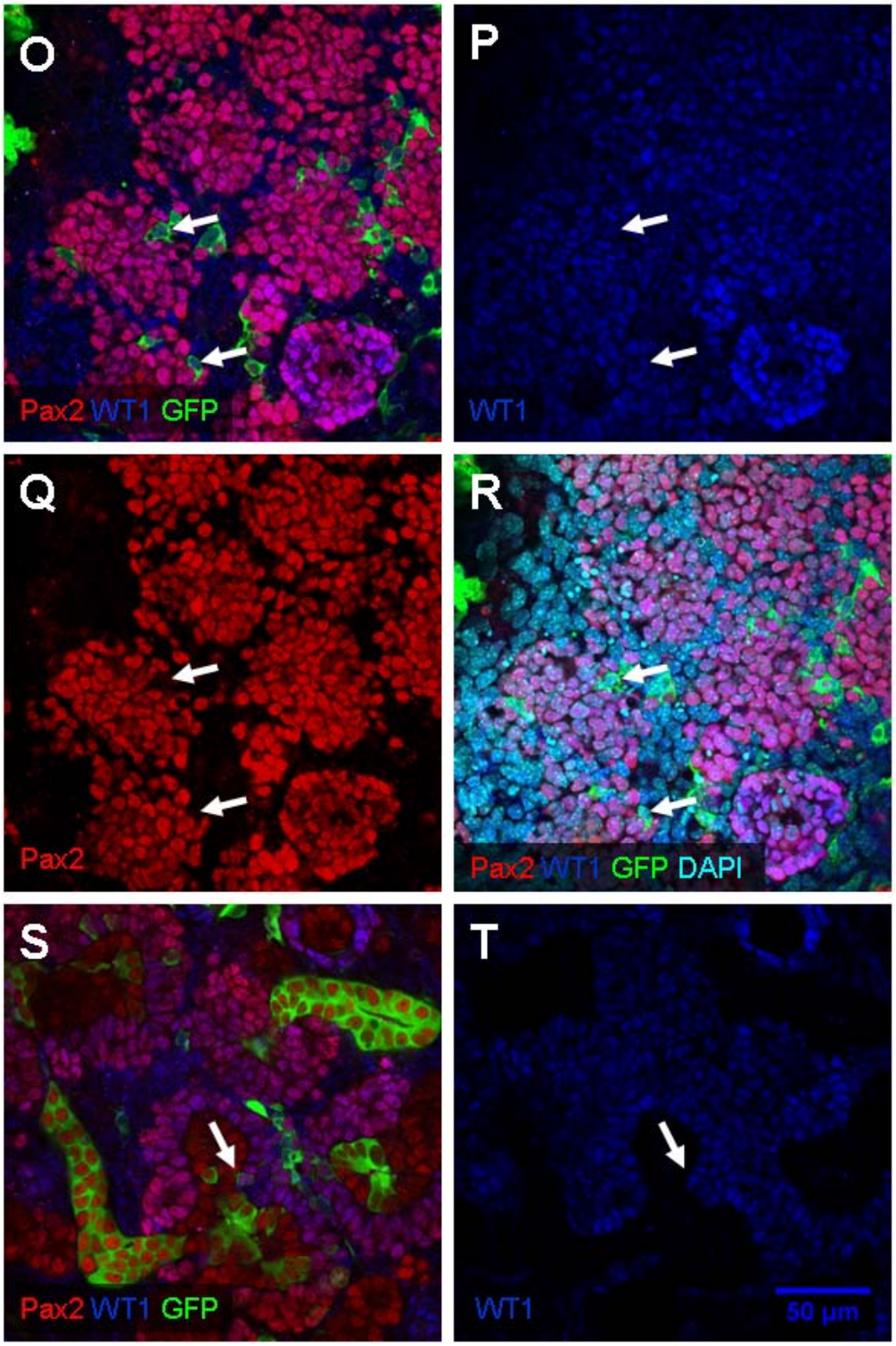
O
Pax2 WT1 GFP
P
WT1
Q
Pax2
R
Pax2 WT1 GFP DAPI
S
Pax2 WT1 GFP
T
WT1
50 µm

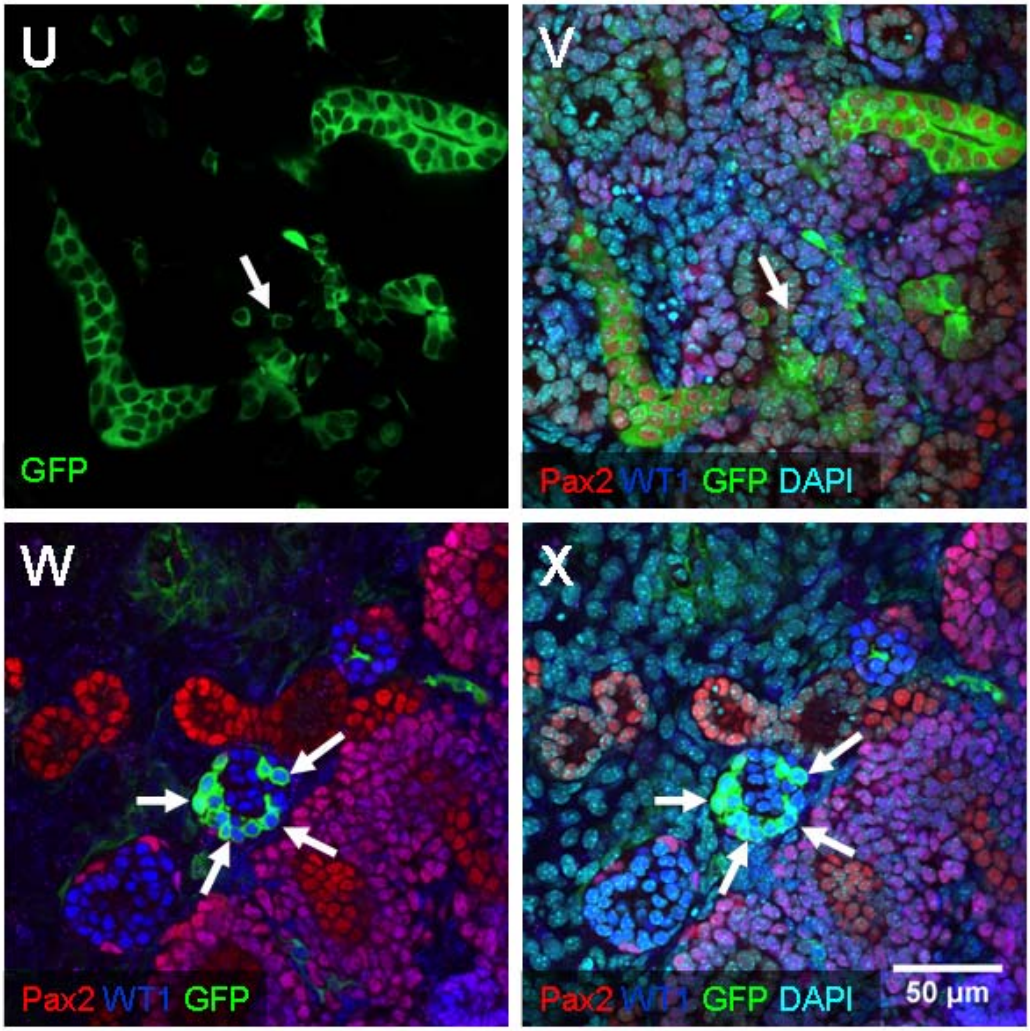

Figure 6.2.10 – Pax2 and WT1 expression of tauGFP E9.5 cells after an 8-day culture in the organotypic pellets
A, B, C and D – most tauGFP+ cells found in the organotypic pellets were Pax2- WT1- (arrows)
C and D – some tauGFP+ cells forming chimeric structures with renal epithelia were Pax2- and exhibited an uncharacteristic for renal tubules morphology (arrows)
E, F, G and H - demonstrate that rarely WT cells, which have already formed tubules, co-express Pax2 and WT1 (arrows)
I and J – show that some tauGFP+ cells integrating in renal epithelia express Pax2+; these were negative for WT1 (arrows)
K , L, M, N, O, P, Q, R – show tauGFP cells expressing low levels of WT1, as characteristic of the condensing mesenchyme (arrows); the tauGFP+ WT1+cells on the lower side of the panels K, L, M and N show a more loose distribution than wild type cells
S, T, U and V – the arrow points to a tauGFP+ cell, which is also co-expressing Pax2 and WT1, thereby appearing purple in the merged images S and V; U shows that the cells is tauGFP+
W and X – show tauGFP+ cells located in a glomerulus and expressing a high level of GFP+

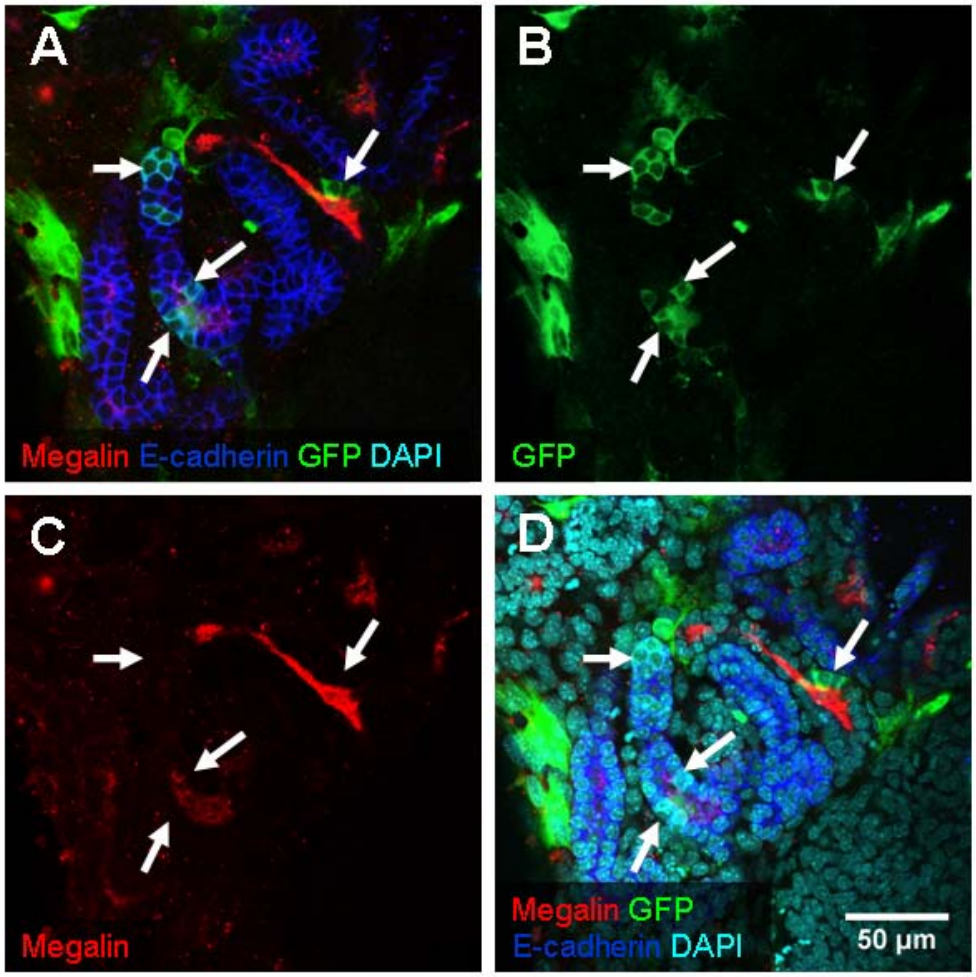

Figure 6.2.11 – Megalin and E-cadherin expression of tauGFP E9.5 cells after an 8-day culture in organotypic reaggregates
A – shows tauGFP+ cells localised into a renal tubules, which express both E-Cadherin and Megalin (arrows); the tubule with three arrows pointing at it expresses high levels of E-cadherin and seems to express low levels of Megalin; the tubule with one arrow pointing at it expresses high levels of Megalin and a very low level of E-cadherin
B and C – show the tauGFP and Megalin channels separately
D – is a merge, of all channels and also shows DAPI nuclear staining

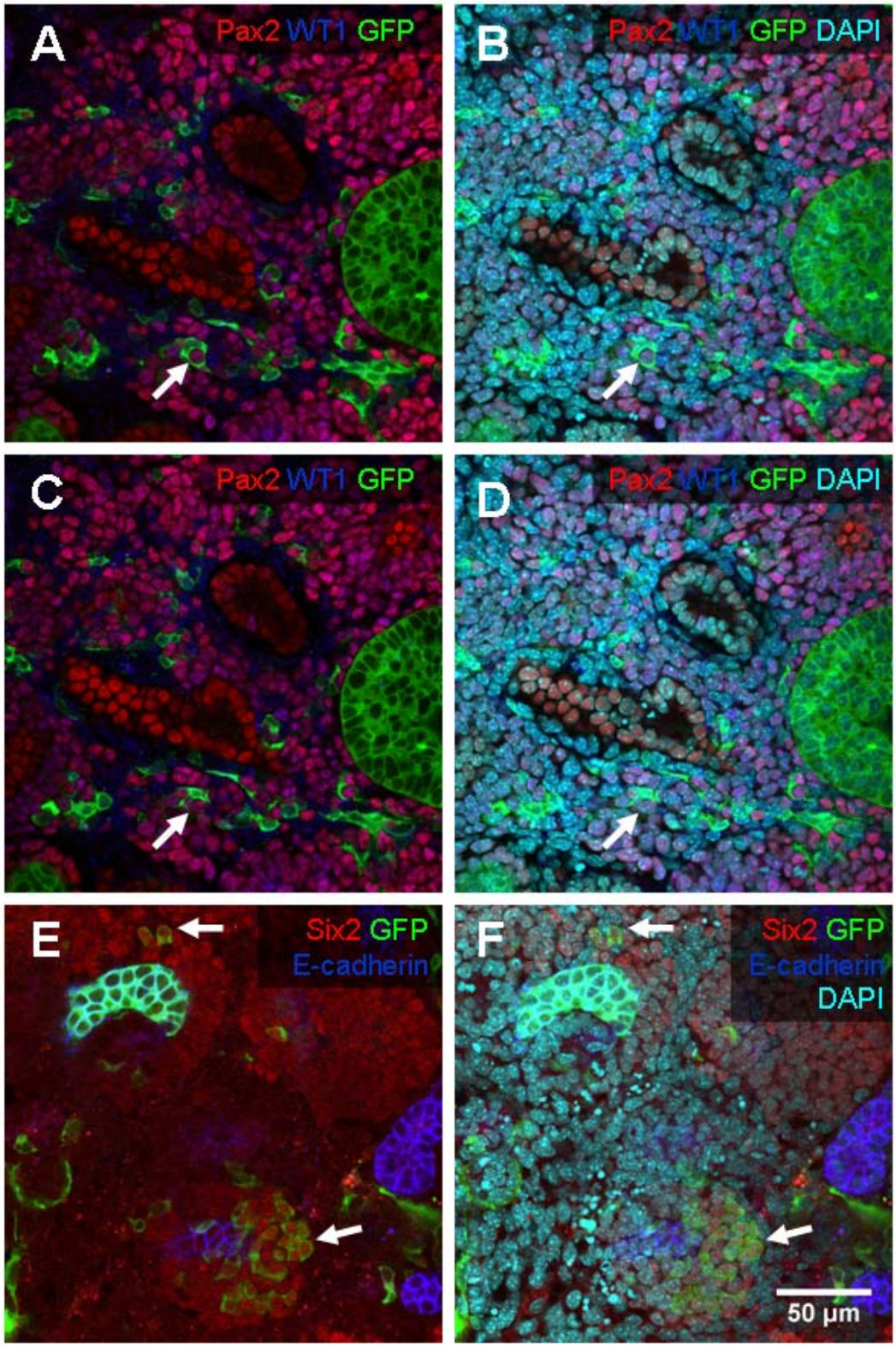

Figure 6.2.12 – Six2 expression of E9.5 tauGFP cells after a 6-day culture in reaggregated organotypic rudiments
A, B, C and D show two consecutive confocal sections of reaggregated pellets containing E9.5 cells, which have been stained for Pax2 (red) WT1(blue) and DAPI (in B and D, cyan); in A (and B), a white block arrow points at a cell, which seems to be tauGFP+ Pax2+ and WT1+; in C, the arrow points at the same cell at a distance of 2µm on the z-axis, which is now clearly negative for GFP;
E and F – show tauGFP+ Six+ positive cells in the condensing mesenchyme

6.3 Summary and Discussion

The aim of this chapter was to examine the ability of cells from early embryos to generate renal cells and structures *in vitro* and, by working backwards in development, identify when this ability stops with the decrease of the age of samples. This was done first to understand to what stage embryonic stem cells should be taken, in order for them to become competent to generate renal cells; and second, to contribute to the understanding of how and when the acquisition of renocompetence happens in development. To accomplish this, two independent experimental methods were used. The first method consisted of the disaggregation and reaggregation of E11.5 mouse kidney rudiments to provide a convenient way of mixing test cells into a reassembled growing rudiment capable of UB extension and branching, and nephron production. The populations of cells tested in that case were traced by genetic labelling with GFP (as previously described in this thesis). This approach tested cells' ability to integrate into the structure of UBs and nephrons and their ability to produce kidney cells, according to the criteria described in Chapter 4. The second independent method was ordinary organ culture. It examined the ability of whole pieces of tissue isolated from various embryo stages, to give rise to structures resembling the structures normally produced by an early stage of a developing kidney rudiment – nephrons and UB structures. Although with this method we could expect some structure formation, the resulting structures would not be expected to have the intricate morphology of renal epithelia found *in vivo* or produced in the organ culture system, due to the possible lack of many molecules necessary for their development.

Experiments with labelled cells showed that cells isolated from the caudal parts of E8.5 embryos were already able to give rise to renal tubular cells, although their number relative to control E11.5 experiments was extremely low. E8.5 was the earliest stage tested, which gave a conclusive result. The same result was obtained by organ culture experiments, which showed the formation of a very rudimentary Calbindin+ and Laminin-bound tubule, connected to another Laminin-bound tubule. It should be noted that although the presence of a tubular structure with a basement

membrane, expressing Calbindin strongly suggested that the structure observed was a UB or its precursor, the nephric duct, the same was not true for Laminin-bound Calbindin-negative structures with regard to being a nephron. With respect to the formation of UB-like structures, although the nephric duct cannot be considered equivalent to the UB due to its different temporal developmental origin and lack of branches, it has been shown competent to produce ureteric buds *in vitro* in the right conditions (Sainio et al., 1997). Therefore, for the purposes of this chapter, no attempt was made to examine whether these structures were Calbindin+ Laminin+ ureteric bud fragments or nephric duct fragments. On the other hand, unlike UB-like structures, nephrons were identified by the expression of one rather than two markers (Laminin), general morphology and morphology with respect to neighbouring Calbindin+ structures. Although in the kidney that provides sufficient evidence for recognising a nephron, the same is not true in the developing embryo, where other Laminin-bound ducts exist. Although of a number of molecular markers available Calbindin was the best marker for UB cells, as it is the only one present only in this renal compartment, it has also shown some limitations for distinguishing between UB structures and nephrons. Observations made in Chapter 1 identified that some UB cells downregulate Calbindin expression after CellTracker treatment due to an unknown reason. Also, experiments with disaggregated mesonephroi showed that Calbindin expression in some nephric duct fragments can be downregulated after reaggregation, while other markers were expressed as appropriate (Supplementary Figure 5). Therefore, it could not be excluded that the Calbindin- Laminin+ structures detected in ordinary cultures might not be nephrons, but possibly UB fragments, which have downregulated Calbindin. Another factor that could have an impact on the interpretation of reaggregates with labelled E8.5 cells is the potential presence of fusion events. Experiments with transplanted bone marrow-derived cells have shown that fusion of host and grafted cells is possible and could occur in various experimental conditions (reviewed by Alison et al., 2004). For example, grafted bone marrow cells were seen fused with host hepatocytes (Vassilopoulos et al., 2003; Wang et al., 2003), cardiomyocytes (Alvarez-Dolado et al., 2003) and Purkinje neurons (Weimann et al., 2003; Alvarez-Dolado et al., 2003). Although, cell fusion could potentially be present in any of the cell mixing experiments, it should be

noted that the possibility of such events occurring in organotypic cultures containing E8.5 cell mixes could have a more significant impact on results due to the low numbers of integrating cells. For example, if some cell fusion occurred in the reaggregates, such events would comprise a low percentage of integrating E11.5 or E10.5 cells (as almost all of these integrate), but could be responsible for a significant proportion (up to a 100%) of integrating E8.5 cells. Although no evidence for cell fusion and formation of heterokaryons was seen on the basis of fluorescence microscopy, no experiments were particularly performed to examine this possibility in detail in the reaggregation system. Furthermore, the integration of test cells in renal epithelia was carefully examined by confocal microscopy in three dimensions and the morphology of integrated cells was taken into account. Such an approach makes it less likely to leave fused cells unnoticed.

Tissues from E7.5 embryos were also mixed in the reaggregation system. Unfortunately, the analysis of these could not be completed, due to an abnormal development of the nephrons and UB structures. The reason for these abnormalities was most probably signals released from the early embryo cells. This comes from the fact that in early embryo development, a lot of signalling pathways are active to steer embryogenesis and that it is very likely that some of these could interfere with nephron and UB structure formation. For example, Wnts, FGF and retinoic acid and their production in the correct regions are essential for the correct patterning of the early embryo (Villanueva et al., 2002). Although tissue culture experiments suggested that renal primordia can be formed even at that very early developmental stage, due to the reasons described in the previous paragraph, with the screening tools available both independent methods used were inconclusive for this embryonic stage.

On the basis of this data, E8.5 of mouse embryonic development was concluded to be the earliest stage that contained renocompetent cells. At the same time, in the light of the experiments performed with E7.5 embryos, it could not be excluded that even earlier cells could also posses this ability. A conclusive assessment of this and earlier stages will require the development of a different assay for analysis, due to the

adverse influence of very early embryo cells on reaggregated embryonic kidney cultures and the limitations for analysis of ordinary tissue culture.

It has previously been mentioned that there is a lot of disagreement in the literature about the timing of intermediate mesoderm specification (Figures 6.1.3). This made it difficult to identify whether at E8.5 the intermediate mesoderm is already specified or whether the prospective intermediate mesodermal cells have not progressed to that stage, yet. This would mean that at E8.5, the earliest lineage that will give rise to the kidney has reached the stage of being mesoderm or intermediate mesoderm. According to Kaufman (2001) the intermediate mesoderm gets specified around E9.0 of mouse embryonic development. This would suggest that at E8.5, mesodermal cells have not yet become allocated to being intermediate mesoderm. On the other hand, So and Daniellian (1999) have seen Osr1 transcripts at E8.5 (and possibly earlier) suggesting that the intermediate mesoderm might have already been specified. The information in the literature therefore does not allow making a conclusive statement about what developmental stage the cells that will give rise to kidney have reached at E8.5. Experiments will have to be performed to characterise the timing of intermediate mesoderm formation before this can be resolved. In such studies embryos ranging from having 5 to 25 somite pairs could be studied for the formation of intermediate mesoderm. This could be first examined by bright-field microscopy to detect when a distinct region of cells is specified between the lateral and paraxial mesoderm. Furthermore, the onset of expression of a number of genes in the prospective intermediate mesoderm could be studied and linked to the number of somites present at the respective stages. Genes helpful to clarify this process could be Osr1, Lim1, Pax2, Pax8, all of which have been found important for the specification of the nephrogenic field (Chapter 1). Also, it should be taken into account that the timing of intermediate mesoderm specification most likely differs between the anterior and posterior parts of the embryo. Using this information to construct a temporal map of intermediate mesoderm specification along the antero-posterior axis would greatly help for future studies of the renogenic potential of early embryo cells. With regard to defining the stage at which cells acquire renocompetence in early embryo development in particular, it was safer to accept that the intermediate

mesoderm is already specified at E8.5. The results presented in this chapter therefore suggest that the cells of the intermediate mesoderm already possess the competence to give rise to renal cells in the conditions tested. Furthermore, this is also supported by studies with cells from the presumptive metanephrogenic regions of E9.5 embryos, which were also able to integrate into renal epithelia. At this stage no metanephric blastema is yet formed. For E9.5 cells, marker expression studies have revealed that integrating cells are also able to express the markers normally seen during normal kidney development. Markers were expressed as appropriate for all renal compartments. Calbindin and E-cadherin - expressing cells were found in ureteric buds, Megalin and E-cadherin (low) - positive cells were found in nephrons, WT1 (high) cells were seen in glomeruli, and Pax2 or WT1 (low)-positive cells were seen in the condensing mesenchyme. These results strongly suggest that the full nephrogenic capacity of cells is acquired earlier in embryo development than previously thought. Although no metanephric blastema is seen at E9.5, it seems like the cells in the intermediate mesoderm at this stage, which are directly adjacent to the WD at the nephrogenic ridge are already capable of producing the kidney lineages detectable in the corresponding stages of normal kidney development. Still, it should be taken into account that the age of acquisition of full renogenic capacity might be underestimated in these studies, due to the variation in the development of the embryos used in the study.

Further experiments described in this chapter have already reported that mesonephric cells were also able to integrate into the renal structures produced in reaggregated metanephric organotypic cultures. These experiments were performed to understand whether it was possible for integrating cells to come from the transient kidneys present in development and this possibility was confirmed. This being said, I would also like to discuss this possibility with respect to the tissues that have been isolated for mixing in the reaggregation system (summarised in Figure 6.2.1). As implied by the schematic, for the stages E11.5 and E10.5, only metanephrogenic tissues were mixed – either E11.5 metanephric kidney rudiments or E10.5 metanephric anlagen with the neighbouring WD). E9.5 is more unclear, although, as indicated the tissues explanted for disaggregation and reaggregation were situated much more posteriorly

than the presumptive zone of mesonephric formation (this can be compared to images of Pax2 and Pax8 staining in the mesonephros of 19-somite stage embryos equivalent to E9.0 (Supplementary Figure 6, from Bouchard et al., 2002). The E9.5 explants were also likely to contain parts of the paraxial mesoderm and surface ectoderm. The literature suggests that the pro- and mesonephrogenic anlagen at E8.5 were also rostral to the isolated tissue and should not have been included in the organotypic reaggregates (Bouchard et al., 2002). Although, more precise methods might be needed to study the development of the three embryonic kidneys with respect to particular markers, the current information hereby presented implies that a contribution from the pro/mesonephros in reaggregates containing E9.5 tissues is unlikely. This could be resolved experimentally by checking whether integrating cells are positive for markers expressed only in the mesonephros, but not in the metanephros, or whether they are negative for markers, which are present only in the metanephros, but not in the mesonephros. Suitable genes could be the Hox11 paralogs, for example, which have been reported to be present only in the metanephros, but not mesonephros (Mugford et al., 2008).

Also, the quantification of the ability of cells from different embryonic stages to integrate in UBs and nephrons also provided interesting observations. First of all, it should be noted that this method of quantification does not correct for the different proportions of UB versus nephrogenic cells that might be present at various stages of development. For example, the number of cells capable of producing nephrons and UBs could be equal at E11.5, but twice as many MM cells could be present at E10.5 when the UB is just starting to form. The change of the proportions of integrating cells with the stepwise decrease in age of embryonic tissues used has been shown in Figure 6.2.7.We can observe that the stepwise decrease of the age of embryonic tissues is accompanied by a steady and significant for all stages decrease in integrating UB cells (as compared to the previous stage). Interestingly, the onset of the capacity of embryonic cells to produce UB structures determined by these experiments (E8.5) coincided with the reported stage of formation of the Wolffian duct (Figure 6.1.3). These observations differed from the ones made for nephrons. The drop in the relative number of cells integrating in nephrons per unit area between

E11.5 and E10.5 was not significant indicating that metanephric mesenchymal cells had the same renogenic capacity at both stages. This is consistent with previous reports that once formed at around E10.5 the metanephric blastema possesses a full nephrogenic capacity (Sariola et al., 2003). On the contrary, a significant drop in renogenic capacity was observed from E10.5 to E9.5, which is consistent with the previously reported times of induction of MM cells (Figure 6.2.3). Still, the experiments described in this chapter have presented evidence that early embryo cells still possess renogenic capacity, which diminishes with the stepwise decrease of the age of embryos used for the studies. As discussed in detail in the introduction section of the chapter, presented this way, the data reflects the chronology of experiments, which is a backward to normal development. This means that when regarded forward to reflect normal development, the renogenic potential of early embryo cells starts with the intermediate mesoderm and increases with the progression of embryo development. However, when examining quantitative data, it should be taken into account that there is one limitation to using them to evaluate the proportion of cells in the isolated tissues, which are able to contribute to renal epithelia. As previously demonstrated, quantification works accurately when it is known that near a 100% of the cells used in the experiment have the ability to contribute to renal epithelia. This is the case when E11.5 embryonic kidney rudiments are used. The situation is similar for tissues isolated from E10.5 embryos are used. Let's say that these experiments measure the probability of one cell to become a kidney cell. When all cells are committed, the probability of them becoming kidney cells is 1. At earlier stages, however, due to the limitations of the dissections, there are cells present in the tissue isolate, which are not capable of producing kidney cells, for example, as they are endodermal or ectodermal derivatives (Figure 6.3.1). In these cases, quantification studies are not directly comparable to E11.5 and E10.5 as the measurement also includes the bias of these cells that do not have the ability to become renal (Figure 6.3.1, B). For example, if three cells are isolated from an E9.5 embryo, let's say that 1 of the cell has a renogenic ability, and 2 cells belong to endoderm and ectoderm and have other fates.

The ideal measurement would be to check whether the 1 cell can form kidney cells without any further instruction when placed in the reaggregation system and exclude from the measurement the two cells that cannot (Figure 6.3.1, C). As currently designed, the quantification measures the ability of all three cells to produce kidney cells, which introduces a bias, as the two cells are not fated to produce renal cells (as illustrated by Figure 6.3.1, B). This bias could be corrected for by experiments, which would determine the frequency of cells used for each experiment that are of the correct lineage. For example, a correcting coefficient could be obtained by isolating the regions used for mixing experiments, staining them for an intermediate mesodermal marker, such as Osr1, and quantifying what percentage of cells from the whole population are Osr1-positive. A similar approach would be to use a transgenic mouse, which has a reporter gene inserted under the regulation of the Osr1 promoter and sorting the cells dissected from regions of interest at each step, which would them allow their direct mixing in the disaggregation-reaggregation system.

On a more general level, it would be interesting to explore whether cells of the posterior intermediate mesoderm present at E9.5 are already committed to generating only kidney cells or whether they have the ability to produce other cell lineages, as well. This would be a second step, which would help us understand the timing and the segregation of different tissue types, and help identify the molecules, which might be involved in the lineage choice of a renal fate.

It is also important to discuss the impact of the results presented in this chapter with regard to ES cell biology as the second aspect of this study was to investigate the acquisition of renogenic capacity of differentiating embryonic stem cells. I have determined that in development, cells resident in the intermediate mesoderm of E9.5 embryos are capable of independently giving rise to kidney cells when placed in the reaggregation system. As currently presented, these data suggest that it should be sufficient to induce ESCs to intermediate mesodermal cells to make them capable of producing renal cells (Figure 6.3.2). A way of testing this would be to generate ESC reporter cell lines for intermediate mesodermal markers. These cells can then be differentiated by various methods, sorted for the intermediate mesodermal marker

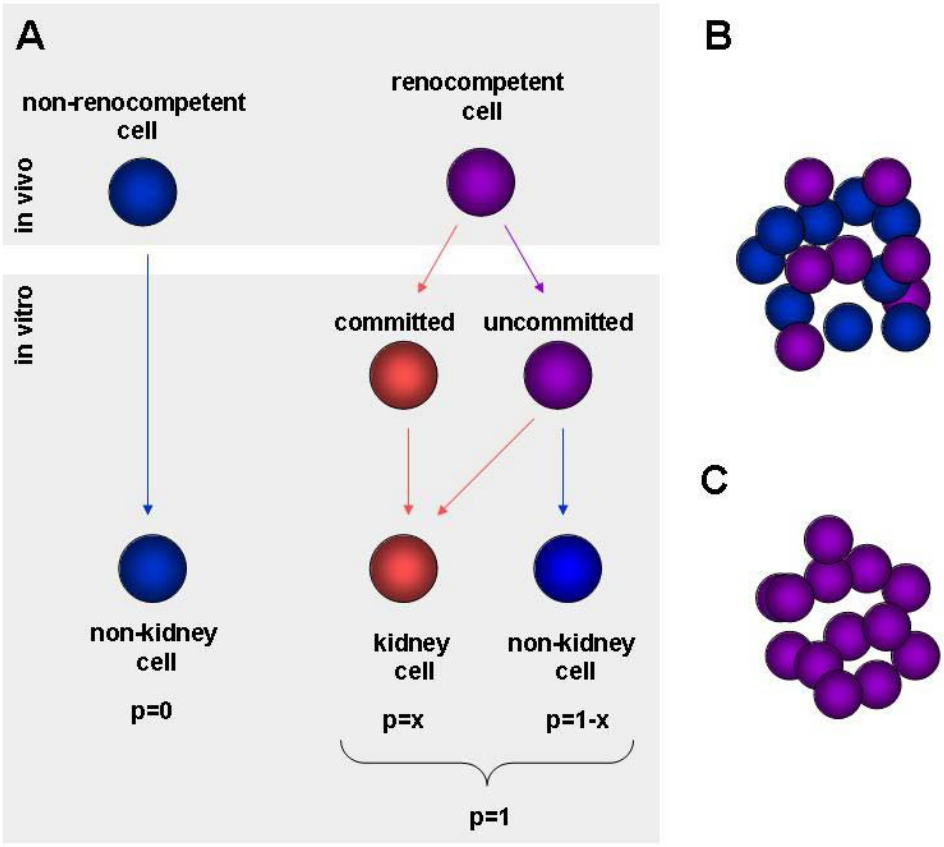

Figure 6.3.1 -The presence of cells allocated to non-kidney lineages creates a bias in quantitative assessment
Tissues isolated from embryos are a mixture of cells, which (1) are destined for non-kidney fates in the embryo and (2) will become kidney cells with the progression of embryonic development (A, B). To determine whether cells from the correct lineage (e.g, intermediate mesoderm) can generate kidney cells independently *in vitro*, the ideal measurement would exclude cells, which have other fates (e.g. ectoderm), as shown in C. In the experiments performed, however, the limitation of the dissection creates a bias by including a mixed population of cells, as shown in B.
p - probability of generating a kidney cell

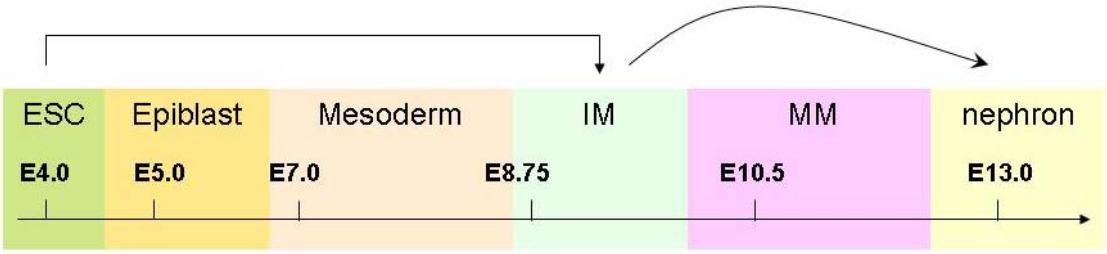

Figure 6.3.2 - Differentiation of ESC to intermediate mesoderm should be sufficient for induction of a renal program in the reaggregation system
Experiments with early embryos have suggested that cells from the intermediate mesoderm are able to produce kidney cells when integrated in the kidney rudiment disaggregation-reaggregation system. This suggests that the differentiation of ESC to the correct type of intermediate mesoderm is sufficient for their acquisition of renocompetence in the environment of a developing kidney rudiment.

and mixed in the disaggregation-reaggregation system to check whether they integrate in renal tubules and express kidney markers after integration. Although, this seems as a straightforward experimental plan, many issues would have to be resolved before such experiments can be undertaken. First, this strategy does not resolve the lack of an efficient method for cell differentiation to intermediate mesoderm. Second, the selection of marker for generation of the transgenic ESC line would be a key step of the experimental planning. Similarly to the lack of a single marker for renal cells, there is no single marker for intermediate mesodermal cells. Foxc1 and Foxc2, for example are expressed in the prospective intermediate mesoderm, but also in the prospective paraxial mesoderm, which gives rise to the somites (Wilm et al., 2004; Sasaki and Hogan, 1993). If cells are sorted for Foxc1/Foxc2 expression in ESC differentiation experiments, this would not necessarily mean that intermediate mesodermal cells are obtained. If only paraxial, rather than intermediate mesodermal Foxc1+ or Foxc2+ cells are obtained, no integration will be observed in the reaggregation system. However, this will not be due to an inability of IM cells to generate renal cells, but to the absence of renogenic cells in the isolate in the first place. Other markers expressed in the mesoderm, pose similar problems. Other candidates that could be considered are Osr1, Lim1, Lhx1, Pax2 and Pax8 (James et al., 2006; Fujii et al., 1994; Cirio et al., 2011; Bouchard et al., 2002). To solve this, a combination of two markers could be used and cells sorted two times. This, however, poses another challenge for further marker expression studies, as the number of channels that can be imaged simultaneously is limited, so this will also have to be taken into account. Furthermore, the IM might contain different cell populations, all of which express the selected markers, but segregate on the basis of the expression of other, also possibly unknown markers. This could potentially also create a bias in the results.

Cell mixing experiments performed in this chapter identified that cells from the intermediate mesoderm have already acquired competence and are able to produce the main types of kidney cells, as shown by marker expression studies. This finding also suggests that ESCs would have to become intermediate mesoderm first, in order to become renocompetent. In addition to experiments with intermediate mesoderm,

in future studies, obtaining results for the renogenic capacity of E7.5 would be important in assessing whether the mesoderm shortly after gastrulation would also be able to integrate into developing renal structures.

Chapter 7

Discussion

7. Discussion

In previous chapters, the acquisition of renocompetence was addressed from several different angles. First, a quantitative system for assessing the renogenic potential of cells on the basis of a combination of marker expression and the functional ability of cells to integrate into renal tubules was devised. Second, it was determined that the microenvironment of a developing kidney rudiment is not sufficient for priming ESCs to become kidney cells. Third, it was determined that although inhibition of Notch signalling seems to increase the proportion of mesodermal at the expense of ectodermal cells in ESC differentiation culture, it was not a good approach for generating ESC-derived renal cells *in vitro* in the conditions tested. Finally, experiments with early embryo cells provided evidence that cells found in the intermediate mesoderm (and possibly even in the mesoderm before intermediate mesoderm formation) are already able to give rise to kidney cells *in vitro*, when explanted from the developing embryo. These results have been summarised and discussed in chapter discussions. The purpose of this last chapter is therefore not to repeat previous material, but rather to build on these results and comments to assess their impact on future directions for embryonic stem cell differentiation to renal cells, kidney development and regenerative medicine and also to assess the limitations of this thesis. The chapter will be concluded by a final short summary of the results obtained during this work.

7.1 Derivation of renal cells from ES cells *in vitro*

7.1.1 Kidney cells and artefacts

This thesis made use of two very different approaches to studying the acquisition of renocompetence. The first approach was to use embryonic stem cells and differentiate them to a renal lineage in vitro. When done successfully, this would allow further studies of what processes and changes take place in cells to instruct pluripotent cells to become renal in the cell culture dish. It would also allow for an extremely convenient tool to model disease or to modify particular properties of these cells and investigate the outcomes of these modifications. For these purposes two approaches have been tested for their ability to produce renal cells entirely *in*

vitro - undifferentiated ESCs or ESCs treated with a Notch inhibitor have been placed in the environment of a developing kidney to test whether they will give rise to kidney cells in these conditions. Steenhard et al. (2005) had already suggested that exposing ESCs to the environment of a developing kidney was sufficient to produce renal cells outside the embryo. It was then surprising to find that although undifferentiated cells placed in disaggregated and then reaggregated E11.5 embryonic kidney cells formed chimeric structures with renal epithelia, they did not express markers normally present in renal epithelia. Interestingly, the formation of embryoid bodies and treatment with Notch inhibitor, which has been reported to favour the formation of mesoderm from ESCs (Nemir er al., 2005; Lowell et al., 2006) did not improve the outcome. As a matter of fact far fewer "test" cells seemed to persist in the reaggregates after culture and almost no cells even forming contacts with renal epithelia were seen. This was also surprising as other sources in the literature suggested that EB formation, even without treatment, induces a spontaneous program of ESC differentiation to renal cells. At the same time, several very important observations were made, which suggested that unusual artefacts might be observed when labelled cells are placed in the environment of a developing kidney rudiment. First, marker expression studies presented in Chapter 4 showed that cells appearing positive for certain renal markers are actually intercalating host kidney cells, which appear to be positive for the tracer, but are not when looked at in three dimensions. A number of staining artefacts, which generate staining in the wrong cellular compartment or generate staining in all fluorescence channels have also been detected. Second, experiments with CellTracker - stained amniotic fluid stem cells (AFSCs) have suggested that labelling reagents might be transferred between cells and being accumulated in nephrons (Supplementary Figure 4). These experiments were based on mixing human CellTracker Green - stained AFSCs with E11.5 embryonic kidney cells. This resulted in green nephrons being detected by confocal microscopy suggesting that AFSCs were able to generate nephrons in the reaggregation system. As an independent confirmation of these results, an old method was used, which allowed to distinguish between mouse and human cells on the basis of nuclear morphology (Moser et al., 1975). Moser et al. (1975) have shown that when stained with DNA-binding compounds mouse nuclei are small, bright and

have chromocentres (dots of high fluorescence intensity), while human ones are large, faint and lack chromocentres. These results have been experimentally confirmed by mixing human ESCs with mouse E11.5 kidney cells (Supplementary Figure 4). Comparisons of images of CellTracker - labelled AFSCs and GFP-labelled hESCs suggested that the green cells seen in AFSC experiments might not be human. But also, we should ask how it is possible for considerable levels of a label to artefactually accumulate in a nephron, in the first place. We could imagine that cells taken away from the environment their favour (for example the cell culture dish) and placed in an adverse for them environment (potentially an embryonic kidney) might die. This will release labelled cell fragments or the soluble, activated (cleaved by intracellular enzymes) CellTracker label in the interstitium. But at the same time, we know that even early nephrons possess some filtrational capabilities as illustrated by their expression of the endocytotic receptor megalin, for example (reviewed by Fisher and Howie, 2006). It is then possible that they filter the low concentrations of released by dead cells dye and progressively accumulate it into their cells. If these results are independently confirmed by other methods, this would suggest that introducing labelled cells into developing kidney rudiments might pose a problem more serious than previously thought.

7.1.2 ESCs – loss of differentiation potential?

But also, the limitations of the experiments presented in this thesis should also be noted. First, for the detailed marker expression studies of undifferentiated ESCs mixed in the reaggregation system only one ESC line was used due to the unavailability of an independent genetically labelled cell line. Performing characterisation of possible karyotypic abnormalities could have revealed genetic changes, which could have interfered with the ability of these cells to generate renal cells. There is a phenomenon, in which pluripotent cells lose their ability to differentiate, but retain their ability to self-renew indefinitely. A very radical example of cells, which have lost their ability to differentiate is the nullipotent embryonal carcinoma cell line 2102Ep (Duran et al., 2001)

7.1.3 Do alternative differentiation programs exist?

It will also be interesting to re-examine the results obtained from mixing undifferentiated ESCs in the reaggregation system from a different perspective. Confocal microscopy has revealed that ESC-derived structures express E-cadherin, but not Pax2, Wt1 and Calbindin. At the same time, the cells formed tubular-like structures, some of which appeared to have a lumen. It would therefore be interesting to ask whether these tubules could be functional renal epithelia even though they didn't express markers normally present in kidney development. Analysis of the expression of proteins, which are markers of later stages of nephron formation might be a suitable way for addressing this. No markers of more mature renal tubules, such as Aquaporin2, KSP-Cadherin and Tamm-Horsfall protein (Takata et al., 2008; Shao et al., 2002; Sikri et al., 1981) have been addressed in this thesis, as their expression hasn't yet been characterised in particularly reaggregated kidney rudiments. I would suggest that this latter option is not likely, as the tubular-like structures produced by ESCs in reaggregates had a rather disorganised appearance and looked phenotypically different in size and shape from host embryonic kidney cells. A more likely option, however, is that ESCs might need more time in the organotypic culture. If ESCs are considered as developmentally equivalent to ICM cells, then the gap between the ICM and the metanephric mesenchyme is more than 5 days of development. To address this problem, reaggregated from embryonic kidney cells pellets containing undifferentiated ESCs could be transplanted under the kidney capsule of adult mice to allow for a long-term culture and re-evaluation of the results with this improved approach. This is not possible *in* vitro culture, as observations have shown that rudiments start to degenerate after 10 days in culture. Also, undifferentiated cells could have been prevented from differentiating in reaggregated pellets by signals secreted by embryonic kidney cells. Evidence was presented in Chapter 4 that expression of Oct4 in at least some ES or ESC-derived cells persists for at least 6 days of culture. Barasch et al. (1999) have reported that LIF is a key regulator of MET in the developing rat kidney. Although the mechanism seems to be different in the mouse (reviewed by Sariola, 2002) the possibility that embryonic kidney cells produce LIF could explain why tauGFP ESCs persisted after mixing with embryonic kidney cells in the reaggregation system. This comes from the fact

that LIF/LIFR/gp130 are major players in embryonic stem cell self-renewal (Niwa et al., 1998).

7.1.4 Cell differentiation is not a stochastic process

ES cell differentiation experiments performed in this thesis allowed making observations about the mechanisms by which these cells generate derivatives of one of the germ layers. It could be hypothesised that there were an equal probability for a cell to become mesoderm, endoderm or ectoderm (p= 1/3). Let's say that once committed to mesoderm, cells can become chordamesoderm, paraxial mesoderm, lateral plate mesoderm or intermediate mesoderm, which has a probability of 1/4, whilst the intermediate mesoderm can give rise to kidneys and gonads (p=1/2). In that case, the overall probability of an ES cell becoming a kidney cell would be:

1/3 x 1/4 x 1/2 = 1/24.

Therefore, if differentiation happened stochastically, $1/24^{th}$ of all ESCs used in experiments should have generated kidney cells. Both of the ESC differentiation strategies tested, mixing untreated ESCs with embryonic kidney cells in reaggregates and pre-treatment of ESCs with γ-secretase inhibitor, did not generate any cells that could be identified as renal. This suggests that the production of kidney cells from ES cells is not a stochastic event. Rather, this implies that an active process (a series of controlled inductive events) is required for the generation of renal tissue. This also raises interesting questions about which tissues or types of cells can be a result of spontaneous differentiation and what are the barriers for all types of cells occurring spontaneously in ESC differentiation.

7.1.5 A very complex differentiation strategy might be necessary for the *in vitro* generation of renal cells

However, the simple explanation for the unsuccessful differentiation of ESCs both when mixed with kidney cells undifferentiated or after being cultured as embryoid bodies and treated with Notch inhibitor, is that they did not receive the signals to induce them acquire renocompetence *in vitro.* Although, no benefit was seen by the

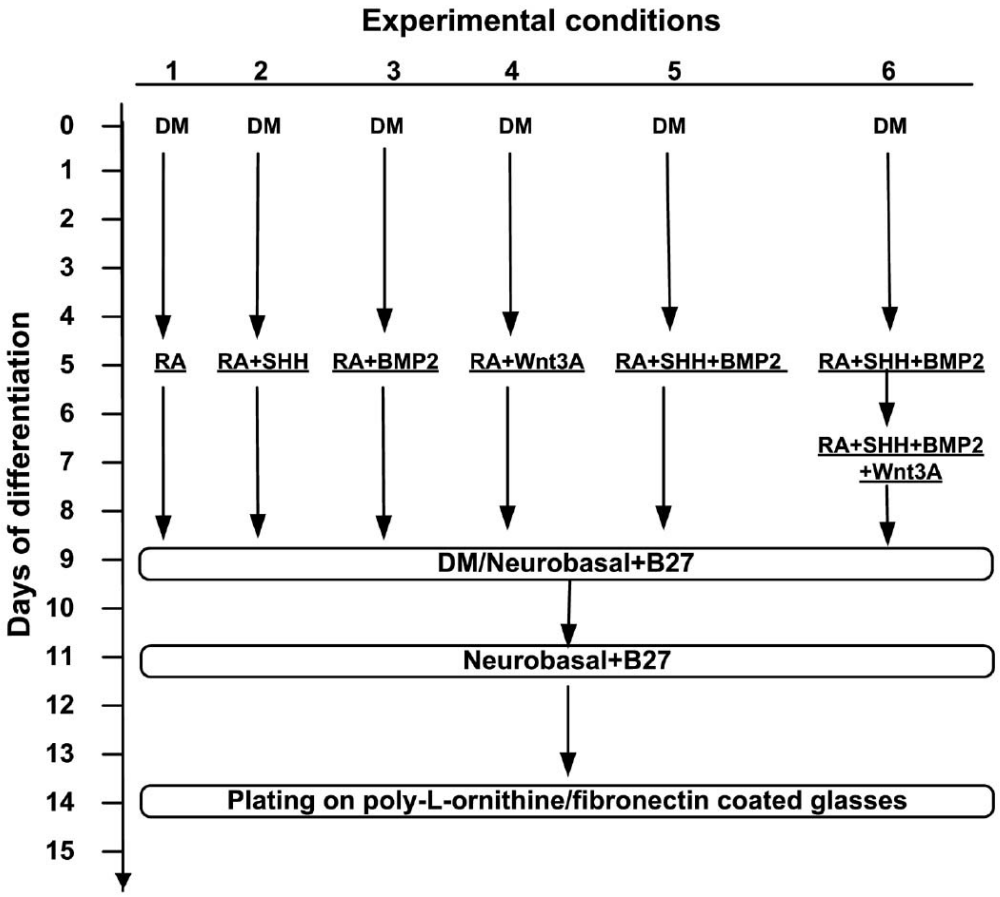

Figure 7.1 - A schematic of an efficient multi-step differentiation strategy for generating dorsal neurons from embryonic stem cells; Murashov et al. (2005)

treatment of differentiating cells with the γ-secretase inhibitor DAPT in the condition tested, modifications of this differentiation strategy could yield a significantly better result. Directed differentiation often requires much more complex multi-step protocols. There are a lot of factors, which can contribute to the differentiation of stem cells - the basal growth medium, the presence or absence of serum, the levels of oxygen, the combination of external signals provided in the medium, the concentration of these signals, the possibility for adhesion to a substrate, the type of substrate and the chronology of applying all these different manipulations. To illustrate the complexity of a successful ES cell differentiation processes, a schematic for the generation of dorsal interneurons has been shown in Figure 7.1 (from Murashov et al., 2005). Murashov et al. (2005) tested 6 different conditions each of which included the consecutive application of at least 4 different types of media. At the same time, this strategy was combined with formation of EBs, plating the formed

EBs, their disaggregation and replating on polyornithine – coated glass slides, all in a defined temporal sequence. For the differentiation of ES cells to kidney cells, protocols with a similar complexity may be required to either recapitulate the molecular signals present in *in vivo* embryonic development, or to find alternative combinations of molecules and treatments, which generate kidney cells efficiently.

It seems like the generation of renal cells is much more difficult than generating other cells types. One of the reasons for this might be the fact that from a developmental point of view, the kidney is a very late organ. In other words, kidney cells get specified much later in embryo development than other cell types. For example, the metanephros starts to form at about E10.5, when a metanephric blastema is visible and the ureteric bud is recognisable only as an enlargement of the Wolffian duct. At that point in embryonic development, most organs and systems have already formed or have started forming. For example, the following structures can be seen - forebrain, midbrain, hindbrain, spinal cord, notochord, lens vesicle, olfactory pits, primitive gut, maxillary and mandibular components of the first branchial arch, fore- and hindlimb buds, elongated tail, a primitive heart showing processes of septation, thyroid primordium with evidence of canalisation, lung buds and primitive liver (Kaufman, 2001). It is well known that embryonic stem cells easily generate certain cell types even by spontaneous differentiation - for example, cells of the nervous system and beating cardiomyocytes (Brüstle et al., 1997 and van Laake et al, 2007). This is also consistent with their developmental counterparts, the brain and heart, arising much earlier than the metanephros. Late organs such as the metanephros might need an intricate sequence of signals, which due to its complexity might be extremely difficult to identify and reproduce *in vitro*. Although not all processes taking part in the *in vivo* induction of intermediate mesoderm have been elucidated, evidence from the literature provides information indicative of such a complexity. For example, it has been reported that signals from the surface ectoderm are essential for nephric duct formation in the chick (Obara-Ishihara, 1999). The authors hypothesised that the surface ectoderm might secrete factors that directly support nephric duct progenitor differentiation or that it could be responsible for the regulation of factors expressed in the lateral or paraxial mesoderm, thus acting

indirectly in the induction process. Furthermore, Obara-Ishihara (1999) have identified that the surface ectoderm regulates Bmp4 mRNA expression levels in lateral mesoderm and reported that the delivery of BMP4 in the culture medium rescues the initiation of the nephric duct. As this was determined by monitoring Pax2 levels, it rather proves the importance of BMP4 for Pax2 induction, but does not exclude the possibility that other factors from the paraxial mesoderm might also be needed for the normal progression of early or later nephrogenesis. Similarly, Mauch et al. (2000) presented evidence that signals from the paraxial mesoderm are required for pronephros formation in the chick. All this evidence collectively demonstrated that neighbouring tissues exert a considerable influence on intermediate mesoderm for kidney specification. In addition, above, only the specification of intermediate mesoderm to renal components was discussed. It is very important to note that the specification of intermediate mesoderm itself is likely to require another set of signals. Not only is the expression of the right molecules needed, but it is needed at the right levels as embryo development is frequently patterned as a response to chemical gradients. James and Schultheiss (2005) conducted a very extensive study about the role of Bmp proteins on the specification of mesoderm after gastrulation in the chick. They discovered that when administered at early stages of development, Bmp2 was able to induce expression of intermediate mesodermal genes in regions, which normally get restricted to paraxial mesoderm. In *in vitro* experiments, they demonstrated that, surprisingly, low levels of Bmp were much more efficient in generating mesoderm than high levels, which emphasised on the importance of the concentration of signalling molecules. Also apart from positive regulation, inhibitory regulation is also necessary for specification of the intermediate mesoderm (Figure 7.2) and therefore likely to be needed for ESC differentiation. Foxc1 and Foxc2 have been reported to balance paraxial and intermediate mesodermal fate (Wilm et al, 2004). Mouse embryos lacking these genes exhibited expansion of the intermediate mesoderm into the paraxial domain. Similar results were obtained in chick embryos, where gain of function negatively regulated intermediate mesoderm formation, while Foxc1 and Foxc2 misexpression in the prospective intermediate mesoderm seemed to drive it to a more paraxial fate (Wilm et al, 2004).

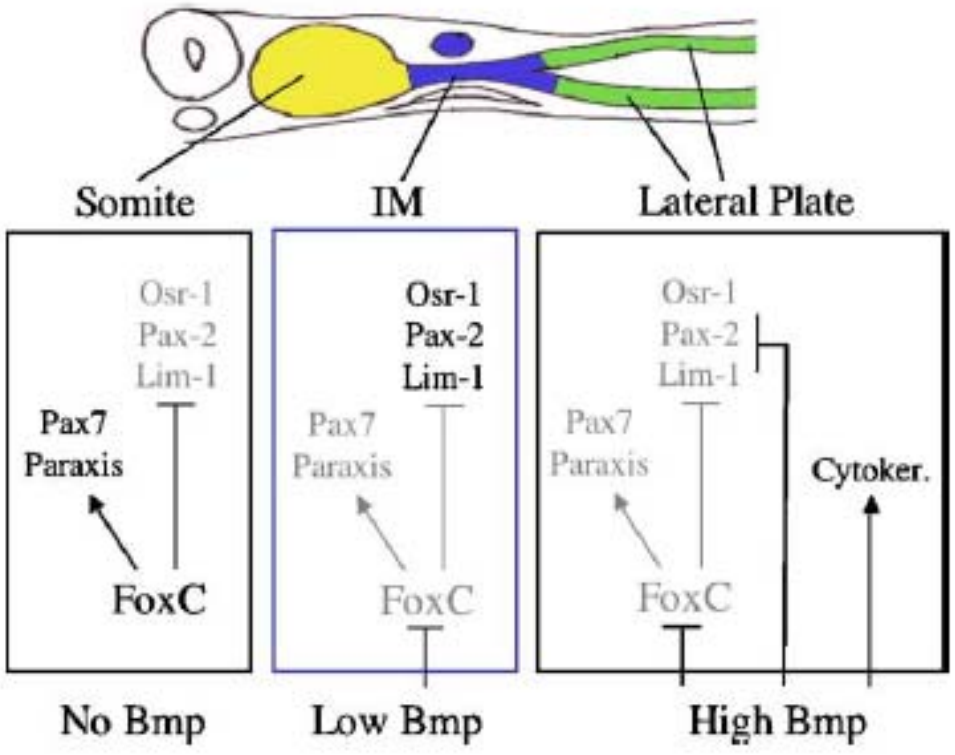

Figure 7.2 - Model of the regulation of mesodermal gene expression by Bmp signalling (from Wilm et al., 2004)
There is a low expression of Bmp signalling in the somites. Foxc1/2 and other paraxial transcription factors activate somite gene expression and and repress IM gene expression. Low levels of Bmp in the IM lead to a repression of somite genes, which “unlocks” the expression of IM genes.

These examples describe the complexity of the processes governing intermediate mesoderm specification, some of which are still poorly understood. On the basis of the data presented in this thesis and the information about intermediate mesoderm and renal tissue specification, two important factors for designing an efficient strategy for differentiation of ES cells to renal cells have been identified. First, the mechanisms that govern development (and intermediate mesoderm development, in particular) have to be very well understood - the interplay between gene networks clarified, the regulatory functions of more genes uncovered and the role and levels of signals for correct patterning established. In this number, gene expression profiling patterns for the different germ layers and their subdivisions would be extremely useful, as this would allow the monitoring of cell differentiation and specification at smaller, more accurate increments (rather than the stages that are currently accepted as preceding the renal lineage - mesoderm and intermediate mesoderm). The second

step in the successful design of a protocol for directed differentiation to renal cells would be an efficient approach to monitor the changes of gene expression and functional abilities of the produced cells at different stages of the differentiation process, where the incremental changes from the developmental studies suggested above could be recognised. Also, the processes happening in differentiating EBs or monolayers in general have to be mapped with respect to all germ layers and their derivatives in various strictly defined conditions, as this would give more information about the pathways that are active at different time points in differentiation and allow hypothesising about the regulatory interplay that takes place between them.

7.2 Contribution to embryo and kidney development

7.2.1 Defining kidney progenitor cells in early embryos

The "backwards" experiments performed as a part of this thesis have offered new insight on when renocompetence is acquired during embryo development. Similarly to ESCs, which produce kidney cells when injected into blastocysts but have more difficulty doing so *in vitro,* the fact that early embryo cells will eventually produce kidney cells in the embryo does not necessarily mean that they will be able to do so autonomously when explanted from the embryo. Studies in this thesis have shown that cells at the stage when the intermediate mesoderm is already specified are already able to become a part of renal tubules and express renal markers. The discovery that renocompetent cells are present in the intermediate mesoderm before the formation of a metanephric blastema raises many further interesting questions, the answers of which would lead to a much better understanding of how renocompetence is acquired. For example, a logical continuation of these experiments would be to use transgenic mice carrying reporters under the promoters of genes important for mesoderm and intermediate mesoderm formation. Such genes would be Brachyury, Eomes, Goosecoid, Osr1, Lim1, Lhx1 Pax2 and Pax8 (Wilkinson et al., 1990; Ciruna and Rossant, 1999; Blum et al., 1992; James et al., 2006; Fujii et al., 1994; Cirio et al., 2011; Bouchard et al., 2002). Nephrogenic regions could be dissected from E8.5 and E9.5 embryos, made into single-cell suspensions and sorted for marker expression. The sorted cells could then be mixed

in the reaggregation system to identify which populations of cells are renogenic. This approach has a significant advantage over using genetically modified ES cells for the same purposes. This is the fact that the definition of regions in embryo development helps explant only relevant regions and circumvent the problem of expression of these markers in other tissues. One example is Pax2, which is expressed in both the kidney and the brain (Dressler et al., 1990). Dissecting only the relevant region would allow examining only potentially renogenic, but not neurogenic Pax2+ cells.

Cell sorting for different markers would also allow using the reaggregation system quantitatively to compare the integration efficiencies of embryo-derived cell populations. Such experiments might help identify which the early progenitor cells in early embryos are and what combinations of markers they express. Furthermore, double reporter mice can help identify these progenitors even more accurately.

7.2.2 Are cells present in the mesoderm prior to intermediate mesoderm formation renocompetent?

Some aspects of studying kidney development include understanding how kidney primordia form. Experiments with E8.5 embryos in which the mesoderm is specified but no intermediate mesoderm is yet present have also raised interesting questions about embryo development. Although, experiments with these embryos were inconclusive they also did not reject the possibility that E8.5 cells may also be competent to give rise to kidney cells in the reaggregation system. If future experiments manage to resolve this, a lot of insight could be gained about the allocation of prospective renal cells in gastrulating embryos. Different regions of mesoderm could be dissected from gastrulas or sorted cells used to test different populations in the reaggregation system. This would allow mapping the location of the renogenic progenitors normally present in embryo development. It would also allow examining embryos at different stages of gastrulation to investigate whether renogenic cells might arise with the formation of posterior mesoderm only, or whether anterior mesoderm can also generate kidney cells. The possibility for cells from the mesoderm to give rise to metanephric cells would provide interesting insight about the acquisition of renocompetence in early embryo development. The

metanephros comes from the posterior mesoderm and intermediate mesoderm. If anterior mesodermal cells had the ability to give rise to metanephric cells, this could suggest that many mesodermal cells might have a renogenic ability at different points in time. This would raise the question of whether all or most mesodermal cells could be renogenic when provided with the right signals. For example, renogenic competence could be acquired and then lost in a wave from the anterior to the posterior until the correct signals become available to "stabilise" the persistence of these cells. The segmentation clock responsible for somite formation, for example, acts in an anterior-to-posterior manner, where anterior somites are formed first, followed by the formation of posterior somites with the progression of development (reviewed by Pourquie, 2003). Renocompetent cells could be specified in a similar antero-posterior fashion. Anterior cells might be competent to respond to the signals that would lead them to a renal fate, but might not receive the right nephrogenic signals, which could cause them to lose this renogenic potential. At the same time more caudal cells could acquire such a competence with the progression of development. Only more caudal signals (in the right combination and concentration) could then be able to induce the formation of the metanephros. Since the metanephros is formed on the same caudal plane as the hind limb buds, it might be interesting to investigate whether the signals responsible for hind limb bud development also instruct the formation of the metanephros. For example, FGF10 specifies the area of limb formation and at the same time has a role in the early stages of kidney development (Ohuchi et al., 1997; Michos et al., 2010). Also, if the anterior intermediate mesoderm indeed contains renocompetent cells, it would be interesting to investigate whether these cells are related to the formation of the pronephros and mesonephros. This hypothesis could be tested by checking whether anterior renocompetent cells, destined to give rise to the pro- or mesonephros would be able to generate metanephric cells when transplanted to the metanephrogenic signals of embryos. The reverse experiment of transplanting early metanephric primordia to regions, which normally give rise to the pro- or mesonephros could provide still more insight on whether potential anterior and posterior renogenic cells actually have the same properties.

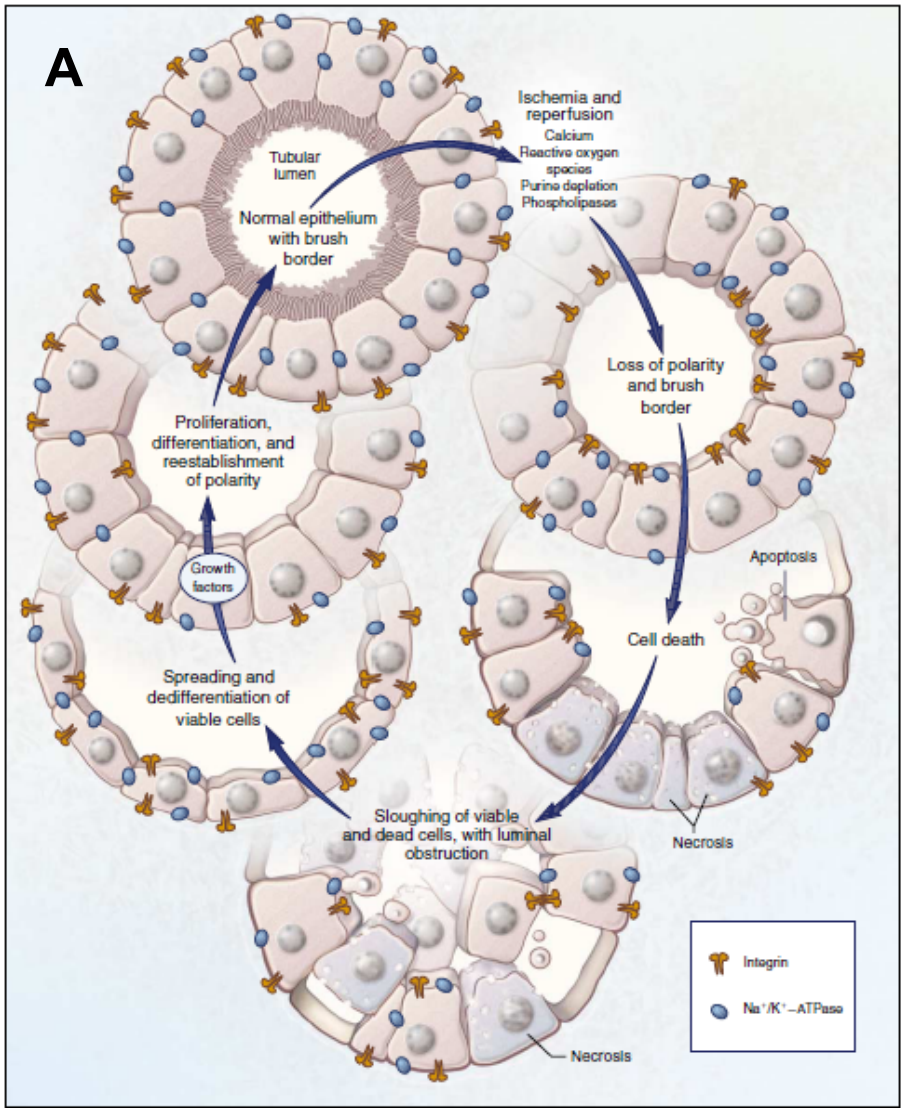

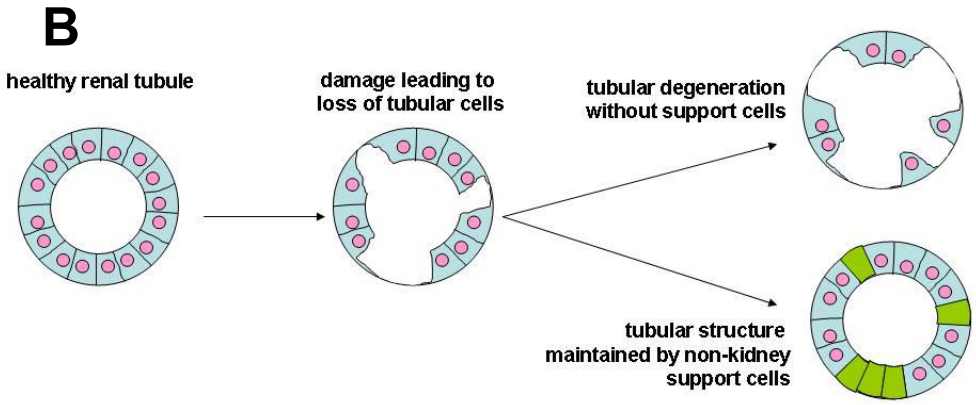

Figure 7.3 - Renal injury and prevention of progressive damage by structural support
A - morphologic changes of proximal tubules after ischemia/reperfusion; loss of brush order, loss of polarity and redistribution of integrins and Na^+/K^+-ATPase; from Thadhani et al. (1996)
B – tubular damage leads to a loss of tubular cells; exogenous cells (green) might provide structural support to renal epithelia preventing further damage; progressive degeneration is likely when nothing is administered

7.3 Potential applications in regenerative medicine

As covered more extensively in section 1.7 of Chapter 1, ESC-derived renal cells could be useful for many translational applications. A few examples are: using *in vitro* generated kidney cells to assess drug efficacy and renotoxicity; seeding ESC-derived cells in medical devices to recapitulate the physiological function of kidneys more closely; or directly transplanting *in vitro* generated renal cells into patients to replace damaged or lost cells. Even though the experiments presented in this thesis could not show any usefulness of ES cells for any of these, they were important for identifying a novel approach to cell replacement therapies. The potential use of ESC-derived cells directly in regenerative medicine could be to inject them in damaged kidneys to replace the cells that have been lost. This addresses the problem that when tubular cells are damaged they can no longer contribute to filtration until replaced by new cells to carry out this function. At the same time, there is another factor that leads to renal failure. Once tubular cells are damaged and start to be shed off, they leave gaps in the renal tubules, which if serious enough lead to the collapse of the whole nephron (Figure 7.3, Thadhani et al., 1996). The use of non-kidney cells could be, to fill in the gaps in damaged nephrons to offer structural support and protect renal tubules from further damage. So rather then restorative effect, this approach would offer renoprotection. In Chapter 4, I have demonstrated that Oct4+ cells and other non-kidney cells are able to form chimeric structures with renal epithelia. This provides the first proof-of principle that non-kidney cells could potentially be used as a “glue” to “patch up” damaged nephronal areas. Of course, a lot of experimental work is outstanding to accumulate further proof that this approach might be useful. First of all, in the experiments presented in this thesis, ES cells have been used to show that non-renal cells can form chimeric structures with renal epithelia. This still does not resolve the issue of safety of ESCs for regenerative therapies, as undifferentiated cells in cell transplants could lead to tumour formation. As previously discussed adhesion molecules are likely to be responsible for the formation of structures. Work with ES cells could be done to determine whether this is the case and identify, which are the molecules mediating chimeric structure formation and find other physiologically occurring, stem cell-derived or transgenically-generated cells with the respective properties. Experiments in this

thesis have shown that in chimeric structures both renal cells and ESC-derived cells express E-cadherin. Experiments with the disaggregation-reaggregation system could be used to check whether loss of E-cadherin in ES cells would prevent the formation of chimeric structures. This could be done by treating ESCs with siRNAs for E-cadherin before mixing them with embryonic kidney cells. This could also be done by generating genetically modified ESCs containing floxed E-cadherin. Recombination can be induced by the application of cell-permeable Cre-recombinase (Jo et al., 2001; Patsch et al., 2011) before mixing with embryonic kidney cells and reaggregation. After the molecule(s) mediating the formation of chimeric structures has (have) been identified, experiments could be performed to identify cell types expressing this (these) molecule(s). Then the cells could be tested in the reaggregation system to confirm their ability to make kidney structures. Then these cells could be injected into the kidneys of mice with experimentally-induced kidney injury (for example by cisplatin administration or glycerol injection) to test the behaviour of the cells after transplantation. Although many challenges lie ahead of this approach, many of these challenges also apply to the use of ESC-derived cells. For example, issues about the delivery of the cells to the kidney are still an important problem for related cell replacement therapies. But if this method proves efficacious for blocking the progressiveness of renal injury, it might show even more advantages than ESC-derived cells. For example, an embryonic or even adult cell line with the derived properties could be established. This does not raise the ethical and safety concerns of using embryonic stem cells. Virtually, unlimited numbers of cells could be obtained and no expensive growth factors would be necessary (such as the ones that would have to be used for ESC differentiation). Also, the use of a cell line rather than generating new batches of cells de novo every time, would allow for the standardised use of the same cells every time. These initial, but important steps could be taken to investigate whether grafting cells for renoprotection of degenerating renal epithelia could be a useful strategy for addressing this problem in patients, in the future.

7.4 Limitations of this thesis

Before the global impact of this thesis could be finally summarised the limitations of the studies in this work should also be acknowledged. Most of these have been addressed in chapter discussions and in the current chapter, as they had to be taken into account for the interpretation of the results. This section provides a summary of the issues that were not resolved by this thesis, but might have an impact on the conclusions made.

Embryonic stem cell differentiation:

- the use of only one cell line for ESC differentiation experiments (this cell line could have lost in particular some of its ability to generate kidney cells)
- no karyotypic analysis was performed to confirm that the used ES cells were genetically stable
- although the ability of ES cells to generate embryoid bodies and to give rise to derivatives of the three germ layers is routinely used to confirm the pluripotency of cells, this is not the most accurate method as cell lined might still be biased to forming particular lineages. A better method could be provided for by performing ES cell injections into blastocysts to generate chimeric mice, which could then be analysed for ES cell contribution in different organs.

Developmental studies:

- the difficulty of cell identification on the basis of marker expression profiles still remains
- the presence of fusion events of host and test cells has not been addressed by specifically designed experiments
- ideally, for an accurate quantification, in quantitative studies measuring the proportions of renogenic cells at different embryo stages the numbers of cells of the correct lineage present in tissue isolates would have to be determined
- although tissue culture experiments provide a good independent check for reaggregation studies, there are serious limitations to using Calbindin and Laminin for structure identification

- although, all developmental studies suggested that some cells resident in the intermediate mesoderm present before the formation of a nephric duct or metanephric blastema are renocompetent, mesoderm before the formation of intermediate mesoderm could not be evaluated; a new approach would have to be designed to study this particular stage
- although the time frame of acquisition of renocompetence in embryo development was defined, the time interval obtained is still very wide; experiments should be performed to narrow it down by correlating stages to the number of somites present rather than days of embryonic development
- ways would have to be devised to isolate renocompetent renal progenitors to maintain and propagate them in *in vitro* cultures; this would allow studying their properties more closely

7.5 Summary of the impact of this work

In the beginning of this thesis, discussions on the potential impact of this work have identified that there are three interconnected areas, which will benefit from the work performed herein - kidney development, embryonic stem cell differentiation and traditional or regenerative medicine (Figure 1.6). After considering the results from this work, it is important to summarise the conclusions obtained in the context of each of these three different areas.

With respect to stem cell biology, the experiments in this work have identified that:

- undifferentiated embryonic stem cells are not capable of producing kidney cells when placed in the reaggregation-disaggregation system
- inhibition of Notch signalling in the conditions tested does not improve the differentiation of ES cells to renal cells
- ES cells might first have to be differentiated to intermediate mesodermal cells to be primed to acquire renocompetence before they can produce kidney cells autonomously, in *in vitro* systems

With respect to developmental biology, experiments have suggested that:

- renocompetence is acquired early in embryo development

- the intermediate mesoderm already contains renocompetent cells
- the first renocompetent cells appear in the intermediate mesoderm at E8.5 of mouse development or earlier
- intermediate mesodermal cells from the prospective metanephrogenic regions of E9.5 embryos are competent to give rise to the major cell types present in early kidney development

Regenerative medicine:

- both ESC and developmental studies have shown that non-kidney cells are able to become a part of renal tubules; this might open a whole new approach for regenerative medicine, where non-kidney cells could be integrated into damaged renal tubules for providing structural rather than functional support and therefore protect them from further degeneration

References

Abelev, G.I. (1971). Alpha-fetoprotein in ontogenesis and its association with malignant tumors. Advances in Cancer Research *14*, 295-358.

Abrahamson, D.R. (1985). Origin of the glomerular basement membrane visualized after in vivo labeling of laminin in newborn rat kidneys. The Journal of Cell Biology *100*, 1988-2000.

Abrahamson, D.R., Hudson, B.G., Stroganova, L., Borza, D.B., and St John, P.L. (2009). Cellular origins of type IV collagen networks in developing glomeruli. Journal of the Americal Society of Nephrology *20*, 1471-1479.

Alison, M.R., Poulsom, R., Otto, W.R., Vig, P., Brittan, M., Direkze, N.C., Lovell, M., Fang, T.C., Preston, S.L. and Wright, N.A. (2004). Recipes for adult stem cell plasticity: fusion cuisine or readymade? Journal of Clinical Pathology *57*, 113–120.

Alvarez-Dolado, M., Pardal, R., Garcia-Verdugo, J.M., Fike, J.R., Lee, H.O., Pfeffer, K., Lois, C., Morrison, S.J. and Alvarez-Buylla, A. (2003). Fusion of bone-marrow-derived cells with Purkinje neurons, cardiomyocytes and hepatocytes. Nature *425*, 968–973.

Artavanis-Tsakonas, S., Rand, M.D., and Lake, R.J. (1999). Notch signaling: cell fate control and signal integration in development. Science *284*, 770-776.

Aruffo, A., Stamenkovic, I., Melnick, M., Underhill, C.B., and Seed, B. (1990). CD44 is the principal cell surface receptor for hyaluronate. Cell *61*, 1303-1313.

Auerbach, R., and Grobstein, C. (1958). Inductive interaction of embryonic tissues after dissociation and reaggregation. Experimental Cell Research *15*, 384-397.

Avilion, A.A., Nicolis, S.K., Pevny, L.H., Perez, L., Vivian, N., and Lovell-Badge, R. (2003). Multipotent cell lineages in early mouse development depend on SOX2 function. Genes and Development *17*, 126-140.

Barajas, L. (1979). Anatomy of the juxtaglomerular apparatus. The American Journal of Physiology *237*, F333-343.

Barak, H., Rosenfelder, L., Schultheiss, T.M., and Reshef, R. (2005). Cell fate specification along the anterior-posterior axis of the intermediate mesoderm. Developmental Dynamics *232*, 901-914.

Barasch, J., Yang, J., Ware, C.B., Taga, T., Yoshida, K., Erdjument-Bromage, H., Tempst, P., Parravicini, E., Malach, S., Aranoff, T.*, et al.* (1999). Mesenchymal to epithelial conversion in rat metanephros is induced by LIF. Cell *99*, 377-386.

Bard, J.B., Gordon, A., Sharp, L., and Sellers, W.I. (2001). Early nephron formation in the developing mouse kidney. Journal of Anatomy *199*, 385-392.

Barker, N., Bartfeld, S., and Clevers, H. (2010). Tissue-resident adult stem cell populations of rapidly self-renewing organs. Cell Stem Cell *7*, 656-670.

Batchelder, C.A., Lee, C.C., Matsell, D.G., Yoder, M.C., and Tarantal, A.F. (2009). Renal ontogeny in the rhesus monkey (Macaca mulatta) and directed differentiation of human embryonic stem cells towards kidney precursors. Differentiation *78*, 45-56.

Becker, A.J., Mc, C.E., and Till, J.E. (1963). Cytological demonstration of the clonal nature of spleen colonies derived from transplanted mouse marrow cells. Nature *197*, 452-454.

Beddington, R.S. (1982). An autoradiographic analysis of tissue potency in different regions of the embryonic ectoderm during gastrulation in the mouse. Journal of Embryology and Experimental Morphology *69*, 265-285.

Beddington, R.S., and Robertson, E.J. (1999). Axis development and early asymmetry in mammals. Cell *96*, 195-209.

Bell, E., Moore, H., Mitchie, C., Sher, S., and Coon, H. (1984). Reconstruction of a thyroid gland equivalent from cells and matrix materials. The Journal of Experimental Zoology *232*, 277-285.

Bell, E., Sher, S., Hull, B., Merrill, C., Rosen, S., Chamson, A., Asselineau, D., Dubertret, L., Coulomb, B., Lapiere, C.*, et al.* (1983). The reconstitution of living skin. The Journal of Investigative Dermatology *81*, 2s-10s.

Bettenhausen, B., Hrabe de Angelis, M., Simon, D., Guenet, J.L., and Gossler, A. (1995). Transient and restricted expression during mouse embryogenesis of Dll1, a murine gene closely related to Drosophila Delta. Development *121*, 2407-2418.

Blaumueller, C.M., Qi, H., Zagouras, P., and Artavanis-Tsakonas, S. (1997). Intracellular cleavage of Notch leads to a heterodimeric receptor on the plasma membrane. Cell *90*, 281-291.

Blum, M., Gaunt, S.J., Cho, K.W., Steinbeisser, H., Blumberg, B., Bittner, D., and De Robertis, E.M. (1992). Gastrulation in the mouse: the role of the homeobox gene goosecoid. Cell *69*, 1097-1106.

Bouchard, M., Souabni, A., Mandler, M., Neubuser, A., and Busslinger, M. (2002). Nephric lineage specification by Pax2 and Pax8. Genes and Development *16*, 2958-2970.

Bridges, C.B. (1917). Deficiency. Genetics *2*, 445-465.

Brinster, R.L. (1974). The effect of cells transferred into the mouse blastocyst on subsequent development. The Journal of Experimental Medicine *140*, 1049-1056.

Brodbeck, S., Besenbeck, B., and Englert, C. (2004). The transcription factor Six2 activates expression of the Gdnf gene as well as its own promoter. Mechanisms of Development *121*, 1211-1222.

Brophy, P.D., Ostrom, L., Lang, K.M., and Dressler, G.R. (2001). Regulation of ureteric bud outgrowth by Pax2-dependent activation of the glial derived neurotrophic factor gene. Development *128*, 4747-4756.

Bruce, S.J., Rea, R.W., Steptoe, A.L., Busslinger, M., Bertram, J.F., and Perkins, A.C. (2007). In vitro differentiation of murine embryonic stem cells toward a renal lineage. Differentiation *75*, 337-349.

Brun, P., Dupret, J.M., Perret, C., Thomasset, M., and Mathieu, H. (1987). Vitamin D-dependent calcium-binding proteins (CaBPs) in human fetuses: comparative distribution of 9K CaBP mRNA and 28K CaBP during development. Pediatric Research *21*, 362-367.

Brüstle, O., Spiro, A.C., Karram, K., Choudhary, K., Okabe, S., and McKay, R.D. (1997). In vitro-generated neural precursors participate in mammalian brain development. Proceedings of the National Academy of Sciences of the United States of America *94*, 14809-14814.

Bulger, R.E., Cronin, R.E., and Dobyan, D.C. (1979). Survey of the morphology of the dog kidney. The Anatomical Record *194*, 41-65.

Bullock, S.L., Fletcher, J.M., Beddington, R.S., and Wilson, V.A. (1998). Renal agenesis in mice homozygous for a gene trap mutation in the gene encoding heparan sulfate 2-sulfotransferase. Genes and Development *12*, 1894-1906.

Burdsal, C.A., Damsky, C.H., and Pedersen, R.A. (1993). The role of E-cadherin and integrins in mesoderm differentiation and migration at the mammalian primitive streak. Development *118*, 829-844.

Burke, A.C. (2000). Hox genes and the global patterning of the somitic mesoderm. Current Topics in Developmental Biology *47*, 155-181.

Bytyqi, A.H., Bachmann, G., Rieke, M., Paraoanu, L.E., and Layer, P.G. (2007). Cell-by-cell reconstruction in reaggregates from neonatal gerbil retina begins from the inner retina and is promoted by retinal pigmented epithelium. The European Journal of Neuroscience *26*, 1560-1574.

Cano-Gauci, D.F., Song, H.H., Yang, H., McKerlie, C., Choo, B., Shi, W., Pullano, R., Piscione, T.D., Grisaru, S., Soon, S.*, et al.* (1999). Glypican-3-deficient mice exhibit developmental overgrowth and some of the abnormalities typical of Simpson-Golabi-Behmel syndrome. The Journal of Cell Biology *146*, 255-264.

Cano, A., Perez-Moreno, M.A., Rodrigo, I., Locascio, A., Blanco, M.J., del Barrio, M.G., Portillo, F., and Nieto, M.A. (2000). The transcription factor snail controls epithelial-mesenchymal transitions by repressing E-cadherin expression. Nature Cell Biololy *2*, 76-83.

Carroll, T.J., and McMahon, A.P. (2003). Overview: The Molecular Basis of Kidney Develoment. In The Kidney: From Normal Development to Congenital Disease, P.D. Vize, A.S. Woolf, and J.B.L. Bard, eds. (London, Academic Press), pp. 343-370.

Chambers, I., Colby, D., Robertson, M., Nichols, J., Lee, S., Tweedie, S., and Smith, A. (2003). Functional expression cloning of Nanog, a pluripotency sustaining factor in embryonic stem cells. Cell *113*, 643-655.

Cheng, H.T., Kim, M., Valerius, M.T., Surendran, K., Schuster-Gossler, K., Gossler, A., McMahon, A.P., and Kopan, R. (2007). Notch2, but not Notch1, is required for proximal fate acquisition in the mammalian nephron. Development *134*, 801-811.

Cheng, H.T., and Kopan, R. (2005). The role of Notch signaling in specification of podocyte and proximal tubules within the developing mouse kidney. Kidney International *68*, 1951-1952.

Cheng, H.T., Miner, J.H., Lin, M., Tansey, M.G., Roth, K., and Kopan, R. (2003). Gamma-secretase activity is dispensable for mesenchyme-to-epithelium transition but required for podocyte and proximal tubule formation in developing mouse kidney. Development *130*, 5031-5042.

Cheng, L., Arata, A., Mizuguchi, R., Qian, Y., Karunaratne, A., Gray, P.A., Arata, S., Shirasawa, S., Bouchard, M., Luo, P., *et al.* (2004). Tlx3 and Tlx1 are post-mitotic selector genes determining glutamatergic over GABAergic cell fates. Nature Neuroscience *7*, 510-517.

Chew, J.L., Loh, Y.H., Zhang, W., Chen, X., Tam, W.L., Yeap, L.S., Li, P., Ang, Y.S., Lim, B., Robson, P., *et al.* (2005). Reciprocal transcriptional regulation of Pou5f1 and Sox2 via the Oct4/Sox2 complex in embryonic stem cells. Molecular and Cellular Biology *25*, 6031-6046.

Chi, N., and Epstein, J.A. (2002). Getting your Pax straight: Pax proteins in development and disease. Trends in Genetics *18*, 41-47.

Cho, E.A., Patterson, L.T., Brookhiser, W.T., Mah, S., Kintner, C., and Dressler, G.R. (1998). Differential expression and function of cadherin-6 during renal epithelium development. Development *125*, 803-812.

Chuai, M., Zeng, W., Yang, X., Boychenko, V., Glazier, J.A., and Weijer, C.J. (2006). Cell movement during chick primitive streak formation. Developmental Biology *296*, 137-149.

Cirio, M.C., Hui, Z., Haldin, C.E., Cosentino, C.C., Stuckenholz, C., Chen, X., Hong, S.K., Dawid, I.B., and Hukriede, N.A. (2011). Lhx1 is required for specification of the renal progenitor cell field. PLoS One *6*, e18858.

Ciruna, B.G., and Rossant, J. (1999). Expression of the T-box gene Eomesodermin during early mouse development. Mechanisms of Development *81*, 199-203.

Daniel, T.O., and Abrahamson, D. (2000). Endothelial signal integration in vascular assembly. Annual Review of Physiology *62*, 649-671.

Daudet, N., and Lewis, J. (2005). Two contrasting roles for Notch activity in chick inner ear development: specification of prosensory patches and lateral inhibition of hair-cell differentiation. Development *132*, 541-551.

Davies, J. (1950). The pronephros and the early development of the mesonephros in the duck. Journal of Anatomy *84*, 95-103.

Davies, J. (1994). Control of calbindin-D28K expression in developing mouse kidney. Developmental Dynamics *199*, 45-51.

Davies, J.A. (2006). A method for cold storage and transport of viable embryonic kidney rudiments. Kidney International *70*, 2031-2034.

Davies, J.A. (2010). The embryonic kidney: isolation, organ culture, immunostaining and RNA interference. Methods in Molecular Biololy *633*, 57-69.

Davies, J.A., Perera, A.D., and Walker, C.L. (1999). Mechanisms of epithelial development and neoplasia in the metanephric kidney. International Journal of Developmental Biology *43*, 473-478.

de Martino, C., and Zamboni, L. (1966). A morphologic study of the mesonephros of the human embryo. Journal of Ultrastructure Research *16*, 399-427.

De Strooper, B., Annaert, W., Cupers, P., Saftig, P., Craessaerts, K., Mumm, J.S., Schroeter, E.H., Schrijvers, V., Wolfe, M.S., Ray, W.J., *et al.* (1999). A presenilin-1-dependent gamma-secretase-like protease mediates release of Notch intracellular domain. Nature *398*, 518-522.

Dehbi, M., Ghahremani, M., Lechner, M., Dressler, G., and Pelletier, J. (1996). The paired-box transcription factor, PAX2, positively modulates expression of the Wilms' tumor suppressor gene (WT1). Oncogene *13*, 447-453.

Dexter, J. (1914). Nabours's Breeding Experiments with Grasshoppers. The American Naturalist *48*, 317-320.

Dovat, S., and Feig, S.A. (1997). The use of umbilical cord blood stem cells for hematopoietic reconstitution. The Western Journal of Medicine *166*, 342-343.

Downs, K.M., and Davies, T. (1993). Staging of gastrulating mouse embryos by morphological landmarks in the dissecting microscope. Development *118*, 1255-1266.

Dressler, G.R. (2011). Patterning and early cell lineage decisions in the developing kidney: the role of Pax genes. Pediatric Nephrololgy *26*, 1387-1394.

Dressler, G.R., Deutsch, U., Chowdhury, K., Nornes, H.O., and Gruss, P. (1990). Pax2, a new murine paired-box-containing gene and its expression in the developing excretory system. Development *109*, 787-795.

Drummond, I.A., and Majumdar, A. (2003). The pronephric glomus and vasculature. In The Kidney: From Normal Development to Congenital Disease, P.D. Vize, A.S. Woolf, and J.B.L. Bard, eds. (London, Academic Press), pp. 61-71.

Drummond, I.A., Majumdar, A., Hentschel, H., Elger, M., Solnica-Krezel, L., Schier, A.F., Neuhauss, S.C., Stemple, D.L., Zwartkruis, F., Rangini, Z., *et al.* (1998). Early development of the zebrafish pronephros and analysis of mutations affecting pronephric function. Development *125*, 4655-4667.

Ducibella, T., and Anderson, E. (1975). Cell shape and membrane changes in the eight-cell mouse embryo: prerequisites for morphogenesis of the blastocyst. Developmental Biology *47*, 45-58.

Dudley, A.T., Lyons, K.M., and Robertson, E.J. (1995). A requirement for bone morphogenetic protein-7 during development of the mammalian kidney and eye. Genes and Development *9*, 2795-2807.

Dudley, A.T., and Robertson, E.J. (1997). Overlapping expression domains of bone morphogenetic protein family members potentially account for limited tissue defects in BMP7 deficient embryos. Developmental Dynamics *208*, 349-362.

Dunn, N.R., Winnier, G.E., Hargett, L.K., Schrick, J.J., Fogo, A.B., and Hogan, B.L. (1997). Haploinsufficient phenotypes in Bmp4 heterozygous null mice and modification by mutations in Gli3 and Alx4. Developmental Biology *188*, 235-247.

Dunwoodie, S.L., Henrique, D., Harrison, S.M., and Beddington, R.S. (1997). Mouse Dll3: a novel divergent Delta gene which may complement the function of other Delta homologues during early pattern formation in the mouse embryo. Development *124*, 3065-3076.

Duran, C., Talley, P.J., Walsh, J., Pigott, C., Morton, I.E., and Andrews, P.W. (2001). Hybrids of pluripotent and nullipotent human embryonal carcinoma cells: partial retention of a pluripotent phenotype. International Journal of Cancer *93*, 324-332.

Ekblom, P. (1989). Developmentally regulated conversion of mesenchyme to epithelium. The Faseb Journal *3*, 2141-2150.

Ekblom, P., Alitalo, K., Vaheri, A., Timpl, R., and Saxen, L. (1980). Induction of a basement membrane glycoprotein in embryonic kidney: possible role of laminin in morphogenesis. Proceedings of the National Academy of Sciences of the United States of America *77*, 485-489.

Enomoto, H., Araki, T., Jackman, A., Heuckeroth, R.O., Snider, W.D., Johnson, E.M., Jr., and Milbrandt, J. (1998). GFR alpha1-deficient mice have deficits in the enteric nervous system and kidneys. Neuron *21*, 317-324.

Evans, M.J., and Kaufman, M.H. (1981). Establishment in culture of pluripotential cells from mouse embryos. Nature *292*, 154-156.

Fanto, M., and Mlodzik, M. (1999). Asymmetric Notch activation specifies photoreceptors R3 and R4 and planar polarity in the Drosophila eye. Nature *397*, 523-526.

Farquhar, M.G., Wissig, S.L., and Palade, G.E. (1961). Glomerular permeability. I. Ferritin transfer across the normal glomerular capillary wall. The Journal of Experimental Medicine *113*, 47-66.

Fisher, C.E., and Howie, S.E. (2006). The role of megalin (LRP-2/Gp330) during development. Developmental Biology *296*, 279-297.

Fitzgerald, K., Wilkinson, H.A., and Greenwald, I. (1993). glp-1 can substitute for lin-12 in specifying cell fate decisions in Caenorhabditis elegans. Development *119*, 1019-1027.

Fleming, R.J. (1998). Structural conservation of Notch receptors and ligands. Seminars in Cell and Developmental Biololgy *9*, 599-607.

Fortini, M.E., and Artavanis-Tsakonas, S. (1994). The suppressor of hairless protein participates in notch receptor signaling. Cell *79*, 273-282.

Fowler, J., Cohen, L., and Jarvis, P. (1998). Practical statistics for field biology, 2nd edn (Chichester, John Wiley and Sons).

Fraser, E.A. (1920). The Pronephros and early development of the Mesonephros in the Cat. Journal of Anatomy *54*, 287-304 287.

Fraser, E.A. (1950). The development of the vertebrate excretory system. Biological Reviews *25*, 159-187.

Friebova-Zemanova, Z., and Goncharevskaya, O.A. (1982). Formation of the chick mesonephros. Anatomy and Embryology *165*, 125-139.

Frise, E., Knoblich, J.A., Younger-Shepherd, S., Jan, L.Y., and Jan, Y.N. (1996). The Drosophila Numb protein inhibits signaling of the Notch receptor during cell-cell interaction in sensory organ lineage. Proceedings of the National Academy of Sciences of the United States of America *93*, 11925-11932.

Fujii, T., Pichel, J.G., Taira, M., Toyama, R., Dawid, I.B., and Westphal, H. (1994). Expression patterns of the murine LIM class homeobox gene lim1 in the developing brain and excretory system. Developmental Dynamics *199*, 73-83.

Gage, F.H. (2000). Mammalian neural stem cells. Science (New York, NY *287*, 1433-1438.

Garcia-Martinez, V., and Schoenwolf, G.C. (1993). Primitive-streak origin of the cardiovascular system in avian embryos. Developmental Biology *159*, 706-719.

Gardner, R.L. (1968). Mouse chimeras obtained by the injection of cells into the blastocyst. Nature *220*, 596-597.

Georgas, K., Rumballe, B., Valerius, M.T., Chiu, H.S., Thiagarajan, R.D., Lesieur, E., Aronow, B.J., Brunskill, E.W., Combes, A.N., Tang, D., *et al.* (2009). Analysis of early nephron patterning reveals a role for distal RV proliferation in fusion to the ureteric tip via a cap mesenchyme-derived connecting segment. Developmental Biology *332*, 273-286.

Gilbert, S.F. (2000). Developmental Biology, 6th edn (Suntherland (MA), Sinauer Associates, Inc.).

Goormaghtigh, N. (1940). Histological changes in the ischemic kidney: With special reference to the juxtaglomerular apparatus. The American Journal of Pathology *16*, 409-416 405.

Gray, H. (1918). Anatmy of the human body, 20 edn (Philadelphia, Lea and Febiger).
Greenwald, I. (2005). LIN-12/Notch signaling in C. elegans. WormBook, 1-16.

Grobstein, C. (1953a). Inductive epitheliomesenchymal interaction in cultured organ rudiments of the mouse. Science *118*, 52-55.

Grobstein, C. (1953b). Morphogenetic interaction between embryonic mouse tissues separated by a membrane filter. Nature *172*, 869-870.

Grobstein, C. (1955). Inductive interaction in the development of the mouse metanephros. Journal of Experimental Zoology *130*, 319-339.

Grote, D., Souabni, A., Busslinger, M., and Bouchard, M. (2006). Pax 2/8-regulated Gata 3 expression is necessary for morphogenesis and guidance of the nephric duct in the developing kidney. Development *133*, 53-61.

Grubb, G.R., Yun, K., Williams, B.R., Eccles, M.R., and Reeve, A.E. (1994). Expression of WT1 protein in fetal kidneys and Wilms' tumors. Laboratory Investigation *71*, 472-479.

Gulyas, B.J. (1975). A reexamination of cleavage patterns in eutherian mammalian eggs: rotation of blastomere pairs during second cleavage in the rabbit. The Journal of Experimental Zoology *193*, 235-248.

Halban, P.A., Powers, S.L., George, K.L., and Bonner-Weir, S. (1987). Spontaneous reassociation of dispersed adult rat pancreatic islet cells into aggregates with three-dimensional architecture typical of native islets. Diabetes *36*, 783-790.

Hallgrimsson, B., Benediktsson, H., and Vize, P.D. (2003). Anatomy and histology of the human urinary system. In The Kidney: From Normal Development to Congenital Disease, P.D. Vize, A.S. Woolf, and J.B.L. Bard, eds. (London, Academic Press), pp. 149-164.

Hartman, B.H., Reh, T.A., and Bermingham-McDonogh, O. (2010). Notch signaling specifies prosensory domains via lateral induction in the developing mammalian inner

ear. Proceedings of the National Academy of Sciences of the United States of America *107*, 15792-15797.

Hartwig, S., Ho, J., Pandey, P., Macisaac, K., Taglienti, M., Xiang, M., Alterovitz, G., Ramoni, M., Fraenkel, E., and Kreidberg, J.A. (2010). Genomic characterization of Wilms' tumor suppressor 1 targets in nephron progenitor cells during kidney development. Development *137*, 1189-1203.

Hatini, V., Huh, S.O., Herzlinger, D., Soares, V.C., and Lai, E. (1996). Essential role of stromal mesenchyme in kidney morphogenesis revealed by targeted disruption of Winged Helix transcription factor BF-2. Genes and Development *10*, 1467-1478.

Haugan, B.M., Halberg, K.A., Jespersen, A., Prehn, L.R., and Mobjerg, N. (2010). Functional characterization of the vertebrate primary ureter: structure and ion transport mechanisms of the pronephric duct in axolotl larvae (Amphibia). BMC Developmental Biology *10*, 56.

Hauser, P.V., De Fazio, R., Bruno, S., Sdei, S., Grange, C., Bussolati, B., Benedetto, C., and Camussi, G. (2010). Stem Cells Derived from Human Amniotic Fluid Contribute to Acute Kidney Injury Recovery. The American Journal of Pathology *177*, 2011-2021.

Hay, E.D. (1995). An overview of epithelio-mesenchymal transformation. Acta anatomica *154*, 8-20.

Heidrich, H.G., Kinne, R., Kinne-Saffran, E., and Hannig, K. (1972). The polarity of the proximal tubule cell in rat kidney. Different surface charges for the brush-border microvilli and plasma membranes from the basal infoldings. The Journal of Cell Biology *54*, 232-245.

Heitzler, P., and Simpson, P. (1991). The choice of cell fate in the epidermis of Drosophila. Cell *64*, 1083-1092.

Hellmich, H.L., Kos, L., Cho, E.S., Mahon, K.A., and Zimmer, A. (1996). Embryonic expression of glial cell-line derived neurotrophic factor (GDNF) suggests multiple developmental roles in neural differentiation and epithelial-mesenchymal interactions. Mechanisms of Development *54*, 95-105.

Hendry, C., Rumballe, B., Moritz, K., and Little, M.H. (2011). Defining and redefining the nephron progenitor population. Pediatric Nephrology *26*, 1395-1406.

Herrera, M.B., Bussolati, B., Bruno, S., Morando, L., Mauriello-Romanazzi, G., Sanavio, F., Stamenkovic, I., Biancone, L., and Camussi, G. (2007). Exogenous mesenchymal stem cells localize to the kidney by means of CD44 following acute tubular injury. Kidney International *72*, 430-441.

Herzlinger, D., Koseki, C., Mikawa, T., and al-Awqati, Q. (1992). Metanephric mesenchyme contains multipotent stem cells whose fate is restricted after induction. Development *114*, 565-572.

Herzlinger, D., Qiao, J., Cohen, D., Ramakrishna, N., and Brown, A.M. (1994). Induction of kidney epithelial morphogenesis by cells expressing Wnt-1. Developmental Biology *166*, 815-818.

Hoar, R.M. (1976). Comparative developmental aspects of selected organ systems. II. Gastrointestinal and urogenital systems. Environmental Health Perspectives *18*, 61-66.

Hohenstein, P., and Hastie, N.D. (2006). The many facets of the Wilms' tumour gene, WT1. Human Molecular Genetics *15 Suppl 2*, R196-R201.

Holtfreter, J. (1933). Der Einfluss von Wirtsalter und verschiedenen Organbezirken auf die Differenzierung von angelagertem Gastrulaektoderm. W Roux Arch EntwMech Org *127*, 610-775.

Holtfreter, J. (1944). Experimental studies on the development of the pronephos. Rev Can Biol *3*, 220-250.

Howland, R.B. (1921). Experiments on the effect of removal of the pronephros of Amblystoma punctatum. Journal of Experimental Zoology *32*, 355-396.

Humes, H.D., Buffington, D.A., MacKay, S.M., Funke, A.J., and Weitzel, W.F. (1999). Replacement of renal function in uremic animals with a tissue-engineered kidney. Nature Biotechnology *17*, 451-455.

Humes, H.D., Weitzel, W.F., Bartlett, R.H., Swaniker, F.C., Paganini, E.P., Luderer, J.R., and Sobota, J. (2004). Initial clinical results of the bioartificial kidney containing human cells in ICU patients with acute renal failure. Kidney International *66*, 1578-1588.

Inman, K.E., and Downs, K.M. (2006). Localization of Brachyury (T) in embryonic and extraembryonic tissues during mouse gastrulation. Gene Expression Patterns *6*, 783-793.

James, R.G., Kamei, C.N., Wang, Q., Jiang, R., and Schultheiss, T.M. (2006). Odd-skipped related 1 is required for development of the metanephric kidney and regulates formation and differentiation of kidney precursor cells. Development *133*, 2995-3004.

James, R.G., and Schultheiss, T.M. (2005). Bmp signaling promotes intermediate mesoderm gene expression in a dose-dependent, cell-autonomous and translation-dependent manner. Developmental Biology *288*, 113-125.

Jarriault, S., Le Bail, O., Hirsinger, E., Pourquie, O., Logeat, F., Strong, C.F., Brou, C., Seidah, N.G., and Isra l, A. (1998). Delta-1 activation of notch-1 signaling results in HES-1 transactivation. Molecular and Cellular Biology *18*, 7423-7431.

Jo, D., Nashabi, A., Doxsee, C., Lin, Q., Unutmaz, D., Chen, J., and Ruley, H.E. (2001). Epigenetic regulation of gene structure and function with a cell-permeable Cre recombinase. Nature Biotechnology *19*, 929-933.

Johnsson, C., Tufveson, G., Wahlberg, J., and Hallgren, R. (1996). Experimentally-induced warm renal ischemia induces cortical accumulation of hyaluronan in the kidney. Kidney International *50*, 1224-1229.

Jokalainen, P. (1963). An electron microscopic study of the early development of the rat metanephric nephron. Acta Anatomica *47*, 1-73.

Karner, C.M., Das, A., Ma, Z., Self, M., Chen, C., Lum, L., Oliver, G., and Carroll, T.J. (2011). Canonical Wnt9b signaling balances progenitor cell expansion and differentiation during kidney development. Development *138*, 1247-1257.

Kaufman, M.H. (2001). The Atlas of Mouse Development, fourth printing, second edn (Cambridge, University Press).

Kestila, M., Lenkkeri, U., Mannikko, M., Lamerdin, J., McCready, P., Putaala, H., Ruotsalainen, V., Morita, T., Nissinen, M., Herva, R.*, et al.* (1998). Positionally cloned gene for a novel glomerular protein--nephrin--is mutated in congenital nephrotic syndrome. Molecular Cell *1*, 575-582.

Kidd, S., Kelley, M.R., and Young, M.W. (1986). Sequence of the notch locus of Drosophila melanogaster: relationship of the encoded protein to mammalian clotting and growth factors. Molecular and Cellular Biology *6*, 3094-3108.

Kim, D., and Dressler, G.R. (2005). Nephrogenic factors promote differentiation of mouse embryonic stem cells into renal epithelia. Journal of the American Society of Nephrology *16*, 3527-3534.

Kingsbury, B.F. (1920). The Developmental Origin of the Notochord. Science *51*, 190-193.

Kispert, A., Vainio, S., and McMahon, A.P. (1998). Wnt-4 is a mesenchymal signal for epithelial transformation of metanephric mesenchyme in the developing kidney. Development *125*, 4225-4234.

Kobayashi, A., Valerius, M.T., Mugford, J.W., Carroll, T.J., Self, M., Oliver, G., and McMahon, A.P. (2008). Six2 defines and regulates a multipotent self-renewing nephron progenitor population throughout mammalian kidney development. Cell Stem Cell *3*, 169-181.

Kobayashi, T., Tanaka, H., Kuwana, H., Inoshita, S., Teraoka, H., Sasaki, S., and Terada, Y. (2005). Wnt4-transformed mouse embryonic stem cells differentiate into renal tubular cells. Biochemical and Biophysical Research Communications *336*, 585-595.

Koopman, P., and Cotton, R.G. (1984). A factor produced by feeder cells which inhibits embryonal carcinoma cell differentiation. Characterization and partial purification. Experimental Cell Research *154*, 233-242.

Kopan, R., and Ilagan, M.X. (2009). The canonical Notch signaling pathway: unfolding the activation mechanism. Cell *137*, 216-233.

Kramer, J., Steinhoff, J., Klinger, M., Fricke, L., and Rohwedel, J. (2006). Cells differentiated from mouse embryonic stem cells via embryoid bodies express renal marker molecules. Differentiation *74*, 91-104.

Krebs, L.T., Iwai, N., Nonaka, S., Welsh, I.C., Lan, Y., Jiang, R., Saijoh, Y., O'Brien, T.P., Hamada, H., and Gridley, T. (2003). Notch signaling regulates left-right asymmetry determination by inducing Nodal expression. Genes and Development *17*, 1207-1212.

Kreidberg, J.A., Donovan, M.J., Goldstein, S.L., Rennke, H., Shepherd, K., Jones, R.C., and Jaenisch, R. (1996). Alpha 3 beta 1 integrin has a crucial role in kidney and lung organogenesis. Development *122*, 3537-3547.

Kreidberg, J.A., Sariola, H., Loring, J.M., Maeda, M., Pelletier, J., Housman, D., and Jaenisch, R. (1993). WT-1 is required for early kidney development. Cell *74*, 679-691.

Kume, T., Deng, K., and Hogan, B.L. (2000a). Minimal phenotype of mice homozygous for a null mutation in the forkhead/winged helix gene, Mf2. Molecular and Cellular Biology *20*, 1419-1425.

Kume, T., Deng, K., and Hogan, B.L. (2000b). Murine forkhead/winged helix genes Foxc1 (Mf1) and Foxc2 (Mfh1) are required for the early organogenesis of the kidney and urinary tract. Development *127*, 1387-1395.

Kuure, S., Sainio, K., Vuolteenaho, R., Ilves, M., Wartiovaara, K., Immonen, T., Kvist, J., Vainio, S., and Sariola, H. (2005). Crosstalk between Jagged1 and GDNF/Ret/GFRalpha1 signalling regulates ureteric budding and branching. Mechanisms of Development *122*, 765-780.

Labastie, M.C., Catala, M., Gregoire, J.M., and Peault, B. (1995). The GATA-3 gene is expressed during human kidney embryogenesis. Kidney International *47*, 1597-1603.

Lai, E.C. (2004). Notch signaling: control of cell communication and cell fate. Development *131*, 965-973.

Laitinen, L., Virtanen, I., and Saxen, L. (1987). Changes in the glycosylation pattern during embryonic development of mouse kidney as revealed with lectin conjugates. Journal of Histochemistry and Cytochemistry *35*, 55-65.

Landreth, K.S. (2002). Critical windows in development of the rodent immune system. Human and Experimental Toxicology *21*, 493-498.

Lawrence, W.D., Whitaker, D., Sugimura, H., Cunha, G.R., Dickersin, G.R., and Robboy, S.J. (1992). An ultrastructural study of the developing urogenital tract in early human fetuses. American Journal of Obstetrics and Gynecology *167*, 185-193.

Lawson, K.A., Meneses, J.J., and Pedersen, R.A. (1991). Clonal analysis of epiblast fate during germ layer formation in the mouse embryo. Development *113*, 891-911.

Leunda-Casi, A., de Hertogh, R., and Pampfer, S. (2001). Control of trophectoderm differentiation by inner cell mass-derived fibroblast growth factor-4 in mouse blastocysts and corrective effect of FGF-4 on high glucose-induced trophoblast disruption. Molecular Reproduction and Development *60*, 38-46.

Leveen, P., Pekny, M., Gebre-Medhin, S., Swolin, B., Larsson, E., and Betsholtz, C. (1994). Mice deficient for PDGF B show renal, cardiovascular, and hematological abnormalities. Genes and Development *8*, 1875-1887.

Li, M., Pevny, L., Lovell-Badge, R., and Smith, A. (1998). Generation of purified neural precursors from embryonic stem cells by lineage selection. Current Biology *8*, 971-974.

Lindsell, C.E., Shawber, C.J., Boulter, J., and Weinmaster, G. (1995). Jagged: a mammalian ligand that activates Notch1. Cell *80*, 909-917.

Little, M.H., Brennan, J., Georgas, K., Davies, J.A., Davidson, D.R., Baldock, R.A., Beverdam, A., Bertram, J.F., Capel, B., Chiu, H.S., *et al.* (2007). A high-resolution anatomical ontology of the developing murine genitourinary tract. Gene Expression Patterns *7*, 680-699.

Liu, L., Dunn, S.T., Christakos, S., Hanson-Painton, O., and Bourdeau, J.E. (1993). Calbindin-D28k gene expression in the developing mouse kidney. Kidney International *44*, 322-330.

Lowell, S., Benchoua, A., Heavey, B., and Smith, A.G. (2006). Notch promotes neural lineage entry by pluripotent embryonic stem cells. PLoS Biology *4*, e121.

Lu, W., Peissel, B., Babakhanlou, H., Pavlova, A., Geng, L., Fan, X., Larson, C., Brent, G., and Zhou, J. (1997). Perinatal lethality with kidney and pancreas defects in mice with a targetted Pkd1 mutation. Nature Genetics *17*, 179-181.

Lundgren, S., Carling, T., Hjalm, G., Juhlin, C., Rastad, J., Pihlgren, U., Rask, L., Akerstrom, G., and Hellman, P. (1997). Tissue distribution of human gp330/megalin, a putative Ca(2+)-sensing protein. Journal of Histochemistry and Cytochemistry *45*, 383-392.

Lusis, M., Li, J., Ineson, J., Christensen, M.E., Rice, A., and Little, M.H. (2010). Isolation of clonogenic, long-term self renewing embryonic renal stem cells. Stem Cell Research *5*, 23-39.

MacKay, G.E., Keighren, M.A., Wilson, L., Pratt, T., Flockhart, J.H., Mason, J.O., Price, D.J., and West, J.D. (2005). Evaluation of the mouse TgTP6.3 tauGFP transgene as a lineage marker in chimeras. Journal of Anatomy *206*, 79-92.

Madsen, K.M., Nielsen, S., and Craig Tisher, C. (2007). Anatomy of the kidney. In Brenner and Rector's The Kidney, B.M. Brenner, ed. (Philadelphia, Saunders), pp. 25-80.

Mae, S., Shirasawa, S., Yoshie, S., Sato, F., Kanoh, Y., Ichikawa, H., Yokoyama, T., Yue, F., Tomotsune, D., and Sasaki, K. (2010). Combination of small molecules

enhances differentiation of mouse embryonic stem cells into intermediate mesoderm through BMP7-positive cells. Biochemical and Biophysical Research Communications *393*, 877-882.

Maeshima, A., Yamashita, S., and Nojima, Y. (2003). Identification of renal progenitor-like tubular cells that participate in the regeneration processes of the kidney. Journal of the American Society of Nephrology *14*, 3138-3146.

Mah, S.P., Saueressig, H., Goulding, M., Kintner, C., and Dressler, G.R. (2000). Kidney development in cadherin-6 mutants: delayed mesenchyme-to-epithelial conversion and loss of nephrons. Developmental Biology *223*, 38-53.

Martin, G.R. (1981). Isolation of a pluripotent cell line from early mouse embryos cultured in medium conditioned by teratocarcinoma stem cells. Proceedings of the National Academy of Sciences of the United States of America *78*, 7634-7638.

Matta, S.G., Wobken, J.D., Williams, F.G., and Bauer, G.E. (1994). Pancreatic islet cell reaggregation systems: efficiency of cell reassociation and endocrine cell topography of rat islet-like aggregates. Pancreas *9*, 439-449.

Mauch, T.J., Yang, G., Wright, M., Smith, D., and Schoenwolf, G.C. (2000). Signals from trunk paraxial mesoderm induce pronephros formation in chick intermediate mesoderm. Developmental Biology *220*, 62-75.

McBurney, M.W. (1976). Clonal lines of teratocarcinoma cells in vitro: differentiation and cytogenetic characteristics. Journal of Cellular Physiology *89*, 441-455.

McConnell, M.J., Cunliffe, H.E., Chua, L.J., Ward, T.A., and Eccles, M.R. (1997). Differential regulation of the human Wilms tumour suppressor gene (WT1) promoter by two isoforms of PAX2. Oncogene *14*, 2689-2700.

McCright, B., Gao, X., Shen, L., Lozier, J., Lan, Y., Maguire, M., Herzlinger, D., Weinmaster, G., Jiang, R., and Gridley, T. (2001). Defects in development of the kidney, heart and eye vasculature in mice homozygous for a hypomorphic Notch2 mutation. Development *128*, 491-502.

McCulloch, E.A., and Till, J.E. (1960). The radiation sensitivity of normal mouse bone marrow cells, determined by quantitative marrow transplantation into irradiated mice. Radiation Research *13*, 115-125.

McIntosh, J.E., Bourdeau, J.E., and Taylor, A.N. (1986). Immunohistochemical localization of calbindin-D28k during the development of the rabbit nephron. The Anatomical Record *215*, 383-389.

McLaren, A. (1976). Mammalian Chimaeras (Cambridge, Cambridge University Press).
Mendelsohn, C., Batourina, E., Fung, S., Gilbert, T., and Dodd, J. (1999). Stromal cells mediate retinoid-dependent functions essential for renal development. Development *126*, 1139-1148.

Michos, O., Cebrian, C., Hyink, D., Grieshammer, U., Williams, L., D'Agati, V., Licht, J.D., Martin, G.R., and Costantini, F. (2010). Kidney development in the absence of Gdnf and Spry1 requires Fgf10. PLoS Genetics *6*, e1000809.

Miner, J.H. (2011). Glomerular basement membrane composition and the filtration barrier. Pediatric Nephrololgy. Pediatric Nephrology *26*, 1413-1417.

Miner, J.H., and Li, C. (2000). Defective glomerulogenesis in the absence of laminin alpha5 demonstrates a developmental role for the kidney glomerular basement membrane. Developmental Biology *217*, 278-289.

Mitsui, K., Tokuzawa, Y., Itoh, H., Segawa, K., Murakami, M., Takahashi, K., Maruyama, M., Maeda, M., and Yamanaka, S. (2003). The homeoprotein Nanog is required for maintenance of pluripotency in mouse epiblast and ES cells. Cell *113*, 631-642.

Miyamoto, N., Yoshida, M., Kuratani, S., Matsuo, I., and Aizawa, S. (1997). Defects of urogenital development in mice lacking Emx2. Development *124*, 1653-1664.

Miyazaki, Y., Oshima, K., Fogo, A., Hogan, B.L., and Ichikawa, I. (2000). Bone morphogenetic protein 4 regulates the budding site and elongation of the mouse ureter. The Journal of Clinical Investigation *105*, 863-873.

Mizumoto, H., Ishihara, K., Nakazawa, K., Ijima, H., Funatsu, K., and Kajiwara, T. (2008). A new culture technique for hepatocyte organoid formation and long-term maintenance of liver-specific functions. Tissue Engineering, Part C, Methods *14*, 167-175.

Mobjerg, N., Larsen, E.H., and Jespersen, A. (2000). Morphology of the kidney in larvae of Bufo viridis (Amphibia, Anura, Bufonidae). Journal of Morphology *245*, 177-195.

Mohr, O.L. (1919). Character Changes Caused by Mutation of an Entire Region of a Chromosome in Drosophila. Genetics *4*, 275-282.

Moore, M.W., Klein, R.D., Farinas, I., Sauer, H., Armanini, M., Phillips, H., Reichardt, L.F., Ryan, A.M., Carver-Moore, K., and Rosenthal, A. (1996). Renal and neuronal abnormalities in mice lacking GDNF. Nature *382*, 76-79.

Morgan, T.H., and Bridges, C.B. (1916). Sex-linked inheritance in Drosophila (Washington, Carnegie Institution of Washington).

Morigi, M., Imberti, B., Zoja, C., Corna, D., Tomasoni, S., Abbate, M., Rottoli, D., Angioletti, S., Benigni, A., Perico, N., *et al.* (2004). Mesenchymal stem cells are renotropic, helping to repair the kidney and improve function in acute renal failure. Journal of the American Society of Nephrology *15*, 1794-1804.

Morizane, R., Monkawa, T., and Itoh, H. (2009). Differentiation of murine embryonic stem and induced pluripotent stem cells to renal lineage in vitro. Biochemical and Biophysical Research Communication *390*, 1334-1339.

Moser, F.G., Dorman, B.P., and Ruddle, F.H. (1975). Mouse-human heterokaryon analysis with a 33258 Hoechst-Giemsa technique. The Journal of Cell Biology *66*, 676-680.

Mounier, F., Hinglais, N., Brehier, A., Thomasset, M., Lacoste, M., Sich, M., and Gubler, M.C. (1987). Ontogenesis of 28 kDa vitamin D-induced calcium-binding protein in human kidney. Kidney International *31*, 121-129.

Mugford, J.W., Sipila, P., McMahon, J.A., and McMahon, A.P. (2008). Osr1 expression demarcates a multi-potent population of intermediate mesoderm that undergoes progressive restriction to an Osr1-dependent nephron progenitor compartment within the mammalian kidney. Developmental Biology *324*, 88-98.

Muller, U., Wang, D., Denda, S., Meneses, J.J., Pedersen, R.A., and Reichardt, L.F. (1997). Integrin alpha8beta1 is critically important for epithelial-mesenchymal interactions during kidney morphogenesis. Cell *88*, 603-613.

Mulnard, J., and Huygens, R. (1978). Ultrastructural localization of non-specific alkaline phosphatase during cleavage and blastocyst formation in the mouse. Journal of Embryology and Experimental Morphology *44*, 121-131.

Mummery, C.L., van den Eijnden-van Raaij, A.J., Feijen, A., Freund, E., Hulskotte, E., Schoorlemmer, J., and Kruijer, W. (1990). Expression of growth factors during the differentiation of embryonic stem cells in monolayer. Developmental Biology *142*, 406-413.

Mundel, P., and Shankland, S.J. (2002). Podocyte biology and response to injury. Journal of the American Society of Nephrology *13*, 3005-3015.

Mundlos, S., Pelletier, J., Darveau, A., Bachmann, M., Winterpacht, A., and Zabel, B. (1993). Nuclear localization of the protein encoded by the Wilms' tumor gene WT1 in embryonic and adult tissues. Development *119*, 1329-1341.

Murashov, A.K., Pak, E.S., Hendricks, W.A., Owensby, J.P., Sierpinski, P.L., Tatko, L.M., and Fletcher, P.L. (2005). Directed differentiation of embryonic stem cells into dorsal interneurons. The FASEB Journal *19*, 252-254.

Nagy, A., Gocza, E., Diaz, E.M., Prideaux, V.R., Ivanyi, E., Markkula, M., and Rossant, J. (1990). Embryonic stem cells alone are able to support fetal development in the mouse. Development *110*, 815-821.

Nagy, A., Rossant, J., Nagy, R., Abramow-Newerly, W., and Roder, J.C. (1993). Derivation of completely cell culture-derived mice from early-passage embryonic stem cells. Proceedings of the National Academy of Sciences of the United States of America *90*, 8424-8428.

Narlis, M., Grote, D., Gaitan, Y., Boualia, S.K., and Bouchard, M. (2007). Pax2 and pax8 regulate branching morphogenesis and nephron differentiation in the developing kidney. Journal of the American Society of Nephrology *18*, 1121-1129.

Nemir, M., Croquelois, A., Pedrazzini, T., and Radtke, F. (2006). Induction of cardiogenesis in embryonic stem cells via downregulation of Notch1 signaling. Circulation Research *98*, 1471-1478.

Niederreither, K., Subbarayan, V., Dolle, P., and Chambon, P. (1999). Embryonic retinoic acid synthesis is essential for early mouse post-implantation development. Nature Genetics *21*, 444-448.

Nishinakamura, R., Matsumoto, Y., Nakao, K., Nakamura, K., Sato, A., Copeland, N.G., Gilbert, D.J., Jenkins, N.A., Scully, S., Lacey, D.L., *et al.* (2001). Murine homolog of SALL1 is essential for ureteric bud invasion in kidney development. Development *128*, 3105-3115.

Niwa, H., Burdon, T., Chambers, I., and Smith, A. (1998). Self-renewal of pluripotent embryonic stem cells is mediated via activation of STAT3. Genes and Development *12*, 2048-2060.
Noden, D.M., and Francis-West, P. (2006). The differentiation and morphogenesis of craniofacial muscles. Developmental Dynamics *235*, 1194-1218.

O'Connor R, J. (1938). Experiments on the development of the pronephric duct. Journal of Anatomy *73*, 145-154 141.

Obara-Ishihara, T., Kuhlman, J., Niswander, L., and Herzlinger, D. (1999). The surface ectoderm is essential for nephric duct formation in intermediate mesoderm. Development *126*, 1103-1108.

Ohuchi, H., Nakagawa, T., Yamamoto, A., Araga, A., Ohata, T., Ishimaru, Y., Yoshioka, H., Kuwana, T., Nohno, T., Yamasaki, M., *et al.* (1997). The mesenchymal factor, FGF10, initiates and maintains the outgrowth of the chick limb bud through interaction with FGF8, an apical ectodermal factor. Development *124*, 2235-2244.

Oliver, G., Wehr, R., Jenkins, N.A., Copeland, N.G., Cheyette, B.N., Hartenstein, V., Zipursky, S.L., and Gruss, P. (1995). Homeobox genes and connective tissue patterning. Development *121*, 693-705.

Oliver, J.A., Barasch, J., Yang, J., Herzlinger, D., and Al-Awqati, Q. (2002). Metanephric mesenchyme contains embryonic renal stem cells. American Journal of Physiology *283*, F799-809.

Ordahl, C.P., and Le Douarin, N.M. (1992). Two myogenic lineages within the developing somite. Development *114*, 339-353.

Papaioannou, V.E. (1982). Lineage analysis of inner cell mass and trophectoderm using microsurgically reconstituted mouse blastocysts. Journal of Embryology and Experimental Morphology *68*, 199-209.

Papaioannou, V.E., Gardner, R.L., McBurney, M.W., Babinet, C., and Evans, M.J. (1978). Participation of cultured teratocarcinoma cells in mouse embryogenesis. Journal of Embryology and Experimental Morphology *44*, 93-104.

Papaioannou, V.E., McBurney, M.W., Gardner, R.L., and Evans, M.J. (1975). Fate of teratocarcinoma cells injected into early mouse embryos. Nature *258*, 70-73.

Patsch, C., Kesseler, D., and Edenhofer, F. (2011). Genetic engineering of mammalian cells by direct delivery of FLP recombinase protein. Methods *53*, 386-393.

Pearson, S., Sroczynska, P., Lacaud, G., and Kouskoff, V. (2008). The stepwise specification of embryonic stem cells to hematopoietic fate is driven by sequential exposure to Bmp4, activin A, bFGF and VEGF. Development *135*, 1525-1535.

Pichel, J.G., Shen, L., Sheng, H.Z., Granholm, A.C., Drago, J., Grinberg, A., Lee, E.J., Huang, S.P., Saarma, M., Hoffer, B.J., *et al.* (1996). Defects in enteric innervation and kidney development in mice lacking GDNF. Nature *382*, 73-76.

Piotrowska-Nitsche, K., and Zernicka-Goetz, M. (2005). Spatial arrangement of individual 4-cell stage blastomeres and the order in which they are generated correlate with blastocyst pattern in the mouse embryo. Mechanisms of Development *122*, 487-500.

Plisov, S.Y., Yoshino, K., Dove, L.F., Higinbotham, K.G., Rubin, J.S. and Perantoni, A.O. (2001). TGF beta 2, LIF and FGF2 cooperate to induce nephrogenesis. Development *128*, 1045-1057

Poulson, D.F. (1937). Chromosomal Deficiencies and the Embryonic Development of Drosophila Melanogaster. Proceedings of the National Academy of Sciences of the United States of America *23*, 133-137.

Pourquie, O. (2003). The segmentation clock: converting embryonic time into spatial pattern. Science *301*, 328-330.

Pratt, H.P., Ziomek, C.A., Reeve, W.J., and Johnson, M.H. (1982). Compaction of the mouse embryo: an analysis of its components. Journal of Embryology and Experimental Morphology *70*, 113-132.

Pratt, T., Sharp, L., Nichols, J., Price, D.J., and Mason, J.O. (2000). Embryonic stem cells and transgenic mice ubiquitously expressing a tau-tagged green fluorescent protein. Developmental Biology *228*, 19-28.

Pritchard-Jones, K., Fleming, S., Davidson, D., Bickmore, W., Porteous, D., Gosden, C., Bard, J., Buckler, A., Pelletier, J., Housman, D., *et al.* (1990). The candidate Wilms' tumour gene is involved in genitourinary development. Nature *346*, 194-197.

Prozialeck, W.C., Lamar, P.C., and Appelt, D.M. (2004). Differential expression of E-cadherin, N-cadherin and beta-catenin in proximal and distal segments of the rat nephron. BMC Physiology *4*, 10.

Prusa, A.R., Marton, E., Rosner, M., Bernaschek, G., and Hengstschlager, M. (2003). Oct-4-expressing cells in human amniotic fluid: a new source for stem cell research? Human Reproduction *18*, 1489-1493.

Prusa, A.R., Marton, E., Rosner, M., Bettelheim, D., Lubec, G., Pollack, A., Bernaschek, G., and Hengstschlager, M. (2004). Neurogenic cells in human amniotic fluid. American Journal of Obstetrics and Gynecology *191*, 309-314.

Puschel, A.W., Westerfield, M., and Dressler, G.R. (1992). Comparative analysis of Pax-2 protein distributions during neurulation in mice and zebrafish. Mechanisms of Development *38*, 197-208.

Putaala, H., Soininen, R., Kilpelainen, P., Wartiovaara, J., and Tryggvason, K. (2001). The murine nephrin gene is specifically expressed in kidney, brain and pancreas: inactivation of the gene leads to massive proteinuria and neonatal death. Human Molecular Genetics *10*, 1-8.

Qi, H., Rand, M.D., Wu, X., Sestan, N., Wang, W., Rakic, P., Xu, T., and Artavanis-Tsakonas, S. (1999). Processing of the notch ligand delta by the metalloprotease Kuzbanian. Science *283*, 91-94.

Qiao, J., Cohen, D., and Herzlinger, D. (1995). The metanephric blastema differentiates into collecting system and nephron epithelia in vitro. Development *121*, 3207-3214.

Qiao, J., Uzzo, R., Obara-Ishihara, T., Degenstein, L., Fuchs, E., and Herzlinger, D. (1999). FGF-7 modulates ureteric bud growth and nephron number in the developing kidney. Development *126*, 547-554.

Quaggin, S.E., Schwartz, L., Cui, S., Igarashi, P., Deimling, J., Post, M., and Rossant, J. (1999). The basic-helix-loop-helix protein pod1 is critically important for kidney and lung organogenesis. Development *126*, 5771-5783.

Raatikainen-Ahokas, A., Hytonen, M., Tenhunen, A., Sainio, K., and Sariola, H. (2000). BMP-4 affects the differentiation of metanephric mesenchyme and reveals an early anterior-posterior axis of the embryonic kidney. Developmental Dynamics *217*, 146-158.

Ravin, H.A., Zacks, S.I., and Seligman, A.M. (1952). Histochemical localization of acetyl cholinesterase in the central nervous system and myoneural junction. Journal of the National Cancer Institute *13*, 257-259.

Ray, W.J., Yao, M., Mumm, J., Schroeter, E.H., Saftig, P., Wolfe, M., Selkoe, D.J., Kopan, R., and Goate, A.M. (1999). Cell surface presenilin-1 participates in the gamma-secretase-like proteolysis of Notch. The Journal of Biological Chemistry *274*, 36801-36807.

Ren, X., Zhang, J., Gong, X., Niu, X., Zhang, X., Chen, P., and Zhang, X. (2010). Differentiation of murine embryonic stem cells toward renal lineages by conditioned medium from ureteric bud cells in vitro. Acta Biochimica et Biophysica Sinica *42*, 464-471.

Rodda, D.J., Chew, J.L., Lim, L.H., Loh, Y.H., Wang, B., Ng, H.H., and Robson, P. (2005). Transcriptional regulation of nanog by OCT4 and SOX2. The Journal of Biological Chemistry *280*, 24731-24737.

Ross, E.A., Williams, M.J., Hamazaki, T., Terada, N., Clapp, W.L., Adin, C., Ellison, G.W., Jorgensen, M., and Batich, C.D. (2009). Embryonic stem cells proliferate and differentiate when seeded into kidney scaffolds. Journal of the American Society of Nephrology *20*, 2338-2347.

Rossant, J. (1975). Investigation of the determinative state of the mouse inner cell mass. I. Aggregation of isolated inner cell masses with morulae. Journal of Embryology and Experimental Morphology *33*, 979-990.

Ruotsalainen, V., Ljungberg, P., Wartiovaara, J., Lenkkeri, U., Kestila, M., Jalanko, H., Holmberg, C., and Tryggvason, K. (1999). Nephrin is specifically located at the slit diaphragm of glomerular podocytes. Proceedings of the National Academy of Sciences of the United States of America *96*, 7962-7967.

Rupprecht, H.D., Drummond, I.A., Madden, S.L., Rauscher, F.J., 3rd, and Sukhatme, V.P. (1994). The Wilms' tumor suppressor gene WT1 is negatively autoregulated. The Journal of Biological Chemistry *269*, 6198-6206.

Ruzicka, D.L., and Schwartz, R.J. (1988). Sequential activation of alpha-actin genes during avian cardiogenesis: vascular smooth muscle alpha-actin gene transcripts mark the onset of cardiomyocyte differentiation. The Journal of Cell Biology *107*, 2575-2586.

Ryan, G., Steele-Perkins, V., Morris, J.F., Rauscher, F.J., 3rd, and Dressler, G.R. (1995). Repression of Pax-2 by WT1 during normal kidney development. Development *121*, 867-875.

Sainio, K. (2003). Development of the mesonephric kidney. In The Kidney: From Normal Development to Congenital Disease, P.D. Vize, A.S. Woolf, and J.B.L. Bard, eds. (London, Academic Press), pp. 75-84.

Sainio, K., Suvanto, P., Davies, J., Wartiovaara, J., Wartiovaara, K., Saarma, M., Arumae, U., Meng, X., Lindahl, M., Pachnis, V.*, et al.* (1997). Glial-cell-line-derived neurotrophic factor is required for bud initiation from ureteric epithelium. Development *124*, 4077-4087.

Sakurai, H., Bush, K.T., and Nigam, S.K. (2001). Identification of pleiotrophin as a mesenchymal factor involved in ureteric bud branching morphogenesis. Development *128*, 3283-3293.

Samakovlis, C., Manning, G., Steneberg, P., Hacohen, N., Cantera, R., and Krasnow, M.A. (1996). Genetic control of epithelial tube fusion during Drosophila tracheal development. Development *122*, 3531-3536.

Sanchez, M.P., Silos-Santiago, I., Frisen, J., He, B., Lira, S.A., and Barbacid, M. (1996). Renal agenesis and the absence of enteric neurons in mice lacking GDNF. Nature *382*, 70-73.

Sariola, H. (2002). Nephron induction. Nephrology Dialysis Transplantation *17 Suppl 9*, 88-90.

Sariola, H., and Philipson, L. (1999). Bridge over troubled waters. Nature Medicine *5*, 22-23.

Sariola, H., Sainio, K., and Bard, J. (2003). Fates of the metanephric mesenchyme. In The Kidney: From Normal Development to Congenital Disease, P. Vise, A. Woolf, and J. Bard, eds. (London, Academic Press), pp. 181-193.

Sasaki, H., and Hogan, B.L. (1993). Differential expression of multiple fork head related genes during gastrulation and axial pattern formation in the mouse embryo. Development *118*, 47-59.

Satchell, S.C., and Braet, F. (2009). Glomerular endothelial cell fenestrations: an integral component of the glomerular filtration barrier. American Journal of Physiology Renal physiology *296*, F947-956.

Sawtell, N.M., and Lessard, J.L. (1989). Cellular distribution of smooth muscle actins during mammalian embryogenesis: expression of the alpha-vascular but not the gamma-enteric isoform in differentiating striated myocytes. The Journal of Cell Biology *109*, 2929-2937.

Saxen, L. (1987). Organogenesis of the kidney (Cambridge, Cambridge University Press).

Saxen, L., Vainio, T., and Toivonen, S. (1962). Effect of polyoma virus on mouse kidney rudiment in vitro. Journal of the National Cancer Institute *29*, 597-631.

Schedl, A., and Hastie, N.D. (2000). Cross-talk in kidney development. Current Opinion in Genetics and Development *10*, 543-549.

Schlondorff, D., and Banas, B. (2009). The mesangial cell revisited: no cell is an island. Journal of the American Society of Nephrology *20*, 1179-1187.

Scholer, H.R., Dressler, G.R., Balling, R., Rohdewohld, H., and Gruss, P. (1990). Oct-4: a germline-specific transcription factor mapping to the mouse t-complex. The EMBO Journal *9*, 2185-2195.

Schroeder, T., Meier-Stiegen, F., Schwanbeck, R., Eilken, H., Nishikawa, S., Hasler, R., Schreiber, S., Bornkamm, G.W., and Just, U. (2006). Activated Notch1 alters differentiation of embryonic stem cells into mesodermal cell lineages at multiple stages of development. Mechanisms of Development *123*, 570-579.

Schuchardt, A., D'Agati, V., Larsson-Blomberg, L., Costantini, F., and Pachnis, V. (1994). Defects in the kidney and enteric nervous system of mice lacking the tyrosine kinase receptor Ret. Nature *367*, 380-383.

Sekine, M., Monkawa, T., Morizane, R., Matsuoka, K., Taya, C., Akita, Y., Joh, K., Itoh, H., Hayashi, M., Kikkawa, Y.*, et al.* (2011). Selective depletion of mouse kidney proximal straight tubule cells causes acute kidney injury. Transgenic Research.

Self, M., Lagutin, O.V., Bowling, B., Hendrix, J., Cai, Y., Dressler, G.R., and Oliver, G. (2006). Six2 is required for suppression of nephrogenesis and progenitor renewal in the developing kidney. The EMBO Journal *25*, 5214-5228.

Seydoux, G., and Greenwald, I. (1989). Cell autonomy of lin-12 function in a cell fate decision in C. elegans. Cell *57*, 1237-1245.

Shao, X., Johnson, J.E., Richardson, J.A., Hiesberger, T., and Igarashi, P. (2002). A minimal Ksp-cadherin promoter linked to a green fluorescent protein reporter gene exhibits tissue-specific expression in the developing kidney and genitourinary tract. Journal of the American Society of Nephrology *13*, 1824-1836.

Shawber, C., Boulter, J., Lindsell, C.E., and Weinmaster, G. (1996). Jagged2: a serrate-like gene expressed during rat embryogenesis. Developmental Biology *180*, 370-376.

Sheridan, J.M., Taoudi, S., Medvinsky, A., and Blackburn, C.C. (2009). A novel method for the generation of reaggregated organotypic cultures that permits juxtaposition of defined cell populations. Genesis *47*, 346-351.

Shutter, J.R., Scully, S., Fan, W., Richards, W.G., Kitajewski, J., Deblandre, G.A., Kintner, C.R., and Stark, K.L. (2000). Dll4, a novel Notch ligand expressed in arterial endothelium. Genes and Development *14*, 1313-1318.

Sikri, K.L., Foster, C.L., MacHugh, N., and Marshall, R.D. (1981). Localization of Tamm-Horsfall glycoprotein in the human kidney using immuno-fluorescence and immuno-electron microscopical techniques. Journal of Anatomy *132*, 597-605.

Silva, J., Barrandon, O., Nichols, J., Kawaguchi, J., Theunissen, T.W., and Smith, A. (2008). Promotion of reprogramming to ground state pluripotency by signal inhibition. PLoS Biology *6*, e253.

Siminovitch, L., McCulloch, E.A., and Till, J.E. (1963). The distribution of colony-forming cells among spleen colonies. Journal of Cellular Physiology *62*, 327-336.

Skeggs, L.T., Jr., Marsh, W.H., Kahn, J.R., and Shumway, N.P. (1954). The existence of two forms of hypertensin. The Journal of Experimental Medicine *99*, 275-282.

Smith, A.G. (2001). Embryo-derived stem cells: of mice and men. Annual Review of Cell and Developmental Biology *17*, 435-462.

Smith, A.G., Heath, J.K., Donaldson, D.D., Wong, G.G., Moreau, J., Stahl, M., and Rogers, D. (1988). Inhibition of pluripotential embryonic stem cell differentiation by purified polypeptides. Nature *336*, 688-690.

Smith, A.G., and Hooper, M.L. (1987). Buffalo rat liver cells produce a diffusible activity which inhibits the differentiation of murine embryonal carcinoma and embryonic stem cells. Developmental Biology *121*, 1-9.

Smith, C., and Mackay, S. (1991). Morphological development and fate of the mouse mesonephros. Journal of Anatomy *174*, 171-184.

Smith, E.M., Mitsi, M., Nugent, M.A., and Symes, K. (2009). PDGF-A interactions with fibronectin reveal a critical role for heparan sulfate in directed cell migration during Xenopus gastrulation. Proceedings of the National Academy of Sciences of the United States of America *106*, 21683-21688.

Smith, J.L., Gesteland, K.M., and Schoenwolf, G.C. (1994). Prospective fate map of the mouse primitive streak at 7.5 days of gestation. Developmental Dynamics *201*, 279-289.

So, P.L., and Danielian, P.S. (1999). Cloning and expression analysis of a mouse gene related to Drosophila odd-skipped. Mechanisms of Development *84*, 157-160.

St John, P.L., and Abrahamson, D.R. (2001). Glomerular endothelial cells and podocytes jointly synthesize laminin-1 and -11 chains. Kidney International *60*, 1037-1046.

Stark, K., Vainio, S., Vassileva, G., and McMahon, A.P. (1994). Epithelial transformation of metanephric mesenchyme in the developing kidney regulated by Wnt-4. Nature *372*, 679-683.

Steenhard, B.M., Isom, K.S., Cazcarro, P., Dunmore, J.H., Godwin, A.R., St John, P.L., and Abrahamson, D.R. (2005). Integration of embryonic stem cells in metanephric kidney organ culture. Journal of the American Society of Nephrology *16*, 1623-1631.

Stemple, D.L. (2005). Structure and function of the notochord: an essential organ for chordate development. Development *132*, 2503-2512.

Sugi, Y., and Lough, J. (1992). Onset of expression and regional deposition of alpha-smooth and sarcomeric actin during avian heart development. Developmental Dynamics *193*, 116-124.

Taira, M., Otani, H., Jamrich, M., and Dawid, I.B. (1994). Expression of the LIM class homeobox gene Xlim-1 in pronephros and CNS cell lineages of Xenopus embryos is affected by retinoic acid and exogastrulation. Development *120*, 1525-1536.

Takahashi, K., and Yamanaka, S. (2006). Induction of pluripotent stem cells from mouse embryonic and adult fibroblast cultures by defined factors. Cell *126*, 663-676.

Takata, K., Matsuzaki, T., Tajika, Y., Ablimit, A., and Hasegawa, T. (2008). Localization and trafficking of aquaporin 2 in the kidney. Histochemistry and Cell Biology *130*, 197-209.

Takezawa, T., Inoue, M., Aoki, S., Sekiguchi, M., Wada, K., Anazawa, H., and Hanai, N. (2000). Concept for organ engineering: a reconstruction method of rat liver for in vitro culture. Tissue Engineering *6*, 641-650.

Tam, P.P., and Behringer, R.R. (1997). Mouse gastrulation: the formation of a mammalian body plan. Mechanisms of Development *68*, 3-25.

Thadhani, R., Pascual, M., and Bonventre, J.V. (1996). Acute renal failure. The New England Journal of Medicine *334*, 1448-1460.

Theiler, K. (1989). The House Mouse: Atlas of Embryonic Development (New York, Springer-Verlag).

Thomas, P., and Beddington, R. (1996). Anterior primitive endoderm may be responsible for patterning the anterior neural plate in the mouse embryo. Current Biology *6*, 1487-1496.

Thomson, J.A., Itskovitz-Eldor, J., Shapiro, S.S., Waknitz, M.A., Swiergiel, J.J., Marshall, V.S., and Jones, J.M. (1998). Embryonic stem cell lines derived from human blastocysts. Science *282*, 1145-1147.

Till, J.E., and Mc, C.E. (1961). A direct measurement of the radiation sensitivity of normal mouse bone marrow cells. Radiation Research *14*, 213-222.

Till, J.E., McCulloch, E.A., and Siminovitch, L. (1964). A Stochastic Model of Stem Cell Proliferation, Based on the Growth of Spleen Colony-Forming Cells. Proceedings of the National Academy of Sciences of the United States of America *51*, 29-36.

Toivonen, S., and Saxen, L. (1955). The simultaneous inducing action of liver and bone-marrow of the guinea-pig in implantation and explantation experiments with embryos of Triturus. Experimental Cell Research *Suppl* 3, 346-357.

Torban, E., Dziarmaga, A., Iglesias, D., Chu, L.L., Vassilieva, T., Little, M., Eccles, M., Discenza, M., Pelletier, J., and Goodyer, P. (2006). PAX2 activates WNT4 expression during mammalian kidney development. The Journal of Biological Chemistry *281*, 12705-12712.

Torres, M., Gomez-Pardo, E., Dressler, G.R., and Gruss, P. (1995). Pax-2 controls multiple steps of urogenital development. Development *121*, 4057-4065.

Tsai, M.S., Hwang, S.M., Tsai, Y.L., Cheng, F.C., Lee, J.L., and Chang, Y.J. (2006). Clonal amniotic fluid-derived stem cells express characteristics of both mesenchymal and neural stem cells. Biology of Reproduction *74*, 545-551.

Unbekandt, M., and Davies, J.A. (2010). Dissociation of embryonic kidneys followed by reaggregation allows the formation of renal tissues. Kidney International *77*, 407-416.

Vainio, S., and Lin, Y. (2002). Coordinating early kidney development: lessons from gene targeting. Nature Reviews *3*, 533-543.

van Laake, L.W., Passier, R., Monshouwer-Kloots, J., Verkleij, A.J., Lips, D.J., Freund, C., den Ouden, K., Ward-van Oostwaard, D., Korving, J., Tertoolen, L.G., *et al.* (2007). Human embryonic stem cell-derived cardiomyocytes survive and mature in the mouse heart and transiently improve function after myocardial infarction. Stem Cell Research *1*, 9-24.

Vassilopoulos, G., Wang, P.R., Russell, D.W. (2003). Transplanted bone marrow regenerates liver by cell fusion. Nature *422*, 901–904.

Vega, Q.C., Worby, C.A., Lechner, M.S., Dixon, J.E., and Dressler, G.R. (1996). Glial cell line-derived neurotrophic factor activates the receptor tyrosine kinase RET and promotes kidney morphogenesis. Proceedings of the National Academy of Sciences of the United States of America *93*, 10657-10661.

Vestweber, D., Gossler, A., Boller, K., and Kemler, R. (1987). Expression and distribution of cell adhesion molecule uvomorulin in mouse preimplantation embryos. Developmental Biology *124*, 451-456.

Vetter, M.R., and Gibley, C.W., Jr. (1966). Morphogenesis and histochemistry of the developing mouse kidney. Journal of Morphology *120*, 135-155.

Vigneau, C., Polgar, K., Striker, G., Elliott, J., Hyink, D., Weber, O., Fehling, H.J., Keller, G., Burrow, C., and Wilson, P. (2007). Mouse embryonic stem cell-derived embryoid bodies generate progenitors that integrate long term into renal proximal tubules in vivo. Journal of the American Society of Nephrology *18*, 1709-1720.

Villanueva, S., Glavic, A., Ruiz, P., and Mayor, R. (2002). Posteriorization by FGF, Wnt, and retinoic acid is required for neural crest induction. Developmental Biology *241*, 289-301.

Vize, P.D., Carroll, T.J., and Wallingford, J.B. (2003a). Induction, development, and physiology of the pronephric tubules. In The Kidney: From Normal Development to Congenital Disease, P.D. Vize, A.S. Woolf, and J.B.L. Bard, eds. (London, Academic Press), pp. 19-47.

Vize, P.D., Jones, E.A., and Pfister, R. (1995). Development of the Xenopus pronephric system. Developmental Biology *171*, 531-540.

Vize, P.D., Woolf, A.S., and Bard, J.B.L. (2003b). The Kidney: From Normal Development to Congenital Disease, 1 edn (London, Academic Press).

Wald, A., and Wolfowitz, J. (1939). Confidence Limits for Continuous Distribution Functions. The Annals of Mathematical Statistics *10*, 105-118.

Walmsley, S.J., Broeckling, C., Hess, A., Prenni, J., and Curthoys, N.P. (2010). Proteomic analysis of brush-border membrane vesicles isolated from purified proximal convoluted tubules. American Journal of Physiology Renal Physiology *298*, F1323-1331.

Wang. X., Willenbring, H., Akkari, Y., Torimaru, Y., Foster, M., Al-Dhalimy, M., Lagasse, E., Finegold, M., Olson, S. and Grompe, M. (2003). Cell fusion is the principal source of bone-marrow-derived hepatocytes. Nature *422*, 897–901.

Watanabe, T., and Raff, M.C. (1990). Rod photoreceptor development in vitro: intrinsic properties of proliferating neuroepithelial cells change as development proceeds in the rat retina. Neuron *4*, 461-467.

Watson, A.J., Damsky, C.H., and Kidder, G.M. (1990). Differentiation of an epithelium: factors affecting the polarized distribution of Na+,K(+)-ATPase in mouse trophectoderm. Developmental Biology *141*, 104-114.

Weimann, J.M., Charlton, C.A., Brazelton, T.R., Hackman, R.C., Blau, H.M. (2003). Contribution of transplanted bone marrow cells to Purkinje neurons in human adult brains. Proceedings of the National Academy of Sciences of the United States of America *100*, 2088–2093.

Weimann, J.M., Weimann, J.M., Johansson, C.B., Trejo, A., Blau, H.M. (2003). Stable reprogrammed heterokaryons form spontaneously in Purkinje neurons after bone marrow transplant. Nature Cell Biology *5*, 959–966.

Weingarten, M.D., Lockwood, A.H., Hwo, S.Y., and Kirschner, M.W. (1975). A protein factor essential for microtubule assembly. Proceedings of the National Academy of Sciences of the United States of America *72*, 1858-1862.

Weissman, I.L., Anderson, D.J., and Gage, F. (2001). Stem and progenitor cells: origins, phenotypes, lineage commitments, and transdifferentiations. Annual Review of Cell and Developmental Biology *17*, 387-403.

West, J.D. (1984). Cell markers. In Chimeras in Developmental Biology, N.L. Douarin, and A. McLaren, eds. (London, Academic Press), pp. 39-63.

Wharton, K.A., Johansen, K.M., Xu, T., and Artavanis-Tsakonas, S. (1985). Nucleotide sequence from the neurogenic locus notch implies a gene product that shares homology with proteins containing EGF-like repeats. Cell *43*, 567-581.

Wilkinson, D.G., Bhatt, S., and Herrmann, B.G. (1990). Expression pattern of the mouse T gene and its role in mesoderm formation. Nature *343*, 657-659.

Wilkinson, H.A., Fitzgerald, K., and Greenwald, I. (1994). Reciprocal changes in expression of the receptor lin-12 and its ligand lag-2 prior to commitment in a C. elegans cell fate decision. Cell *79*, 1187-1198.

Williams, R.L., Hilton, D.J., Pease, S., Willson, T.A., Stewart, C.L., Gearing, D.P., Wagner, E.F., Metcalf, D., Nicola, N.A., and Gough, N.M. (1988). Myeloid leukaemia inhibitory factor maintains the developmental potential of embryonic stem cells. Nature *336*, 684-687.

Wilm, B., James, R.G., Schultheiss, T.M., and Hogan, B.L. (2004). The forkhead genes, Foxc1 and Foxc2, regulate paraxial versus intermediate mesoderm cell fate. Developmental Biology *271*, 176-189.

Wilson, A., and Radtke, F. (2006). Multiple functions of Notch signaling in self-renewing organs and cancer. FEBS Letters *580*, 2860-2868.

Wolfe, M.S., and Kopan, R. (2004). Intramembrane proteolysis: theme and variations. Science *305*, 1119-1123.

Wu, G., Markowitz, G.S., Li, L., D'Agati, V.D., Factor, S.M., Geng, L., Tibara, S., Tuchman, J., Cai, Y., Park, J.H., *et al.* (2000). Cardiac defects and renal failure in mice with targeted mutations in Pkd2. Nature Genetics *24*, 75-78.

Xu, P.X., Adams, J., Peters, H., Brown, M.C., Heaney, S., and Maas, R. (1999). Eya1-deficient mice lack ears and kidneys and show abnormal apoptosis of organ primordia. Nature Genetics *23*, 113-117.

Yang, C.H., Axelrod, J.D., and Simon, M.A. (2002). Regulation of Frizzled by fat-like cadherins during planar polarity signaling in the Drosophila compound eye. Cell *108*, 675-688.

Ying, Q.L., Wray, J., Nichols, J., Batlle-Morera, L., Doble, B., Woodgett, J., Cohen, P., and Smith, A. (2008). The ground state of embryonic stem cell self-renewal. Nature *453*, 519-523.

Zhou, W., Boucher, R.C., Bollig, F., Englert, C., and Hildebrandt, F. (2010). Characterization of mesonephric development and regeneration using transgenic zebrafish. American Journal of Physiology *299*, F1040-1047.

Zhou, X., Sasaki, H., Lowe, L., Hogan, B.L., and Kuehn, M.R. (1993). Nodal is a novel TGF-beta-like gene expressed in the mouse node during gastrulation. Nature *361*, 543-547.

Appendix I

Publications

SHORT REPORT

Organogenesis 7:2, 1-5; April/May/June 2011; © 2011 Landes Bioscience

An improved kidney dissociation and re-aggregation culture system results in nephrons arranged organotypically around a single collecting duct system

Veronika Ganeva, Mathieu Unbekandt and Jamie A. Davies*

University of Edinburgh Centre for Integrative Physiology; Hugh Robson Building; Edinburgh, Scotland UK

Key words: renal, tissue engineering, kidney development, ureteric bud, branching, organ culture, 3Rs

Methods for constructing engineered "tissues" from simple suspensions of cells are valuable for investigations into basic developmental biology and for tissue engineering. We recently published a method for producing embryonic renal tissues from suspensions of embryonic mouse renal cells. This method reproduced the anatomies and differentiation states of nephrons and stroma very well; it had the limitation, however, that what would in normal development be a single, highly-branched collecting duct tree leading to a ureter developed, in the engineered system, as a multitude of very small collecting duct trees. These were isolated from each other and therefore would not be effective for draining urine to a common exit, were the tissue to be supplied with blood and physiologically active. Here, we report an improvement on the original method; it results in the formation of nephrons arranged around one single collecting duct tree as would happen in a normal kidney.

Introduction

Developing methods for reconstructing organ rudiments from simple suspensions of cells is important for several reasons. For basic science, it allows researchers to investigate processes of self-organization;[1,2] it also allows them to make fine-grained chimaeras of wild-type and mutant cells to determine whether mutations act in a cell-autonomous manner and whether they bias a cell's choice of fates. For clinical application, an ability to reconstruct organ rudiments from suspensions of cells that have no a priori spatial information is critical to the aim of producing tissues de novo from stem cells cultured in bulk.[3,4]

Recently, we published a method for reconstruction of embryonic kidney tissues from suspensions of cells.[5] For this method, cell suspensions are obtained by enzyme-assisted disaggregation of E11.5 mouse kidney rudiments, followed by temporary pharmacological inhibition of ROCK to reduce loss of cells during this single-cell suspension phase of the experiment. The suspended cells are re-aggregated and they form tubes that express markers typical of ureteric bud/collecting duct. Near these tubes, nephron progenitors form from the mesenchyme and go through their normal morphological sequence of development to produce nephrons with defined Bowman's capsules, proximal tubules and distal tubules; each expresses specific markers in their usual stages and places. The nephrons connect to the nearby ureteric bud/collecting duct structures to make a continuous lumen, as in normal development. In our original report and also in a second paper,[6] we demonstrated the utility of the system for making fine-grained chimaeras and for siRNA-mediated knockdown of gene expression.

The system, as we described it, has one serious anatomical deficiency: because the ureteric bud-derived cells re-aggregate to form multiple small branching ureteric buds rather than one large one, the normal tree-like arrangement of the kidney is missing. At high magnification, a section of the re-aggregated tissue is difficult to distinguish from a section of the cortex of a normal developing kidney but at low magnification the difference is obvious; there is no one, dominating collecting duct tree and therefore none of the cortical-medullary differences in tissue organization that would normally be imposed by such a tree. Functionally, this deficiency would be serious for any attempts towards practical renal tissue engineering, because urine made by the nephrons needs to drain away via the collecting ducts: multitudes of isolated small collecting ducts will not achieve this, whereas a single collecting duct system leading to a ureter would. The cortico-medullary organization imposed by a single collecting duct tree on the kidney is also important, in a normal kidney, for water recovery by counter-current multiplication.

Work published by Grobstein over half a century ago suggested that it is possible to combine intact metanephrogenic mesenchyme tissue with an intact ureteric bud and induce development of both nephrons and ureteric bud.[7] Similarly, Auerbach and

*Correspondence to: Jamie A. Davies; Email: jamie.davies@ed.ac.uk
Submitted: 01/10/11; Accepted: 01/12/11
DOI:

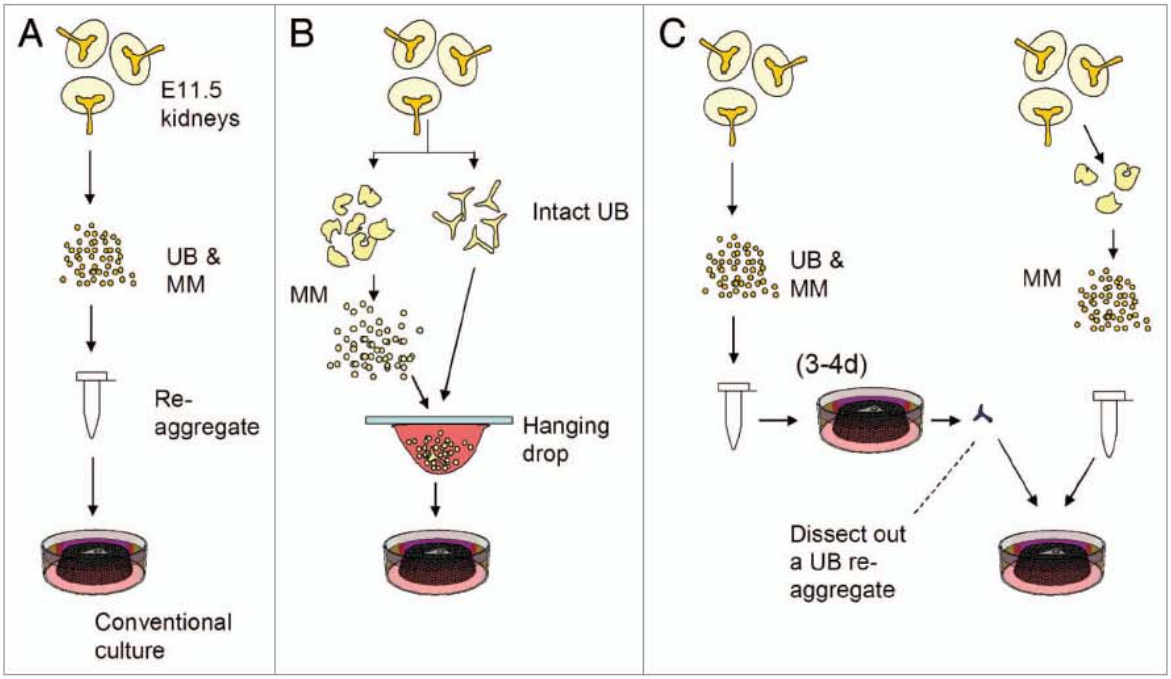

Figure 1. Diagrams to represent the original disaggregation–re-aggregation method, and the improved methods reported here. (A) Depicts the original method of Unbekandt and Davies,[5] in which whole E11.5 kidneys are disaggregated, re-aggregated and cultured. (B) Depicts "method 1" of this paper, in which disaggregated mesenchyme cells (MM) are combined with intact ureteric buds (UB) in hanging drops, then cultured. (C) Depicts "method 2" of this paper, in which the original method is used first to create re-aggregated tissue, then a single "ureteric bud" is dissected from the re-aggregate and combined with re-aggregated mesenchyme.

Grobstein showed that it was possible to combine disaggregated metanephrogenic mesenchyme with a surrogate inducer (spinal cord rather than ureteric bud) and still obtain nephrons.[8] Here, we combine these classical approaches with our modern, pharmacology-assisted dissociation-reaggregation method[5] to generate reaggregate tissues based on a single ureteric bud. We do this two ways (Fig. 1); in one, disaggregated mesenchyme is recombined with an intact ureteric bud, and in the other, disaggregated mesenchyme is combined with a single ureteric bud fragment that has re-aggregated from a previous round of disaggregation and re-aggregation. Both methods result in the reconstruction of organ rudiments that are based on a single branched collecting duct tree; the first method is easier, while the second is more powerful in that it allows formation of the entire renal structure from simple suspensions of cells.

Results

Method 1: combining intact ureteric bud with dissociated metanephric mesenchyme results in an organotypic arrangement of tissues. Our first method combines an intact ureteric bud, isolated straight from an embryo, with a disaggregated and re-aggregated mesenchymal compartment. Metanephric mesenchyme was isolated from E11.5 mouse kidneys and was reduced to a suspension of individual cells. The suspension was then placed in a hanging drop to which a ureteric bud, also isolated from E11.5 kidneys but not disaggregated, was added.[5] Cells placed in the hanging drop congregated at its bottom to make a coherent mass (Fig. 2A). After a day, this mass was transferred to a normal renal organ culture environment, consisting of a polycarbonate filter at the surface of medium.

Under these conditions, mesenchyme of the cultures formed a number of developing nephrons located near to the upper branches of the single collecting duct tree (Fig. 2B). This arrangement contrasts with the random disposition of nephrons and small 'ureteric buds' that is produced when an entire kidney rudiment is disaggregated and re-aggregated (Fig. 2C).[5] The general layout of the tissues compares well with those of embryonic kidneys cultured intact using the traditional method of growing them on filters at the surface of medium[10,11] (Fig. 2D). There is, though, some difference in the shape of the collecting duct system: some of it initially extends around the edge of the aggregate and some branches therefore extend inwards.

Method 2: combining a single re-aggregated ureteric bud cyst with re-aggregated mesenchyme results in an organotypic arrangement of tissues. Our second method uses only tissues that have been re-aggregated from cell suspensions. The first step is a conventional disaggregation and re-aggregation of a complete kidney, using the technique already described in reference 5. As reported before, after 4 or 5 days (1 in ROCK inhibitor and 3 or 4 without), many ureteric bud cysts and nephrons form in these re-aggregates (Fig. 3A and C). Ureteric bud cysts were then isolated, by micro-dissection, from these re-aggregates and were placed on a filter at the surface of conventional medium. To each ureteric bud was added a pellet of mesenchyme, re-aggregated from a suspension of individual, disaggregated mesenchyme cells.

Under these conditions, the re-aggregated ureteric bud 'cyst' developed into a single, extensively-branched ureteric bud/collecting duct system over 3–4 days (Fig. 3B and D). Adjacent to the branches of the bud, nephrons formed, showing their normal morphology and they appeared to connect to the bud/collecting duct system (Fig. 3B and D). The branching was directed outwards as usual. Essentially, the anatomy is typical of that of a normal, intact embryonic kidney (Fig. 2D).

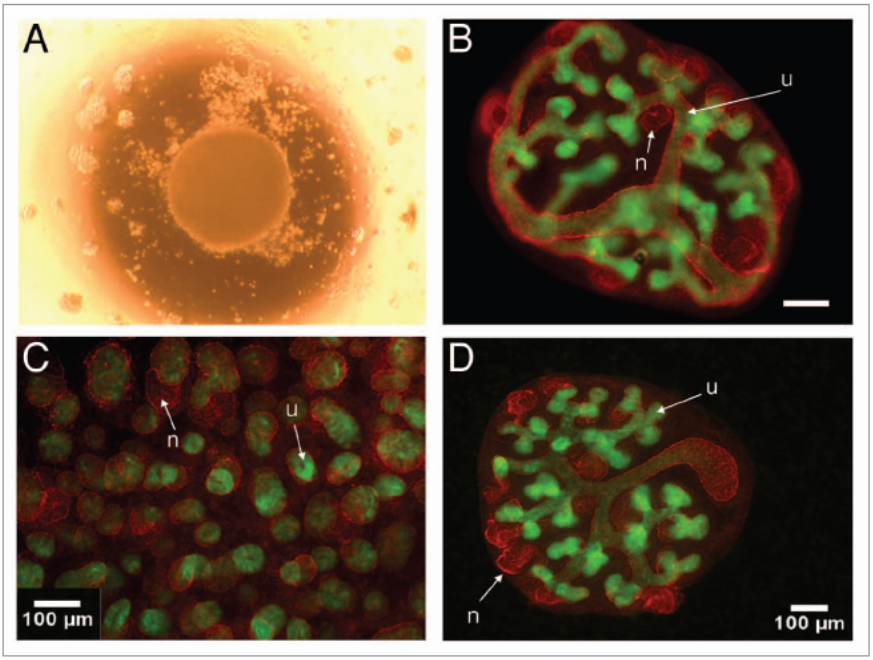

Figure 2. Method 1: combination of re-aggregated mesenchyme with an intact ureteric bud. (A) Metanephrogenic mesenchyme cells form a compact mass at the bottom of a hanging drop. (B) When a ureteric bud is added to the hanging drop, and the resulting tissue mass is transferred to a conventional organ culture system 24 h later, it goes on to develop over the next 3 days to produce a branching ureteric bud ("u", expressing calbindin-D^{28k}: green, as well as laminin: red) and comma- and S-shaped developing nephrons ("n", red only) form near the tips of some of its branches. (C) In a standard reaggregate, made by disaggregation of the complete kidney,[5] short tubules of both types are present ("u", "n" as before) but large-scale organization is not apparent. (D) An intact kidney in organ culture, shown for the purposes of comparison, labels as before.

Discussion

In this short report, we have demonstrated two methods for producing re-aggregated embryonic renal tissues that have a significantly more organotypic arrangement of tissues than do tissues produced in the basic dissociation and re-aggregation method.[5,6] The key improvement is that these techniques result in nephrons being arranged as they should be in relation to a single, branching ureteric bud.

The first method, use of an intact ureteric bud, is the simplest and quickest, and it is suitable where there is no reason for dissociating the bud in the first place. Experiments on the basic developmental biology of nephrons, or on the ability of putative stem cells to integrate into nephrons and produce their specialized cell types, would be examples of such experiments. By including a step that involves the mesenchyme being a suspension of individual cells, the method allows the mixing of cells with different genotypes to make chimaeras for testing the cell autonomy of mutations or the effects of mutation in fate choice, but only within the mesenchyme-derived compartment (we have already demonstrated use of these techniques for the whole kidney re-aggregation system[5,6]).

The second method is more involved, but it retains the full power of the original dissociation-re-aggregation method to produce all of the tissues from simple suspensions of cells. This will allow the production of fine-grained chimaeras of all tissue types, even using different genotypes for mesenchyme and bud. Importantly, it means that a kidney that is properly-arranged around a single ureteric bud/collecting duct tree can be made from simple suspensions of cells, something that might be very important for building renal tissue from cultures of stem cells, which is a major research goal in the field.[12-15]

The basic disaggregation—re-aggregation method facilitates research on the processes of self-organization that take place at small scales, for example in the formation of nephrons. The systems described here, which have correctly-arranged large-scale anatomies, could extend this to accommodate research into process of self-organization at the whole-organ scale, for example cortical-medullary organization, directional growth of loops of Henle etc., in culture.[16] We therefore believe them to be of potential importance to basic research as well as tissue engineering. Furthermore, being culture, based they have the potential to contribute to a reduction in in vivo experimentation, at least in the initial stages of exploratory research.

Materials and Methods

Culture medium. Kidney culture medium (KCM) consisted of Eagle's MEM (Sigma cat # M5650) with 1% Penicillin/Streptomycin (Sigma cat # P4333) and 10% foetal calf serum (BioSera).

Dissection and disaggregation of embryonic kidney rudiments. E11.5 embryonic kidney rudiments were dissected, dissociated and then re-aggregated as we have described before.[5] For experiments that required them, intact ureteric buds were isolated by incubating kidneys in 2x Trypsin/EDTA solution (Sigma cat # T4174) in Eagle's MEM (Sigma cat # M5650) for 2 min at 37°C, transferring them to KCM to quench the trypsinization, and pulling ureteric buds away from their mesenchymes using 25-gauge needles. Ureteric buds were examined carefully to ensure that they were clean of mesenchyme cells (most were: the trypsinization separates the two tissues along the basement membrane). Mesenchymes destined for diasaggregation were

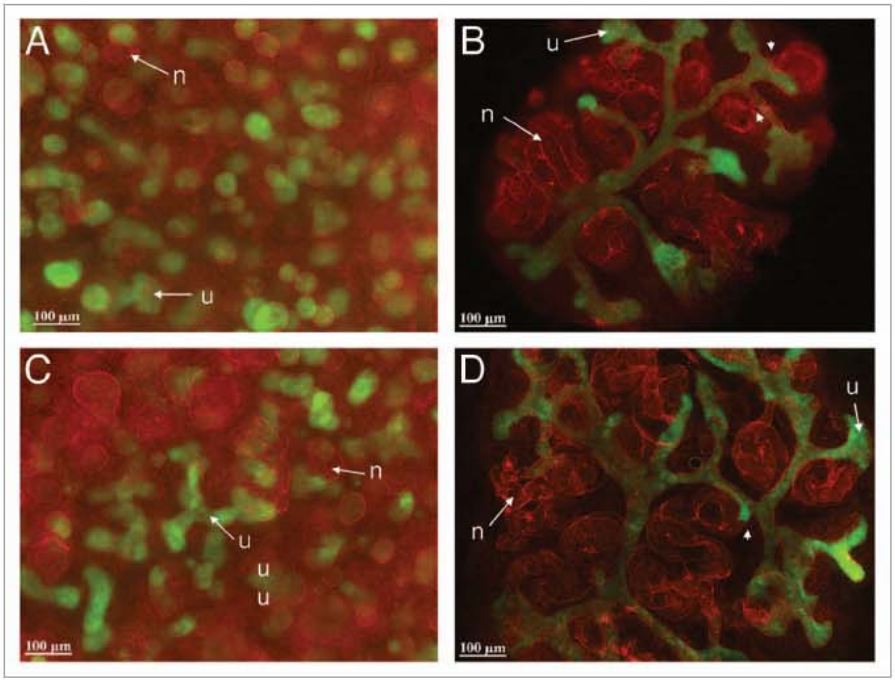

Figure 3. Method 2: both ureteric bud and mesenchyme coming from cell suspensions. To prepare re-aggregated ureteric buds for later combination with mesenchyme, dissociated E11 mouse embryonic kidney cells were reaggregated and cultured for one day with 1.25 µM glycyl-H1152-dihydrochloride and then for 3 (A) or 4 days (C) in plain kidney culture medium. Many cyst-like ureteric bud structures ("u", green, with red border) and primitive nephrons ("n" red border only) form in these conditions: the green immunostain detects CalbindinD^{28K} and the red detects laminin. A single ureteric bud structure was isolated from these reaggregates and cultured for 3 days (D) or 4 days (B) with a reaggregate of dissociated mesenchymal cells. Under these conditions, the ureteric bud 'u' structure grows and branches to make a tree characteristic of normal developing kidneys, and many nephrons 'n' can be observed, connecting to them (arrowheads).

isolated from E11.5 kidney rudiments. 10–15 mesenchymes were incubated for 2 minutes at 37°C degrees in PBS with 0.5x Trysin/EDTA and then in KCM to quench the trypsin effect. They were then placed in a 0.5 ml microcentrifuge tube containing 200 µL KCM and dissociated by vigorous trituration using a 200 µl Gilson tip, until a homogeneous suspension with no visible clumps was obtained. The cell suspension was filtered through a 40 micron cell strainer (Millipore) and the total number of cells was counted. Batches of about 10^5 mesenchymal cells were reaggregated by centrifuging them 3,000 rpm (800 g) for 2 minutes. For re-combination with an intact ureteric bud (i.e., 'method 1'), the resulting pellet was re-suspended in 25 µl KCM, which is enough for two hanging drops; for some hanging drop experiments, 10 µmol/L of the ROCK inhibitor Y27632 (Sigma) was included but this was later found this to be unnecessary for use with hanging drops that included intact ureteric buds. For re-combination with a ureteric bud re-aggregated cyst (i.e., 'method 2'), the pellet detached from the border of the tube, care being taken to keep it intact.

Re-aggregation of mesenchyme cell suspensions with an intact ureteric bud. Initial recombination of ureteric buds and mesenchyme suspensions was performed by a variation of the hanging drop method used by Sainio et al. for culture of ureteric buds.[9] 25 µL of mesenchyme suspension, made as above, was pipetted onto the inside of a 3.5 cm Petri dish lid to make two similarly-sized, separate drops and a single intact ureteric bud was added to each. The lid was inverted and placed over the Petri dish containing containing 2 mL of KCM to buffer the hanging drops against drying out. The dish lid was tapped gently to encourage suspended cells to sediment to the bottom of the hanging drop, and the drops were incubated overnight at 37°C, 5% CO_2. The recombined tissues were then transferred carefully, by pipette, to the top of a filter on a Trowell screen (as described for re-aggregated pellets[5]) and incubated for 3–5 days in plain KCM (with no Y27632).

Re-aggregation of mesenchyme re-aggregates with ureteric bud re-aggregates. First, conventional whole-kidney re-aggregates were produced using the standard method.[5] These were cultured for one day in presence of ROCK inhibitor (1.25 µM glycyl-H1152-dihydrochloride) and then for 3 or 4 days in KCM. Single ureteric bud cysts were identified by their size and shape and were dissected manually from these re-aggregates. Each individual cyst was placed in culture, on a polycarbonate filter at the culture medium/atmosphere interface and covered with a pellet containing about 10^5 re-aggregated mesenchymal cells, prepared as described above. The recombined tissues were incubated for 3 or 4 days in plain KCM at 37°C, 5% CO_2. A culture time of 3 days was applied when the initial conventional reaggregate, from which the ureteric bud rudiment was taken, was 1 day with ROCK inhibitor and 4 days without, and a culture time of 4 days was applied when the initial culture was 1 day with ROCK inhibitor and 3 days without, so that the total culture time from beginning to end, from the point of view of the ureteric bud, was always 8 days.

Immunohistochemistry. Tissues were fixed in methanol at -20°C and either stored in this liquid at this temperature until needed, or left for at least 10 minutes for fixation. Fixed specimens were washed in PBS for 30 minutes at room temperature and then incubated with a solution of primary antibodies diluted 1 in 100 in PBS overnight at 4°C. Primary antibodies were mouse anti-Calbindin (ab82812, Abcam) and rabbit anti-Laminin (L9393, Sigma). Samples were washed for 30 minutes in PBS and then incubated overnight at 4°C with secondary antibodies diluted 1 in 100 in PBS. Secondary antibodies were goat anti-mouse IgG-FITC (F0257, Sigma) and goat anti-rabbit IgG-TRITC (T5268, Sigma). A final wash in PBS was performed for at least 30 minutes. Images were obtained with Zeiss Imager A1 (Carl Zeiss, Welwyn Garden City, UK), Leica Ortholux II (Leica Microsystems GmbH, Wetzlar, Germany) and HUND

Wetzlar Wilovert (Helmut Hund GmbH, Wetzlar, Germany) microscopes. Whenever necessary, separate channels were merged, aligned and modified using the NIH software ImageJ version 1.43.

Acknowledgements

This work was supported by NC3Rs grant G0700480; V.G.'s studentship was supported by the EU KidStem Marie Curie Research Training Network grant FP6 036097-2; and M.U.'s salary by the EU Star-t-rek network FP7 223007. We thank Peter Hohenstein, Guangping Tai and Elise Cachat for their helpful comments.

Note

Because this manuscript includes this Journal's Editor-on-Chief amongst its authors, an anonymous peer review of this paper was organized, and all editorial decisions were made, by another member of the Editorial Board.

References

1. Davies J. Mechanisms of Morphogenesis. Burlington, MA: Academic Press 2005.
2. Camazine S, Deneubourg JL, Franks NR, Sneyd J, Theraulaz G, Bonabeau E. Self-organization in biological systems. Princeton, NJ: Princeton University Press 2001.
3. Rustad KC, Sorkin M, Levi B, Longaker M, Gurtner GC. Strategies for organ level tissue engineering. Organogenesis 2010; 6:151-7.
4. Layer PG, Robitzki A, Rothermel A, Willbold E. Of layers and spheres: The reaggregate approach in tissue engineering. Trends Neurosci 2002; 25:131-4.
5. Unbekandt M, Davies JA. Dissociation of embryonic kidneys followed by reaggregation allows the formation of renal tissues. Kidney Int 2009; 77:407-16.
6. Siegel N, Rosner M, Unbekandt M, Fuchs C, Slabina N, Dolznig H, et al. Contribution of human amniotic fluid stem cells to renal tissue formation depends on mTOR. Hum Mol Genet 2010; 19:3320-31.
7. Grobstein C. Inductive interaction in the development of the mouse metanephros. J Exp Zool 1955; 136:319-35.
8. Auerbach R, Grobstein C. Inductive interaction of embryonic tissues after dissociation and reaggregation. Exp Cell Res 1958; 15:384-97.
9. Sainio K, Suvanto P, Davies J, Wartiovaara J, Wartiovaara K, Saarma M, et al. Glial-cell-line-derived neurotrophic factor is required for bud initiation from ureteric epithelium. Development 1997; 124:4077-87.
10. Davies JA. The embryonic kidney: Isolation, organ culture, immunostaining and RNA interference. Methods Mol Biol 2010; 633:57-69.
11. Saxen L. Organogenesis of the Kidney. Cambridge, MA: Cambridge University Press 1987.
12. Rosines E, Johkura K, Zhang X, Schmidt HJ, Decambre M, Bush KT, et al. Constructing kidney-like tissues from cells based on programs for organ development: toward a method of in vitro tissue engineering of the kidney. Tissue Eng Part A 2010; 16:2441-55.
13. Perin L, Giuliani S, Sedrakyan S, DA Sacco S, De Filippo RE. Stem cell and regenerative science applications in the development of bioengineering of renal tissue. Pediatr Res 2008; 63:467-71.
14. Yokoo T, Fukui A, Matsumoto K, Kawamura T. Kidney regeneration by xeno-embryonic nephrogenesis. Med Mol Morphol 2008; 41:5-13.
15. Rastogi A, Nissenson AR. Technological advances in renal replacement therapy: Five years and beyond. Clin J Am Soc Nephrol 2009; 4:132-6.
16. Sebinger DD, Unbekandt M, Ganeva VV, Ofenbauer A, Werner C, Davies JA. A novel, low-volume method for organ culture of embryonic kidneys that allows development of cortico-medullary anatomical organization. PLoS ONE 2010; 5:10550.

OPEN ACCESS Freely available online

PLoS one

A Novel, Low-Volume Method for Organ Culture of Embryonic Kidneys That Allows Development of Cortico-Medullary Anatomical Organization

David D. R. Sebinger[1], Mathieu Unbekandt[2], Veronika V. Ganeva[2], Andreas Ofenbauer[1], Carsten Werner[1], Jamie A. Davies[2]*

1 Max Bergmann Center of Biomaterials, Leibniz-Institut für Polymerforschung Dresden, Dresden, Germany, **2** Centre for Integrative Physiology, University of Edinburgh, Edinburgh, Scotland

Abstract

Here, we present a novel method for culturing kidneys in low volumes of medium that offers more organotypic development compared to conventional methods. Organ culture is a powerful technique for studying renal development. It recapitulates many aspects of early development very well, but the established techniques have some disadvantages: in particular, they require relatively large volumes (1–3 mls) of culture medium, which can make high-throughput screens expensive, they require porous (filter) substrates which are difficult to modify chemically, and the organs produced do not achieve good cortico-medullary zonation. Here, we present a technique of growing kidney rudiments in very low volumes of medium–around 85 microliters–using silicone chambers. In this system, kidneys grow directly on glass, grow larger than in conventional culture and develop a clear anatomical cortico-medullary zonation with extended loops of Henle.

Citation: Sebinger DDR, Unbekandt M, Ganeva VV, Ofenbauer A, Werner C, et al. (2010) A Novel, Low-Volume Method for Organ Culture of Embryonic Kidneys That Allows Development of Cortico-Medullary Anatomical Organization. PLoS ONE 5(5): e10550. doi:10.1371/journal.pone.0010550

Editor: Patrick Callaerts, Katholieke Universiteit Leuven, Belgium

Received February 12, 2010; **Accepted** April 16, 2010; **Published** May 10, 2010

Funding: This work was supported by the European Union - EU Framework 6 (EuReGene: LSHG-CT-2004-005085), EU and Framework 7 (MRTN-CT-2006-036097 KidStem and HEALTH-F5-2008-223007 STAR-T REK) and National Centre for 3Rs (G0700480). The funders had no role in study design, data collection and analysis, decision to publish, or preparation of the manuscript.

Competing Interests: The authors have declared that no competing interests exist.

* E-mail: jamie.davies@ed.ac.uk

Introduction

This paper describes a method for organ culture of developing kidneys that improves on conventional methods in terms of both economy and organotypic realism.

Organ culture of embryonic kidney rudiments has been established for almost ninety years. The earliest methods suspended renal rudiments in Carrell flasks in semi-solid media, such as clotted owl plasma [1–6]. The clot system, which yielded good though variable development, was replaced in the 1960s by a simpler system in which kidney rudiments are grown on filters supported on a metal grid at a gas-medium interface [7–9]. This is the system generally used to this day, with the occasional variation of using filter inserts designed for multiwell plates, still at a gas-medium interface, in place of pieces of filter supported on steel grids. The filter supports are used because culture in simple liquid hanging drops, which works well for other organs such as salivary glands, does not work well for kidneys and their development in such systems is very poor.

Organ culture of kidney rudiments has been, and continues to be, very valuable in the study of renal development [3;10–13]. The system has been used to study the dynamics of normal development by time-lapse photography, initially by brightfield microscopy and more recently with fluorescent reporter proteins [8;14]. It has been used to study the developmental functions of specific molecules by experimental addition of exogenous growth factors [15], function-blocking antibodies [16], vitamins [17], oligosaccharides [18], drugs [19], antisense oligonucleotides [20] and short interfering RNAs [21;22]. It has also been used to test the cell autonomy of mutations by production of chimaeric recombinant kidneys [23].

Useful as it is, the established culture system suffers from a number of limitations. It requires volumes of media of the order of millilitres, which limits its use in high-throughput screens that require high concentrations of expensive reagents such as siRNAs, and it requires supporting filters that are significantly harder to modify with custom substrates than is glass. Also, while cultured kidneys show good development of the branched collecting duct system and of nephrons to the S-shaped stage and beyond, including differentiation of specific regions such as proximal tubule, distal tubule etc, they do not show development of a distinct renal medulla into which Loops of Henle extend. In conventional culture, the loops of Henle do not form [24] while in culture systems that optimize the maturation of nephrons, such as those using hyaluronic acid, loops of Henle form but are arranged haphazardly rather than extending into the medulla [25].

In this paper, we describe a simple culture system that allows kidney rudiments to be cultured directly on glass coverslips in just 85 µl of medium. The development of these kidneys is superior to traditional methods when compared by any of the usual metrics (overall size, nephron number and the extent of ureteric bud branching) and they show correct cortico-medullary zonation. This new technique therefore offers considerable advantages, of economy and realism of development, over the established method.

Materials and Methods

Organ culture

Organ rudiments were microdissected from E11.5 NMRI or CD1 mouse embryos; they were pooled and assigned randomly to control or experimental groups. For conventional culture, the rudiments were placed on 5 µm pore-size polycarbonate filters at the bottom of a well insert in a six well plate (Corning, Costar), or on top of a stainless steel Trowell grid in a 3.5 cm culture dish in kidney culture medium (KCM: Eagle's minimal essential medium with Earle's salts and non-essential amino acids (GIBCO), 10% foetal bovine serum (Biochrom/Biosera) and 1% penicillin/streptomycin (Sigma)). For some experiments, 1 nM TGF-β (Sigma T7039) or 100 ng/ml GDNF (Sigma G1777) were added.

Low-volume cultures used sterilized silicone rings (flexiPERM Cone shape A, Greiner BioOne), on 22×22 mm coverslips (Menzel Gläser, Germany), cleaned in 5:1:1 H_2O:H_2O_2:NH_4OH (10 min, 70°C), in tissue culture dishes (35×10 mm, Sarstedt/Greiner). Kidney rudiments were placed close to the middle of the circle; medium carried over in this pipetting operation was removed and replaced by the final KCM culture medium (70–200 µl), the complete enclosed area of the coverslip being wetted. The dish surrounding the silicone ring was filled with PBS containing 1% penicillin/streptomycin). All cultures were incubated at 5% CO2 at 37°C, medium being changed every 2 days.

For time lapse movies, cultures were placed in the incubation chamber of a Zeiss Axiovert 200 microscope and images were taken every 10 or 15 min. NIH ImageJ 1.37v. was used to create time lapse movies. Phase contrast images of living cultures were taken every 12 h using an Olympus IX50 microscope.

Fixation and immuno/lectin fluorescence

Kidney rudiments were fixed in methanol at −20°C, washed in PBS 10 min, then incubated in primary antibody in PBS, overnight at 4°C. Primary antibodies were anti-laminin (1:100 Sigma L9393), anti-calbindin D28k (1:100 Sigma C9848),), anti-megalin (1:150, obtained from Thomas Wilnow), anti-human-Wilms' Tumour 1 (1:50, Dako M3561), anti-Pax-2 (1:100, Covance PRB-276P) and anti-E-cadherin (1:100, BD Transduction Laboratories 610181). Samples were washed for at least 30 min in PBS then incubated with appropriate secondary antibodies overnight at 4°C. The secondary antibodies used were: anti-rabbit IgG - TRITC (1:100, Sigma T6778), anti-mouse IgG–TRITC (1:100, Sigma T5393) and anti-mouse IgG - FITC (1:100, Sigma F6257). For antibody/lectin co-stainings, all solutions contained 1% milk powder in PBS and 10 ng/ml lectin from *Dolichos biflorus*-FITC (Sigma L9142) was included with the secondary antibody. Finally the samples were washed in PBS and mounted on slides.

Cell proliferation and apoptosis detection assay

BrdU (5-bromo-2-deoxy-uridine) was added to the medium of kidney rudiments in culture 4 hours before fixation to a final concentration of 100 µM. Detection was performed as described by [26] except that cell death detection master mix (In Situ Cell

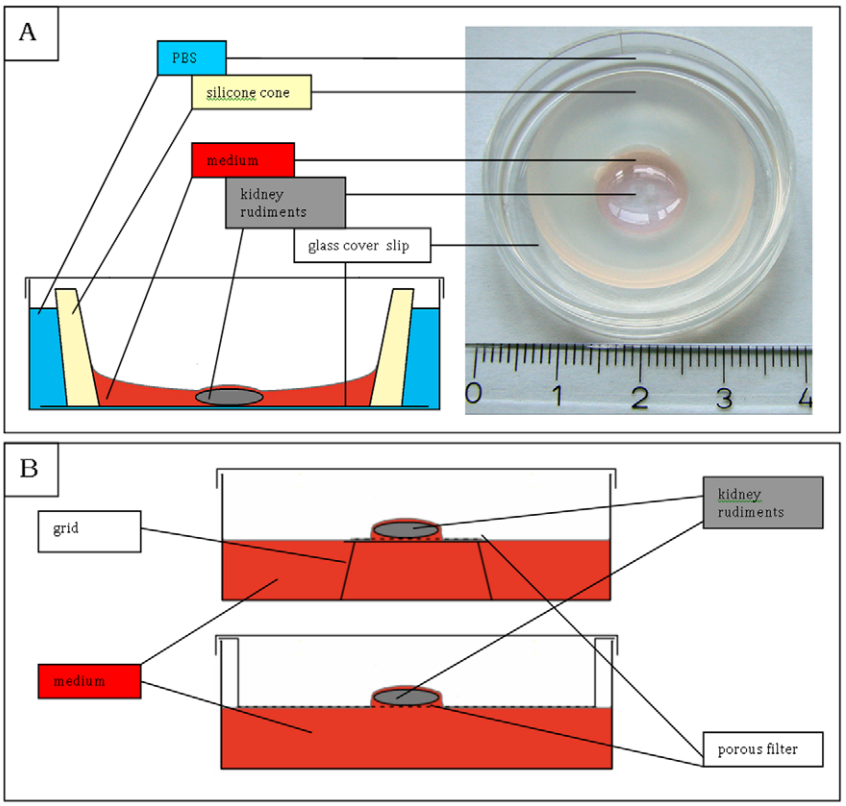

Figure 1. Methods for embryonic kidney culture. (A) The low-volume culture method described in this paper, drawn from the side and photographed from above. (B) Conventional, high volume culture either on a membrane on a Trowell grid (above) or on the membrane at the bottom of a well insert (below). The blue in (A) depicts PBS, the red in all diagrams depicts culture medium, yellow in (A) symbolizes the silicone ring and dark grey the embryonic kidney rudiments. The numbered divisions on the ruler are centimetres.
doi:10.1371/journal.pone.0010550.g001

Death Detection Kit, TMR red, Roche 12156792910) was added along with primary antibodies. Samples were washed for 30 min in PBS and incubated in secondary antibodies overnight at 4°C. After a PBS wash, 1 µg/ml DAPI (Sigma) in PBS was added for 20 min. Finally the samples were washed in PBS and mounted on slides.

Morphometric quantification

Immunostained samples were examined on a confocal laser scanning microscope (TCS SP5, Leica Microsystems, Wetzlar, Germany). Serial 5-µm optical sections of each kidney were acquired. FITC, TRITC and DAPI emissions were acquired sequentially. Ureteric bud tips and nephrons were counted manually. Area was defined manually and measured using NIH ImageJ 1.37v (http://rsb.info.nih.gov/nih-image/).

Measurement of cytokines

Right and left kidneys of the same embryo were dissected and allocated randomly to either conventional culture or the new method. Supernatants conditioned from 0–2 d 2–4 d were collected and diluted in fresh medium to a standard total of 3 ml. Expression of 40 cytokines was assessed using R&D systems' mouse cytokine array panel according to the manufacturer's directions. Experiments were performed in triplicate.

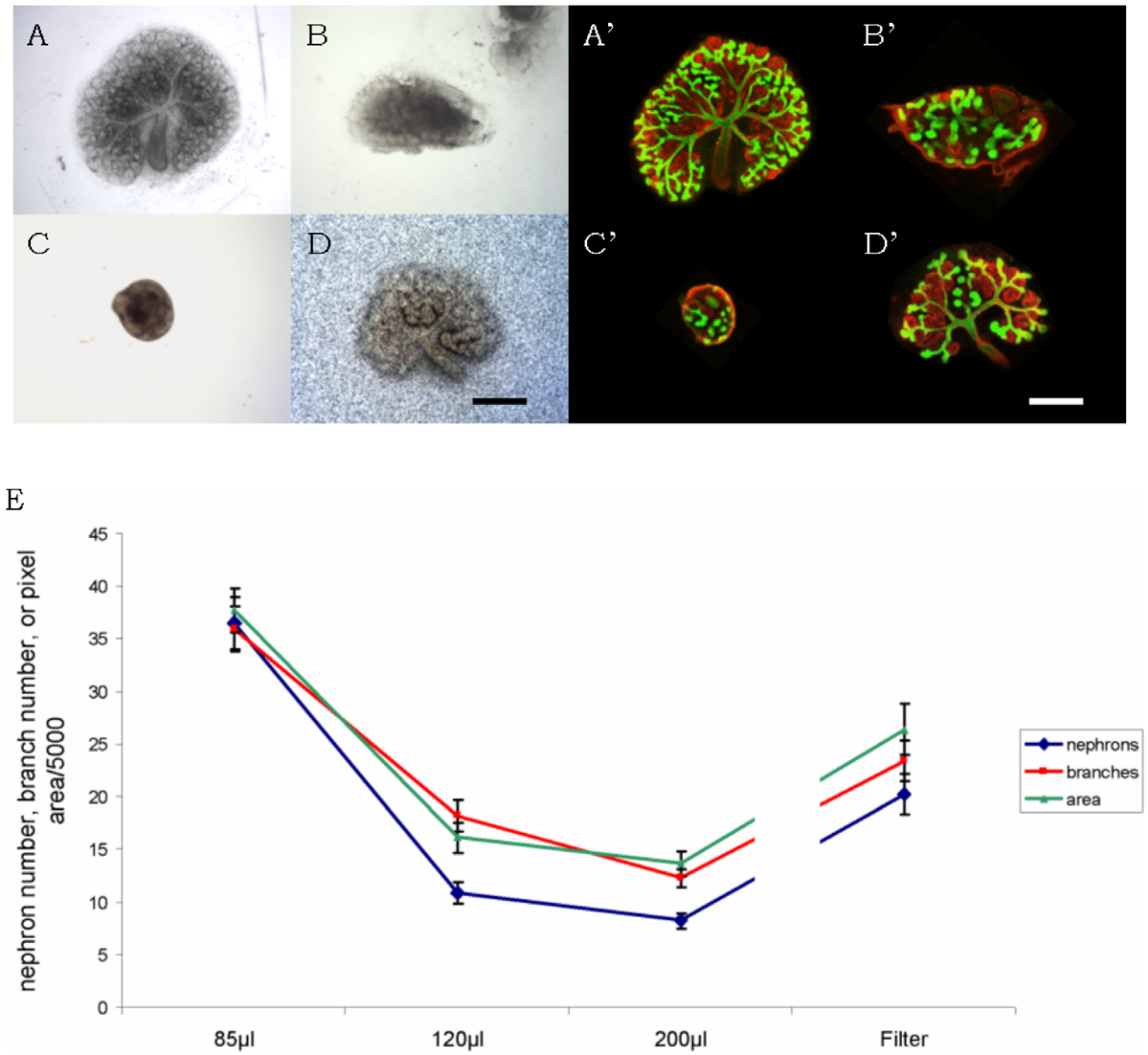

Figure 2. Development of mouse kidney rudiments in conventional culture and on glass inside silicone rings. (A–C) show phase contrast views of kidney rudiments grown for 4 days in silicone rings on glass in 85 µl, 120 µl and 200 µl respectively, while (D) shows a kidney grown in the conventional system (on a filter on a Trowell grid: the 'noise' in the background is the filter). On glass, the lowest volume, 85 µl, shows the best development, resulting in a larger kidney than the conventional system. (A'–D') show kidneys grown in the same conditions as (A–D) but stained for basement membrane marker laminin (red) and the ureteric bud marker calbindin-D_{28k} (green). (E) shows a quantitative analysis of area, nephron and bud tip numbers for each of these culture conditions. Error bars depict standard errors of the mean and are derived from at least 49 kidneys in total, from six different runs of the experiment, each run using between 6 and 18 kidneys. Scale bars = 500 µm.
doi:10.1371/journal.pone.0010550.g002

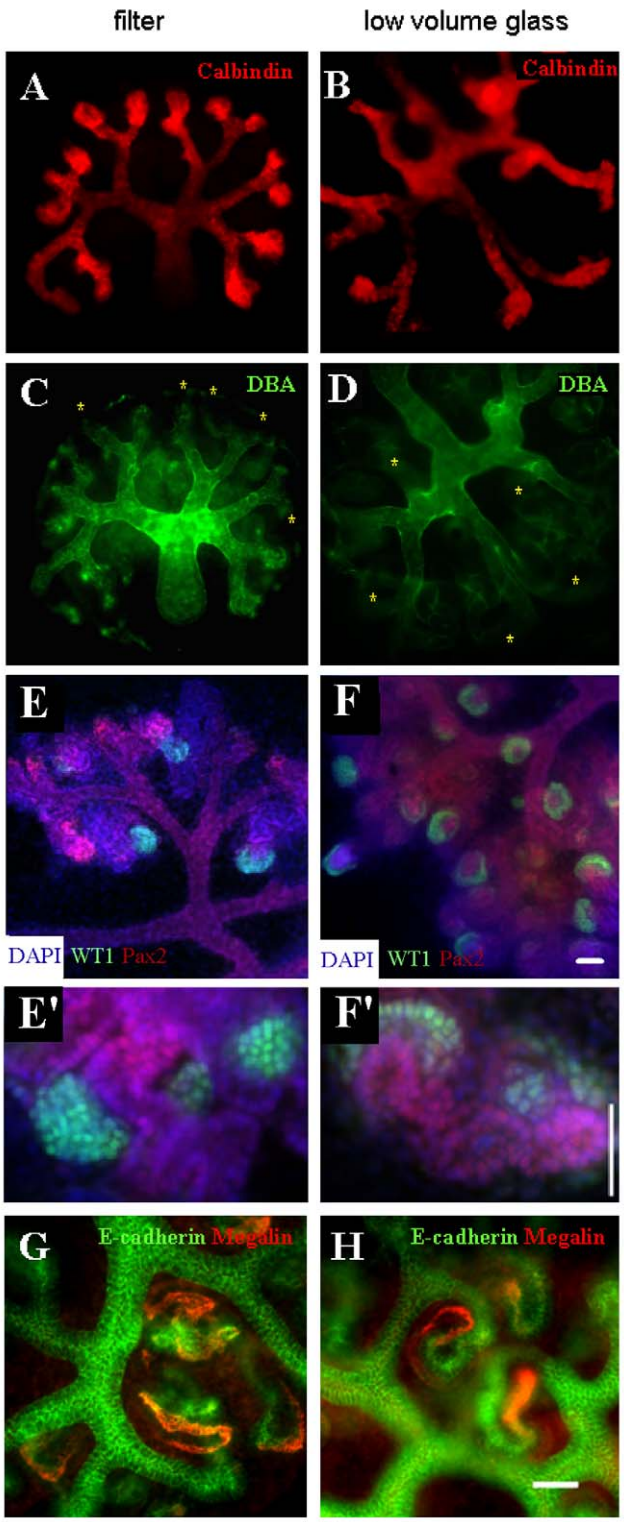

Figure 3. Normal segmentation of nephrons grown on filters (A, C, E, G) and in low volumes on glass (B, D, F, H). (A, B) show kidneys stained for calbindin, which stains the whole ureteric bud; (C, D) show kidneys stained for Dolichos biflorus agglutinin (DBA), which stains only the bud stalk–the 'missing' tips visible in A,B but not in C,D are marked with yellow stars; (E, F) show kidneys stained for the WT1, which is expressed strongly in crescents that consist of developing podocytes: in these images, staining for Pax2, expressed in bud, condensates and early nephrons, is used to reveal the general structure of the rudiment and to place the developing podocytes in their anatomical context: higher power views are shown in E′ and F′, revealing the nuclear location of WT1. (G, H) show higher power views of kidneys stained for the ureteric bud and distal tubule marker, E-cadherin, and the proximal tubule marker megalin; the expression of each of these markers is similar in both culture systems. Scale bars = 50 μm; the scale bar shown in F applies to A–F, that shown in F′ to E′ and F′, and that shown in H applies to G and H.
doi:10.1371/journal.pone.0010550.g003

Surface tension measurements

DOPC (1,2-dioleoyl-sn-glycero-3-phosphocholine; Sigma P6354) was added to and dispersed at 1 mg/ml in KCM by 30 min. of sonication on ice. Surface tension was determined using the pendant drop-method based on the Young-Laplace equation [27]. After calibrating the system (Contact Angle System OCA 30, DataPhysics Instruments, Germany) with degassed water, the surface tensions of KCM and KCM with DOPC were measured.

Animals

The animals from which tissue samples were obtained, bred and kept according to relevant UK Home Office guidance (http://scienceandresearch.homeoffice.gov.uk/animal-research/legislation/index.html) and the Animals (Scientific Procedures) Act, 1986, available from the same website: they were killed by trained technical staff according to a method listed in Schedule 1 of that Act. Ethical approval for keeping the animals and obtaining these tissue samples was approved by the University of Edinburgh's local ethics approvals process.

Results

Kidney rudiments develop well on glass if cultured in low volumes of medium

We began this work with the aim of growing embryonic kidney rudiments on glass coverslips that could be coated easily with defined matrix components. To define a small culture area on the glass, we used FlexiPERM silicone rings, each with the approximate shape of a decapitated cone, the smallest end of which defined a 1 cm^2 (i.e. 5.6 mm radius) circle (Fig 1A). It was at once clear that kidney rudiments did not grow well when supplied with large volumes of media in this system. Smaller volumes, of 85, 90, 120 or 200 μl were therefore tried (volumes of 70 μl and less were found to be insufficient to wet the whole circle permanently). Development of the organ rudiments after four days in each condition was quantified by measuring rudiment area, number of ureteric bud tips (2 at the time of isolation) and number of nephrons (0 at the time of isolation).

Control kidneys, cultured by the conventional Trowell method (Fig 1B) developed normally, showing a calbindin-positive ureteric bud that was well-branched (mean 23.4, $\sigma = 16$, $n = 49$) and many developing nephrons (mean 20.2, $\sigma = 16$, $n = 49$), identifiable by their shapes and by their laminin-rich basement membranes and absence of calbindin staining (Fig 2D, D′). In 200 μl medium, many times deeper than the height of the kidney, kidneys remained rounded and developed poorly (Fig 2C, C′), showing less than half the ureteric bud branches and nephrons of control kidneys grown on conventional Trowell filters. This was expected from previous reports (see Introduction). With lower volumes of medium, however (Fig 2A, A′, B, B′), the extent of development improved (Fig 2E). In the optimum volume - 85 μl - kidney rudiments covered significantly more area (42%) than did filter-grown controls and they produced 46% more ureteric bud tips and 81% more nephrons. The variability between kidneys was also

reduced (standard deviations in measurements of area, branch number and nephron number were all only about four fifths as large, as a proportion of the means to which they applied, as they were for filter-grown controls). Adding 500 µl of culture medium to kidney rudiments that had already been cultured in 85 µl for 1 day of culture caused the kidneys to round up and to cease developing well: they therefore require low volumes continuously, and not just to promote initial settling on the glass.

The nephrons and ureteric bud branches of kidneys grown in conventional organ culture showed patterns of gene expression similar to those observed *in vivo*, as has been described before [28–31]. The ureteric bud, for example, expressed calbindin D_{28K} (Fig 3A) and was divided into a stalk region that bound *Dolichos biflorus* lectin and a tip region that did not (Fig 3C) [32;33] (Fig 3C). The nephrons showed correctly-restricted expression of markers; for example, the most proximal ends of the nephrons differentiated into podocytes that expressed high levels of WT1 (Fig 3E: the weak expression of WT1 in condensing mesenchyme is normal and reflects an earlier role for that protein in nephron development [21]), the proximal tubules expressed megalin and the distal

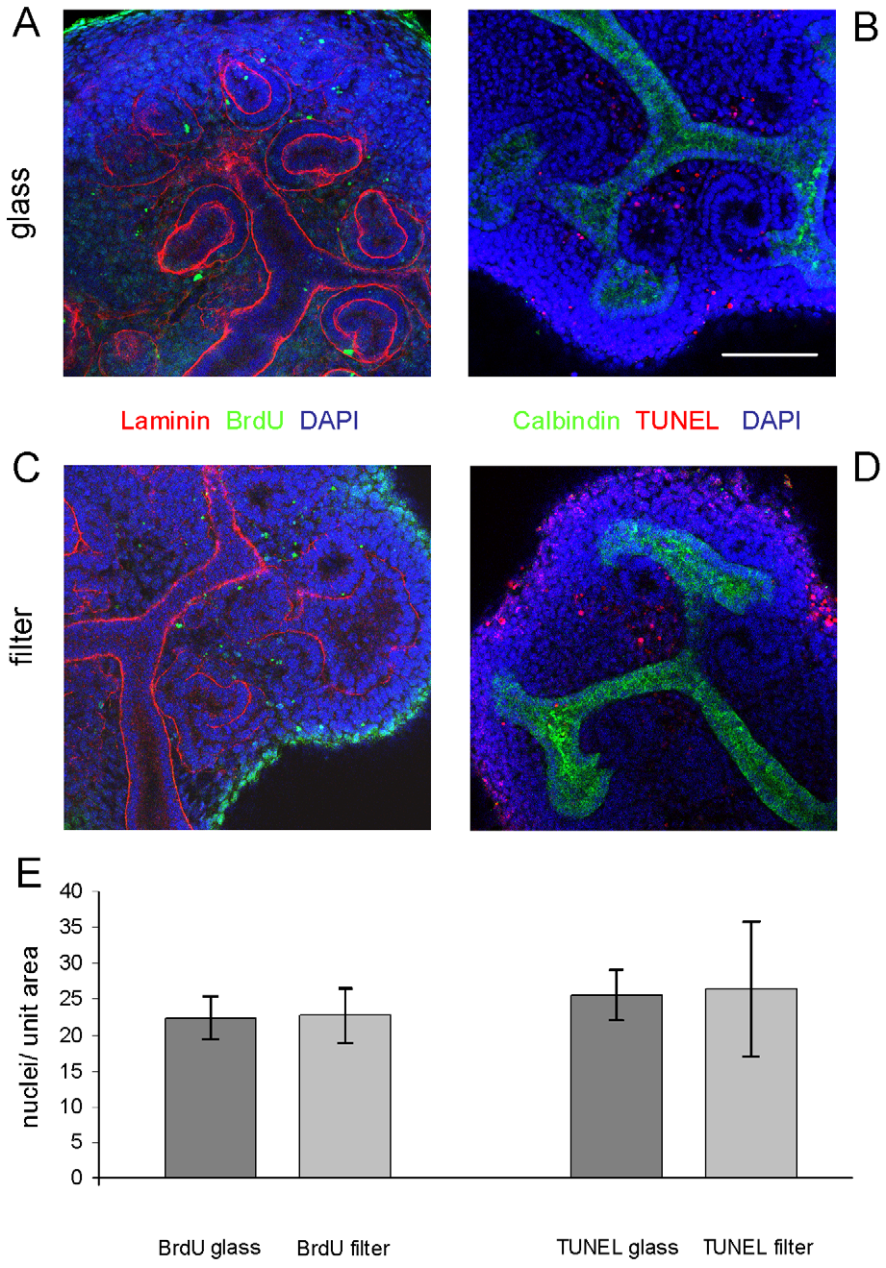

Figure 4. There is no significant difference after two days in rates of proliferation or cell death in nephrons formed in the two culture systems. Proliferation was measured using BrdU incorporation and apoptosis by terminal end labelling (TUNEL); source images typical of those analysed quantitatively are shown for BrdU (A glass; C filter) and TUNEL (B glass; D filter). Over many such images, the numbers of BrdU or TUNEL-positive nuclei per unit area of visible nephron cross-section were counted. The data, from ten filter-grown kidneys and thirty one glass-grown ones, (E) show no evidence for difference between culture systems (a two-tailed Student's t-test yields $p = 0.93$ and $p = 0.94$ for BrdU and TUNEL respectively). Scale bar is 100 µm.
doi:10.1371/journal.pone.0010550.g004

tubules and ureteric bud expressed E-cadherin (Fig 3G). Nephrons and ureteric buds of kidneys grown using our low volume culture system showed the same organotypic expression of segment marker genes. Ureteric buds were divided correctly into tip and stalk zones (Fig 3B, D), developing podocytes expressed WT1 (Fig 3F), proximal tubules expressed megalin and distal tubule expressed E-cadherin (Fig 3H). Rates of cell proliferation and apoptosis in nephrons, measured by BrdU incorporation and Terminal deoxynucleotidyl transferase dUTP nick end labelling (TUNEL) respectively, were not significantly different in the two culture systems after two days (Fig 4).

Kidney rudiments grown in the low volume system show typical responses to positive and negative morphogens

Conventional kidney organ culture has been used to identify various diffusible regulators of renal development, by applying suspected regulators to the medium and observing any changes to subsequent morphogenesis. We have tested kidneys growing in the low volume system for their response to two known modulators of morphogenesis, one positive and one negative. This had two purposes; (a) to verify the normality of development and (b) to check that the culture volume used is not so small that these regulators become quickly exhausted or inactivated by cellular secretions. The factors we used were TGF-β, a known inhibitor of ureteric bud branching [34] and GDNF, a known activator [35].

Exogenous TGF-β, applied at 1 nM for four days [36], had similar effects on the development of kidneys in conventional and low volume culture, although the inhibitory effects were a little less dramatic in the low volume method (Fig 5). Exogenous GDNF, added at a final concentration of 100 ng/ml again for four days [36] significantly increased branching morphogenesis in both systems so that more than a doubling of the amount of nephrons and ureteric bud branches was achieved.

Kidney rudiments develop cortico-medullary zonation when cultured in this system

Kidney rudiments developing in conventional organ culture show excellent recapitulation of *in vivo* development at a fine scale but one important large-scale aspect of development is typically lost, or at least seriously under-developed. *In vivo*, growth and extension of stalks of the ureteric bud and the Loops of Henle divides the kidney into two broad zones, an outer cortex containing the glomeruli and ureteric bud tips, and an inner medulla that is dominated by straight tubules of the collecting duct

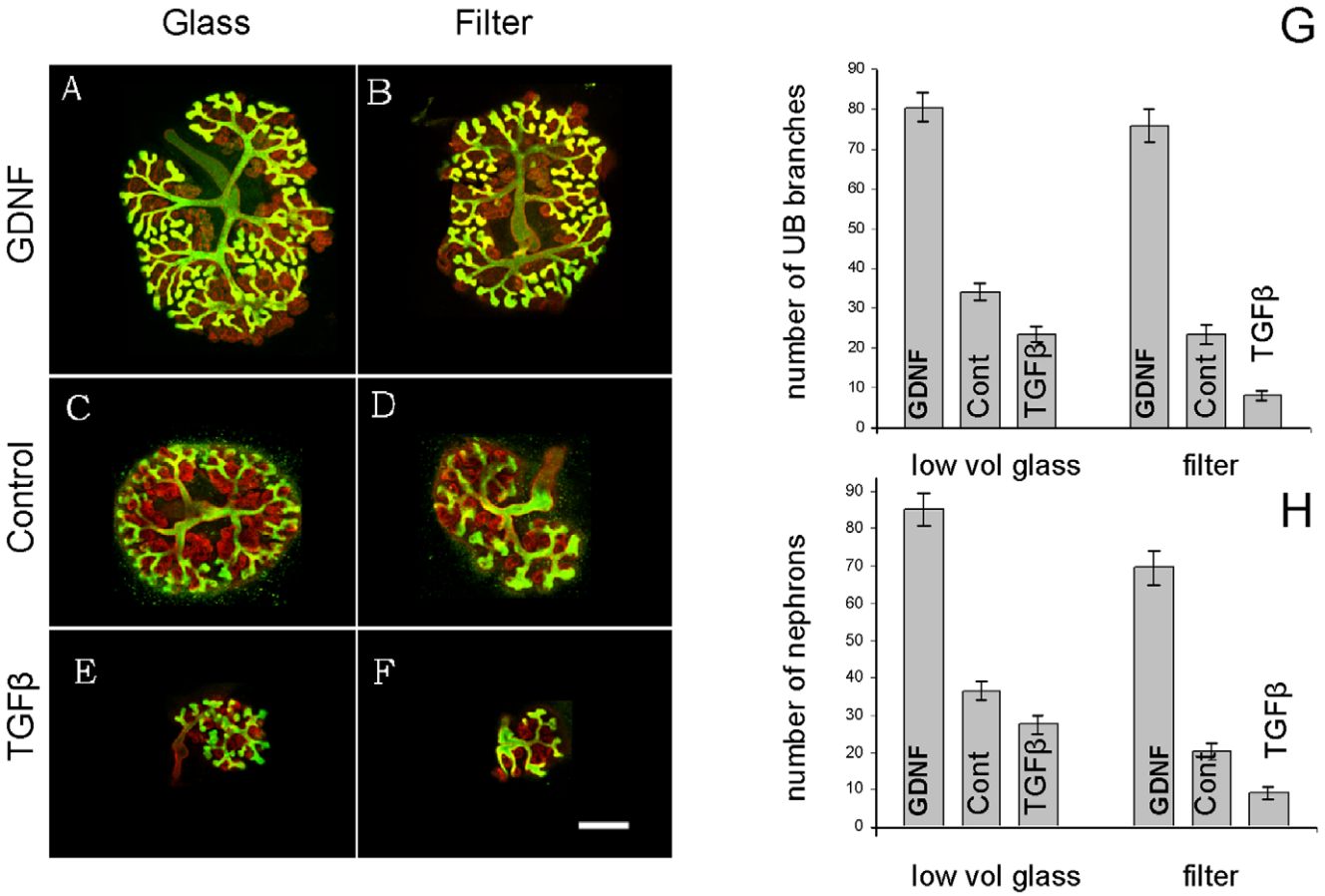

Figure 5. Kidneys grown in the low volume glass system show normal responses to known morphogens. (A, B) show the enhanced development of kidneys grown in 100 ng/ml GDNF in the low volume glass system and on conventional filters, stained for laminin (red) and calbindin-D_{29k} (green). (C, D) show kidneys grown in control medium and (E, F) show the decreased development of kidneys cultured in the presence of 1 nM TGFβ. (G) shows the effects of these molecules on ureteric bud (UB) branching, in the low volume and the filter systems and (H) shows their effects on nephron number. Each bar represents data from between 10 and 71 kidneys. All values in (G) and (H) differ significantly from their respective controls, by a two-tailed Student's t-test assuming unequal variances, the weakest difference (that between nephrons in control and TGFβ, on glass) still having a p-value of 0.009. Scale bar 500 μm.
doi:10.1371/journal.pone.0010550.g005

system and the loops of Henle. This organization is critical to the urine-concentrating activity of the metanephros, so lack of a good culture model to allow the development of cortico-medullary differences to be studied is a serious limitation to the field.

Long-term (10-day) culture in our low volume system resulted in a substantial increase in area of the organ rudiment and the formation of distinct cortical and medullary zones (Fig 6A). The forming glomeruli were restricted to the cortical zone and the medullary zone contained ureteric bud/collecting duct tubules and also loops of Henle (Fig 6B). The new culture system therefore has the substantial advantage, beyond economy with reagents, that it shows more anatomically realistic renal development.

Kidney rudiments cultured in the low volume system show less evidence for stress than those grown in conventional organ culture

Tissues subject to stress secrete specific cytokines that interact with cells of the immune system to initiate an inflammatory response [37]. These cytokines include tissue inhibitor of metalloproteinase I (TIMP1), monocyte chemotactic protein 1 (MCP1, also called JE), the neutrophil chemokine CXCL1 (also called KC) and interferon gamma (IFNγ) [38–41]. Release of these proteins into medium can therefore be used as an indicator for how stressed cells are in culture [42–46].

Medium from kidneys cultured conventionally in 3 mls of medium contained significant amounts of TIMP1 and MCP1 and smaller but still detectable amounts of CXCL1 (not shown) and IFNγ (Fig 7). Medium from the low volume glass culture system showed lower amounts of TIMP1 and less or equal of the other pro-inflammatory cytokines, measured over either first 48 h or the subsequent 48 h of culture (Fig 7), though the effects were stronger by the second 48 h. These results suggest that the cells in this system were significantly less stressed than those in conventional culture.

Kidney rudiments may grow better in low culture volumes because of a requirement for effects of surface tension

Something that the conventional high-volume filter method of culture has in common with the low-volume method, but not with the much less effective high-volume methods (including our use of 120 and 200 µl instead of 85 µl the silicone rings), is that the organ rudiment is at the gas-medium interface. There are two reasons that this might be important. One is improved access to oxygen, although this seems unlikely since kidneys grow very well in conventional culture in low (3%) oxygen systems [47]. The other is the effect of the surface itself. Molecules of liquid are mutually attractive. Those in the bulk liquid are surrounded by other molecules on all sides so therefore experience no directional force. Those at a gas-liquid interface surface still have other attractive molecules to the side of them and below them but not above them, so they experience a net average force pulling them back into the bulk liquid. For this reason, surfaces are drawn in until balanced by compressive forces in the bulk liquid, and liquids minimize their free surface area. Actions that would expand the surface area of a liquid work against this tendency to minimize surface are therefore met with an opposing force, usually called surface tension. Where the liquid over a culture substrate is shallow compared to the height of the organ culture itself, the raised profile of the organ forces the surface of the liquid to be larger than it would otherwise

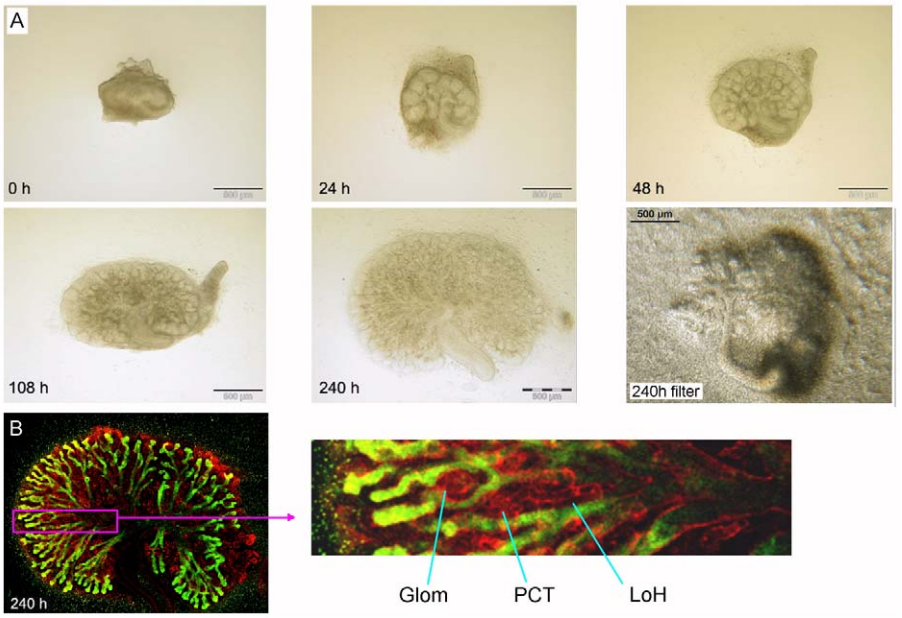

Figure 6. Kidneys grown on glass develop organotypic features including cortico-medially zonation. (A) Shows a time course of development to 240 h (10 d). From about 108 h (4.5 d), the kidney spreads out enough that it begins to divide into two zones, an outer medullary zone that features many nephrons and an inner medulla that contains more elongated tubules (mainly collecting ducts at this stage). By 240 h (10 d), this effect has become more marked. The last panel of (A) shows a kidney rudiment cultured on a filter for 240 h: the organ occupies less area and there is less evidence of corticomedullary zonation. The 'grain' in the photograph is an optical effect of the filter pores, which are beneath the kidney; their absence in bright field imaging is another advantage of the glass system. (B) A high-power view of part of a 240 h kidney shows that nephrons (red) are arranged organotypically, with the glomerulus ('Glom') and proximal convoluted tubule ('PCT') in the cortex and a loop of Henle ('LoH') extending down into the medulla, forming a tight hair-slide shape parallel to the collecting ducts (green). Green = calbindin, red = laminin.
doi:10.1371/journal.pone.0010550.g006

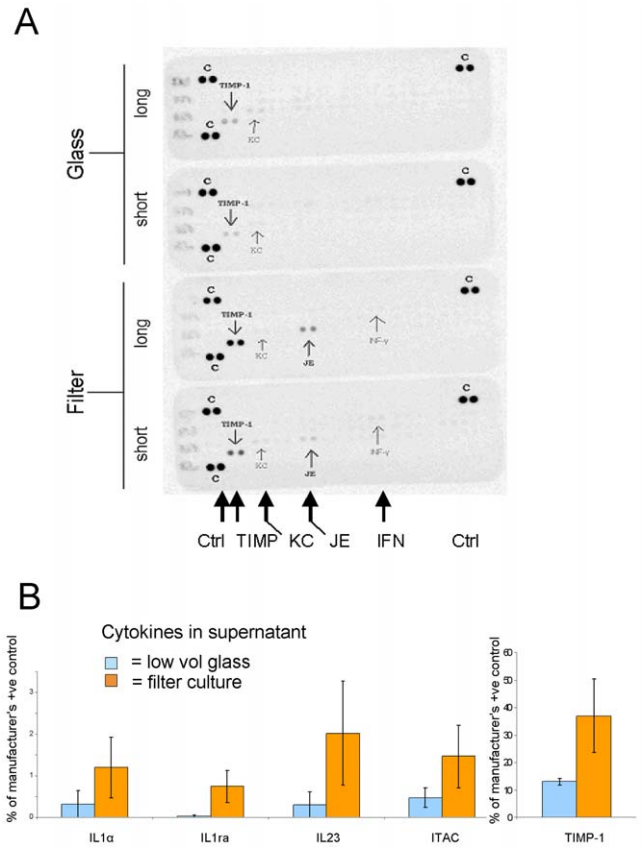

Figure 7. Kidneys grown in the low-volume glass system show less evidence of stress. In (A) the samples labelled 'short' are of medium conditioned from day 0–2 and those labelled 'long' are from days 2–4. Spots marked 'C' are positive controls (to verify the detection kit). The other spots, of TIMP1, KC, JE and IFNγ represent these markers of cellular stress (see main text). (B) shows, quantitatively, the results of these molecules on the arrays, as means of three runs. The Y axis is % relative to the signal provided by the manufacturers' positive control. The right-most part of the graph, showing TIMP (also shown as a spot in A), is plotted to a different y axis. Although the data for each of the molecules, each individual array spot being derived from 3 pooled kidneys and 3 independent arrays being run for each condition, suggests a decrease on glass, the variation in measurement is so large that no one individual molecule has a change that can be regarded as significant at the conventional $p \leq 0.05$ (most have $p \approx 0.1$). As all molecules are markers for the same physiological state (cellular stress), however, their measurements can be pooled for a one-tailed, paired Student's t-test that uses all 15 experiment-control measurement pairs together (the 15 pairs coming from 5 target molecules x 3 runs each). Viewed this way, the data show that glass culture does produce a significant reduction in production of these stress proteins ($p = 0.05$). Elements on the spot arrays not shown in this graph showed no significant differences.
doi:10.1371/journal.pone.0010550.g007

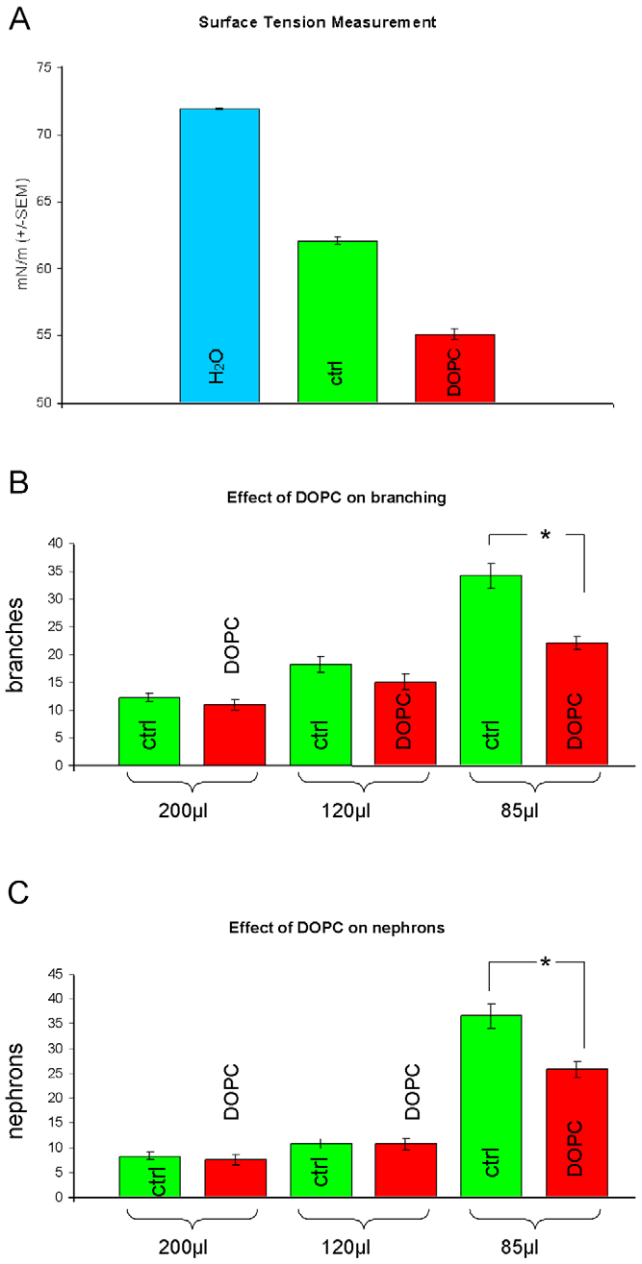

Figure 8. Reduction of surface tension influences development of cultured kidney rudiments. In (A) the reduction of surface tension by the addition of the surfactant DOPC to the medium is demonstrated; data represent means of a minimum of 18 measurements. (B and C) show the influence of the surfactant on ureteric bud branching and amount of nephrons, respectively, if compared to the control; each bar represents data from a minimum of 17 kidneys. The asterisk indicates significant difference ($p = 3.4 \times 10^{-6}$ for branches and 3.3×10^{-4} for nephrons) by a two-tailed Student's t-test assuming unequal variances.
doi:10.1371/journal.pone.0010550.g008

be and the organ will experience a flattening force due to surface tension.

It is therefore possible that the flattening effect of surface tension is important to renal development *in vitro*. We tested this idea by using a surfactant to reduce surface tension in the medium to see if this mimicked the effect of a high volume of medium. The surfactant used, 1,2-dioleoyl-sn-glycero-3-phosphocholine (DOPC), reduces surface tension by forming phospholipid bilayers (rather than the monolayers formed by typical lab detergents) at the air-medium interface [48]. Direct measurements of surface tension in untreated and DOPC treated medium confirmed the surface tension-lowering effects of DOPC (Fig 8A).

The presence of DOPC had no significant effect on the (already poor) development of kidneys under large volumes of medium, as would be expected since these should be relatively free from surface effects (Fig 8B, C). In the low-volume (85 µl) system, though, the presence of DOPC significantly reduced the renal

area, the number of ureteric bud tips formed and the number of nephrons formed. This is compatible with the hypothesis that surface tension is important.

Discussion

In this report, we have described an improved technique for organ culture of mouse metanephric organ rudiments that is very economical of medium, shows quantitatively better development and also shows cortico-medullary zonation absent in the conventional method. It also uses a transparent substrate, useful for live imaging, that can also be coated easily with experimental custom substrates.

Conventional culture and the low-volume method described here both have the kidney supported at the air-medium interface, with only a thin film of medium covering it; larger volumes of medium, even in exactly the same system, support development significantly less well. There are two obvious *a priori* hypotheses for the importance of the surface: access to oxygen, or the physical compression effect of surface tension. Previous reports of normal development of cultured kidneys in just 3–5% oxygen [47;49] make the first of these unlikely. We have shown that lowering the surface tension of the medium using a surfactant results in quantitatively poorer development. This supports the surface tension hypothesis but does not prove it, for the lipid bilayer formed at the surface by the surfactant may also affect the diffusion of gases. To formally prove the biophysical hypothesis that kidneys do better if gently squashed, it would be necessary to vary physical forces only with no effect on chemistry [50]. A possible, though technically difficult, way to achieve this might be to culture kidney rudiments on glass, under large volumes of medium, in a centrifuge.

As well as producing quantitatively better development, the culture system showed a quantitatively strongly reduced expression of markers of cellular stress. As well as arguing for the superiority of the new culture system, this finding highlights a potential but rarely measured problem in organ culture systems; the cells involved might actually be under considerable stress. Some of the molecules they produce as a result of this (and that we measured), such as IFN-γ, will probably only be bioactive in the context of an animal with an immune system but others, such as MMP9 (matrix metalloproteinase-9) and its antagonist Timp-1 (tissue inhibitor of metalloproteinase 1), are important in matrix turnover during development [51] and may therefore lead to culture results not reflecting those obtained *in vivo*. In the kidney itself, there are instances of this: endogenously-produced HGF is needed for collecting duct branching in culture, for example, but $HGF^{-/-}$ mice have normal kidneys [52]. It may be that one explanation of why in vivo and in vitro results do not always agree is a reflection of cellular stress, with measureable induction of protein expression, rather than the often-assumed explanation that the intact body provides some diffusible factor from elsewhere, that can perform the same function as the molecule under study and therefore creates redundancy in vivo, but not in vitro.

In summary, we have presented a culture method that extends the range of questions that can be addressed in culture to include those connected to corticomedullary zonation and loop of Henle formation, and have made culture conditions more economical of medium supplements. As well as making developmental processes more easily visible, this method has the potential to significantly reduce animal use by allowing the control of these aspects of kidney development to be studied in vitro, for example by using siRNAs, rather than by extensive breeding of genetically-modified mice.

Acknowledgments

We would like to thank the following for their advice, support and gifts of reagents; Louise Cooper, Petra Gruber, Jussi Helppi, Ina Kurth, Peter Hohenstein, Susann Malik, Kerstin Menzer, Anke Münch-Wuttke, Patricia Murray, Lars Renner, Philipp Seib, Thomas Wilnow and Ralph Zimmermann.

Author Contributions

Conceived and designed the experiments: AO CW JAD. Performed the experiments: DS MU VG AO. Analyzed the data: DS MU VG AO. Wrote the paper: DS JAD. Supervised Sebinger and Ganeva in some experiments in the UK: MU. Supervised Sebinger when working in Germany: CW.

References

1. Rienhoff W (1922) Development and growth of the metanephros or permanent kidney in chick embryos. John's Hopkins Hosp Bull 33: 392–406.
2. Grobstein C (1953) Morphogenetic interaction between embryonic mouse tissues separated by a membrane filter. Nature 172: 869–870.
3. Gleucksohn-Waelsch S, Rota TR (1963) Development in organ tissue culture of kidney rudiments from mutant mouse embryos. Dev Biol 7: 432–444.
4. Auerbach R, Grobstein C (1958) Inductive interaction of embryonic tissues after dissociation and reaggregation. Exp Cell Res 15: 384–397.
5. Grobstein C (1953) Inductive epitheliomesenchymal interaction in cultured organ rudiments of the mouse. Science 118: 52–55.
6. Grobstein C (1953) Epithelio-mesenchymal specificity in the morphogenesis of mouse submandibular rudiments *in vitro*. J Exp Zool 124: 383–414.
7. Saxen L, Vainio T, Toivonen (1962) Effect of polyoma virus on mouse kidney rudiment in vitro. J Natl Cancer Inst 29: 597–631.
8. Saxen L, Wartiovaara J (1966) Cell contact and cell adhesion during tissue organization. Int J Cancer 1: 271–290.
9. Saxen L, Koskimies O, Lahti A, Miettinen H, Rapola J, et al. (1968) Differentiation of kidney mesenchyme in an experimental model system. Adv Morphog 7: 251–293.
10. Bard JB, Ross AS (1991) LIF, the ES-cell inhibition factor, reversibly blocks nephrogenesis in cultured mouse kidney rudiments. Development 113: 193–198.
11. Davies J (1994) Control of calbindin-D28K expression in developing mouse kidney. Dev Dyn 199: 45–51.
12. Michos O, Goncalves A, Lopez-Rios J, Tiecke E, Naillat F, et al. (2007) Reduction of BMP4 activity by gremlin 1 enables ureteric bud outgrowth and GDNF/WNT11 feedback signalling during kidney branching morphogenesis. Development.
13. Thesleff I, Ekblom P (1984) Role of transferrin in branching morphogenesis, growth and differentiation of the embryonic kidney. J Embryol Exp Morphol 82: 147–161.
14. Watanabe T, Costantini F (2004) Real-time analysis of ureteric bud branching morphogenesis in vitro. Dev Biol 271: 98–108.
15. Sainio K, Suvanto P, Davies J, Wartiovaara J, Wartiovaara K, et al. (1997) Glial-cell-line-derived neurotrophic factor is required for bud initiation from ureteric epithelium. Development 124: 4077–4087.
16. Woolf AS, Kolatsi-Joannou M, Hardman P, Andermarcher E, Moorby C, et al. (1995) Roles of hepatocyte growth factor/scatter factor and the met receptor in the early development of the metanephros. J Cell Biol 128: 171–184.
17. Rogers SA, Droege D, Dusso A, Hammerman MR (2004) Incubation of metanephroi with vitamin d(3) increases numbers of glomeruli. Organogenesis 1: 52–54.
18. Davies JA, Yates EA, Turnbull JE (2003) Structural determinants of heparan sulphate modulation of GDNF signalling. Growth Factors 21: 109–119.
19. Fisher CE, Michael L, Barnett MW, Davies JA (2001) Erk MAP kinase regulates branching morphogenesis in the developing mouse kidney. Development 128: 4329–38.
20. Sainio K, Saarma M, Nonclercq D, Paulin L, Sariola H (1994) Antisense inhibition of low-affinity nerve growth factor receptor in kidney cultures: power and pitfalls. Cell Mol Neurobiol 14: 439–457.
21. Davies JA, Ladomery M, Hohenstein P, Michael L, Shafe A, et al. (2004) Development of an siRNA-based method for repressing specific genes in renal organ culture and its use to show that the Wt1 tumour suppressor is required for nephron differentiation. Hum Mol Genet 13: 235–246.
22. Lee WC, Berry R, Hohenstein P, Davies J (2008) siRNA as a tool for investigating organogenesis: The pitfalls and the promises. Organogenesis 4: 176–181.
23. Kreidberg JA, Sariola H, Loring JM, Maeda M, Pelletier J, et al. (1993) WT-1 is required for early kidney development. Cell 74: 679–691.
24. Avner ED, Ellis D, Temple T, Jaffe R (1982) Metanephric development in serum-free organ culture. In Vitro 18: 675–682.

25. Rosines E, Schmidt HJ, Nigam SK (2007) The effect of hyaluronic acid size and concentration on branching morphogenesis and tubule differentiation in developing kidney culture systems: potential applications to engineering of renal tissues. Biomaterials 28: 4806–4817.
26. Davies JA, Garrod DR (1995) Induction of early stages of kidney tubule differentiation by lithium ions. Dev Biol 167: 50–60.
27. Hansen F, Rodsrud G (1991) Surface Tension by pendant drop I. A fast standard instrument using computer image analysis. J Colloid Interface Sci 141: 1–0.
28. Buckler AJ, Pelletier J, Haber DA, Glaser T, Housman DE (1991) Isolation, characterization, and expression of the murine Wilms' tumor gene (WT1) during kidney development. Mol Cell Biol 11: 1707–1712.
29. Liu L, Dunn ST, Christakos S, Hanson-Painton O, Bourdeau JE (1993) Calbindin-D28k gene expression in the developing mouse kidney. Kidney Int 44: 322–330.
30. Vestweber D, Kemler R, Ekblom P (1985) Cell-adhesion molecule uvomorulin during kidney development. Dev Biol 112: 213–221.
31. Yamagata M, Kimoto A, Michigami T, Nakayama M, Ozono K (2001) Hydroxylases involved in vitamin D metabolism are differentially expressed in murine embryonic kidney: application of whole mount in situ hybridization. Endocrinology 142: 3223–3230.
32. Michael L, Sweeney DE, Davies JA (2007) The lectin Dolichos biflorus agglutinin is a sensitive indicator of branching morphogenetic activity in the developing mouse metanephric collecting duct system. J Anat 210: 89–97.
33. Laitinen L, Virtanen I, Saxen L (1987) Changes in the glycosylation pattern during embryonic development of mouse kidney as revealed with lectin conjugates. J Histochem Cytochem 35: 55–65.
34. Sakurai H, Nigam SK (1997) Transforming growth factor-beta selectively inhibits branching morphogenesis but not tubulogenesis. Am J Physiol 272: F139–F146.
35. Towers PR, Woolf AS, Hardman P (1998) Glial cell line-derived neurotrophic factor stimulates ureteric bud outgrowth and enhances survival of ureteric bud cells in vitro. Exp Nephrol 6: 337–351.
36. Michael L, Davies JA (2004) Pattern and regulation of cell proliferation during murine ureteric bud development. J Anat 204: 241–255.
37. Hightower LE, White FP (1981) Cellular responses to stress: comparison of a family of 71–73-kilodalton proteins rapidly synthesized in rat tissue slices and canavanine-treated cells in culture. J Cell Physiol 108: 261–275.
38. Engelmyer E, van Goor H, Edwards DR, Diamond JR (1995) Differential mRNA expression of renal cortical tissue inhibitor of metalloproteinase-1, -2, and -3 in experimental hydronephrosis. J Am Soc Nephrol 5: 1675–1683.
39. Matsushima K, Oppenheim JJ (1989) Interleukin 8 and MCAF: novel inflammatory cytokines inducible by IL 1 and TNF. Cytokine 1: 2–13.
40. Shibata F, Kato H, Konishi K, Okumora A, Ochiai H, et al. (1996) Differential changes in the concentrations of cytokine-induced neutrophil chemoattractant (CINC)-1 and CINC-2 in exudate during rat lipopolysaccharide-induced inflammation. Cytokine 8: 222–226.
41. McEarchern JA, Besselsen DG, Akporiaye ET (1999) Interferon gamma and antisense transforming growth factor beta transgenes synergize to enhance the immunogenicity of a murine mammary carcinoma. Cancer Immunol Immunother 48: 63–70.
42. Peterson JM, Pizza FX (2009) Cytokines derived from cultured skeletal muscle cells after mechanical strain promote neutrophil chemotaxis in vitro. J Appl Physiol 106: 130–137.
43. Tan HK, Lee MM, Yap MG, Wang DI (2008) Overexpression of cold-inducible RNA-binding protein increases interferon-gamma production in Chinese-hamster ovary cells. Biotechnol Appl Biochem 49: 247–257.
44. Nedachi T, Fujita H, Kanzaki M (2008) Contractile C2C12 myotube model for studying exercise-inducible responses in skeletal muscle. Am J Physiol Endocrinol Metab 295: E1191–E1204.
45. Pillai RG, Beutelspacher SC, Larkin DF, George AJ (2008) Upregulation of chemokine expression in murine cornea due to mechanical trauma or endotoxin. Br J Ophthalmol 92: 259–264.
46. Carlson C, Hussain SM, Schrand AM, Braydich-Stolle LK, Hess KL, et al. (2008) Unique cellular interaction of silver nanoparticles: size-dependent generation of reactive oxygen species. J Phys Chem B 112: 13608–13619.
47. Loughna S, Yuan HT, Woolf AS (1998) Effects of oxygen on vascular patterning in Tie1/LacZ metanephric kidneys in vitro. Biochem Biophys Res Commun 247: 361–366.
48. Tajima K, Gershfeld NL (1985) Phospholipid surface bilayers at the air-water interface. I. Thermodynamic properties. Biophys J 47: 203–209.
49. Akimoto T, Hammerman MR, Kusano E (2005) Low ambient o(2) enhances ureteric bud branching in vitro. Organogenesis 2: 17–21.
50. Voronov DA, Taber LA (2002) Cardiac looping in experimental conditions: effects of extraembryonic forces. Dev Dyn 224: 413–421.
51. Kossakowska AE, Edwards DR, Lee SS, Urbanski LS, Stabbler AL, et al. (1998) Altered balance between matrix metalloproteinases and their inhibitors in experimental biliary fibrosis. Am J Pathol 153: 1895–1902.
52. Schmidt C, Bladt F, Goedecke S, Brinkmann V, Zschiesche W, et al. (1995) Scatter factor/hepatocyte growth factor is essential for liver development. Nature 373: 699–702.

Appendix II

Supplementary Figures

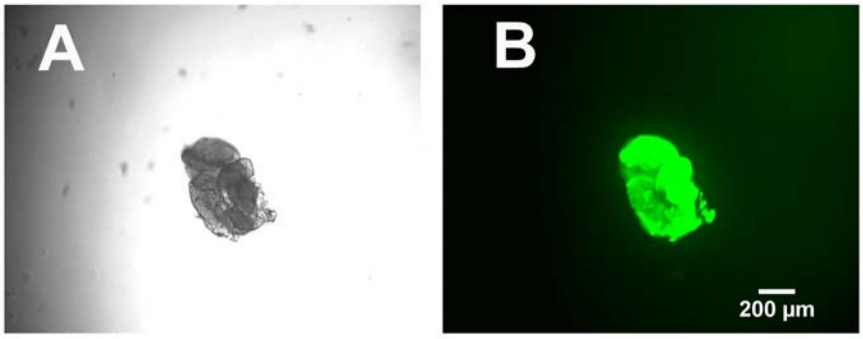

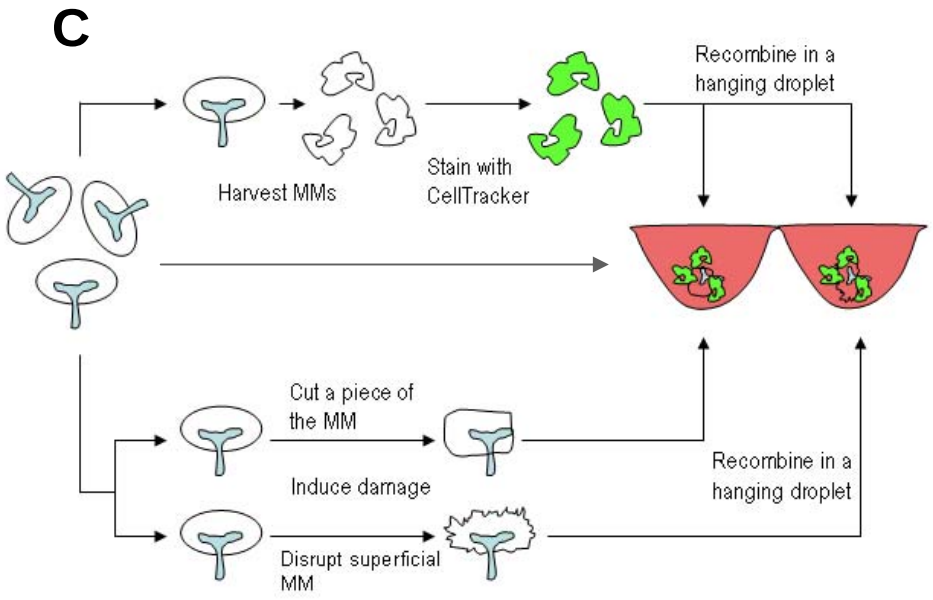

Supplementary Figure 1 – Testing the ability of CellTracker-stained MMs to integrate into host kidney rudiments
A and B – verification of CellTracker staining of whole isolated metanephric mesenchymes, A (bright field) and B (CellTracker fluorescence showing complete staining of the MMs)
C – Schematic illustration of the experimental setup for testing the ability of CellTracker-stained mesenchymes to integrate in host kidney rudiments. Either whole (undamaged) host kidney rudiments were used, or kidney rudiments in which superficial physical damage was induced to improve the integration of exogenous stained MMs

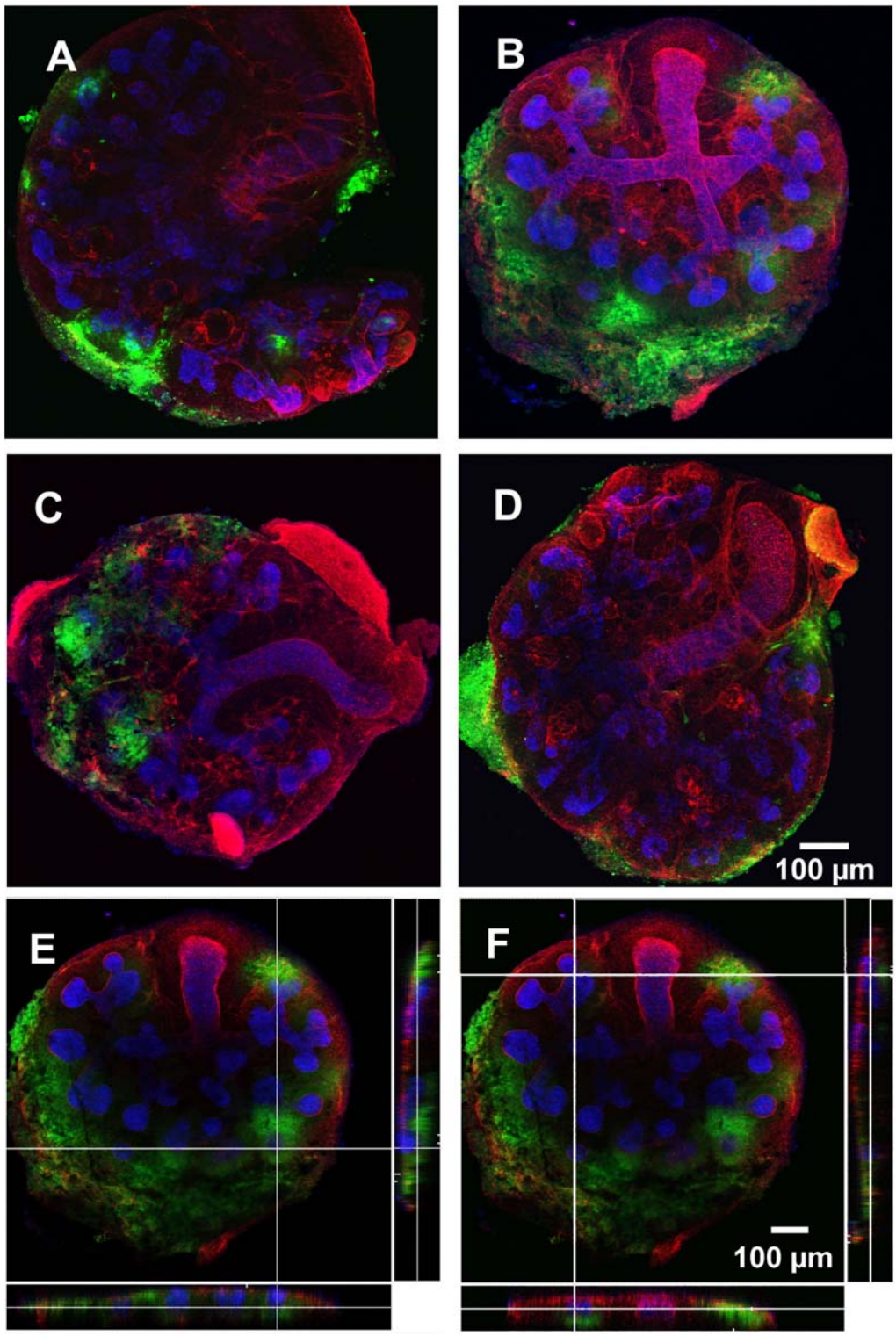

Supplementary Figure 2 - Immunohistochemistry of kidney rudiments combined with CellTracker-stained mesenchymes in a hanging droplet
After being kept for 24h in a hanging droplet the samples were transferred to filter culture and kept for further 3 days before fixation with 4% PFA. Undamaged host kidney rudiments were used.
Blue – Calbindin, red – Laminin, green – CellTracker-stained MMs
A, B, C, D – four different samples showing some integration of CT-labelled MM cells. In E and F, sections along the Z-axis are shown at the right and bottom part of the images to demonstrate that although CT-labelled MM cells have invaded the host kidney rudiment, no nephrons are formed. E and F show the same sample.

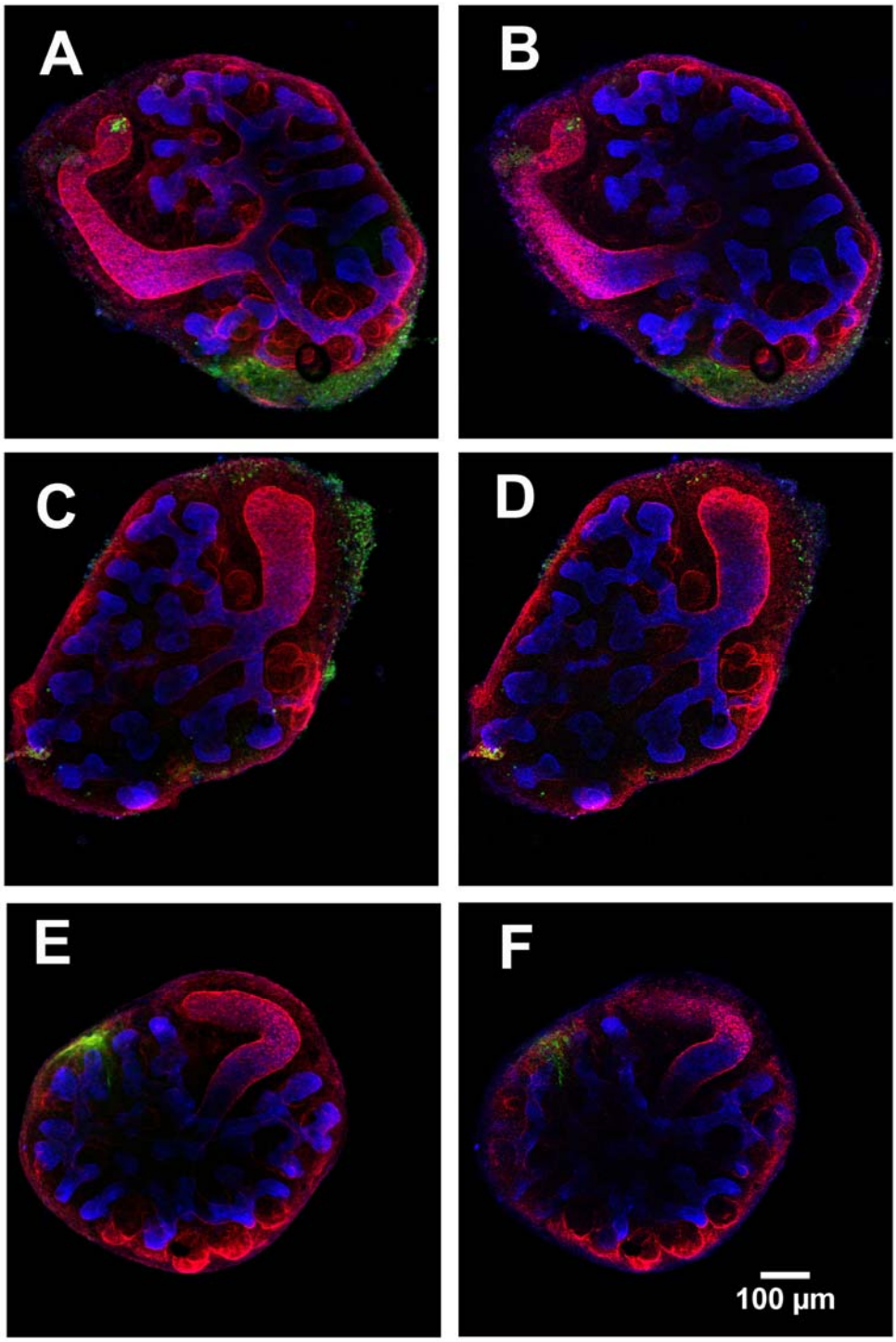

Supplementary Figure 3 - Immunohistochemistry of kidney rudiments combined with CellTracker-stained mesenchymes after induction of mechanical damage

After being kept for 24h in a hanging droplet the samples were transferred to a filter culture and kept for further 3 days before fixation with 4% PFA.
Blue – Calbindin, red – Laminin, green – CellTracker-stained MMs
A, C, E – stacks of confocal sections
B, D, F – confocal sections showing the integration of grafted CellTracker-labelled MM cells. The grafted cells do not integration in nephrons and the efficiency of invasion of host tissue is low.

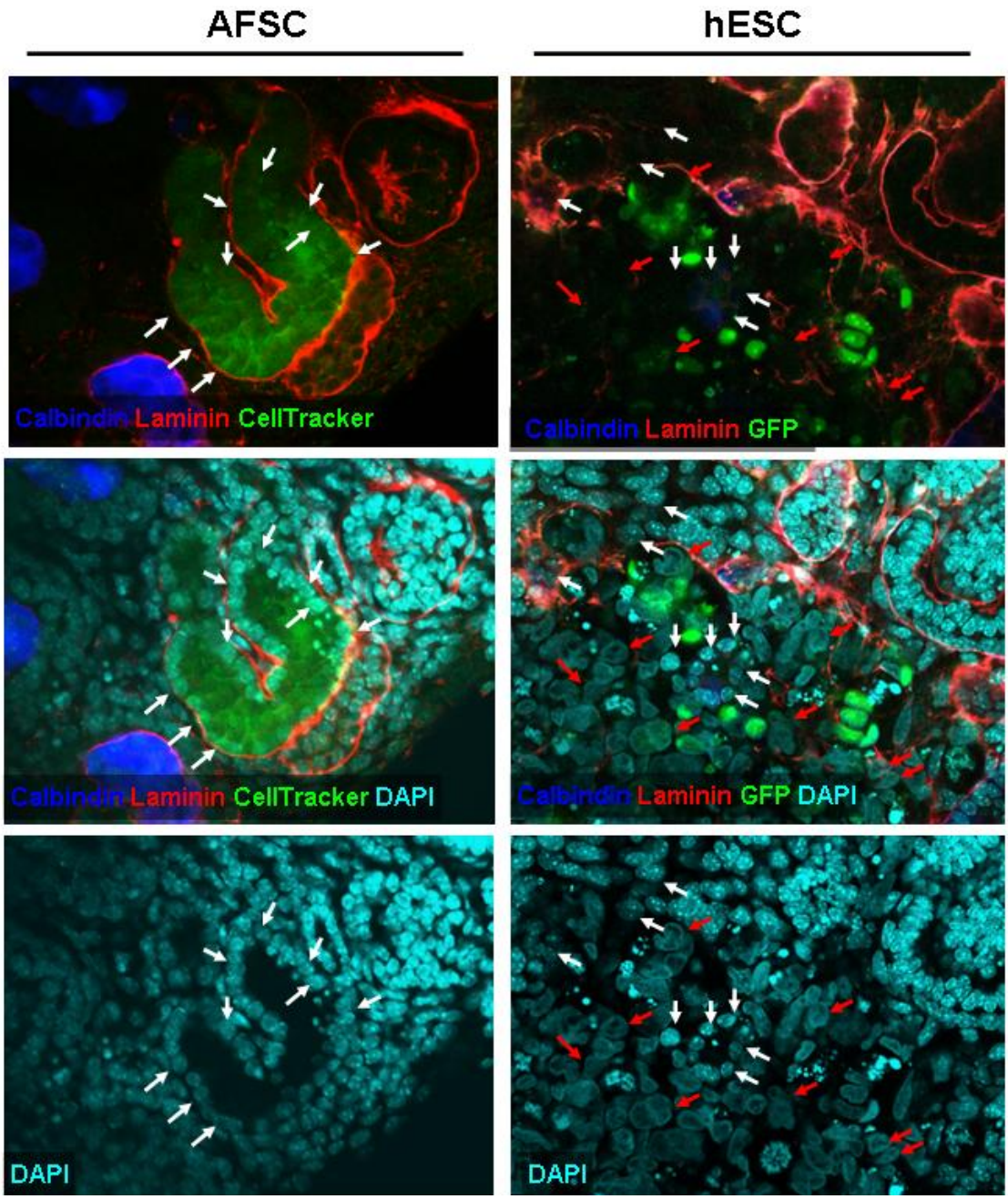

Supplementary Figure 4: Possible CellTracker artefacts in the disaggregation-reaggregation system

The first row shows confocal micrographs of Q1 human amniotic fluid stem cells (AFSCs) stained with CellTracker Green, mixed with disaggregated E11.5 kidney rudiments, reaggregated and cultured for 8D. The images show a CellTracker+ nephron suggesting that AFSCs successfully formed a nephron in the reaggregate. At the same time, reports have shown that mouse and human nuclei can be distinguished on the basis of a nuclear stain Moser et al., 1975). Mouse nuclei are brighter and show many lighter speckles - chromocentres. In contrast, human nuclei are larger, fainter and lack chromocentres. These data have also been confirmed by a control experiment with mixing GFP-tagged human ESCs into reaggregates (second row in the figure). Human nuclei (red arrows) are distinguishable from mouse nuclei (white arrows) in a large number of the cases. Please, note that not all hESCs are GFP+ due to the mosaicism of the cell line, as previously reported in Chapter 4. Re-evaluating the AFSC integration by looking at the nuclei suggests that the cells in the nephron might be mouse cells, as they are small, bright and have chromocentres (white arrows). This might suggest that the CellTracker dye could be filtered through and accumulated by renal tubules thereby creating artefacts.

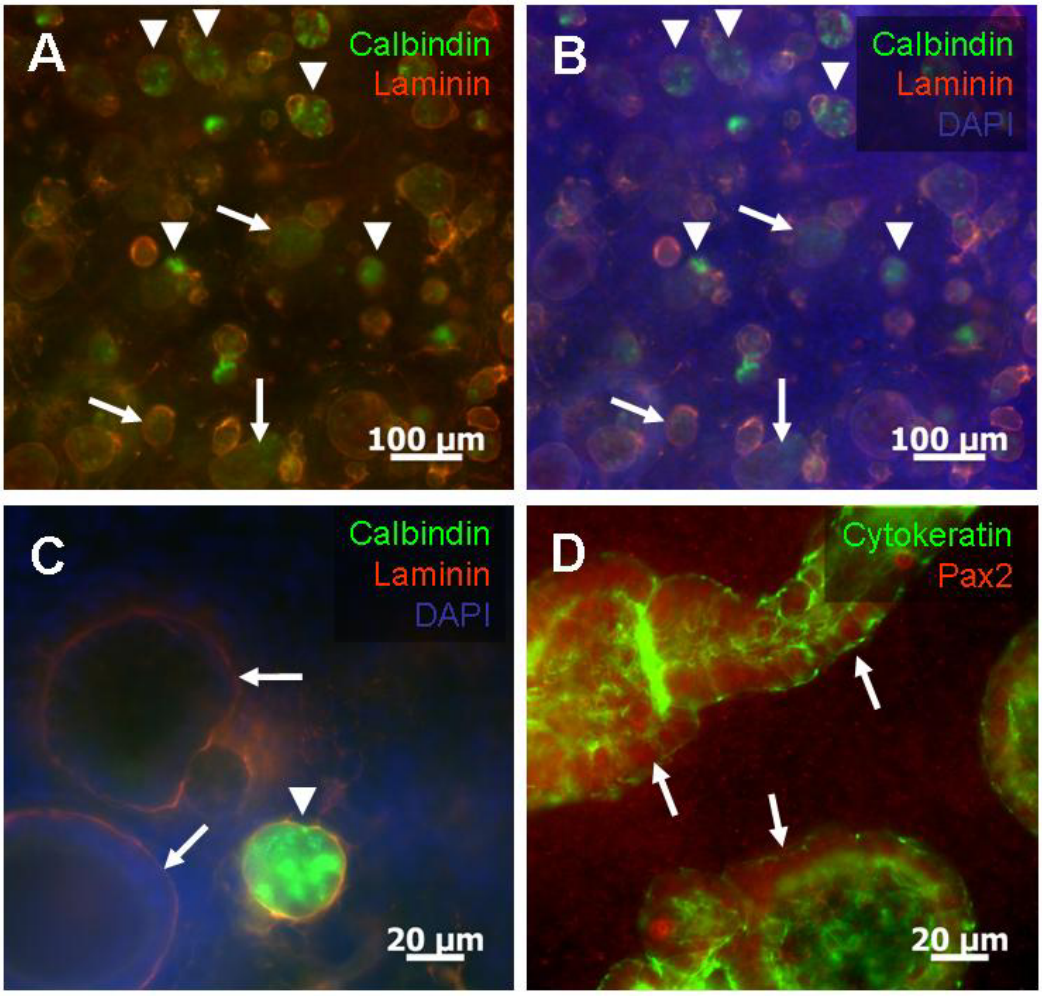

Supplementary Figure 5 - Structures formed by disaggregated and then reaggregated mesonephroi show different intensities of Calbindin staining
Disaggregated and reaggregated mesonephroi show structure formation (A, B, C and D). A and B – reformed structures show a weak (arrows) or strong (arrowheads) Calbindin staining. C – both reformed mesonephric nephrons (arrow, Laminin+ Calbindin-) and WD fragments (arrowhead, Laminin+ Calbindin-) were observed. Expression of Cytokeratin and Pax2 was normal.

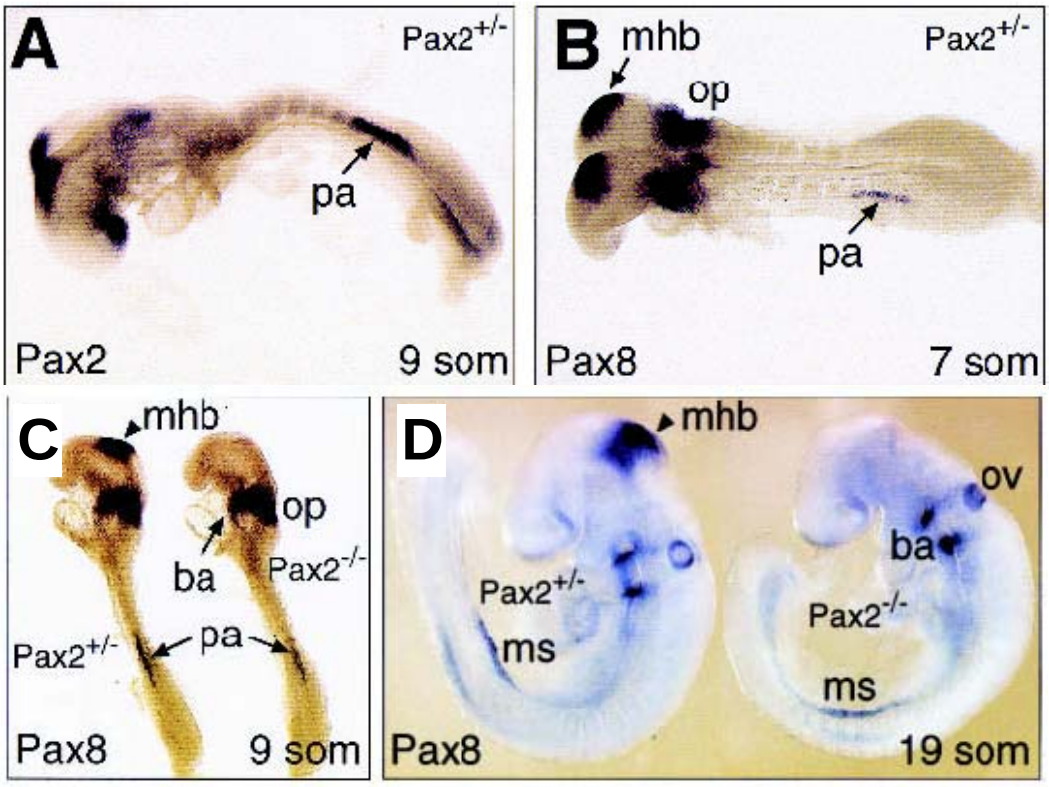

Supplementary Figure 6 - Pax2 and Pax8 expression at the onset of kidney development (modified from Bouchard et al., 2002)
A – initiation of *Pax* gene expression in the pronephric anlage of *Pax2*+/- embryos. *Pax8* expression was first detected by *in situ* hybridisation at the 7-somite stage in the intermediate mesoderm at the level of the 5th and 6th somites, corresponding to the pronephric anlagen (B). *Pax2* was also detected in the pronephric anlagen at the 9–somite stage (A). Initiation of Pax2 expression was reported to happen at the 8-somite stage (Bouchard et al., 2002, not shown)
E - shows the expression of *Pax8* in Pax2+/- and Pax2-/- embryos at the 9-somite stage
F – shows *Pax8* expression in the mesonephros of a 19-somite stage embryo
(from Bouchard et al., 2002)

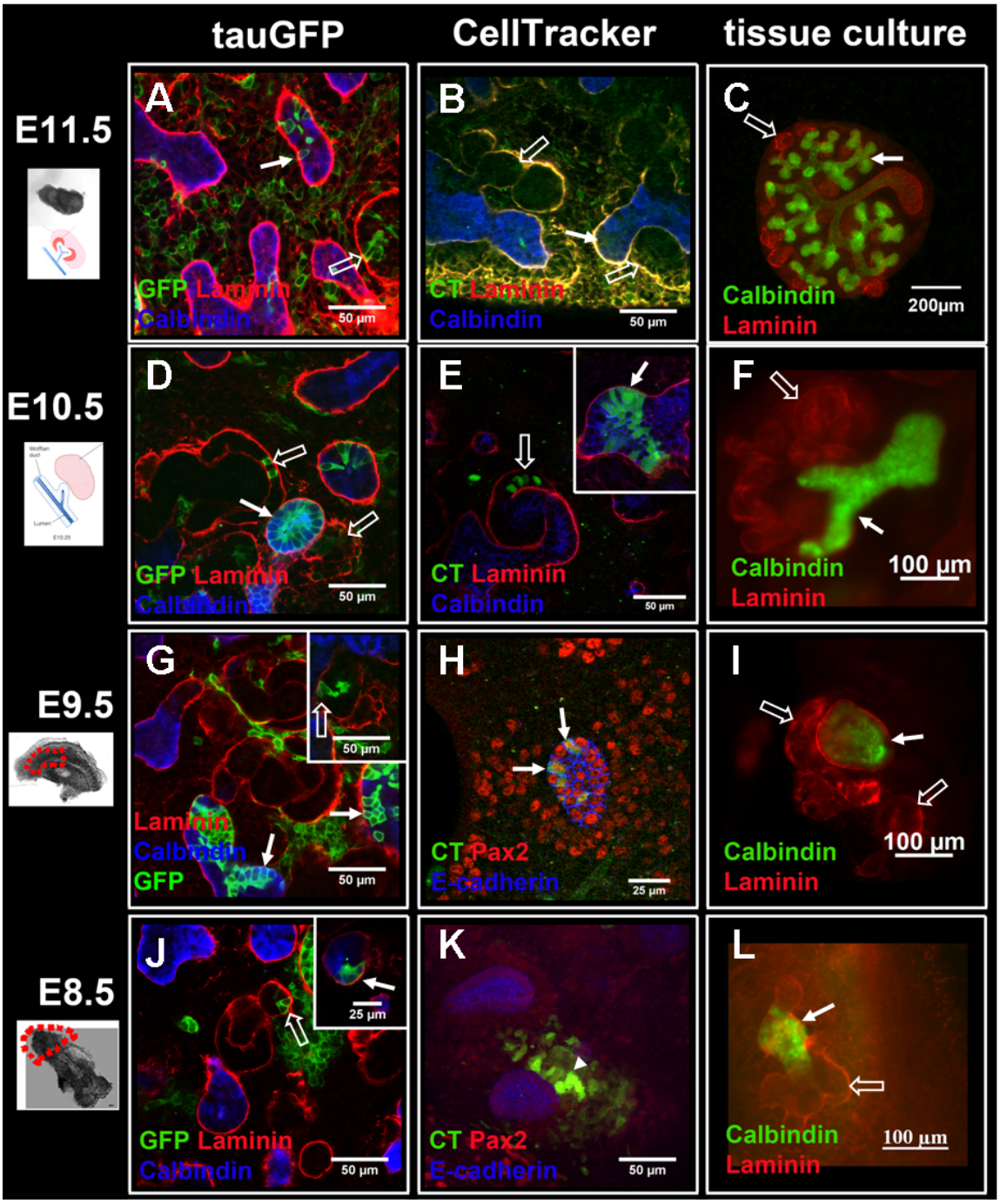

Supplementary Figure 7 – The ability of cells and tissues from different embryonic stages to integrate into renal epithelia and generate renal-like structures in organ culture
The respective embryonic stage is shown on the left; the isolated region was shown by a red dotted line if necessary; block arrows indicate cells integrating in UBs or forming Calbindin+ UB-like structures in the last column of images; open arrows indicate cells integrating in nephrons or the formation of nephron-like structures in the last column of images
A, D, G and J show that tauGFP+ cells from E11.5 metanephroi were able to integrate into both nephrons and UBs, where at least some of the integrating UB cells were Calbindin+; B, E, H and K show integration experiments performed with CellTracker-stained cells; Integration in both nephrons and UBs can be seen in B and E; integration in UB only in H, and no integration in K; organ culture experiments in C, F, I and L show that the tissues isolated from different embryonic stages (as indicated in the diagrammatic panels on the left) for both UB-like and nephron-like structures; the ability of Calbindin + structures to branch disappeared in I and L.